

**CASCADE RADICAL CYCLIZATION: APPLICATION TO THE DEVELOPMENT OF
NOVEL CAMPTOTHECIN ANALOGS AND A SHORT SYNTHESIS OF LUOTONIN A
AND ITS ANALOGS**

by

Raghuram S. Tangirala

B.Sc., Osmania University, 1996

M.Sc., Indian Institute of Technology Madras, 1998

Submitted to the Graduate Faculty of

Arts and Sciences in partial fulfillment

of the requirements for the degree of

Doctor of Philosophy

University of Pittsburgh

2004

UNIVERSITY OF PITTSBURGH
FACULTY OF ARTS AND SCIENCES

This dissertation was presented

by

Raghuram S. Tangirala

It was defended on

December 16, 2004

and approved by

Professor Peter Wipf

Professor Scott G. Nelson

Professor Jack C. Yalowich

Professor Dennis P. Curran
Dissertation Director

To my mother Vijaya, father Eshwar, my brother Krishna
and my late grandparents to whom this would have meant so much.

Copyright by Raghuram S. Tangirala
2004

CASCADE RADICAL CYCLIZATION: APPLICATION TO THE DEVELOPMENT OF NOVEL CAMPTOTHECIN ANALOGS AND A SHORT SYNTHESIS OF LUOTONIN A AND ITS ANALOGS

Raghuram S. Tangirala, Ph.D.

University of Pittsburgh, 2004

Cascade radical cyclizations have been employed in the synthesis of several novel analogs of camptothecin and luotonin A. The mild conditions of the cyclization allowed for the synthesis of a wide variety of analogs with high functional group tolerance in a modular fashion.

The asymmetric synthesis of a pyridone lactone, a key intermediate in Lavergne and Bigg's synthesis of (*R*)-hCPT, is described. The synthesis furnished the product in good enantiopurity (96% ee) in eleven synthetic steps starting from commercially available 2-methoxypyridine. The key reactions in this synthesis are Sharpless asymmetric epoxidation and Corey-Stille coupling.

Attempts towards a more efficient synthesis of the DE-fragment of (*R*)-hCPT which were not successful, but led to the synthesis of novel non-lactone analogs of camptothecin are discussed. These non-lactone analogs contain either a cyclic ether or an α,β -unsaturated lactone in place of the α -hydroxy- δ -lactone as the E-ring of camptothecin. Despite possessing interesting structural features, these analogs were shown to be biologically inactive in the topo I inhibition assays as well as cell growth inhibition studies.

The semi-synthesis and biological evaluation of E-ring open form analogs of camptothecin was developed. This analog synthesis evolved from an interesting report by Stewart and coworkers of the X-ray crystal structure of topo I-DNA-topotecan ternary complex. Amongst the six open form analogs synthesized, the hydrazides showed activity comparable to

that of camptothecin in the DNA cleavage assays. This activity may be due to the reclosure to camptothecin under the assay conditions.

20-Fluorocamptothecin was accidentally discovered upon fluorination of the tertiary alcohol of CPT with DAST at $-78\text{ }^{\circ}\text{C}$. This discovery led to the stereoselective total synthesis of racemic, *20R*- and *20S*-fluorocamptothecin. It was concluded from the biological data that the fluorination occurred with inversion of configuration.

The total synthesis of luotonin A, a recently isolated topo I poison, and its analogs using the radical cascade cyclization strategy, was accomplished. A concise, modular approach was undertaken for the synthesis of all the analogs of luotonin A. This exercise would provide more insight into the structure-activity relationships of this new drug candidate.

The development of camptothecin analogs with interesting biological properties and differing mainly in the D, E rings was the central theme of the research work described in this thesis. Knowledge acquired from this research can be used for future discovery and development of potential drug candidates.

TABLE OF CONTENTS

PREFACE	xvi
1. BACKGROUND	1
1.1. Camptothecin.....	1
1.2. Mechanism of Action.....	3
1.3. Structure-Activity Relationships.....	5
1.4. Various Total Syntheses of CPT.....	9
1.5. Silatecans.....	12
1.6. Homocamptothecin and Homosilatecans.....	13
2. ASYMMETRIC SYNTHESIS OF LAVERGNE-BIGG DE FRAGMENT OF (R)-hCPT	17
2.1. Introduction.....	17
2.2. Asymmetric Synthesis of the Lavergne-Bigg DE Fragment.....	21
2.3. Summary.....	27
3. NEW ASYMMETRIC APPROACHES TO THE DE-FRAGMENT OF (R)-hCPT AND SYNTHESIS OF NON-LACTONE E-RING ANALOGS OF CPT	28
3.1. Introduction.....	28
3.2. Homologation Approaches to the Synthesis of the DE-Fragment of (R)-hCPT.....	29
3.2.1. Synthesis of the Substrate 49 for Homologation Studies.....	31
3.2.2. Attempted Homologation of 49 with 1,3-Dithiane derived Phosphonate.....	32
3.2.3. Attempted Homologation using α -Aminoacetonitriles.....	34
3.2.4. Attempted Homologation using Tosylmethyl Isocyanide (TosMIC).....	35
3.3. Epoxidation/Dihydroxylation Approaches to the Synthesis of the DE Fragment of (R)-hCPT.....	39
3.3.1. Synthesis of the Enelactone 71	41
3.3.1.1. Attempted Synthesis of 71 by Metathesis Approach.....	41
3.3.1.2. Synthesis of 71 by Ni (II)/Zn Catalyzed Cyclization.....	44
3.3.1.3. Synthesis of 71 using Stille Coupling.....	46
3.3.1.4. Modeling and Variable Temperature NMR Studies of 71	48
3.3.2. Dihydroxylations and Epoxidations of Olefin 71	51
3.3.2.1. Dihydroxylation Studies of Olefin 71	52
3.3.2.2. Epoxidation Studies of Olefin 71	53
3.3.3. Novel Non-Lactone Analogs of Camptothecin – Synthesis.....	55
3.3.4. Novel Non-Lactone Analogs of Camptothecin – Biological Evaluation.....	59
3.4. Summary.....	61
4. E-RING OPEN-FORM ANALOGS OF CAMPTOTHECIN	62
4.1. Introduction.....	62
4.2. Synthesis of the E-ring Open Form Analogs of CPT.....	63
4.3. Biological Evaluation of the E-ring Open Form Analogs of CPT.....	67
4.4. Summary.....	71
5. 20-FLUOROCAMPTOTHECINS: AN ACCIDENTAL DISCOVERY	72
5.1. Introduction.....	72

5.2.	Synthesis and Biological Evaluation of Analogs of 20-Fluorocamptothecin.....	75
5.3.	Stereoselective Total Synthesis of 20 <i>S</i> and 20 <i>R</i> -Fluorocamptothecin	76
5.4.	Summary	82
6.	TOTAL SYNTHESIS OF LUOTONIN A AND ITS ANALOGS USING CASCADE RADICAL CYCLIZATION	83
6.1.	Introduction.....	83
6.2.	Synthetic Approaches to Luotonin A.....	84
6.3.	Total Synthesis of Luotonin A.....	85
6.4.	Synthesis of Analogs of Luotonin A.....	87
6.5.	Summary.....	95
7.	SUMMARY AND CONCLUSIONS	96
8.	EXPERIMENTAL.....	100
	APPENDIX.....	160
	NMR and LCMS Data of Representative Compounds.....	160
	BIBLIOGRAPHY.....	207

LIST OF TABLES

Table 3.1 Homologation of Aldehyde 49 with TosMIC - Reaction Conditions.....	37
Table 5.1 Comparison of DAST and Deoxofluor for the Fluorination of 108	79
Table 6.1 Building Blocks for the Luotonin Library	89
Table 6.2 Luotonin Library - Compound Numbers and Isolated Yields from Column Chromatography	91
Table 7.1 Summary of the Biological Results	97

LIST OF FIGURES

Figure 1.1 Structure of (<i>S</i>)-Camptothecin.....	1
Figure 1.2 Structure-Activity Relationships of various CPT derivatives (adapted from ref. 10)...	6
Figure 1.3 Topotecan Binding as the (A) Closed Lactone and (B) Open Carboxylate (reproduced from ref. 12).....	7
Figure 1.4 Various clinically relevant CPT analogs	9
Figure 1.5 Structure of DB-67	12
Figure 1.6 Structure of Homocamptothecin.....	13
Figure 1.7 Structure of Du1441	15
Figure 3.1 MOE Images of the Predicted Lowest Energy Conformer of 71 (A) Front view (B) Side view.....	49
Figure 3.2 Variable Temperature Proton NMR Studies of 71	50
Figure 3.3 Novel Non-Lactone Analogs Reported by Lavielle	56
Figure 3.4 Development of Cyclic Ether Analogs to Camptothecin Derivatives.....	56
Figure 3.5 Topoisomerase Inhibitory DNA Cleavage Assay Results for Non-lactone Analogs 95a,b	60
Figure 4.1 Structural Modifications in Synthesis of E-ring Open Form Analogs	64
Figure 4.2 Results of Topo I Inhibitory Assay of Derivatives 96, 97, 101 & 102	68
Figure 4.3 Results of the Cell Growth Inhibition SRB Assay of Derivatives 96, 97, 101 and 102	70
Figure 5.1 Results of the Topo I Inhibitory DNA Cleavage Assay of Derivatives (<i>S</i>)- 107 , (<i>R</i>)- 107 and <i>rac</i> - 107	80
Figure 6.1 Structures of Luotonin A and Camptothecin.....	83
Figure 6.2 Hecht's E-ring Analogs of Luotonin A.....	87
Figure 6.3 Structures, Amounts and LCMS Purities of Luotonins.....	94

LIST OF SCHEMES

Scheme 1.1 Hydrolysis of camptothecin at physiological pH	2
Scheme 1.2 Mechanism of Action of Camptothecin (adapted from ref. 7).....	4
Scheme 1.3 [4+1] Radical Cascade Cyclization Strategy.....	10
Scheme 1.4 Mechanism of the cascade radical cyclization	11
Scheme 1.5 Lavergne and Bigg's semisynthetic approach to hCPT	14
Scheme 2.1 Comins' strategy of synthesis of the CPT skeleton.....	18
Scheme 2.2 Lavergne-Bigg synthesis of DE fragment of racemic hCPT.....	19
Scheme 2.3 Final steps in the Lavergne-Bigg synthesis of racemic hCPT	20
Scheme 2.4 Resolution strategy in Lavergne-Bigg synthesis of (R)-hCPT.....	20
Scheme 2.5 Initial iodoformylation reactions with 24a and 24b	22
Scheme 2.6 Quéguiner's strategy of selective ortholithiation of 2-methoxypyridine	23
Scheme 2.7 Preparation of the Sharpless asymmetric epoxidation precursor	24
Scheme 2.8 Preparation of ethyl (E)-3-(tributylstannyl)-2-pentenoate	24
Scheme 2.9 Completion of the asymmetric synthesis of (R)-19 and (R)-39	26
Scheme 3.1 Asymmetric Nucleophilic Addition Approach to Ketones Towards the <i>DE</i> -fragment of (R)-hCPT	29
Scheme 3.2 Shibasaki's catalytic enantioselective cyanosilylation of ketones.....	30
Scheme 3.3 Shibasaki's Enantioselective Eyanosilylation of Ketone 45	30
Scheme 3.4 Envisioned Synthesis of (R)-38 from Nitrile 46	31
Scheme 3.5 Synthesis of the Homologation Substrate 49	32
Scheme 3.6 Proposed Homologation of 49 with 1, 3-Dithiane Derived Phosphonate 51	33
Scheme 3.7 Proposed Mechanism for the Generation of 45 in the Homologation of 49 with 51	33
Scheme 3.8 Proposed Homologation of 49 with an Aminoacetonitrile 55	34
Scheme 3.9 Reaction of Adamantanone with TosMIC	35
Scheme 3.10 Proposed Mechanism of Reaction of TosMIC with an Aldehyde	36
Scheme 3.11 Proposed Homologation of Aldehyde 49 with TosMIC	36
Scheme 3.12 Proposed Mechanism of Formation of 45 by Reaction of TosMIC with 49	38
Scheme 3.13 Reaction of TosMIC on Test Substrate 70	39
Scheme 3.14 Synthetic Routes to (R)-38 via Asymmetric Epoxidation/Dihydroxylation of 71 ..	40
Scheme 3.15 Attempted Synthesis of 71 by Metathesis Approach	42
Scheme 3.16 Ni(II)/Zn Catalyzed Regioselective Cyclization of 29b	45
Scheme 3.17 Intramolecular Ni(II)/Zn Catalyzed Cyclization of 84	45
Scheme 3.18 Preparation of Ethyl (Z)-3-(Tributylstannyl)-2-pentenoate	47
Scheme 3.19 Synthesis of 71 by Stille Coupling.....	47
Scheme 3.20 Racemic and Asymmetric Dihydroxylation of 71	52
Scheme 3.21 Racemic Epoxidation of 71	54
Scheme 3.22 Plausible Mechanism of the Unexpected Rearrangement during Epoxidation of 71	54
Scheme 3.23 Synthesis of Four Cyclic Ether Analogs of CPT.....	58
Scheme 3.24 Synthesis of Four Enelactone Analogs of CPT	59

Scheme 4.1 Synthesis of the Hydrazides 96 , 97 and Weinreb Amide 99	65
Scheme 4.2 Synthesis of 17-Deshydroxy Open-form Analogs	66
Scheme 5.1 Proposed Synthesis of 104 from CPT	72
Scheme 5.2 Reaction of CPT with DAST	73
Scheme 5.3 Synthesis of Analogs of 20F-CPT.....	75
Scheme 5.4 Reaction of DAST with DB67	76
Scheme 5.5 Synthesis of 20-Fluorocamptothecin 107	77
Scheme 6.1 Synthetic Approaches to Luotonin A	85
Scheme 6.2 Total Synthesis of Luotonin A	86
Scheme 6.3 Synthesis of Library of Luotonin A Analogs	88
Scheme 6.4 Unexpected Side Reaction of 129{b}	90
Scheme 6.5 Synthesis of 10-hydroxy and 10-aminoluotonins.....	92

LIST OF ABBREVIATIONS

AD-Mix	asymmetric dihydroxylation mixture
AIBN	2,2'-azobisisobutyronitrile
Boc	butyloxycarbonyl
BSA	bovine serum albumin
<i>t</i>BuOK	potassium <i>tert</i> -butoxide
CPT	camptothecin
DABCO	1,4-diazabicyclo[2,2,2]octane
DAST	(diethylamino)sulfur trifluoride
DBU	1,8-diazabicyclo[5,4,0]undec-7-ene
DB67	7- <i>tert</i> -butyldimethylsilyl-10-hydroxycamptothecin
DEAD	diethylazodicarboxylate
(DHQD)₂-AQN	hydroquinidine anthraquinone-1,4-diyl diether
(DHQD)₂-PHAL	hydroquinidine 1,4-phthalazinediyl diether
(DHQD)₂-PYR	hydroquinidine 2,5-diphenyl-4,6-pyrimidinediyl diether
DIBAL	diisobutyl aluminum hydride
DMAP	4-dimethylamino pyridine
DMDO	2,2-dimethyldioxirane
DME	dimethoxyethane
DMF	dimethylformamide
DMSO	dimethyl sulfoxide
DNA	deoxyribonucleic acid

dppe	1,2-bis(diphenylphosphino)ethane
EDTA	ethylenediamine tetraacetic acid
<i>ee</i>	enantiomeric excess
EI	electron ionization
equiv	equivalents
eV	electron volts
FDA	food and drug administration
FTIR	fourier transform infrared spectroscopy
GC	gas chromatography
GI₅₀	growth inhibition 50%
hCPT	homocamptothecin
HMBC	heteronuclear multiple bond coherence
HMPT	hexamethylphosphoramide
HPLC	high pressure liquid chromatography
HRMS	high resolution mass spectrometry
Hz	hertz
IC₅₀	inhibitory concentration 50%
IR	infrared spectroscopy
<i>k_{coal}</i>	coalescence rate constant
KHMDS	potassium hexamethyldisilazide
KOAc	potassium acetate
LAH	lithium aluminum hydride
LCMS	liquid chromatography - mass spectrometry

LDA	lithium diisopropylamide
μM	micromolar
mCPBA	<i>meta</i> -chloroperbenzoic acid
MOE	molecule operating environment
mol%	mole percent
MOM	methoxymethyl
MS	mass spectrometry
<i>m/z</i>	mass to charge ratio
NaOMe	sodium methoxide
nM	nanomolar
NMO	4-methylmorpholine <i>N</i> -oxide
NMR	nuclear magnetic resonance
PBS	phosphate buffer saline
Ph	phenyl
ppm	parts per million
QSAR	quantitative structure-activity relationships
rt	room temperature
Rt	retention time
SAD	sharpless asymmetric dihydroxylation
SAE	sharpless asymmetric epoxidation
SAR	structure-activity relationships
SCLC	small-cell lung cancer
SDS	sodium dodecylsulfate

TBAB	tetra-butyl ammonium bromide
TBHP	<i>tert</i> -butylhydroperoxide
TBS	<i>tert</i> -butyldimethylsilyl
TFA	trifluoroacetic acid
THF	tetrahydrofuran
TLC	thin layer chromatography
TMS	trimethylsilyl
topo I	topoisomerase I
TosMIC	tosylmethyl isocyanide
<i>p</i>TsOH	<i>para</i> -toluenesulfonic acid
TsOMe	methyl tosylate

PREFACE

I would like to take this opportunity to express my gratitude to those people who have made my stay in Pittsburgh pleasant and memorable.

First, I would like to thank my advisor Prof. Dennis P. Curran for the opportunity to work in his group. I thank him for his motivation and guidance in shaping my career towards becoming a good chemist. His patience and calmness in solving problems and his willingness to share freely his knowledge has been an inspiration. He is also a wonderful teacher as was evident from his enthusiastic participation in the Tuesday night super group meetings. I was quite fortunate to have been associated with such an outstanding chemist and a patient teacher.

I also thank Profs. Peter Wipf and Scott Nelson for serving as my committee members at various stages of my graduate student life at Pitt. They have been a source of encouragement and advice throughout my stay at Pitt. My special thanks are due to Prof. Floreancig for guiding me through my research proposal. Thanks are also due to Prof. Jack Yalowich for serving as the external committee member and for helpful suggestions on the camptothecin project. I also would like to thank our collaborators on the camptothecin project, late Prof. Thomas G. Burke and Dr. Brad Anderson and their groups at the University of Kentucky and Dr. Yves Pommier and his group at the National Cancer Institute for all the biological assays.

I would like to thank all the Curran group members, past and present, for helping me get through my graduate school by making every day special. In particular, Drs. Ana Gabarda, David Bom, Wu Du, Thomas Isarno and Rachel Dixon for being great colleagues in the camptothecin project. In particular, my special thanks are due to Rachel who not only helped me with a few data measurements but also was there as a strong moral support during the hectic days in the completion of this thesis. Thanks are also due to Drs. Matthias Pohlman, Stefan Fischer, Jun

Terauchi, Stefan Werner, Arndt Brückner and Qisheng Zhang have been wonderful colleagues and have provided the much needed fun-filled work environment along with interesting chemistry discussions. There was so much to learn from them. It was also a pleasure to work with Youseung Shin, Jonathan Tripp and André Lapierre. In particular, thanks are due to Jon and André for helping me with lab-related and computer issues with a smile. Youseung was a special person from whom one could learn what hard work really meant. Thanks for being a great labmate. Thanks to Venugopal Gudipati, my fellow Indian in the group, for being a good friend and for listening to all my complaints.

I wish to thank Dr. Fu-tyan Lin for the support with the NMR facilities. My special thanks are due to Dr. Kasi Somayajula for his support with the MS facilities in the chemistry department. Kasigaru, as I fondly used to call him, was like a father figure to me during the past five years. I thank him and his wife for making me part of their family. It was home away from home. My thanks are also due to Jonathan Tripp and Venugopal Gudipati for recording several NMR spectra.

Words cannot adequately express my thanks to my friends Dr. Sivaraman Dandapani, Sridhar Rajaram, Vasumathy Rajaraman and Apsara Gopalarathnam for their friendship and the chemistry and non-chemistry discussions. In particular, thanks are due to Siva and Sridhar for always being there during the highs and the lows of my life at Pitt. I will miss all the regular conversations and debates we always had about everything under the sun.

I would like to express my deepest gratitude to the most important people in my life, my parents and my brother. I thank my mother, Vijaya, for her sacrifices throughout her life in bringing me up the way she did. She had supported me in every decision I made and every step I took even if it meant studying in the United States, thousands of miles away from home. I owe

my life and education to my mother whom I will never cease to love, admire and respect. I also thank my father, Eshwar, who probably is the proudest father that I have ever met. He is a forever cheerful person and knows how to live life. I thank him for always being so humorous and lively and making every conversation I ever had with him fun-filled. I thank my brother, Krishna, for being my best friend for the past 27 years. I don't know of a kinder and sweeter human being and I am fortunate to have him as my brother. Thanks for always being there for me, particularly when I needed you the most. And to my late grandparents, this Ph.D. would have meant so much. I dedicate my thesis, although tiny and unnoticeable, to my parents, brother and my grandparents. I couldn't have done this without their love and support.

1. BACKGROUND

1.1. Camptothecin

One of the primary causes for deaths in many parts of the world is cancer.¹ “*Cancer*” is a general name for a condition in which abnormal cells grow in an uncontrolled manner. Cancer can invade and destroy healthy tissues and spread via the bloodstream and lymphatic system to other parts of the body. One of the efficient ways to treat cancer is by chemotherapy in which anti-cancer drugs are used to treat cancerous cells. Chemotherapy either kills or arrests the growth of cancerous cells by targeting specific parts of the cell growth cycle. A wide variety of compounds possessing chemotherapeutic properties have been isolated from natural substances like plants, fungi etc. Taxol is an excellent example of a plant-derived anticancer drug that has achieved tremendous success in cancer chemotherapy. Another important family of plant-derived anticancer drugs that has been the subject of considerable attention is that of the camptothecins (Figure 1.1).

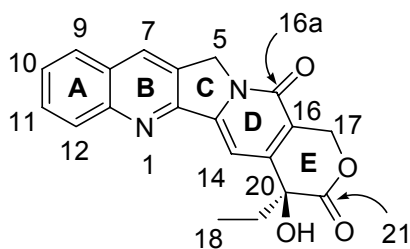
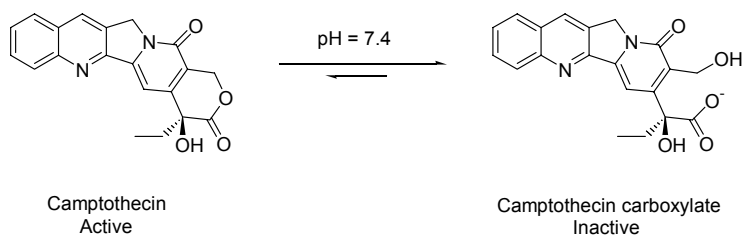


Figure 1.1 Structure of (S)-Camptothecin

Camptothecin (CPT) was isolated by Monroe Wall and Mansukh Wani in 1966 from the extracts of the Chinese tree Xi Shu (*Camptotheca acuminata* of the *Nyssaceae* family) and its

chemical structure was established.² Camptothecin exhibited promising antitumor activity against a wide range of solid tumors and this led to widespread attention.³ Camptothecin soon entered into clinical trials (Phase I and partially Phase II) in the late '60s. However, the clinical development of CPT was halted because of certain severe and unpredictable side effects such as haemorrhagic cystitis and myelosuppression.⁴ It was later learned that CPT failed because it was administered as the water-soluble sodium carboxylate form rather than the water-insoluble camptothecin itself. Unfortunately, this ring-opened carboxylate form of CPT is biologically inactive⁵ (Scheme 1.1).



Scheme 1.1 Hydrolysis of camptothecin at physiological pH

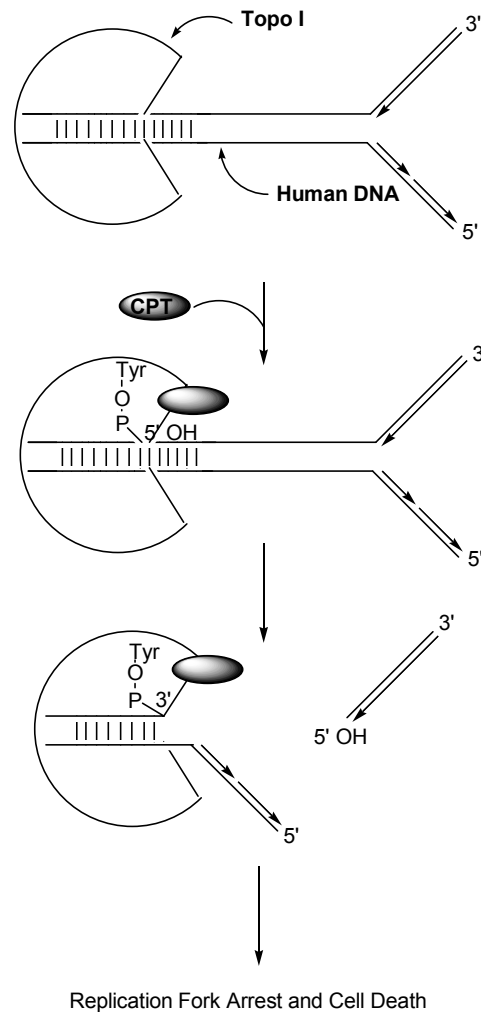
In 1985, the molecular target of CPT, human DNA topoisomerase I, was identified.⁶ This result, coupled with the understanding of the failure of clinical trials of CPT, led to a dramatic increase in research efforts aimed at development of various analogues of CPT which would possess improved water solubility yet retain CPT's unique mechanism of action.

1.2. Mechanism of Action

Topoisomerase I (topo I) is an enzyme that catalyzes the various topoisomerization reactions of DNA (e.g., relaxation/supercoiling, catenation/decatenation) by transient enzyme-linked single-strand breaks.⁷ The primary function of topo I is believed to be the removal of excessive supercoils generated during processes like transcription, replication etc.

DNA relaxation reaction by topo I occurs in three steps. First, a nucleophilic attack by the tyrosine hydroxyl group (#723 of human DNA topo I) on the 3'-phosphate of the phosphodiester linkage gives rise to an enzyme-linked single-strand break. Second, the phosphodiester linkage opposite to the transient break is believed to turn around to undergo the religation reaction. Third, the 5'-hydroxyl group nucleophilically attacks the tyrosyl phosphate to release the tyrosine residue from the phosphate. This constitutes the religation reaction.

Biochemical studies have shown that CPT binds at the interface between the DNA and topo I and inhibits specifically the religation step in the cleavage/religation reaction. It has been learned that CPT binds neither the DNA nor the topo I alone,⁶ but rather interacts with the DNA-topo I complex to form a reversible ternary complex termed as the “*cleavable complex*”. Based on the studies in a cell-free SV40 replication system by Hsiang and Liu, a replication fork collision model⁸ was proposed for the cytotoxicity of CPT as shown in Scheme 1.2.



Scheme 1.2 Mechanism of Action of Camptothecin (adapted from ref. 8)

The reversible topo I-DNA-CPT ternary complexes are not lethal by themselves. However, collision occurring between this complex and the advancing replication fork leads to apoptosis. Three biochemical events have been identified as occurring soon after the collision occurs. These are (a) formation of a double-strand break, (b) irreversible arrest of the replication fork, and (c) formation of topo-I linked DNA break at the site of collision.

It has also been shown that this collision is potentially lethal only if the cleavable complex is formed on the strand complementary to the leading strand of DNA synthesis.⁹

1.3. Structure-Activity Relationships

While efforts to elucidate the mechanism of action of CPT and its binding in the cleavable complex are important to understand its cytotoxicity, it is equally crucial to acquire knowledge about the various structure-activity relationships associated with CPT. CPT itself is not used as a drug for chemotherapy due to its poor blood stability and solubility resulting in loss of activity. Hence it was of considerable importance to determine if substitutions by various hydrophilic and lipophilic groups at different positions on the CPT structure would lead to suitable drug candidates.

Considerable efforts of various research groups around the world have thrown light on the structure-activity relationships in CPT. It is now known that:

- Only the 20*S* enantiomer is active.^{5a,6b,6d}
- The lactone form of E-ring in the CPT structure is crucial for activity. The open hydroxycarboxylate form of CPT is inactive (see Scheme 1.1).
- Changes in the E-ring, for example, replacing lactone by lactam, removal of the 20-hydroxy group, substituting a lactol for the lactone etc., resulted in inactivity with respect to topo I inhibition.^{5b}

Analogs bearing substituents at positions 7, 9, 10 and to some extent 11 either retained the activity of or showed enhanced activity than the parent CPT. Figure 1.2 proposed by Sawada and coworkers summarizes the overall understanding of structure-activity relationships of CPT.¹⁰

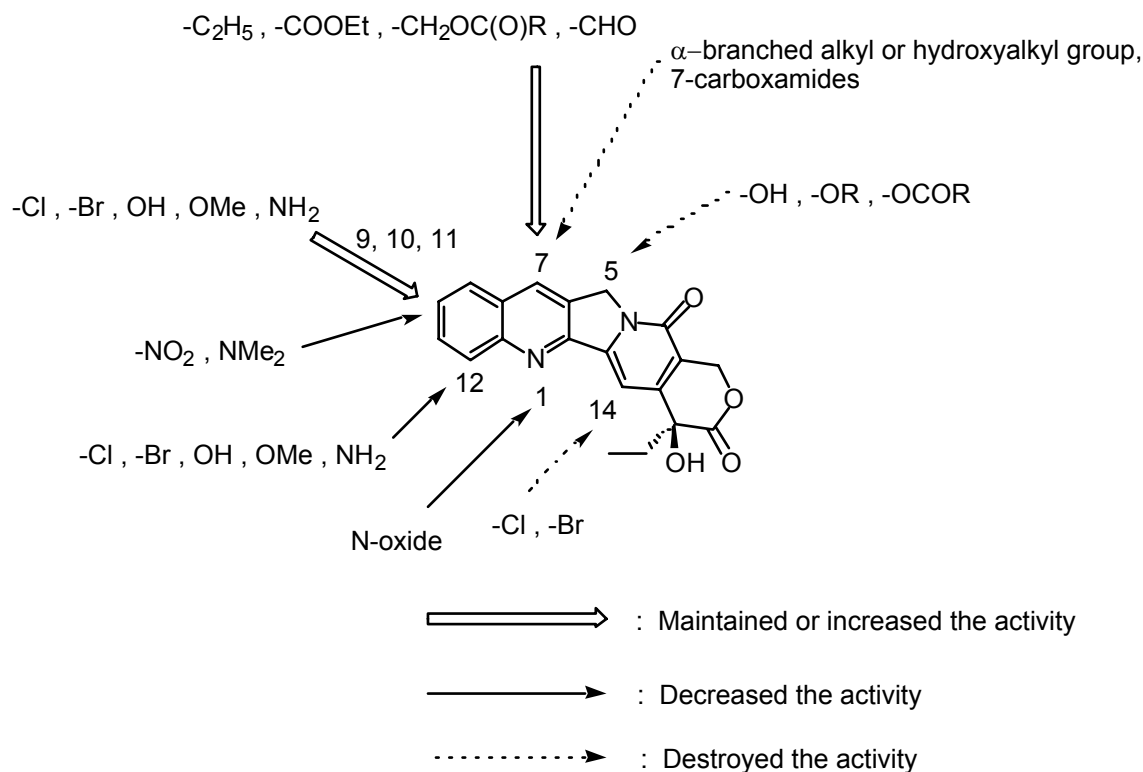


Figure 1.2 Structure-Activity Relationships of various CPT derivatives (adapted from ref. 10)

Two analogs of CPT, topotecan (Hycamptin[®], Smithkline Beecham) and irinotecan (Camptosar[®], Pharmacia-Upjohn), have been approved by the Food and Drug Administration (FDA) for clinical use in the United States. Topotecan is used for the treatment of cisplatin-refractory ovarian carcinoma and for second-line therapy in small-cell lung cancer (SCLC) and irinotecan is used for the treatment of colorectal cancer.¹¹

Recently, Stewart and co-workers reported the X-ray crystal structure of human topoisomerase I covalently joined to double-stranded DNA and bound to topotecan, a clinically approved analog of camptothecin (Figure 1.3).¹² This crystal structure explains a number of structure-activity relationships of the camptothecin family of anticancer drugs. The ternary complex demonstrated that topotecan intercalates at the site of DNA cleavage and is stabilized by base-stacking interactions with both the upstream and the downstream base pairs. The

topotecan, in effect, mimics a DNA base pair and occupies the same space as a base pair in the structure without the drug bound.

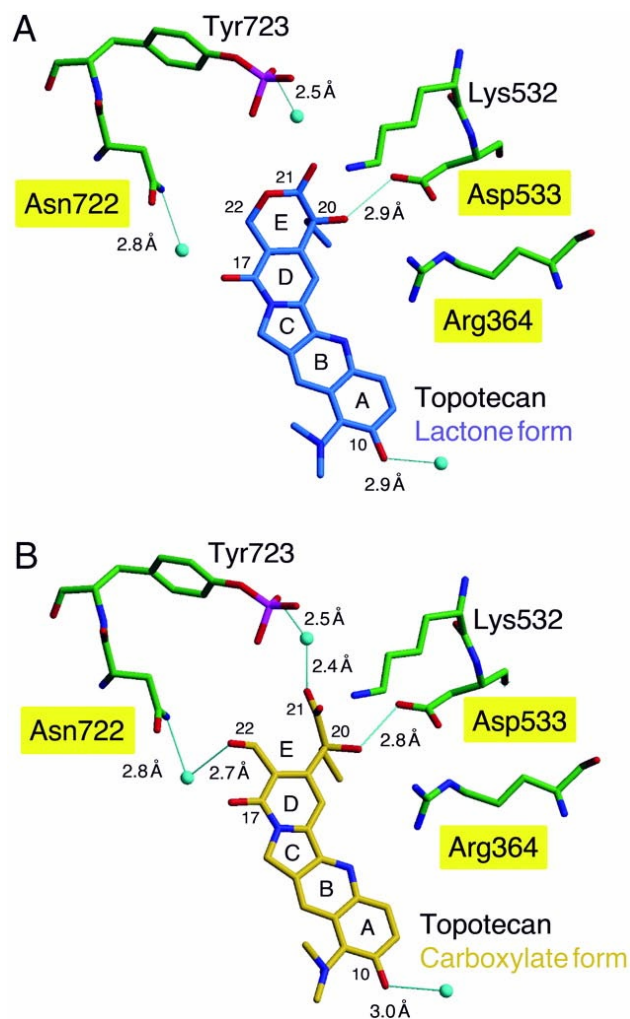


Figure 1.3 Topotecan Binding as the (A) Closed Lactone and (B) Open Carboxylate (reproduced from ref. 12)

The high functional group tolerance demonstrated at positions 7, 9 and 10 positions of CPT could also be explained because these positions face into the major groove of the DNA and modifications that improve solubility, stability etc. would not sterically interfere with the binding of the drug. Also, only one direct hydrogen bonding (20S hydroxyl hydrogen bonds to Asp 533) between the enzyme and topotecan was predicted by the structure model. The SAR studies have

also concluded that 20*R* enantiomer was biologically inactive *in vitro*. This is because, according to the model, the 20*R*-hydroxyl would not be able to contact Asp 533 to participate in the hydrogen bonding and the 20*R*-ethyl group would create a steric hindrance with Asp 533 and Lys 532.

The substitution of hydroxyl group with hydrogen atom (20-deoxy analog) would eliminate hydrogen bonding thus making the analog biologically inactive. Chloro or bromo substitution at the C20 position only partially eliminates the biological activity unlike the case of 20-deoxy analog. This is because the E-ring opening to the carboxylate form is still allowed in the halocamptothecins and therefore water-bridged contacts of the 22-hydroxyl to Asn-722 and 21-carboxylate oxygen to the P-Tyr-723 in the carboxylate model are still allowed. The lactam modification is also inactive due to the change in the hydrogen bond acceptor (OH) to a hydrogen bond donor (NH). Homocamptothecins are potent topo I poisons because the model reveals that there is sufficient space within the binding pocket to accommodate the slightly larger E-ring and the 20*S*-hydroxyl and the hCPT could maintain the critical Asp 533:20*S* hydroxyl hydrogen bonding.

Several novel analogs of CPT have promising activity and are presently undergoing preclinical development. Some of them include exatecan (DX-8951f), rubitecan (9-NC), 9-aminoCPT, lurtotecan (Figure 1.4).^{11,3e,h,i,j}

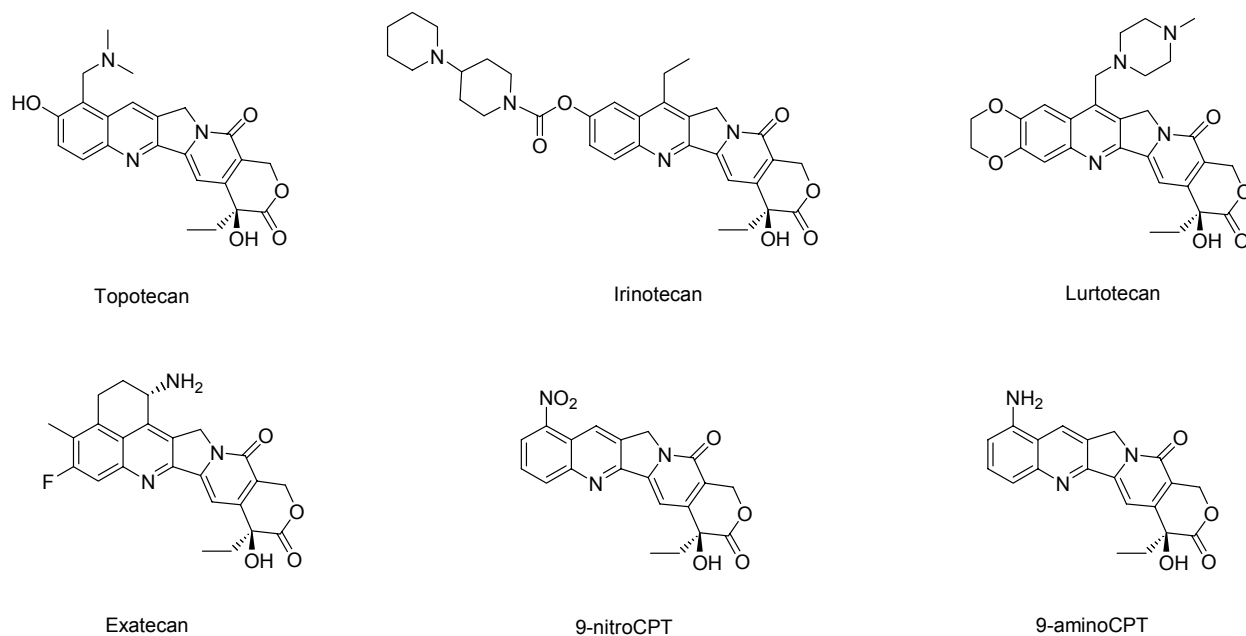
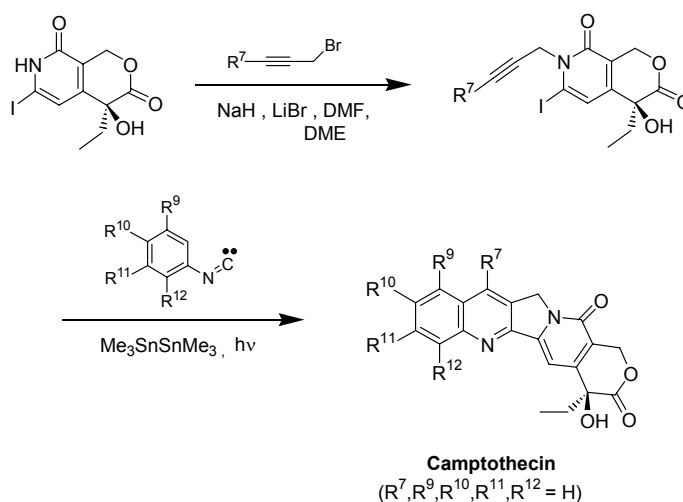


Figure 1.4 Various clinically relevant CPT analogs

1.4. Various Total Syntheses of CPT

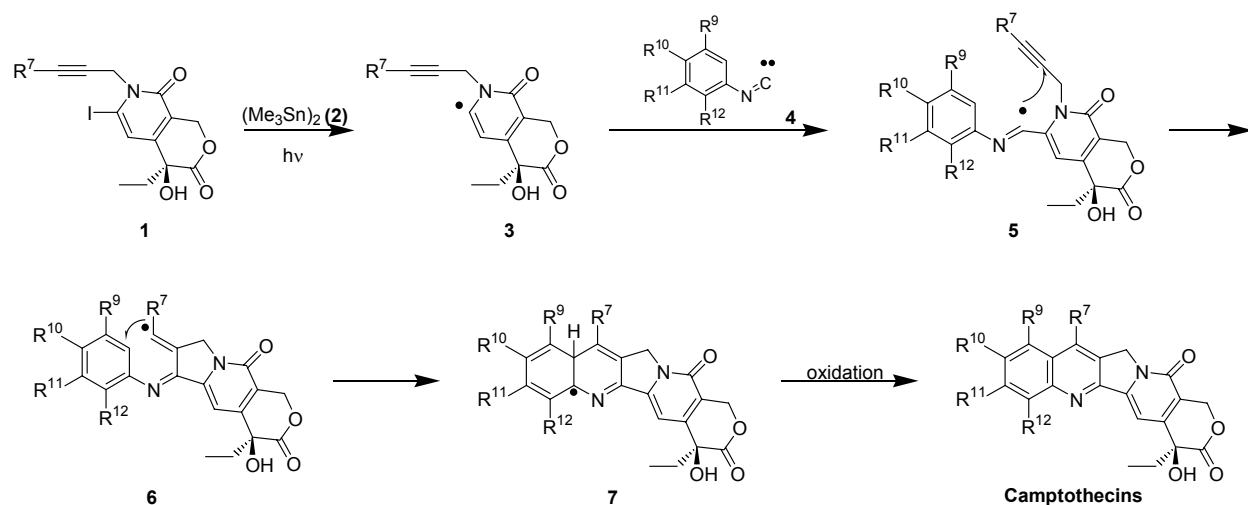
Owing to the promising antitumor activity of CPT, many synthetic strategies have evolved over the last 3 decades aimed at preparing camptothecin.³ⁱ The total syntheses published thus far have focussed mainly on the synthesis of camptothecin itself, in both racemic and enantiopure forms. While several research groups have contributed to the synthesis of racemic CPT,¹³ the first synthesis of (*S*)-CPT was reported by Corey in 1975.¹⁴ This was followed by a host of total syntheses of (*S*)-CPT by Vollhardt, Wani and Wall, Tagawa, Comins and Ciufolini involving either a resolution strategy or an asymmetric synthesis.¹⁵ In 1996, Fortunak reported a novel intramolecular [4+2] cycloaddition strategy for the synthesis of (*S*)-CPT.^{15f} More recently, Snieckus and coworkers reported a convergent synthesis of the ABCD ring system of camptothecin using a combination of directed ortho metalation and Negishi cross-coupling reactions.^{15g}

Most of these syntheses are not amenable to the preparation of a wide variety of known and new CPT analogs. The radical cascade cyclization strategy in the synthesis of CPT developed in the Curran group¹⁶ (Scheme 1.3) stands as an elegant example in overcoming this problem. This strategy, in addition to being modular in nature, is tolerant to a variety of functional groups present in the molecule.



Scheme 1.3 [4+1] Radical Cascade Cyclization Strategy

The key [4+1] radical annulation step is interesting because the pentacyclic skeleton in CPT is assembled in this step by the coupling of DE fragment (iodopyridone) **1** and the A-ring (isonitrile) **4** in one single reaction by a tandem radical cyclization. The accepted mechanism of this [4+1] radical annulation/cyclization reaction is shown below (Scheme 1.4).



Scheme 1.4 Mechanism of the cascade radical cyclization

Pyridonyl radical **3** is formed upon irradiation of **1** in the presence of hexamethylditin **2**. Addition of **3** to the isonitrile **4** gives the corresponding iminoyl radical **5**. This iminoyl radical undergoes a 5-*exo* radical cyclization to give the vinyl radical **6**. Radical **6** adds on to the aromatic ring to give the cyclohexadienyl radical **7**, which oxidatively rearomatizes to give the CPT skeleton. The synthesis of several analogs by this radical cascade cyclization approach is a testimony to the mildness and generality of the strategy.

Shibasaki and coworkers have shown that the key iodopyridone intermediate in the Curran synthetic strategy of CPT could be obtained via an enantioselective cyanosilylation of a suitable ketone.¹⁷ More recently, Hecht and coworkers¹⁷ reported water-soluble camptothecin derivatives, 20-*O*-phosphate and phosphonates, that have inhibited topo I in an enzyme-dependent fashion.¹⁸ Husson and coworkers synthesized racemic 17-methylcamptothecins by a partial synthesis starting from ajmalicine via a sequential oxidation steps and E-ring functionalization.¹⁹

1.5. Silatecans

Originally, camptothecins were administered *in vitro* necessitating the water solubility of the drug. However, Knight and coworkers have shown that certain drugs delivered to the respiratory tract in a liposome formulation may have significant advantages over other modes of administration.^{6f} Also, Burke and coworkers found out that increased lipophilicity of the analogs reduces the *in vivo* hydrolysis of the lactone form of CPT, leading to its improved blood stability without any loss in activity.^{6e} This is thought to be due to a rapid intracellular drug accumulation and tissue distribution that favors lactone stabilization. Hence, in search of better drug candidates, it might prove to be beneficial to test for lipophilic analogs of CPT.

To test the effect of lipophilic analogs, a project aimed at developing various lipophilic analogs of CPT was undertaken in the Curran group in mid 1990s. During the course of these collaborative investigations with the late Prof. T. G. Burke and coworkers (University of Kentucky), it was found that silyl substitution at the 7-position of CPT increased the lactone concentration in the blood.²⁰ This family of camptothecin analogs is now commonly referred to as *silatecans*.

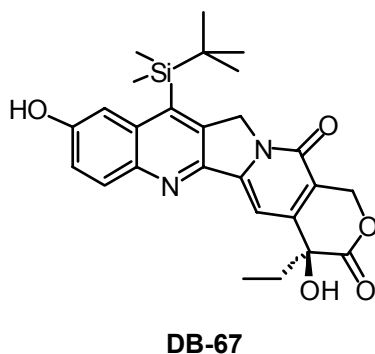


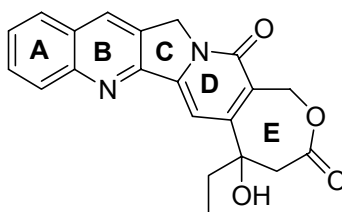
Figure 1.5 Structure of DB-67

Amongst all the silatecans synthesized, DB-67 showed the most promise. DB-67 (Figure 1.5) displayed superior human blood stability when compared to topotecan, irinotecan and many other clinically relevant CPT analogues. DB-67 showed 25-fold increase in lipophilicity compared to CPT and is incorporated quite readily as the lactone form into cellular and liposomal bilayers. Accordingly it was found to possess comparable potency relative to CPT, topotecan and irinotecan.

More recently, work by Merlini and Zunino shows that lipophilicity is the main parameter correlated to cytotoxicity in the QSAR analysis of novel 7-oximinomethyl substituted camptothecins.²¹

1.6. Homocamptothecin and Homosilatecans

The α -hydroxy- δ -lactone functionality in the E-ring was thought to be crucial for the activity of camptothecins. However, the discovery of homocamptothecin by Lavergne and Bigg in early 1997 (Figure 1.6) showed that alteration of the E-ring is possible while still maintaining the biological activity.²²



Homocamptothecin

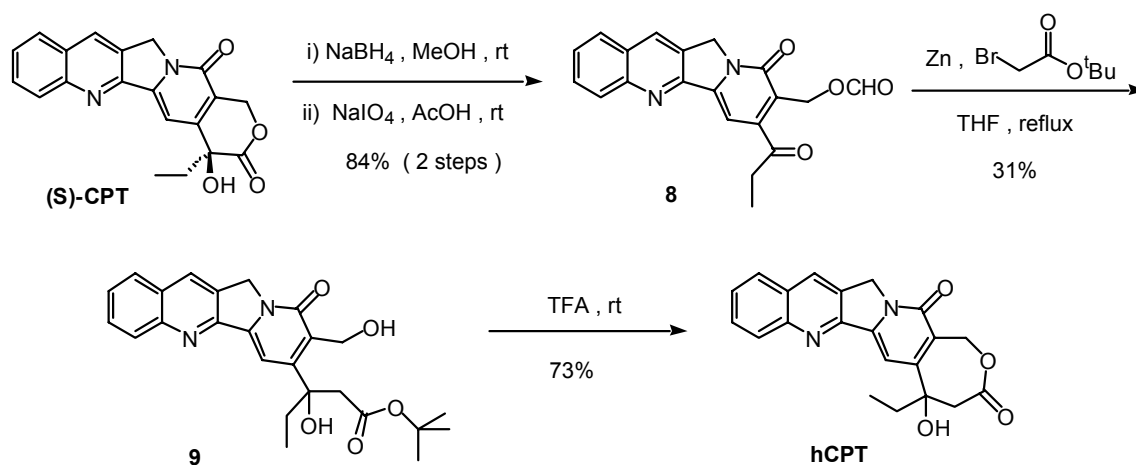
Figure 1.6 Structure of Homocamptothecin

Homocamptothecin (hCPT) is an E-ring expanded analog of CPT. Structurally, this is the result of homologation of the α -hydroxy- δ -lactone of CPT by one methylene group thereby

converting it into a β -hydroxy- δ -lactone. The advantage of hCPT over CPT is that the lactone is much less reactive (although not completely unreactive) due to the methylene spacer and hence less prone to any nucleophilic attack that might lead to the formation of the inactive open carboxylate form.

Homocamptothecin was synthesized by Lavergne and Bigg by a semi-synthetic approach (Scheme 1.5).²² Commercially available (**S**)-CPT was reduced with NaBH₄ to the corresponding hydroxy lactol followed by an oxidative cleavage of the 1,2-diol with NaIO₄ to give achiral ketone **8**. This was subjected to a Reformatsky reaction with *tert*-butyl bromoacetate to give racemic **9** after an aqueous workup. Finally, **9** was converted to racemic hCPT (BN 80245) by treatment with TFA at room temperature.

During the biological evaluation, hCPT was found to inhibit topo I mediated DNA relaxation with an activity comparable to that of CPT and, in addition, proved to be considerably more active (IC₅₀ = 16.2 nM) in cell growth inhibition than both CPT (IC₅₀ = 126 nM) and topotecan (IC₅₀ = 601 nM) in the MTT assay.

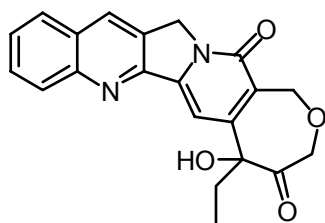


Scheme 1.5 Lavergne and Bigg's semisynthetic approach to racemic hCPT

Hence, on the one hand, CPT analogues with more lipophilic character (the silatecans, e.g., DB-67) help increase its potency and, on the other hand, homologation of the E-ring in CPT also leads to a more potent system than the parent CPT itself. It could be surmised that incorporation of both these features in an analog could lead to greater activity. This led to the development of 7-silylhomocamptothecins or *homosilatecans*.

Indeed, the homosilatecans have displayed markedly enhanced human blood stabilities relative to clinically relevant CPT analogs and are the most blood stable camptothecins to date.²⁰ The homosilatecans showed greater than 80% lactone levels following three hours of incubation in the human blood which is much greater than those exhibited by CPT (~5%) under the same conditions. Also the IC₅₀ cytotoxicity values of the homosilatecans against MDA-MB-435 tumorigenic metastatic human breast cancer cells were in the range of 20-100 nM.²³

Recent work in the Curran group focused on the development of new non-lactone analogs of CPT that might potentially be active and better drug candidates. As part of this work, a novel α -hydroxy keto-ether E-ring analog of CPT and hCPT, **Du1441**, was synthesized and biologically evaluated (Figure 1.7).²⁴



Du1441

Figure 1.7 Structure of Du1441

This analog combines the α -hydroxy carbonyl moiety of CPT with the seven-membered E-ring of hCPT. Despite these similarities, Du1441 was inactive in the preliminary biological

studies. However, the search for non-lactone analogs continues because it has been suggested by current biological and computational studies that the lactone moiety is not opened during the binding of CPT to the topo-I-DNA complex leading to loss of any activity.

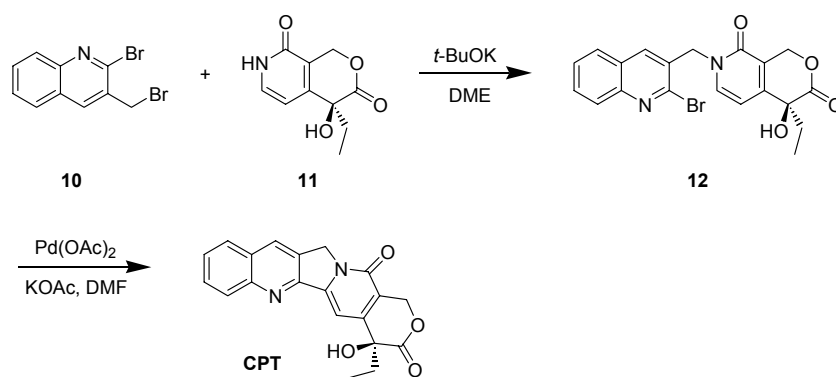
Homocamptothecin can be prepared by semi-synthetic approaches starting from commercially available (*S*)-CPT. However, these approaches are limited to the synthesis of the parent hCPT and a limited set of analogs. In contrast, a total synthesis broadens the scope in preparing a wider variety of analogs. A total synthesis of racemic hCPT was accomplished in late 1990s by Lavergne and Bigg and coworkers.²⁵ An asymmetric total synthesis of (*R*)-hCPT was developed recently in the Curran group which provided access to many of its analogs. In an effort to develop an asymmetric strategy to the synthesis of the key DE-fragment in the Lavergne-Bigg synthesis of hCPT, the Curran asymmetric strategy of synthesis of (*R*)-hCPT was employed successfully. The following chapter describes this synthesis after an introduction to the Lavergne-Bigg synthesis of racemic hCPT.

2. ASYMMETRIC SYNTHESIS OF LAVERGNE-BIGG DE FRAGMENT OF (*R*)-hCPT

2.1. Introduction

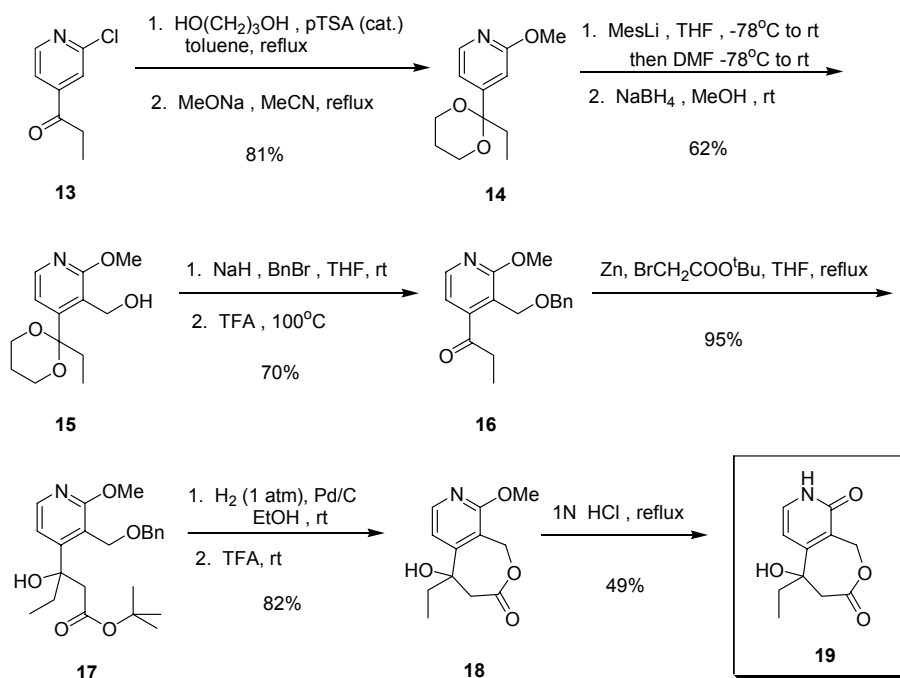
Homosilatecans have showed markedly enhanced human blood stabilities and cell growth and topo I inhibitory activity compared to CPT, topotecan and irinotecan. This biological activity is exhibited by only one enantiomer of hCPT. The absolute configuration of this enantiomer was initially postulated to be *R* on the presumption that CPT and hCPT have the same spatial arrangement of atoms at the stereocenter based on the stereospecific Topo I inhibition and positive rotation of polarized sodium D light. This postulate was later confirmed by the X-ray crystal structure analysis of the quinidium salt of (*R*)-**23** (see Scheme 2.4).²⁷ The biologically active counterpart of (*S*)-CPT is therefore (*R*)-hCPT, because homologation of the lactone changes the substituent priority according to the CIP nomenclature.

Lavergne and Bigg achieved a concise semi-synthesis of racemic hCPT from CPT (see Scheme 1.5, Chapter 1). Following this, they disclosed the total synthesis of racemic hCPT in 1998.²⁰ The construction of the hCPT skeleton in this synthesis was based on Comins' strategy of CPT synthesis:^{11e} N-alkylation of **11** with bromide **10** with ^tBuOK/DME and subsequently closing the C ring in **12** by a Heck coupling reaction to give camptothecin (Scheme 2.1). Comins' strategy was attractive because of the convergent nature of the synthesis and the ready access to various substituted quinolines.²⁶



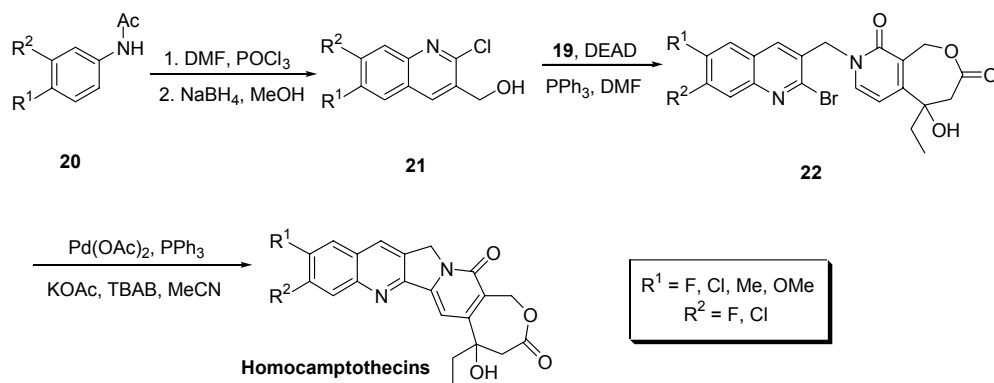
Scheme 2.1 Comins' strategy of synthesis of the CPT skeleton

The Lavergne-Bigg synthesis of the DE-fragment **19** in the synthesis of hCPT is shown in Scheme 2.2. Protection of the pyridine ketone **13** as a ketal (not shown) followed by treatment with NaOMe in acetonitrile under reflux conditions gave substitution product **14**. Methoxypyridine **14** was formylated by treatment with mesityllithium, followed by trapping of the resultant anion with DMF. The resulting aldehyde (not shown) was subsequently reduced by NaBH₄ to the primary alcohol **15**. This was then protected as the benzyl ether and the ketone was deprotected with TFA to afford **16**. Reformatsky reaction of ketone **16** with *t*-butylbromoacetate under reflux conditions gave **17**, which was debenzylated by catalytic hydrogenolysis and the resulting primary alcohol was subsequently lactonized by treatment with TFA to afford **18**. The pyridine lactone **18** was finally demethylated in HCl under reflux conditions to give the desired DE pyridone-lactone **19** in 13% overall yield.



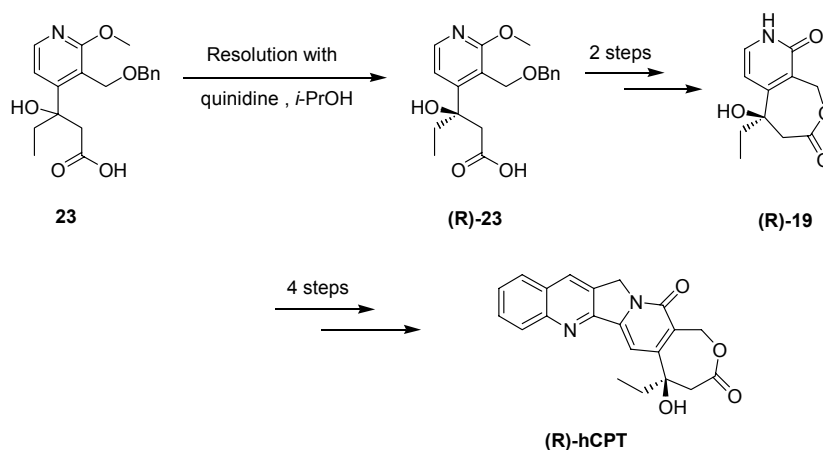
Scheme 2.2 Lavergne-Bigg synthesis of DE fragment of racemic hCPT²²

To make hCPT AB-ring analogs, various substituted quinolines were prepared by the Meth-Cohn protocol (Scheme 2.3).²¹ Acetanilides **20** were subjected to Vilsmeier conditions to give the intermediate 2-chloro-3-quinolinecarboxaldehydes (not shown). These aldehydes were reduced with NaBH₄ to give AB quinolines **21**. DE fragment **19** and the AB quinolines **21** were coupled together by a Mitsunobu reaction to give **22**. Finally an intramolecular Heck reaction of **22** afforded the pentacyclic racemic homocamptothecins.



Scheme 2.3 Final steps in the Lavergne-Bigg synthesis of racemic hCPT

Lavergne and Bigg subsequently reported a total synthesis of (*R*)-hCPT by using a chemical resolution strategy (see Scheme 2.4).²⁷ The Reformatsky adduct **17** was converted to the acid **23** by treatment with TFA (not shown). β -Hydroxy acid **23** was resolved with quinidine to give the desired (*R*)-enantiomer (***R***-**23**) in 70% ee. This was subsequently converted to the pyridone (***R***-**19**) in two steps (Scheme 2.4). Recrystallization of (***R***-**19**) increased the ee to >99% which in 4 steps gave (***R***)-hCPT.



Scheme 2.4 Resolution strategy in Lavergne-Bigg synthesis of (*R*)-hCPT

A major drawback of a resolution strategy in the preparation of enantiomerically pure compounds is that the maximum chemical yield cannot exceed 50%. This is unattractive from a practical standpoint especially when large quantities of the compound are required for biological evaluation. An efficient asymmetric total synthesis could surpass the limitations posed by both the semi-synthetic as well as the resolution strategies.

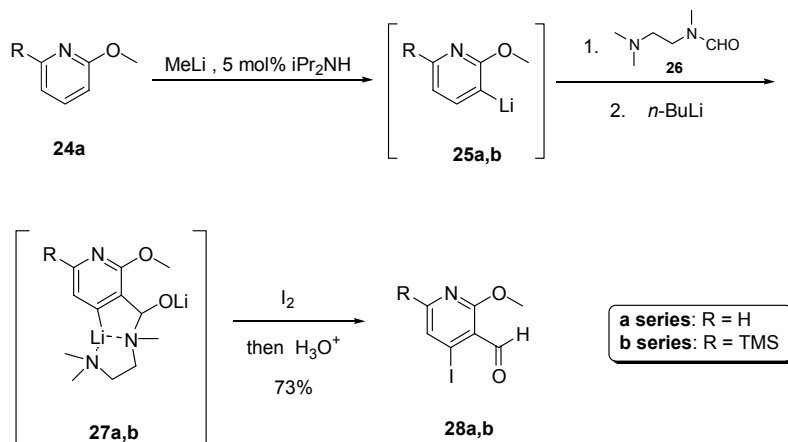
Recently, the first asymmetric synthesis of (*R*)-hCPT developed in the Curran group by Dr. A. E. Gabarda provided access to a number of its analogs in >90% ee (see Schemes 2.7 & 2.9: **b series**).²⁸ The key bond constructing steps involved Corey modified Stille coupling reaction²⁹ and Sharpless asymmetric epoxidation.³⁰ Thus iodopyridine **30b** was treated with vinyl stannane **31** in the presence of LiCl, CuCl and Pd(PPh₃)₄ in DMSO and the reaction mixture heated to 60°C to afford the Stille product **32b** in 80% yield. The α,β -unsaturated ester **32b** was readily reduced to the allylic alcohol **33b** by treatment with LAH. Stoichiometric Sharpless asymmetric epoxidation on **33b** gave the epoxide **34b** in 79% yield and 90% ee. No reaction was observed when catalytic amounts of Ti(OiPr)₄ and diethyltartrate were used. Epoxide **34b** was then converted to lactone (**R**)-**39** in 6 steps.

We set out to apply the asymmetric approach to the preparation of the key DE-fragment of the Lavergne-Bigg synthesis of (*R*)-hCPT in a highly enantiopure form.

2.2. Asymmetric Synthesis of the Lavergne-Bigg DE Fragment

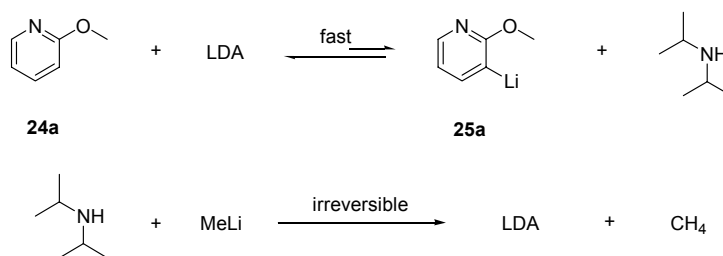
In accordance with Dr. Gabarda's strategy, the asymmetric synthesis of the Lavergne-Bigg DE fragment commenced with the iodoformylation of 2-methoxypyridine **24a** (Scheme 2.5). Iodoformylation was performed following Comins' *ortho*-directed metallation protocol.^{11e} For this, pyridine **24b** was *ortho*-lithiated by *t*-BuLi. Then addition of the formamide **26** followed

by addition of *n*-BuLi and subsequently I₂ gave aldehyde **28b**. However, this procedure cannot be used with pyridine **24a** because of the likelihood of competitive lithiation with butyllithium at the 6-position of the pyridine ring.³¹ This was not a concern with pyridine **24b** because of the blocking provided by the TMS group at the 6-position.



Scheme 2.5 Initial iodoformylation reactions with 24a and 24b

Quéguiner and coworkers have reported the selective ortho lithiation of 2-methoxypyridine at the 3-position by using methyllithium in the presence of catalytic amounts of diisopropylamine.³² Scheme 2.6 shows the proposed roles of LDA and methyllithium in this reaction..



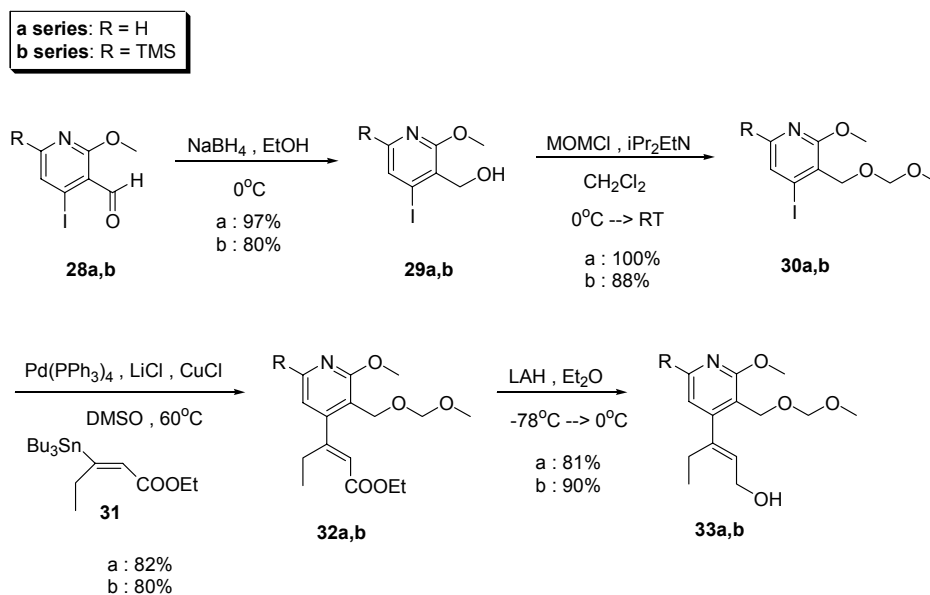
Scheme 2.6 Quéguiner's strategy of selective ortholithiation of 2-methoxypyridine

Reaction of 2-methoxypyridine **24a** with 1.8 equiv of MeLi in the presence of catalytic amounts of diisopropylamine results in a fast overall deprotonation to give **25a**. The small amount of diisopropylamine generated reacts irreversibly with MeLi allowing constant regeneration of a small concentration of LDA, which shifts the equilibrium in favor of the lithio derivative **25a**. This leads to an accumulation in the concentration of **25a** before the electrophile is added.

Based on this literature precedent, we treated 2-methoxypyridine **24a** with methyllithium in the presence of 5 mol% of diisopropylamine. The resultant 3-lithio derivative was quenched with the formamide **26** to afford only the 3-formyl derivative (not shown). We then attempted the one-pot iodoformylation via this strategy as shown in Scheme 2.5.

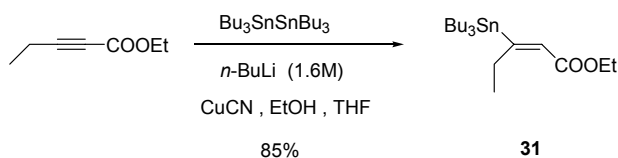
Treatment of 2-methoxypyridine **24a** with methyllithium in the presence of 5 mol% of diisopropylamine was followed by addition of formamide **26**. *n*BuLi was then added to this followed by addition of I₂ to afford iodo aldehyde **28a**. On a 1 mmol scale, **28a** was obtained in 73% yield after purification by column chromatography. The yield suffered, however, when the scale was raised to 19 mmol when only 40% product was isolated. Trapping of the initial lithio derivative **25a** with the formamide **26** gave the α -amino alkoxide *in situ* (not shown). This, on addition of *n*-BuLi, resulted in the dianion **27a** which on reaction with I₂ gave the iodo aldehyde **28a**. Aldehyde **28a** was reduced by NaBH₄ to the corresponding alcohol **29a** in 97% yield

(Scheme 2.7). This was subsequently protected as a MOM ether using the standard protocol³³ to afford **30a** in quantitative yield. Intermediates **29a** and **30a** were used crude in the subsequent reactions.



Scheme 2.7 Preparation of the Sharpless asymmetric epoxidation precursor

The necessary (E)-vinylstannane **31** for the Stille coupling was prepared by the procedure previously published by Piers and coworkers³⁴ (Scheme 2.8). Reaction of the lithium(tributylstannyl)cyanocuprate (formed from treatment of Bu_6Sn_2 with $n\text{-BuLi}$ followed by addition of CuCN) with commercially available ethyl 2-pentynoate at -78°C in THF gave the vinylstannane **31** in 85% yield after distillation at 140°C under a pressure of 0.06 mm Hg.

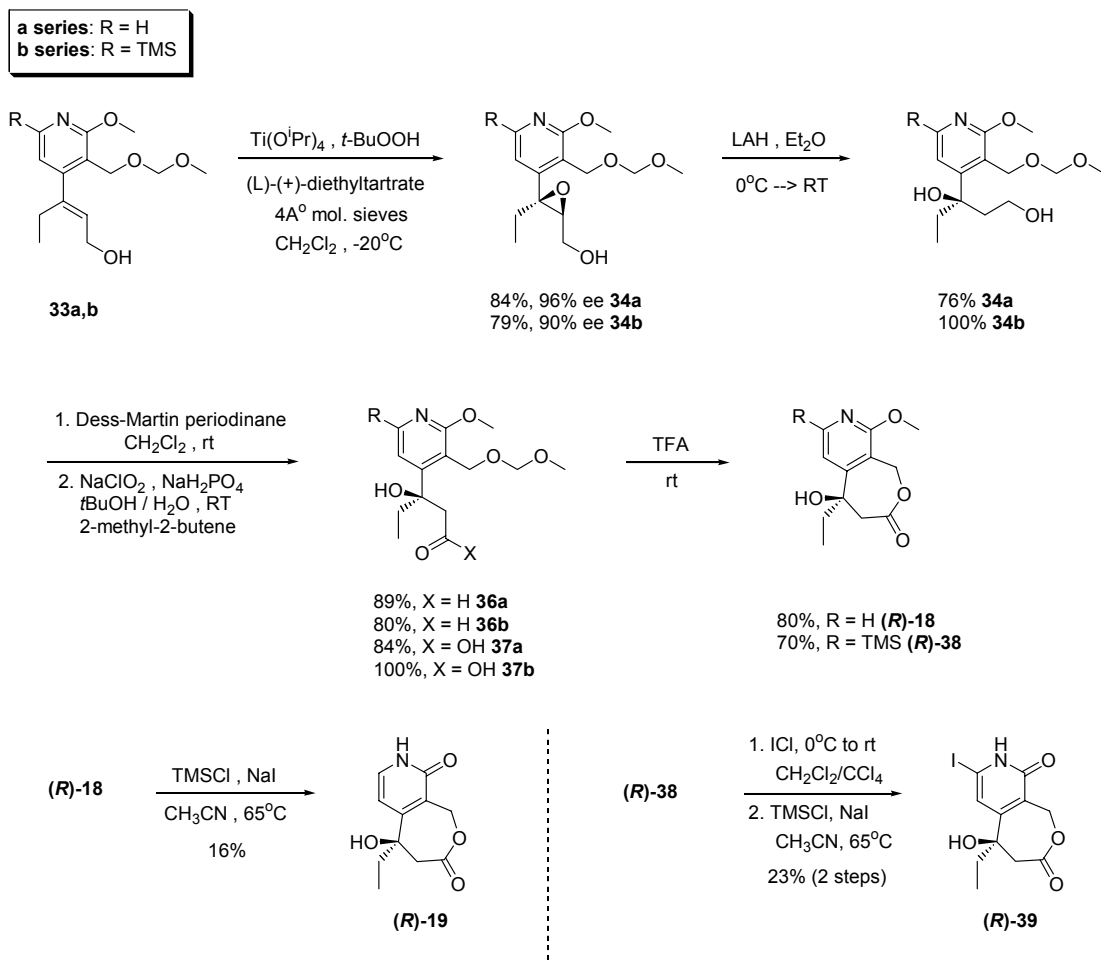


Scheme 2.8 Preparation of ethyl (E)-3-(tributylstannyl)-2-pentenoate

Stille coupling was achieved by first degassing the reaction vessel containing the mixture of LiCl, Pd(PPh₃)₄ and CuCl under high vacuum followed by an Ar purge (Scheme 2.7). Then DMSO, iodopyridine **30a** and the vinylstannane **31** were added and the resulting mixture was degassed by the freeze-thaw process. The mixture was stirred at room temperature for 1 h and then at 60°C for 17 h to afford the Stille product **32a** in 82% yield after column chromatography. The α,β -unsaturated ester **32a** was readily reduced to the allylic alcohol **33a** in 81% yield by treatment with LAH.

Sharpless asymmetric epoxidation (SAE) was successfully carried out on the allylic alcohol **33a** (Scheme 2.9). Keeping in mind the poor results with catalytic SAE during the epoxidation studies in the preparation of (*R*)-hCPT and the subsequent success with the stoichiometric version, only the stoichiometric SAE was attempted.

Thus, *t*BuOOH was added to a mixture of the allylic alcohol **33a**, 4Å molecular sieves, diethyl-L(+)-tartrate and Ti(O^{*i*}Pr)₄ at -20 °C in CH₂Cl₂. After 24 h at room temperature, the reaction was worked up, giving the epoxide **34a** in 84% crude yield. The racemic epoxide was simultaneously prepared from reaction of the allylic alcohol **33a** with mCPBA (not shown). Chiral HPLC analysis (using Chiralcel-OD column) of the epoxide **34a**, with the racemate as the standard, showed the enantiomeric excess to be 96%.



Scheme 2.9 Completion of the asymmetric synthesis of (R)-19 and (R)-39

Epoxide **34a** was then converted to the β -hydroxy carboxylic acid **37a** in three steps with no purification of the intermediates. Reaction of epoxide **34a** with LAH resulted in the regioselective opening of the epoxide to give **35a** in 76% yield. Diol **35a** was then oxidized to the aldehyde **36a** with Dess-Martin periodinane.³⁵ The resultant aldehyde was further oxidized to the β -hydroxy carboxylic acid **37a** using NaClO_2 in *t*-BuOH, buffered with an aqueous solution of NaH_2PO_4 in the presence of 2-methyl-2-butene in 75% crude yield (for 2 steps).

Treatment of this crude acid with TFA at room temperature resulted in an *in situ* deprotection of the MOM group followed by lactonization to give the pyridine lactone (**R**)-**18** in 80% yield. The crude product was used for the subsequent reaction.

Completion of the synthesis was effected by the demethylation of the pyridine lactone **(R)-18** by TMSI generated *in situ*, by the reaction of TMSCl and NaI in acetonitrile, at 65°C. The product, pyridone lactone **(R)-19**, was obtained in a low yield of 16%. No attempts of improving the reaction yield were made.

The enantiomeric excess of the lactone **(R)-19** was presumed to be 96% since no synthetic steps affecting the stereocenter at C20 were involved after the Sharpless asymmetric epoxidation step.

2.3. Summary

The asymmetric synthesis of the pyridone lactone **(R)-19**, a key intermediate in Lavergne and Bigg synthesis of (R)-hCPT, was described. The synthesis furnished the product in an overall yield of 2.9% and with 96% ee in 11 steps starting from 2-methoxypyridine **24a**. Sharpless asymmetric epoxidation and Corey-Stille coupling reactions, developed during the synthesis of (R)-hCPT, were utilized here for key bond constructions. The chemistry described in this chapter provides an easy access to the DE fragment thus establishing a direct route to the desired *R* enantiomer without having to resort to resolution strategies.

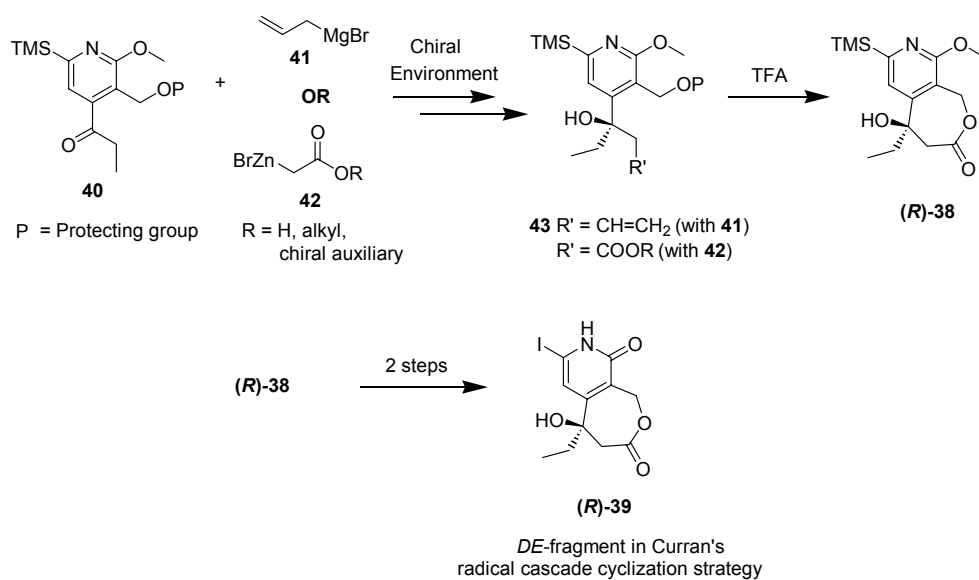
3. NEW ASYMMETRIC APPROACHES TO THE *DE*-FRAGMENT OF (*R*)-hCPT AND SYNTHESIS OF NON-LACTONE *E*-RING ANALOGS OF CPT

3.1. Introduction

The first asymmetric synthesis of (*R*)-hCPT developed in the Curran group has been used to produce several analogs in highly enantioenriched form (*ee* > 90%).²³ However, the synthesis employs stoichiometric quantities of the tartrate and Ti(O^{*i*}Pr)₄ for the Sharpless asymmetric epoxidation to establish the requisite stereocenter. This might be a drawback for large scale preparation of the epoxide. Furthermore, sixteen steps are required to synthesize (*R*)-hCPT and its analogs starting from 2,6-dibromopyridine and the overall yield is about 0.6%. Realizing the need for improvement, we decided to look for a practical alternative route to the synthesis of (*R*)-hCPT.

An attractive approach to synthesize the *DE*-fragment of (*R*)-hCPT (***R***-**39**) is to install the β-hydroxy carboxylic group via an asymmetric nucleophilic addition to the ketone **40** (Scheme 3.1). This approach is more direct and addresses the problems raised by the current synthesis.

The synthesis of enantioenriched tertiary alcohols by the addition of an organometallic reagent to prochiral ketones in the presence of a chiral catalyst is a formidable challenge. Several examples of preparing chiral tertiary alcohols in an indirect fashion (opening of an epoxide, C-H insertion into a secondary alcohol, etc.) are known.³⁶ Diastereo- and enantioselective nucleophilic additions to ketones and pyruvate esters to generate chiral tertiary alcohols have been reported.³⁷



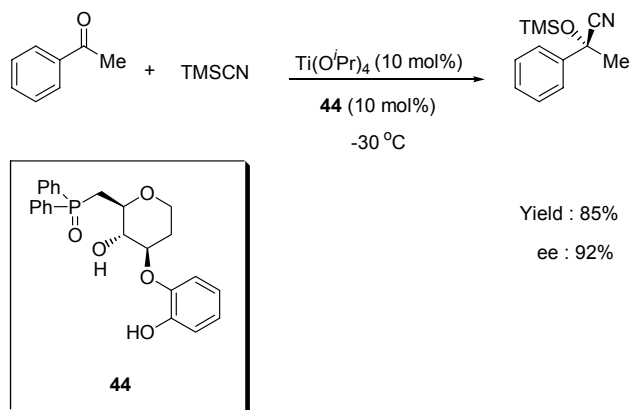
Scheme 3.1 Asymmetric Nucleophilic Addition Approach to Ketones Towards the *DE*-fragment of (*R*)-hCPT

We initially attempted two strategies to access **43**: (a) asymmetric allylation route, or (b) asymmetric enolate addition via the Reformatsky routes. Unfortunately, after considerable experimentation (Scheme 3.1) with the above methods following literature precedents, we failed to achieve satisfactory results.³⁸ This chapter deals with the variety of alternatives we attempted to achieve a more efficient synthesis of the *DE* fragment of (*R*)-hCPT and the unexpected results leading to the synthesis of a small assortment of non-lactone analogs of CPT.

3.2. Homologation Approaches to the Synthesis of the *DE*-Fragment of (*R*)-hCPT

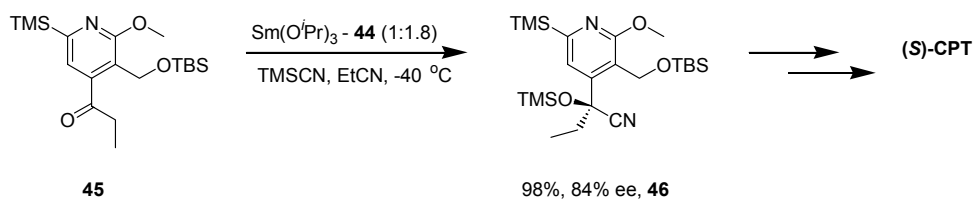
Asymmetric cyanosilylation reactions of ketones to give TMS-protected cyanohydrins have been studied by many research groups with Belokon, Deng, Hoveyda and Snapper making important contributions in this field.³⁹ Shibasaki and coworkers had recently reported an asymmetric cyanosilylation of ketones in the presence of catalytic amounts of the bifunctional catalyst **44** and Ti(O^{*i*}Pr)₄.⁴⁰ The reaction is general and affords TMS-protected cyanohydrins in

good enantioselectivities. An example of this reaction using Shibasaki's conditions is shown in Scheme 3.2.



Scheme 3.2 Shibasaki's catalytic enantioselective cyanosilylation of ketones

Following this work, Shibasaki and coworkers, in collaboration with Prof. Curran and Dr. Du, published the enantioselective synthesis of (*S*)-camptothecin with a modified version of the enantioselective cyanosilylation strategy¹³ (Scheme 3.3).

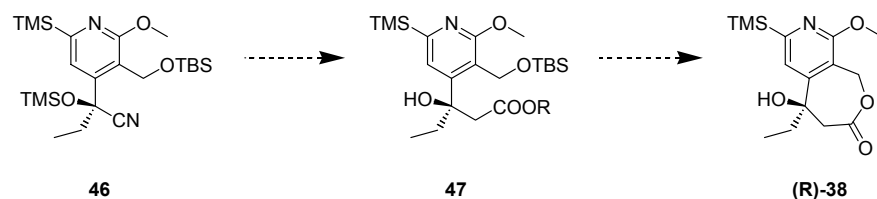


Scheme 3.3 Shibasaki's Enantioselective Cyanosilylation of Ketone 45

Ketone **45** was reacted with TMSCN in the presence of the ligand **44** (9 mol%, see Scheme 3.2) and $\text{Sm(O}^i\text{Pr)}_3$ (5 mol%) in propionitrile. The nitrile **46** was obtained in 98% yield and 84% ee.

In considering ways to synthesize the *DE*-fragment of (*R*)-hCPT, we realized that nitrile **46** could be used as an important intermediate. We envisioned a synthetic sequence in which **46**

or a derivative could be homologated by one carbon to the compound with the desired oxidation state **47**, which could then be carried forward to make the DE lactone of (*R*)-hCPT (Scheme 3.4).

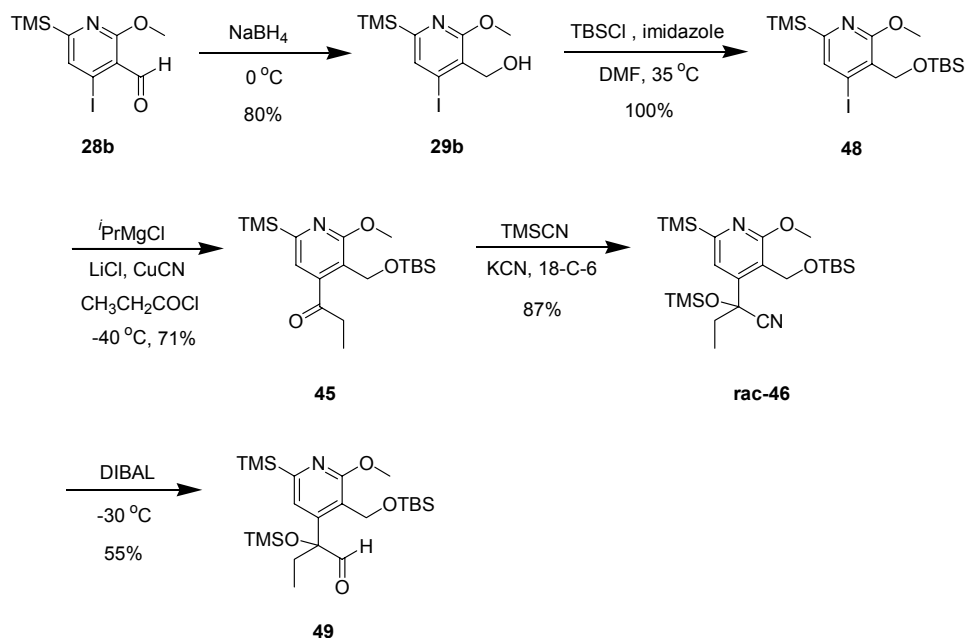


Scheme 3.4 Envisioned Synthesis of (*R*)-38 from Nitrile 46

A few methods have been reported to homologate nitriles to esters or other carboxylic acid derivatives (see Section 3.2.1.). Aldehyde **49** (Scheme 3.5) was determined to be best suited for the one-carbon homologation studies. We screened some of these known methods for reaction with the aldehyde **49**.

3.2.1. Synthesis of the Substrate **49** for Homologation Studies

The synthesis of the homologation precursor **49** was accomplished according to some of the methods developed in the Curran group. Reduction of aldehyde **28b** (Scheme 3.5, see also Scheme 2.7, Chapter 2) by NaBH₄ gave the alcohol **29b** in 89% yield. Protection of the crude alcohol **29b** as a TBS ether with Corey's procedure²⁹ gave **48** in quantitative yield. Iodopyridine **48** was then converted to the corresponding cuprate by treatment with ⁱPrMgCl followed by addition of LiCl and CuCN.⁴¹ The cuprate was quenched with propionyl chloride to provide the TBS-ketone **45** in 71% yield after purification by column chromatography.

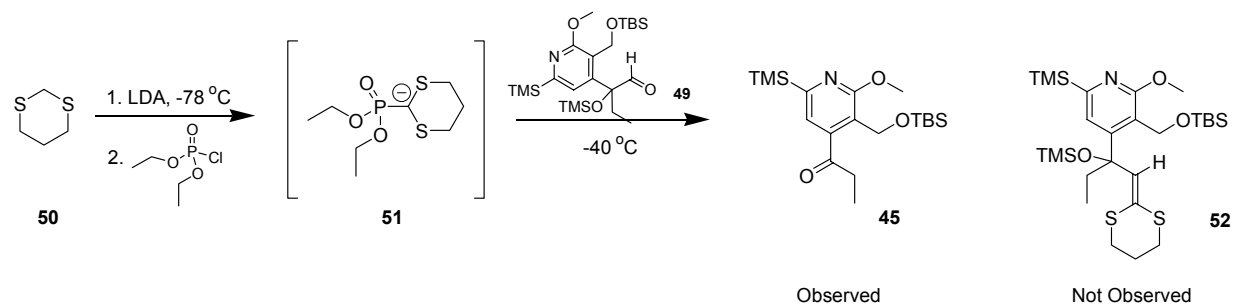


Scheme 3.5 Synthesis of the Homologation Substrate 49

This TBS-ketone was transformed to the corresponding TMS-protected cyanohydrin **rac-46** in 87% yield with TMSCN in the presence of KCN and 18-crown-6. Reduction of the nitrile **rac-46** to the aldehyde **49** took place upon reaction with DIBAL at $-30\text{ }^\circ\text{C}$ to afford **49** in 55% yield. Aldehyde **49** was used as the substrate for all the subsequent homologation studies.

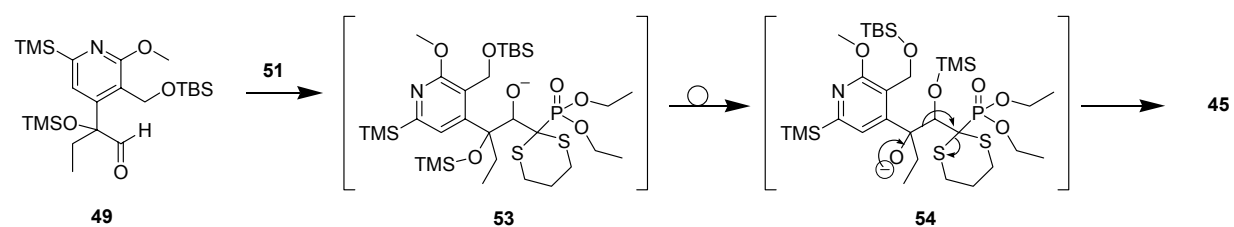
3.2.2. Attempted Homologation of 49 with 1,3-Dithiane derived Phosphonate

In the late 1970s, Jacobine and coworkers reported a procedure for one-carbon homologation of benzaldehyde by a modified Wittig reaction.⁴² Phosphonate esters were prepared by treatment of active methylene compounds with a suitable base and diethyl phosphorochloridate to form the corresponding olefins. We envisioned the use of 1,3-dithiane as the active methylene compound to afford our desired olefin **52** (Scheme 3.6), which upon acid treatment could be transformed to lactone **38** (see Scheme 3.4).



Scheme 3.6 Proposed Homologation of 49 with 1,3-Dithiane Derived Phosphonate 51

Accordingly, 1,3-dithiane **50** was treated with 2 equiv of LDA at $-78\text{ }^{\circ}\text{C}$. The resulting anion was treated with diethyl phosphorochloridate at the same temperature to presumably afford the phosphonate anion **51**. It was determined that 2 equiv of LDA was necessary since the product phosphonate is more acidic than the starting material **50**. The phosphonate anion **51** was then trapped with aldehyde **49** at $-40\text{ }^{\circ}\text{C}$. Unfortunately, the Wittig olefination product **52** was not observed as indicated by ^1H NMR analysis; instead, ketone **45** was formed. The structure of the product **45** was confirmed by spectroscopic techniques. A plausible mechanism for the formation of the ketone **45** is shown in Scheme 3.7.



Scheme 3.7 Proposed Mechanism for the Generation of 45 in the Homologation of 49 with 51

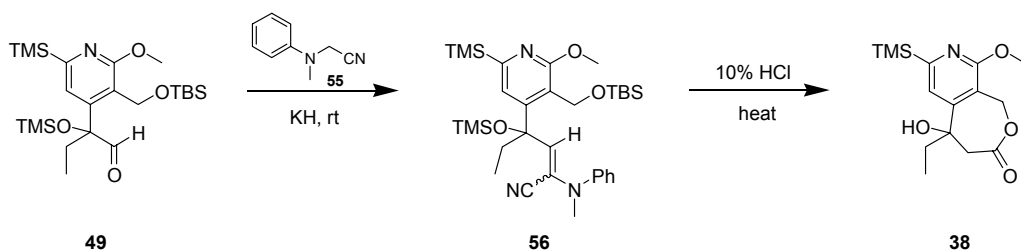
The addition of phosphonate anion **51** (see Scheme 3.6) to the aldehyde **49** results, presumably, in the formation of adduct **53**. This is expected to undergo a regular Wittig olefination by extruding the corresponding phosphate to give **52**. However, **53** undergoes a 1,4-

silyl shift to form the tertiary oxyanion **54**. This can now undergo a sequence of steps, as shown by the movement of arrows, to liberate ketone **45** and β -phosphato acetaldehyde (not shown).

Unfortunately, attempts to use a different base (e.g. *n*BuLi) or conduct the aldehyde addition at different temperatures (e.g. $-40\text{ }^{\circ}\text{C}$, $-15\text{ }^{\circ}\text{C}$) resulted in the formation of **45** and not **52**. We therefore decided to abandon this strategy in favor of a new one.

3.2.3. Attempted Homologation using α -Aminoacetonitriles

Takahashi and coworkers reported an interesting procedure for homologation of aldehydes to carboxylic acids in the early 1980s⁴³ employing α -(*N*-methylanilino)acetonitrile **55**. We expected that the reaction of **49** with **55** under Takahashi's reaction conditions would produce **56** (Scheme 3.8).



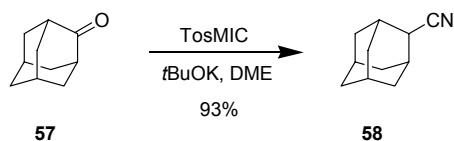
Scheme 3.8 Proposed Homologation of **49 with an Aminoacetonitrile **55****

Potassium hydride was added to a mixture of the aldehyde **49** and the α -aminoacetonitrile **55**⁴⁴ in THF at room temperature. However, no reaction occurred even after stirring overnight for 14 h as indicated by TLC. In this case, both the starting materials remained unaffected (Table 3.1). In an attempt to promote the addition, the reaction mixture was heated to $40\text{ }^{\circ}\text{C}$. This resulted in decomposition as indicated by TLC and ^1H NMR analysis.

Similar results were obtained when LDA or KHMDS in the presence of 18-crown-6 (1 equiv or 2 equiv) was used as the base at room temperature. When nitrile **55** was treated with LDA and the resulting anion was quenched with D₂O, a clean incorporation of deuterium in the alpha position of the nitrile was observed by ¹H NMR spectrum. This indicates that the anion addition of **55** to the aldehyde **49** is the problematic step.

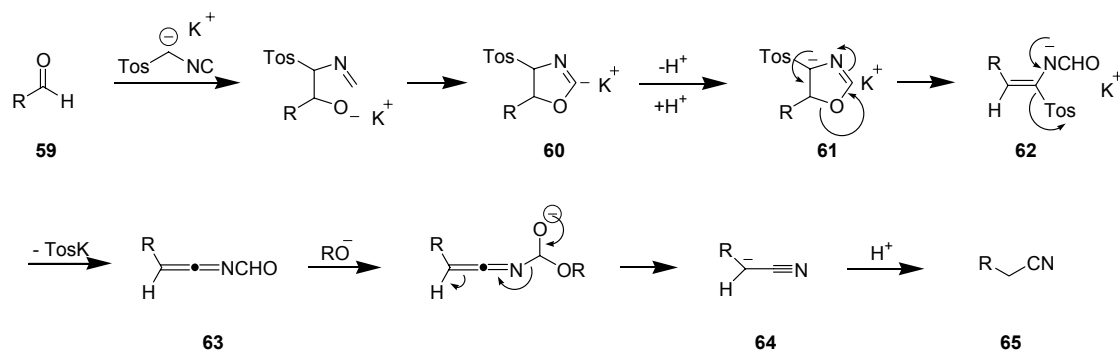
3.2.4. Attempted Homologation using Tosylmethyl Isocyanide (TosMIC)

The chemistry of tosylmethyl isocyanide (TosMIC) is well documented in the synthesis of heterocycles.⁴⁵ In 1977, van Leusen and coworkers used TosMIC as a homologating agent from carbonyl compounds to nitriles.⁴⁶



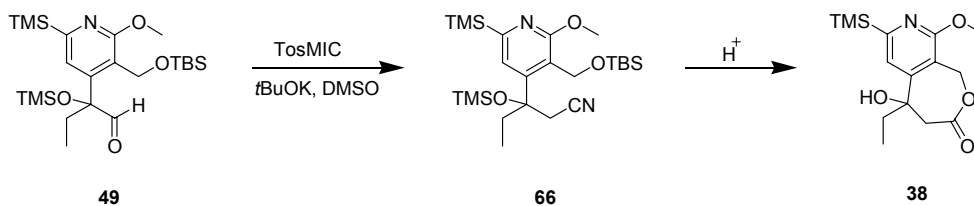
Scheme 3.9 Reaction of Adamantanone with TosMIC

For example, adamantanone **57** was reacted with 1.3 equiv of TosMIC in the presence of a strong base such as *t*BuOK to yield cyanoadamantane **58** in 93% yield. The proposed mechanism of the homologation of an aldehyde **59** with TosMIC is shown in Scheme 3.10. The key step of this reductive cyanation mechanism is the formation of the oxazoline anion **60** following by the opening of the rearranged oxazoline **61** to **62**. Formation of **63** from **62** is accompanied by the precipitation TosK. Hydrolysis of **63** with an alcohol leads to the cyano anion **64** along with the loss of formate ester and the resulting anion **64** is protonated to give the homologated nitrile **65**.



Scheme 3.10 Proposed Mechanism of Reaction of TosMIC with an Aldehyde

The proposed homologation procedure is shown in Scheme 3.11. Aldehyde **49** was added to the anion of TosMIC, generated by the treatment of TosMIC with a strong base such as *t*BuOK (1M solution in THF), and the reaction mixture was stirred at room temperature.



Scheme 3.11 Proposed Homologation of Aldehyde 49 with TosMIC

However, no conversion of the starting material **49** was observed as shown by TLC (entry 1, Table 3.2). Instead, some unidentifiable material was observed in the ^1H NMR spectrum. Suspecting the purity of *t*BuOK solution, we employed solid *t*BuOK under the same reaction conditions (entry 2). However, the result was identical to the previous case in that the same unidentifiable material was obtained.

Table 3.1 Homologation of Aldehyde 49 with TosMIC - Reaction Conditions

S. No.	Reagents	Solvent	Temp.	Comments
1.	<i>t</i> BuOK (liq)	DMSO	rt	Unidentified material
2.	<i>t</i> BuOK (solid)	DMSO	rt	Unidentified material
3.	<i>t</i> BuOK (solid)	DME	rt	45 (<10%) + unidentified mat.
4.	<i>t</i> BuOK (solid) + H ₂ O	DME	rt	No intermediate trapped
5.	NaOEt	DME	rt	Multiple spots on TLC
6. ^{a)}	<i>t</i> BuOK (solid)	DME	rt	45
7. ^{a)}	<i>t</i> BuOK (solid)	DME	0°C	45
8. ^{a)}	<i>t</i> BuOK (solid)	DME	-20°C	45

*

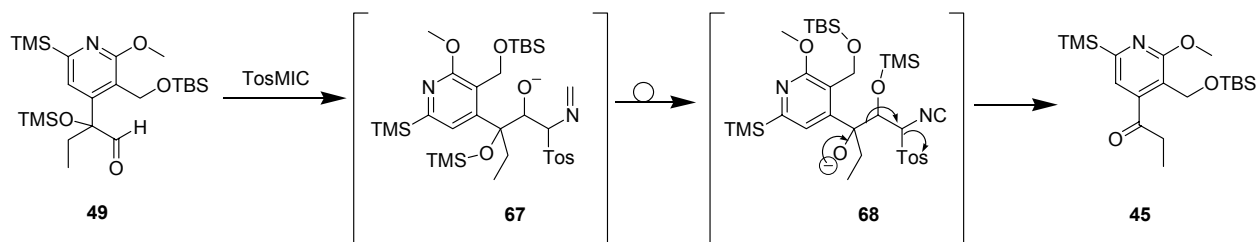
^{a)} These reactions were done using recrystallized TosMIC.

We next decided to explore the solvent conditions. van Leusen and coworkers used DMSO, DME and HMPT in the reaction. Using DME as the solvent (entry 3), we were surprised to observe ketone **45** by ¹H NMR, albeit in small amounts (<10%), along with a majority of unidentifiable material. In an effort to determine whether any intermediate compounds could be trapped, the reaction was repeated under the same conditions but quenched with H₂O (entry 4) which could, in principle, trap the oxazoline or any one of the intermediates formed. Unfortunately, the ¹H NMR spectrum of the crude product indicated the formation of multiple products and was not very informative. Changing the base to NaOEt (entry 5) resulted only in multiple products as indicated by TLC.

Suspecting the quality of TosMIC, we recrystallized it from MeOH. The recrystallized TosMIC was had a sharp melting point at 112°C (lit. 116°-117°C).⁴⁵ The purity of TosMIC was also confirmed by reacting cycloheptanone with TosMIC in the presence of *t*BuOK to afford cyanocycloheptane in 80% yield as reported.⁴⁶

The initial reaction of TosMIC with **49** in the presence of *t*BuOK was repeated with the purified TosMIC at room temperature, 0 °C and -20 °C (entries 6, 7 and 8). In all the three cases, ketone **45** was the sole product of the reaction.

The mechanism of the formation of **45** is presumed to be akin to that of the side reaction observed for the reaction of the 1,3-dithiane derived phosphonate **51** (see Schemes 3.6 & 3.7) with the aldehyde **49**. This proposed mechanism is shown below in Scheme 3.12.

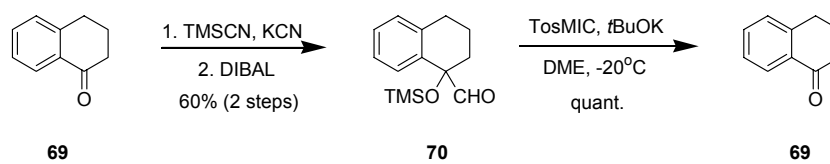


Scheme 3.12 Proposed Mechanism of Formation of 45 by Reaction of TosMIC with 49

After the addition of the anion of TosMIC to the aldehyde **49**, adduct **67** is presumably formed (Scheme 3.12). This adduct undergoes a TMS exchange reaction (as shown in Scheme 3.10) to form the tertiary oxy anion **68** instead of forming the usual oxazoline. This can now undergo a sequence of steps, as shown by the movement of arrows, with the elimination of the tosyl group to liberate ketone **45** and α -isocyanoaldehyde (not shown).

We suspected that this fragmentation behavior was exhibited often by aldehydes with an α -quaternary center bearing a TMS-protected tertiary alcohol, such as **49**. To confirm this,

aldehyde **70** was synthesized by treatment of tetralone **69** with TMSCN in presence of KCN and 18-crown-6 followed by reduction of the resulting nitrile with DIBAL in an overall yield of 60% for two steps (Scheme 3.13). This aldehyde was then subjected to the TosMIC reaction conditions. As expected, the sole product of the reaction was α -tetralone **69**, isolated in quantitative yield.

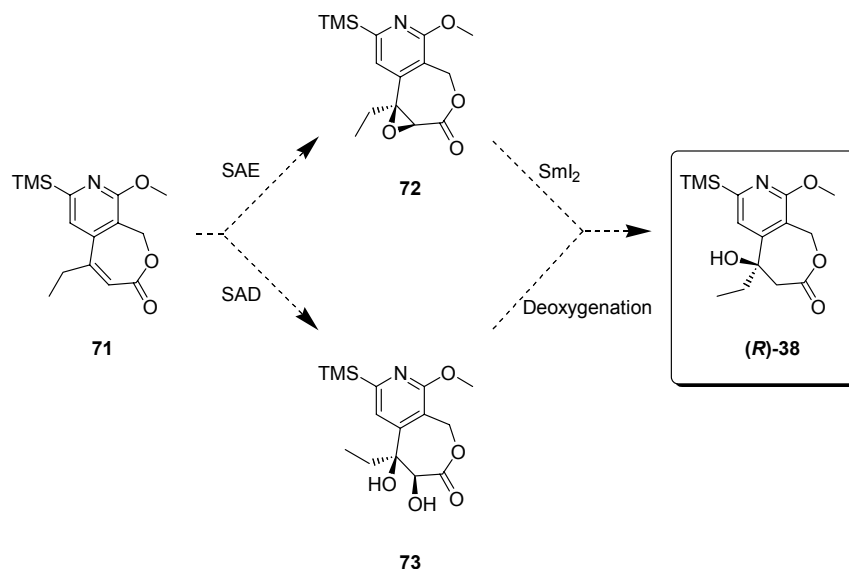


Scheme 3.13 Reaction of TosMIC on Test Substrate **70**

Other strategies such as the Wittig olefination of the aldehyde **49** have also yielded results similar to previously discussed examples and hence not discussed. However, one general observation was that the aldehyde **49** was too hindered and prone to undesirable side reactions which arose from the TMS group migration as discussed in Schemes 3.7 & 3.12. These discouraging results prompted us to abandon the homologation strategy in favor of an entirely new approach towards making the DE fragment of (*R*)-hCPT.

3.3. Epoxidation/Dihydroxylation Approaches to the Synthesis of the *DE* Fragment of (*R*)-hCPT

Synthesis of tertiary alcohols in good to excellent enantioselectivities, by Sharpless asymmetric epoxidation (SAE) or Sharpless asymmetric dihydroxylation (SAD) of olefins, is well documented.⁴⁷ Accordingly, we decided to explore these Sharpless protocols to set the tertiary alcohol stereocenter (Scheme 3.14).



Scheme 3.14 Proposed Synthetic Routes to (*R*)-38 via Asymmetric Epoxidation or Dihydroxylation of 71

Thus, enlactone **71** could be envisioned to undergo an SAE with a suitable chiral ligand to provide the epoxylactone **72** and the epoxide could be opened by SmI₂ to afford the β-hydroxylactone (*R*)-**38**. Alternatively, **71** could be enantioselectively dihydroxylated to give diol **73**, which could be deoxygenated using a literature protocol⁴⁸ to give (*R*)-**38**.

Previous research efforts in the Curran group directed towards the study of Sharpless asymmetric dihydroxylation of the enlactone **71** with commercially available AD-Mix reagents indicated modest yields and enantioselectivities.⁴⁹ For example when **71** was subjected standard Sharpless conditions using DHQD-PYR as the chiral ligand, diol **73** was obtained in 48% yield and 67% ee as indicated by analysis by HPLC. On the other hand, the asymmetric epoxidation route was never previously attempted with **71**.

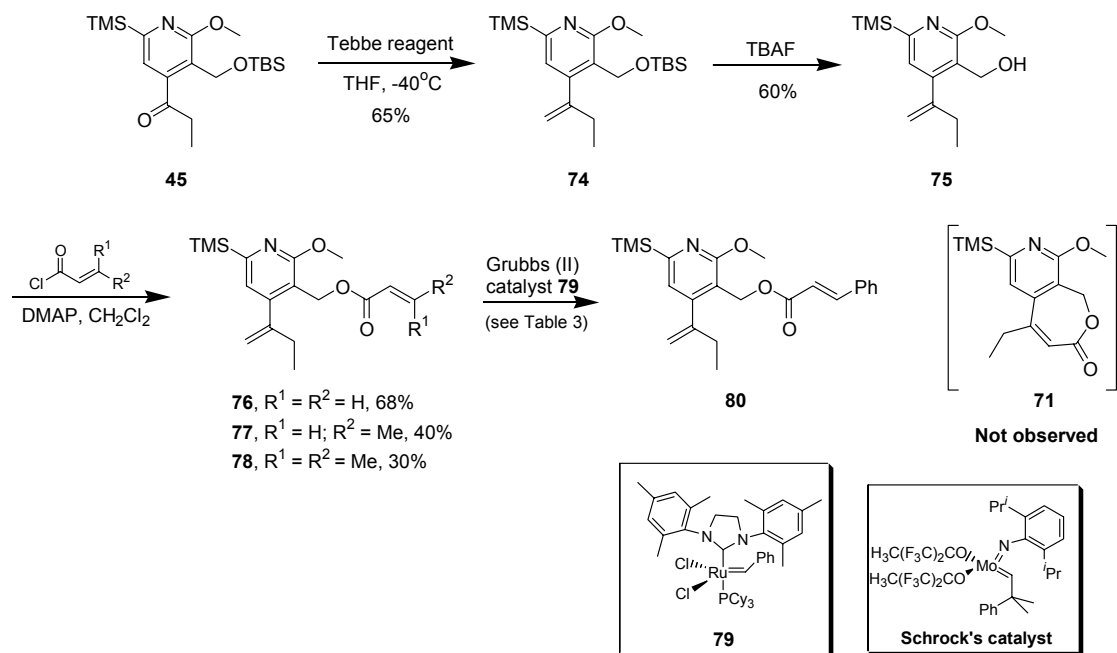
3.3.1. Synthesis of the Enelactone 71

Enelactone **71** was previously prepared⁴⁴ by the dehydration of racemic **38** with Burgess reagent (not shown). However, this procedure involves the synthesis of the racemic lactone first in several steps. To quickly access **71**, we explored a metathesis approach, radical addition to an alkyne, Heck cyclization onto an alkene and Ni(II)/Zn catalyzed cyclization chemistry. We finally successfully utilized the Stille coupling in synthesizing **71**.

3.3.1.1. Attempted Synthesis of 71 by Metathesis Approach

Olefin metathesis has evolved into a versatile and an important tool in synthetic organic chemistry.⁵⁰ In particular, metathesis of enones to access α,β -unsaturated lactones was first reported by Fürstner and coworkers in 2000.⁵¹ They reported the synthesis of enelactones of ring sizes 5, 6 and 7 in good to excellent yields.

Attempts to synthesize the trisubstituted olefin **71** by a metathesis of the corresponding acrylate and 1,1-disubstituted olefin **76** is shown in Scheme 3.15. The suitable substrate for the Grubbs metathesis, **76**, was easily synthesized from the known ketone **45** by first methylenation with the commercially available Tebbe reagent to give the 1,1-disubstituted olefin **74** in 65% yield. Deprotection of the TBS group reveals the benzyl alcohol **75** in 60% yield. The alcohol **75** was treated with acryloyl chloride in the presence of DMAP to obtain **76** in 68% yield. The other two metathesis substrates, **77** and **78**, were also synthesized in a similar fashion using the appropriate acylating agent in 40% and 30% yields, respectively.



Scheme 3.15 Attempted Synthesis of 71 by Metathesis Approach

We first conducted a control reaction to verify the purity and efficacy of the catalyst. Thus, 4-pentenyl ester of acrylic acid was treated with the Grubbs catalyst **79** under the standard metathesis reaction conditions (not shown). The product olefin was obtained in 44% yield with no other product derived from the starting ester validating the reagent purity.

Acrylate **76** was treated with the 2nd generation Grubbs catalyst **79** in refluxing toluene (0.04 M) to effect an intramolecular metathesis reaction. However a TLC analysis showed predominantly the starting acrylate. No desired enolactone was detected either by TLC or ¹H NMR spectroscopy. A number of reaction conditions, by varying the concentration and the temperature, were tested with **76**, **77** and **78** to effect this transformation.

Following the initial failure, we attempted the same metathesis conditions for the substrates **77** and **78**. In both the cases, the substrates remained unreactive under these conditions presumably due to the increase in substitution on the olefins. Increasing the amount of the catalyst used with **78** resulted only in the recovery of the starting acrylates.

We hypothesized that the presence of basic nitrogen in the pyridine ring inhibits the reaction to proceed. It is documented that free amines are incompatible with metathesis reactions owing to the inhibition of the catalyst by basic nitrogen.⁵² In order to circumvent a similar problem in their synthesis of halichlorine, Wright and coworkers conducted their metathesis reactions in the presence of *p*-toluenesulfonic acid to protonate the basic nitrogen *in situ* and allow the reaction to proceed. When olefin **76** was reacted with catalyst **79** in the presence of *p*TsOH, the reaction was messy with the starting material, an unidentified compound and a new compound (which was later identified as **80**) as the major products. Since the catalyst was not inactivated in this reaction, we concluded that our initial hypothesis of catalyst inhibition by the pyridine nitrogen was false.

We next changed the concentration of the reaction. Increasing the concentration of the reaction of **76** to 0.2 M with 20 mol% of the Grubbs catalyst in toluene at room temperature resulted in a new product. However, ¹H NMR analysis revealed that this product was not the desired enelactone **71**. Instead, we obtained the cinnamate ester **80**, which is the metathesis product of the starting enone **76** and styrene, in 28% yield. Presumably, the catalyst **79**, after forming the carbene with the α,β -unsaturated olefin, undergoes metathesis with the styrene that was released in the initial carbene formation (not shown) to form the cinnamate ester. The low yields of the cinnamate ester could be explained by the use of only 20 mol% of the catalyst. Increasing the concentration of the reaction mixture to 0.5 M, however, resulted in the same undesired product **80** in similar yields as above.

Changing reaction conditions in the reaction with the Grubbs catalyst did not yield any desired olefin **71**. We next employed the Schrock catalyst with our substrate **76**. Although no reports of Schrock catalyst used for the metathesis of electron-deficient olefins have been

documented, we decided to apply to our system. Accordingly, substrate **76** was reacted with Schrock catalyst (30 mol%) at 0.04 M concentration in toluene (entry 8). However, only the starting material remained completely unreactive to these conditions. Increasing the concentration to 0.1 M under identical conditions did not improve the reaction outcome either (entry 9).

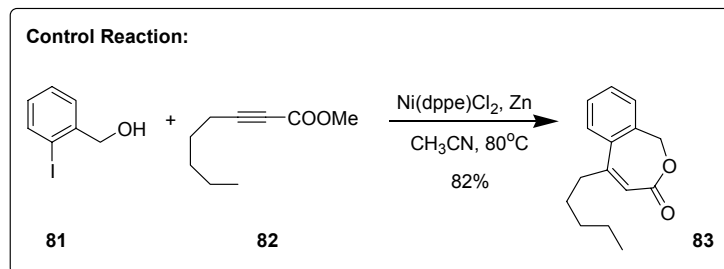
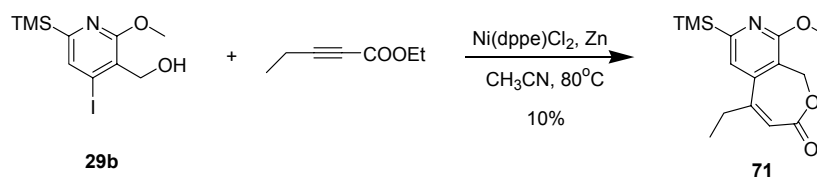
After these unsuccessful attempts to install the olefin by using the metathesis approach, we decided to abandon this strategy and investigate alternative methods for the preparation of the desired enelactone.

3.3.1.2. Synthesis of **71** by Ni (II)/Zn Catalyzed Cyclization

During the course of this work, Cheng and Rayabarapu described a one pot synthesis of 7-membered α,β -unsaturated lactones by a Ni/Zn catalyzed regioselective cyclization of 2-iodobenzyl alcohols with alkyl propiolates.⁵³ The authors reported several examples of trisubstituted olefin products although no heteroaromatic substrates have been examined.

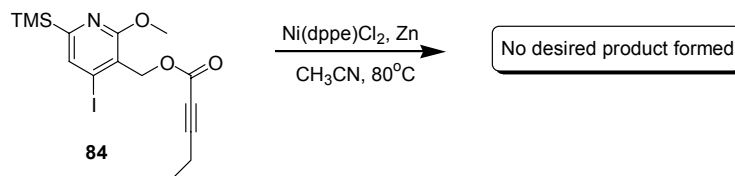
We first checked the quality of our nickel catalyst in a control reaction of 2-iodobenzyl alcohol **81** and methyl 2-octynoate **82** with Ni(dppe)Cl₂ complex in the presence of zinc powder at 80 °C. The product enelactone **83** was isolated in 82% yield (reptd. 81%) after chromatography.

Iodoalcohol **29b** and ethyl 2-pentynoate are the suitable substrates to access to **71** (Scheme 3.16). Accordingly, **29b** and ethyl 2-pentynoate were treated with Ni(dppe)Cl₂ complex in the presence of zinc powder and the reaction mixture was heated in acetonitrile at 80 °C. The reaction mixture showed multiple products as observed by TLC. The desired compound **71** was isolated in a yield of 10% after a difficult column chromatography.



Scheme 3.16 Ni(II)/Zn Catalyzed Regioselective Cyclization of 29b

The reaction parameters that were varied included the solvent, temperature and equivalents of the nickel catalyst. Since acetonitrile was the optimum solvent, we decided to change the solvent to propionitrile which can be used to conduct the reaction at higher temperatures as well. The temperature was varied between 80 °C and 110 °C. The catalyst equivalents were varied between 5 mol% and 1 equiv. Unfortunately, in all the cases, we observed multiple products as indicated by TLC. The ^1H NMR spectra of the crude reaction mixtures (after workup) were identical to each other as well.



Scheme 3.17 Intramolecular Ni(II)/Zn Catalyzed Cyclization of 84

An alternative to the above reaction conditions is the intramolecular variant shown in Scheme 3.17. We reasoned that predisposition of the second substrate would favor the product

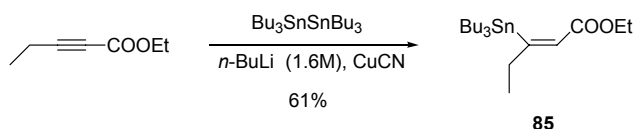
formation. Hence alkynyl ester **84** was subjected to the standard reaction conditions. The reaction mixture showed multiple products, as indicated by TLC, none of which was the desired product. Increasing the amount of the nickel catalyst added did not affect the outcome of the reaction.

Failing Cheng's cyclization protocol, we attempted other intramolecular strategies that can allow access to **71** such as intramolecular radical addition to **84** under $\text{Bu}_3\text{SnH/AIBN}$ conditions, Pd(0) promoted intramolecular Heck reaction conditions of the olefin variant of **84** (not shown) etc. Unfortunately, none of these methods provided us the desired olefin **71** in any reasonable quantities.

3.3.1.3. Synthesis of **71** using Stille Coupling

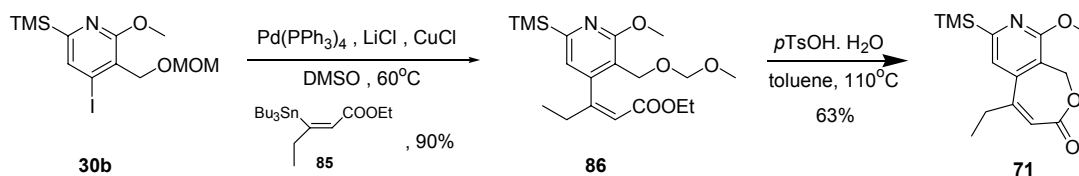
Faced with multiple failures to synthesize **71**, we decided to explore the Stille reaction. We had earlier made use of the Stille reaction in the total synthesis of (*R*)-hCPT (see Chapter 2). Iodopyridine **30b** (Scheme 3.19, see also Scheme 2.7) was subjected to the Stille conditions in the presence of the vinyl stannane **31** as the coupling partner. A similar type of coupling can be envisioned en route to synthesize **71**, albeit with the *Z*-variant of **31**.

The requisite vinyl stannane **85** was synthesized by the procedure that was previously published by Piers and coworkers (Scheme 3.18).³⁴ The lithium(tributylstannyl)cyanocuprate, prepared from treatment of Bu_6Sn_2 with BuLi followed by the addition of CuCN, was reacted with commercially available ethyl 2-pentynoate at $-78\text{ }^\circ\text{C}$ in THF. The vinyl stannane **85** was obtained in 61% yield after distillation at $95\text{-}100\text{ }^\circ\text{C}$ under a pressure of 0.7 mm of Hg.



Scheme 3.18 Preparation of Ethyl (Z)-3-(Tributylstannyl)-2-pentenoate

The Stille coupling was conducted with iodopyridine **30b** in moisture- and oxygen-free conditions. The reaction vessel was degassed under high vacuum followed by Ar purge after all the solid reagents ($\text{Pd}(\text{PPh}_3)_4$, LiCl and CuCl) were added and by the freeze-thaw process after the liquid reagents, DMSO and (Z)-vinylstannane **85**, were added. The reaction mixture was heated to 60 °C under these Corey-modified conditions of reaction with 1,1-disubstituted vinylstannanes.²⁹ The Stille product **86** was obtained in 90% yield after column chromatography.



Scheme 3.19 Synthesis of 71 by Stille Coupling

With the α,β -unsaturated ester **86** in hand, the next step was lactonization with concomitant deprotection of MOM group to give the enlactone **71**. Based on previous experience, our first choice of reagent for this transformation was TFA. Hence, an 0.4 M solution of ester **86** was treated with TFA and stirred at room temperature. This resulted in multiple products as detected by TLC. The desired enlactone **71** could be fished out of the crude reaction mixture in 15% yield after a difficult chromatography. Two other reactions of **86** with TFA were attempted in a similar fashion in higher and lower concentrations compared to the first reaction. Whilst the concentration variation did have an effect, it resulted only in poor yields of **71**.

We next conducted the reaction in the presence of camphor sulfonic acid. Unfortunately, only the starting material was recovered. When the ester **86** was reacted with Bu₂BOTf, TLC indicated the presence of multiple products. Gratifyingly, however, when **86** was stirred for 30 min with 1.5 equiv of *p*TsOH•H₂O, the product enelactone **71** was obtained in a 63% yield after purification by flash column chromatography.

We noticed that if the reaction time exceeds 30 min, we observed progressive decrease of reaction yields with time and also contamination of the reaction mixture with methyl toluenesulfonate (TsOMe). The by-product TsOMe was found to co-elute with the enelactone **71** in many solvent combinations. The presence of TsOMe was confirmed by ¹H NMR analysis combined with GC-MS analysis which clearly showed *m/z* peak corresponding to TsOMe. If the acid catalyzed cyclization is carried out for a period of 12 h or more, the reaction led to complete decomposition of the starting material and no desired product could be detected.

3.3.1.4. Modeling and Variable Temperature NMR Studies of 71

Spectroscopic analysis of the enelactone **71** revealed some interesting dynamic behavior. The two methylene protons on the lactone ring appeared as a broad peak at room temperature centered at 5.14 ppm in the ¹H NMR spectrum. This indicated that the methylene protons are positioned in different chemical environments compared to one another giving rise to two individual resonances at low temperature and at room temperature, the methylene protons resonances average out and coalesce to form one broad peak. This behavior can also be observed with enelactone **83** from the supporting information of the report by Cheng and Rayabarapu⁵³ (see Scheme 3.16). We then decided to study this interesting behavior of **71** by modeling and variable temperature NMR studies.

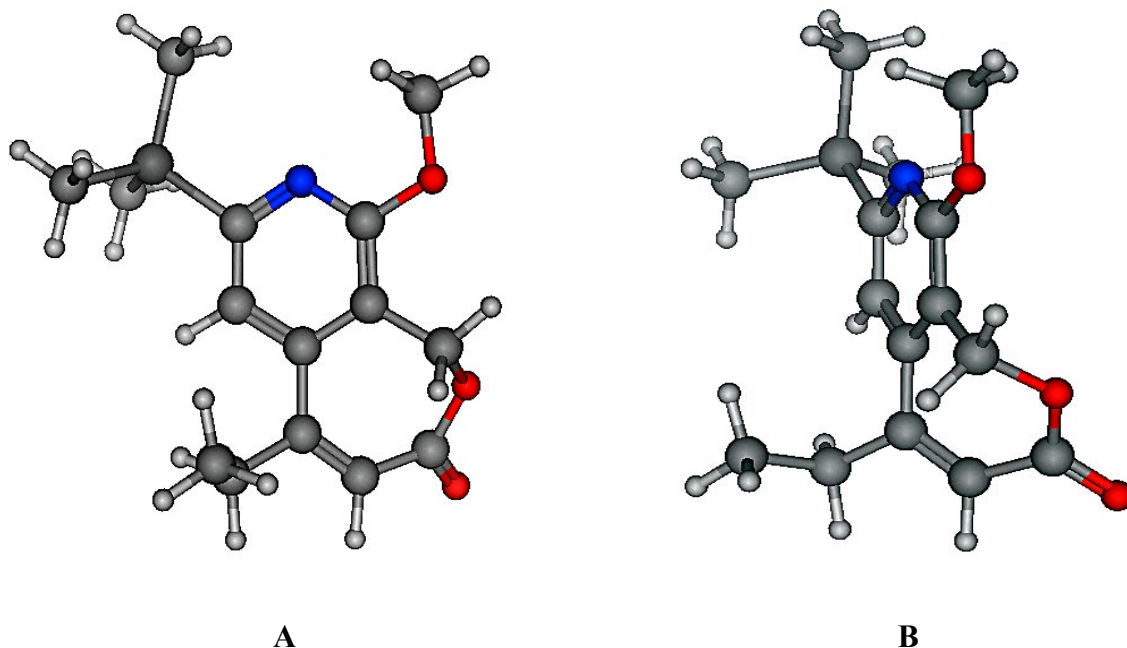


Figure 3.1 MOE Images of the Predicted Lowest Energy Conformer of **71** (A) Front view (B) Side view

To construct a model of **71**, an *in vacuo* conformational search using the MMFF94x force field within the molecular mechanics package MOE⁵⁴ was carried out. Two images of the predicted lowest energy conformer from this study are shown in Figure 3.1. The conformational search revealed a cluster of six lowest energy conformations (representing the different positioning of the groups TMS, ethyl and methoxy in space) all separated from the next highest energy cluster by a gap of 0.8 kcal.mol. This low energy conformation showed that the lactone portion of **71** is puckered (see Figure 3.1B). As a consequence, the two methylene protons are diastereotopic if the interconversion is slow on the NMR time scale.

In order to quantitate this dynamic NMR behavior, we conducted variable temperature NMR studies on **71**. Accordingly ¹H spectra of a CDCl₃ solution of **71** were recorded at temperatures ranging from -40 °C to 50 °C in increments of 10°. The spectra are shown in Figure 3.2.

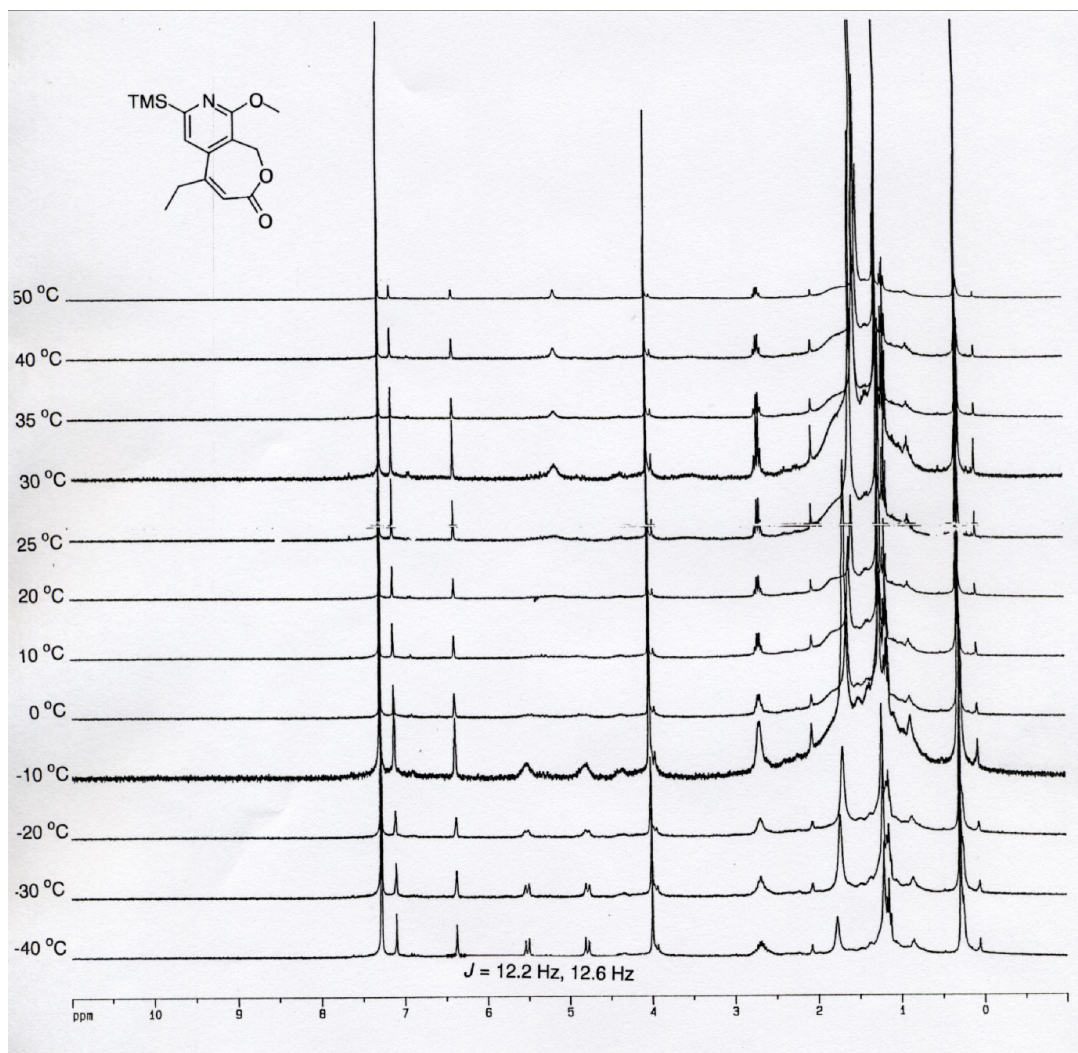


Figure 3.2 Variable Temperature Proton NMR Studies of 71

We observed that as the temperature was raised to 50 °C from room temperature, the broad peak corresponding to the methylene protons at 25 °C gradually sharpened to a singlet at 5.13 ppm. Similarly when the temperature was decreased to -40 °C, the broad peak separates into two doublets at -10 °C (which are coupling partners with $J = 12.4 \text{ Hz}$) at 5.51 and 4.78 ppm respectively.

The coalescence temperature is the temperature at which the two doublets merge to become a broad singlet and this was estimated by inspection to be 15 °C. The rate of site exchange between the two conformations, k_{coal} , can be determined by the following equation,⁵⁵

$$k_{coal} = \frac{1}{2} \pi \sqrt{2 \sqrt{(\nu_1 - \nu_2)^2 + 6J^2}}$$

where J is the coupling constant of the two methylene protons with chemical shifts ν_1 and ν_2 recorded in the units of Hz. Inserting the values of the variables in the equation above with the average coupling constant $J = 12.4$ Hz, the rate constant k_{coal} was determined to be 491 s^{-1} at the coalescence temperature of 15 °C. From this information, the free energy of activation for this exchange was calculated from the Eyring equation shown below,

$$\Delta G^\ddagger = RT_c \ln (hk_{coal}/k_B T_c)$$

where T_c is the coalescence temperature, h is Planck's constant and k_B is Boltzmann's constant. Plugging in the appropriate values into the above equation, the free energy of activation, ΔG^\ddagger , was determined to be $-13.3 \text{ kcal mol}^{-1}$. Thus the enelactone **71** was found to display the interesting behavior of conformational equilibrium with averaging of the two conformers at room temperature.

With the desired enelactone **71** in hand, we next proceeded to explore the dihydroxylation and the epoxidation approaches to make the DE fragment (**R**)-**38** (see Scheme 3.14).

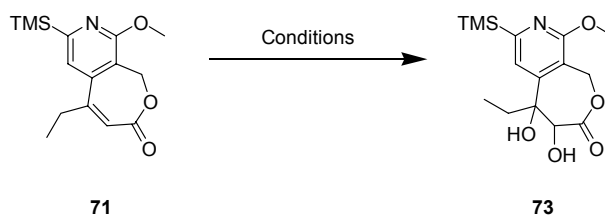
3.3.2. Dihydroxylations and Epoxidations of Olefin **71**

Investigations in the Curran group in the past have shown that the catalytic Sharpless asymmetric dihydroxylations of endocyclic α,β -unsaturated lactones were marred either with poor reactivity of the olefin or with good conversion but low enantioselectivities. In contrast, Sharpless dihydroxylations of exocyclic electron-deficient olefins have shown better selectivities

and good conversions and yields. With this as the background, we first decided to investigate the reactivity with dihydroxylation of racemic **71**.

3.3.2.1. Dihydroxylation Studies of Olefin **71**

Several protocols were attempted to synthesize the racemic diol **73** with different Os sources, bases, oxidants etc. including OsO₄/pyridine, KMnO₄, OsO₄/NMO etc. But in our hands, none of these well established reaction conditions were successful. We observed either the starting material or traces of the desired diol product **73**. We then attempted conditions that mimic those of Sharpless asymmetric dihydroxylation reaction using the combination K₂OsO₂(OH)₄/DABCO instead of the chiral ligand. This reaction showed traces of product **rac-73** along with large amounts of the starting material.



Entry	Reaction conditions	Product	Yield
1.	OsO ₄ , Et ₄ NOAc.H ₂ O, 70% TBHP	rac-73	75%
2.	"Os" source, MeSO ₂ NH ₂ , K ₃ Fe(CN) ₆ , K ₂ CO ₃ , lig*	(S,S)-73	No reaction/ poor yield

Scheme 3.20 Racemic and Asymmetric Dihydroxylation of **71**

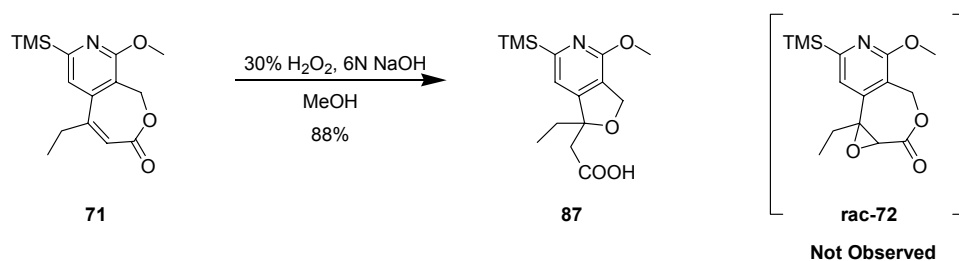
Sharpless and coworkers reported in late '70s a dihydroxylation procedure that works even for trisubstituted and hindered olefins.^{47a} Accordingly, **71** was reacted with OsO₄ in the presence of Et₄NOAc and *t*-butyl hydroperoxide at room temperature to afford the corresponding

diol **rac-73** in 75% yield after the usual workup followed by filtration through a pad of celite (Scheme 3.20).

We then investigated the asymmetric dihydroxylation reaction of **71**. Under standard Sharpless conditions along with different commercially available chiral ligands (DHQD)₂-PHAL, (DHQD)₂-AQN gave unreacted starting material back (Scheme 3.20). Reaction with the ligand (DHQD)₂-PYR gave a 16% yield of (**S,S**)-**73** after 48 hours along with large amounts of starting material left unconsumed as indicated by the TLC. Increase in the amounts of the ligands or the Os source or using different Os sources did not improve the result. In conclusion, dihydroxylation strategy failed to provide a practical means to access lactone (**R**)-**38**.

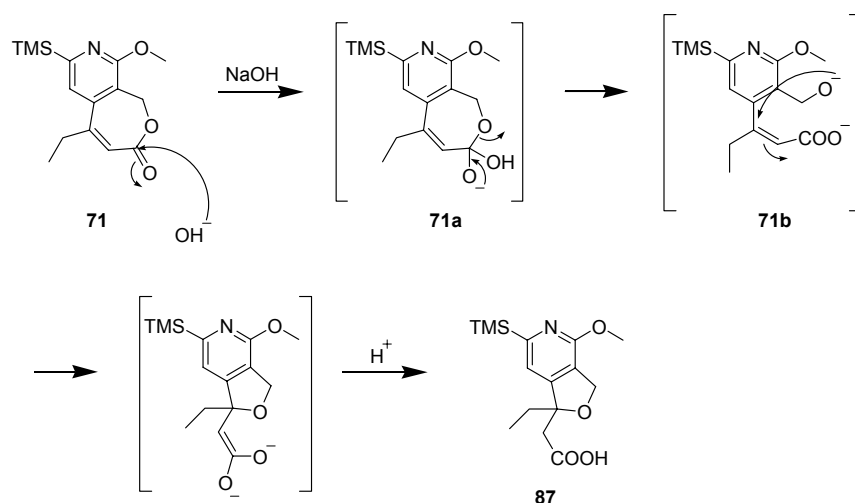
3.3.2.2. Epoxidation Studies of Olefin **71**

We decided to first investigate the reactivity pattern of our olefin **71** by studying the racemic epoxidation of this substrate. Olefin **71** was accordingly reacted with 30% H₂O₂ in the presence of 6N NaOH (Scheme 3.21). TLC analysis indicated the complete consumption of the starting olefin and the appearance of an intense polar product observed under a UV lamp. Unfortunately, none of the desired epoxide **rac-72** was observed in the product mixture as analyzed by ¹H NMR. Instead, the polar spot proved to be the rearranged acid **87** which was isolated in 88% yield after acidification of the crude reaction mixture with 1N HCl followed by a standard aqueous workup. The structure of **87** was confirmed by NMR and MS techniques.



Scheme 3.21 Racemic Epoxidation of 71

We also observed that the same product **87** was obtained even in the absence of 30% H_2O_2 in otherwise identical reaction conditions. These two observations led us to propose the plausible mechanism for this unexpected rearrangement involving the hydroxide (Scheme 3.22).



Scheme 3.22 Plausible Mechanism of the Unexpected Rearrangement during Epoxidation of 71

Thus, under the basic conditions the lactone is converted to the tetrahedral intermediate **71a**, which breaks down to give rise to the alkoxide **71b**. This alkoxide undergoes a conjugate addition to the α,β -unsaturated acid and the resulting carboxylate dianion, after workup, gives the rearranged product **87**. Other known procedures of epoxidation of electron-deficient olefins involving the use of NaOCl /neutral Al_2O_3 , $t\text{BuOOH}$ /DBU did not proceed well in our hands. In

these cases either the unreacted starting material was obtained or the crude reaction mixture displayed an indiscernible ^1H NMR spectrum.

Knowing that the structure of **71** is puckered and that the olefin is slightly out-of-conjugation with the lactone carbonyl moiety, we reasoned that **71** might behave more like a simple, unconjugated olefin. Hence we attempted reaction with mCPBA, DMDO to effect the epoxidation. However, in both the cases, only the starting olefin remained unreacted and none of the desired epoxide **rac-72** was observed.

In spite of the failure with the epoxidation strategy, we identified an interesting rearrangement occurring with the olefin **71**. Capitalizing upon this unexpected result, we turned our attention to developing compounds such as **87** into novel non-lactone analogs of camptothecin.

3.3.3. Novel Non-Lactone Analogs of Camptothecin – Synthesis

Our interest in the development of non-lactone analogs of camptothecin arises from the recent interest shown in the area of E-ring modified camptothecin analogs. Lavielle and coworkers reported the synthesis and pharmacological evaluation of the first biologically active non-lactone analogs of camptothecin (Figure 3.3).⁵⁶

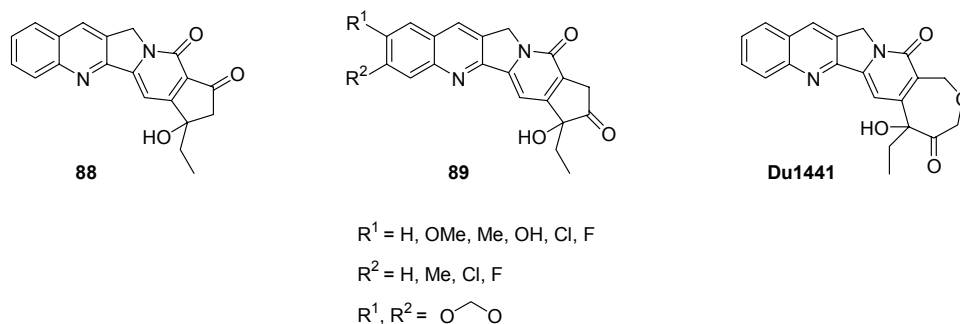


Figure 3.3 Novel Non-Lactone Analogs Reported by Lavielle

They described a series of two different kinds of E-ring ketone derivatives **88** and **89** as shown in Figure 3.3. The topoisomerase inhibitory assay (with CPT and SN-38 as standards) and the cell-growth inhibitory assay (with L1210 leukemia cells) both indicated that the compounds showed reasonable activity (0.06-1.0 μM). In particular, the methylenedioxy derivative ($R^1, R^2 = \text{OCH}_2\text{O}$) showed activity that was comparable to topotecan.

With reference to non-lactone E-ring analogs, the Curran group had also reported the synthesis and biological evaluation of the keto-ether **Du1441**.²⁴ Unfortunately, **Du1441** did not show promise as a topo I poison. We carried through **87** into E-ring modified cyclic ether CPT derivatives (Figure 3.4).

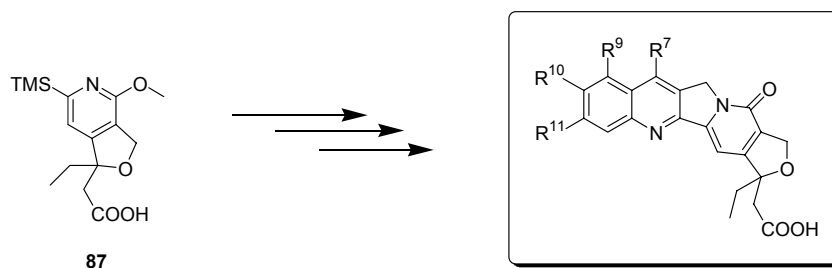
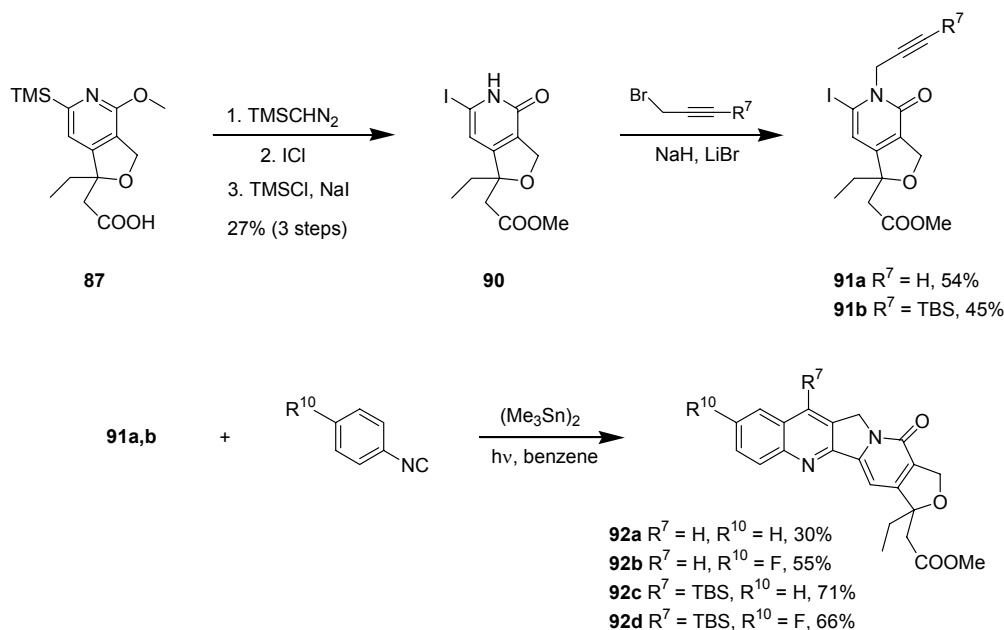


Figure 3.4 Development of Cyclic Ether Analogs to Camptothecin Derivatives

We planned to synthesize four non-lactone analogs with modifications on the 7 and 10 positions of the A & B rings of the final derivatives. Our choices of substitution at the 7-position were H and TBS and at the 10-position were H and F. This selection for the initial set of compounds was based on previous knowledge in the Curran group in this area. Silyl substitution on the 7-position has been shown to increase blood stability of the derivatives and result in an enhanced activity.⁵⁷ In particular, 7-TBS substitution has been very beneficial. Similarly 10-F substitution allows to study effect a hydrogen-bond acceptor while still retaining the size of the group at that position compared to the parent 10-H substituted compound. The synthesis of these analogs is shown in Scheme 3.23.

The synthesis commences with the esterification of the carboxylic acid **87** upon treatment with TMSCHN₂ at room temperature to afford the corresponding methyl ester⁵⁸ (not shown). This protection as the ester ensures that no complications arise due to the free carboxylic acid. This ester is then iododesilylated under standard ICl conditions. The iodine atom in this iodopyridine acts as the radical precursor. Next, the reaction of this methoxy pyridine with *in situ* generated TMSI affords the demethylated iodopyridone **90** in a combined three-step yield of 25%.

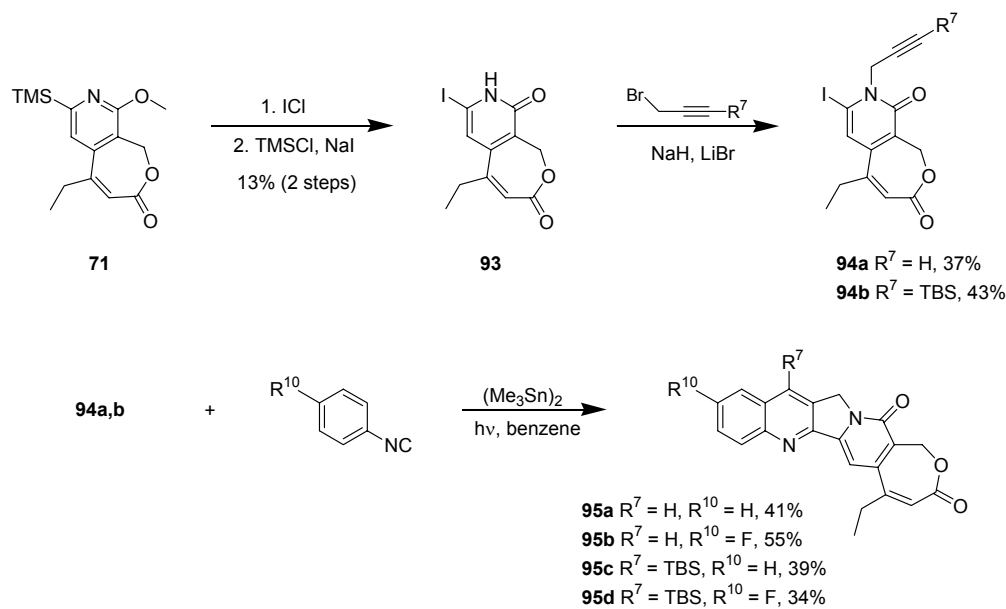
Compound **90** was divided into two portions and propargylated with the two propargyl bromides in the presence of NaH and LiBr to give the corresponding *N*-propargylated pyridones **91a** and **91b** in 54% and 45% yield, respectively. Each of these propargylated pyridones was further divided into two portions and reacted with two *p*-substituted isonitriles under photoirradiation conditions to afford the four camptothecin analogs **92a-d** in 30-71% yield after purification by flash column chromatography. The structures of **92a-d** were confirmed by NMR and MS analysis.



Scheme 3.23 Synthesis of Four Cyclic Ether Analogs of CPT

We realized that E-ring modified analogs without a stereocenter would also be interesting to understand the significance of the tertiary alcohol in CPT and hCPT. To access such type of analogs, we identified the enlactone **71** as a good starting point and decided to develop analogs with the E-ring containing an olefin in the place of the tertiary stereocenter. The synthesis, which closely follows the synthesis of the cyclic ether analogs, is described in Scheme 3.24.

Four analogs with identical substitution patterns to those of the cyclic ethers were synthesized. Thus, enlactone **71** was iododesilylated with ICl and following that it was demethylated with *in situ* generated TMSI to afford iodopyridone **93** in 12% for the two steps. Compound **93** was divided into two portions for the propargylation reaction and then the *N*-propargylated iodopyridones **94a** and **94b**, obtained in 37% and 43% yield respectively, were further divided into two portions each to be reacted with two isonitriles under photoirradiation conditions to give the final enlactone derivatives **95a-d** in about 34-55% yields after purification by column chromatography. The structures of the four enlactones were confirmed by NMR and MS techniques.



Scheme 3.24 Synthesis of Four Enelactone Analogs of CPT

3.3.4. Novel Non-Lactone Analogs of Camptothecin – Biological Evaluation

Eight E-ring modified CPT analogs, four cyclic ethers and four enelactones, were tested by Drs. Y. Pommier, B. Anderson and their coworkers for biological activity in two assays: topoisomerase inhibitory assay and cell growth inhibitory assay. The results from the electrophoresis experiments in the topoisomerase inhibitory assay are shown in Figure 3.5.

The first two lanes in the gel display show the controls DNA and topo I in the absence of CPT or hCPT. As expected, no cleavage products were observed. The third lane shows CPT control and cleavage products are clearly observed. The next two sets of lanes show the hCPT controls, the first set indicates hCPT synthesized by French researchers and the second set hCPT synthesized by our group. Each set is divided into four lanes, represented by concentrations 0.1 μM , 1 μM , 10 μM and 100 μM respectively. The final two sets of lanes show the assay results of analogs **95a** and **95b**. The DNA cleavage products are indicated by arrows in Figure 3.5.

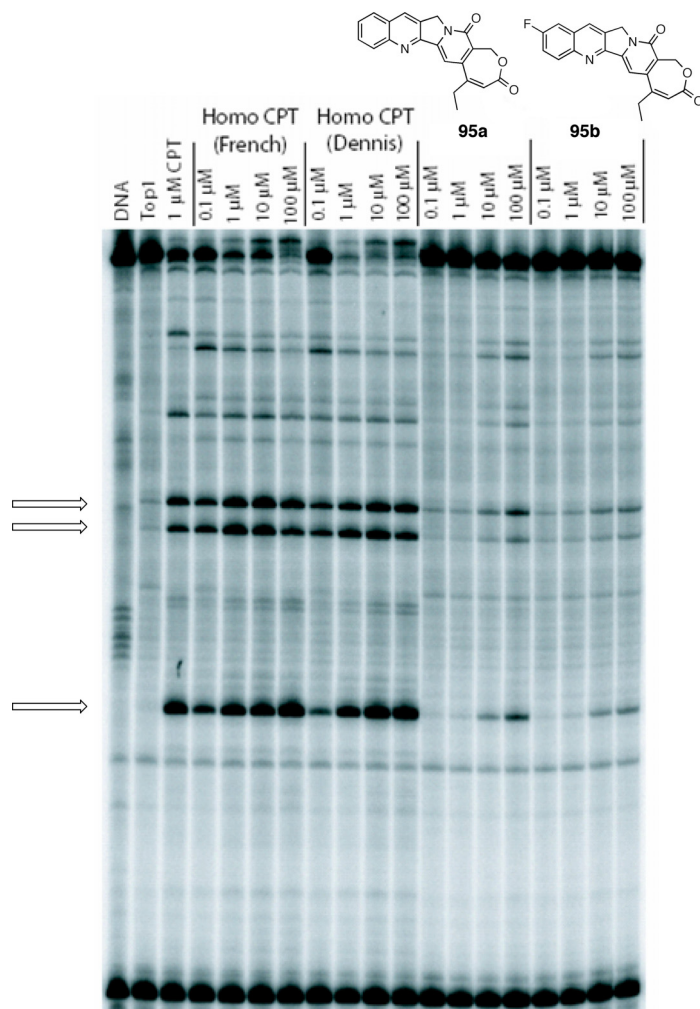


Figure 3.5 Topoisomerase Inhibitory DNA Cleavage Assay Results for Non-lactone Analogs 95a,b

For topo I cleavage assays, labeled DNA (~50 fmole/reaction) was incubated with 5 ng of recombinant topo I with or without the drug at 25 °C in 10μL reaction buffer (10 mM Tris-Cl pH 7.5, 50 mM KCl, 5 mM MgCl₂, 0.1 mM EDTA, 15 μg/mL BSA, final concentrations) for 20 min. Reactions were stopped with SDS (0.5 %). Samples were denatured by the addition of 3.3 volumes of Maxam Gilbert loading buffer (80% formamide, 10 mM sodium hydroxide, 1 mM sodium EDTA, 0.1% xylene cyanol and 0.1% bromophenol blue, pH 8.0). Aliquots were separated in 16% denaturing polyacrylamide gels (7M urea) in 1 X TBE (45 mM Tris, 45 mM

Boric acid, 1 mM EDTA) for 2 h at 40 V/cm at 50 °C. Imaging and quantitation were performed using a Phosphorimager.

The electrophoresis experiments have led to the following results. First, the cyclic ether analogs **92a-d** have shown no activity compared to the standard samples of hCPT. Second, the enelactones **95a-d** showed that the 20-OH group is not *absolutely* required for topoisomerase I poisoning. However, in the absence of the 20-OH group, the drug activity was reduced by about 100-fold. And third, due to the low activity of the parent enelactone **95a**, effects of the substitution could not be assessed accurately.

3.4. Summary

This chapter described our initial efforts to investigate new approaches towards the efficient synthesis of the *DE*-fragment of (*R*)-hCPT. Our efforts in using different homologation approaches to achieve this goal were described. When many of the tested homologation protocols either failed to succeed or furnished unsatisfactory results, we turned our attention to the epoxidation and dihydroxylation procedures in accessing the desired *DE*-fragment. These procedures have not afforded the desired results. However, an unexpected rearrangement in an epoxidation protocol led us to the synthesis of novel non-lactone analogs of camptothecin which can be classified into two categories – cyclic ether analogs and enelactone analogs. Despite the interesting synthetic sequence, these analogs have not shown much promise in the biological activity studies. The development of non-lactone analogs with promising biological activity continues to be of interest in our group and other research laboratories. Further studies in this area may reveal such analogs possessing interesting modifications in the E-ring without compromising the biological activity.

4. E-RING OPEN-FORM ANALOGS OF CAMPTOTHECIN

4.1. Introduction

Recently, Stewart and co-workers reported the X-ray crystal structure of human topoisomerase I covalently joined to double-stranded DNA and bound to topotecan, a clinically approved analog of camptothecin.¹² This crystal structure sheds light on the mechanism of topoisomerase I poisoning by the CPT derivatives. Prior to the disclosure of this report, it had been difficult to study the mechanism of action of CPT because the drug acts as an uncompetitive inhibitor at the binding site and binds only the transient covalent enzyme-substrate complex.⁵⁹

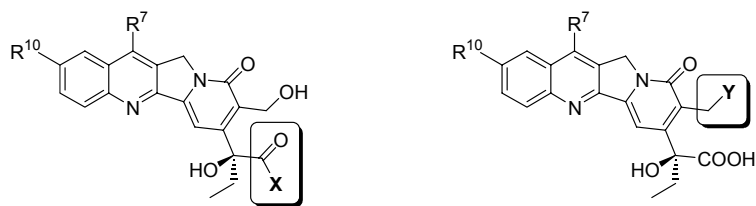
It was reported that topotecan mimics a DNA base pair and binds at the site of DNA cleavage by intercalating between the upstream and downstream base pairs. One of the most striking findings of this report was that the electron density allowed the positioning of both the closed lactone and the open carboxylate conformers of topotecan. An unrestrained full matrix refinement of occupancy factors for both these conformers converged to an occupancy of 37% open carboxylate and 63% closed lactone forms. Fluorescence spectrophotometric measurements of topotecan as a function of pH revealed a similar ratio between the closed (75%) and open (25%) forms. The observed ternary crystal structure also demonstrates that both the closed lactone and the open carboxylate conformers *can* bind within the same intercalation pocket and presumably prevent the religation reaction. These findings are surprising because they contradict conventional wisdom that the ring-opened carboxylate is detrimental to the drug's biological activity (see Scheme 1.1, Chapter 1).

The binding interactions of topotecan within the intercalation pocket (Figure 1.3, Chapter 1) in both the closed and the open forms explain the results of various E-ring modifications reported in literature. The crystal structure model shows that in the closed lactone there is only one direct hydrogen bond between the enzyme and topotecan: the 20(*S*)-hydroxy group hydrogen bonds to Asp533. This stabilizing hydrogen bond interaction is intact in the open carboxylate form arguing against the belief that the open form inactivates the drug. In addition, the open form enjoys two other stabilizing interactions: the water-bridged contacts of the free primary hydroxyl group to Asn722 and the carboxylate oxygen to the P-Tyr723.

This report of the crystal structure opens up new avenues in the field of camptothecin analog synthesis: E-ring open form analogs. Based on the conclusions described above, we initiated a project aimed at the synthesis and biological evaluation of derivatives which resemble the open carboxylate form of camptothecin.

4.2. Synthesis of the E-ring Open Form Analogs of CPT

The two points of modification in the synthesis of open form analogs that we made are shown in Figure 4.1. One of the key features of the open form is the extent to which it can participate in hydrogen bonding. Excluding the tertiary alcohol which is involved in a key stabilizing interaction, we varied the primary hydroxyl group and the carboxylate such that the resulting modifications may enhance or diminish the hydrogen bond interactions.



X = NHNH₂, NHOH etc.

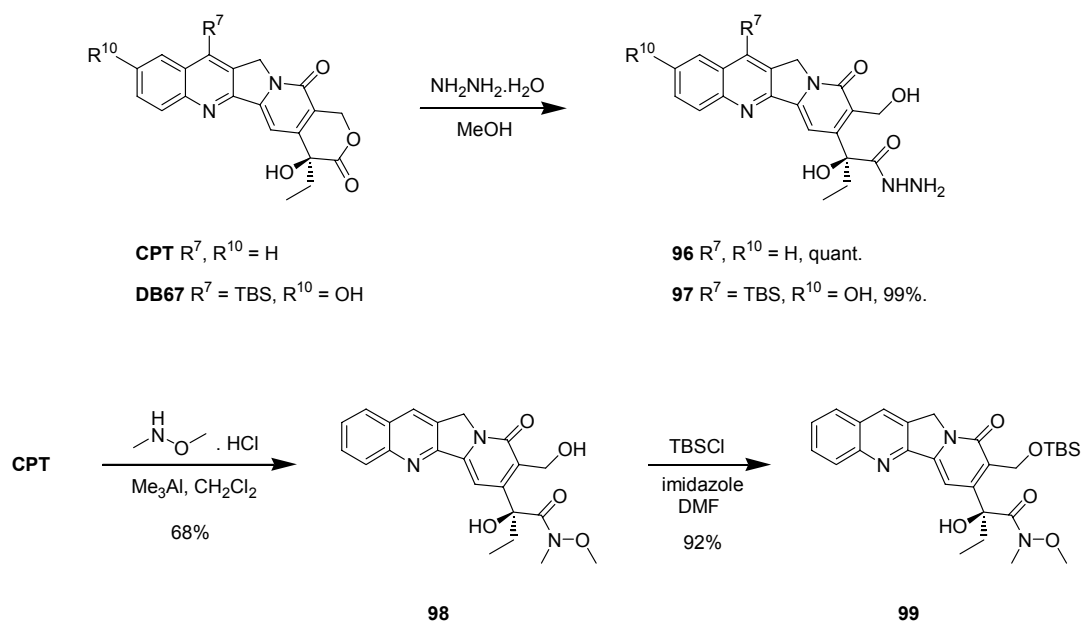
Y = H, F etc.

(R⁷, R¹⁰) = (H, H) or (TBS, OH)

Figure 4.1 Structural Modifications in Synthesis of E-ring Open Form Analogs

The first type of modification we made was to substitute the acid for a hydrazide ($X = \text{NHNH}_2$). The hydrazide can retain the hydrogen bond donor capacity while remaining in the same oxidation state as the parent carboxylate. Secondly, the acid was substituted by the Weinreb amide that will remove the hydrogen bonding interactions due to the lack of donors. This change will help us understand the significance of the hydrogen bonding interactions of the carboxylate.

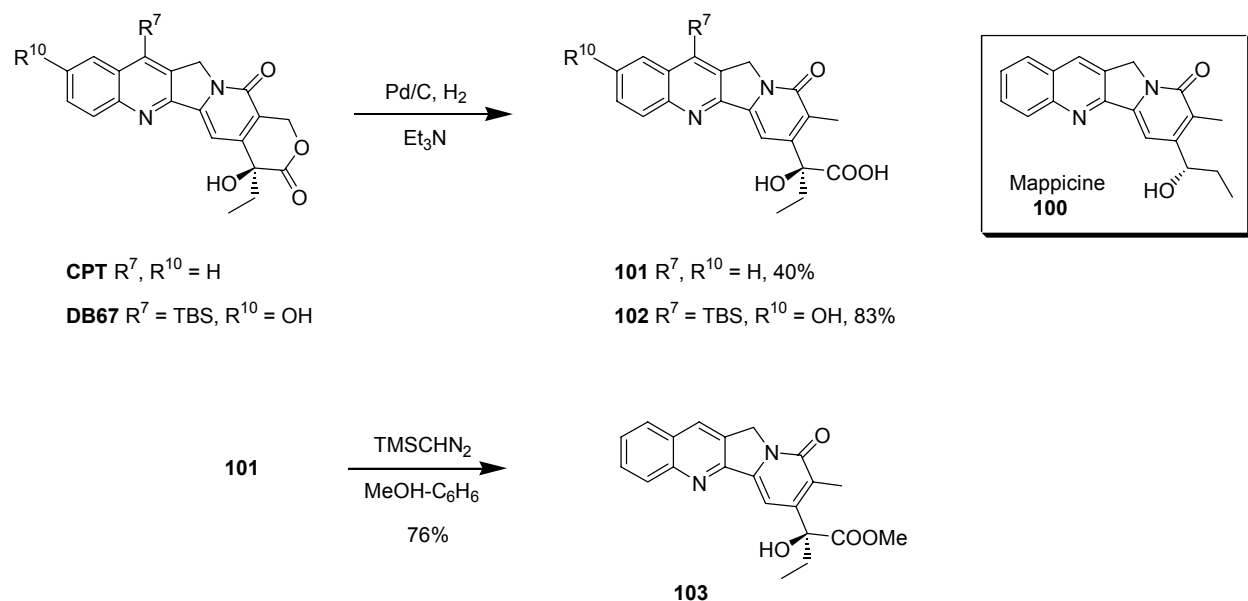
The synthesis of these analogs is shown in Scheme 4.1. Camptothecin (CPT) was treated with an excess of hydrazine monohydrate in methanol at room temperature⁶⁰ to effect the opening of the lactone and form hydrazide **96** in quantitative yield. DB-67 was subjected to identical reaction conditions affording hydrazide **97**, also in near quantitative yield. Both the hydrazides did not require further purification after the workup. The structures of **96** and **97** were confirmed by NMR and MS techniques.



Scheme 4.1 Synthesis of the Hydrazides **96**, **97** and Weinreb Amide **99**

For the synthesis of the Weinreb amide **98**, CPT was added to a mixture of Me_3Al and *N,O*-dimethylhydroxylamine hydrochloride at room temperature to afford **98** in 77% yield.⁶¹ Weinreb amide **98** was quite unstable on standing at room temperature (displayed multiple products as indicated by TLC). However, when the free alcohol in **98** was protected as the TBS ether on treatment with TBSCl and imidazole, the product **99** (obtained in 92% yield) was found to be stable on the bench top as indicated by TLC.

The second point of modification was at the primary alcohol position. We synthesized two derivatives lacking a hydrogen bond donor group i.e., a 17-deshydroxy derivative ($Y = H$ in Figure 4.1) as shown in Scheme 4.2.



Scheme 4.2 Synthesis of 17-Deshydroxy Open-form Analogs

We were particularly interested in the 17-deshydroxy substrate **101** because it combines the structural features of camptothecin and the related mappicine **100**.⁶² A report by the researchers at the Smithkline Beecham Corporation⁶³ describes a semi-synthetic route to **101**. However, no information regarding the biological activity was reported. Employing this procedure, camptothecin (CPT) was subjected to hydrogenolysis reaction using palladium on carbon in the presence of Et_3N and DMF to afford the acid **101** in 40% yield after purification by semi-preparative HPLC using a reverse phase C18 column. DB67 was also submitted to identical reaction conditions but substituting the solvent DMF with MeOH because of better solubility and ease of workup. The product **102** was isolated in a 83% yield after column chromatography. The presence of a carboxylic acid moiety in **101** was confirmed by esterification with trimethylsilyl diazomethane to the corresponding methyl ester **103** in 76% yield.

4.3. Biological Evaluation of the E-ring Open Form Analogs of CPT

All the open-form derivatives of CPT were sent for a preliminary evaluation for any biological activity as shown by the topoisomerase inhibitory assay. The assay conditions were identical to those described in Chapter 3. Figure 4.2 shows an electrophoresis gel display of CPT, the hydrazides **96** and **97** and the acids **101** and **102**. The first two lanes in the gel display show the controls DNA and topo I in the absence of CPT. As expected, no cleavage products were observed. The third set of four lanes shows CPT control and the cleavage products are clearly observed. Each of these four lanes refers to the concentrations 0.1 μM , 1 μM , 10 μM and 100 μM respectively. The next four sets of lanes show the assay results of **101**, **96**, **97** and **102** respectively. The DNA cleavage products are indicated by arrows in Figure 3.5.

The topo I assay shows that the hydrazides **96** and **97** display promising activity that is comparable to that of camptothecin (CPT). One can also note that the hydrazide **97** shows slightly better activity as indicated by the intensity of the cleavage products in the electrophoresis gel display. Unfortunately, the acids **101** and **102** showed no activity at all as indicated by the empty lanes 2 and 5 (Figure 4.3). Weinreb amide **99** also exhibited no activity.

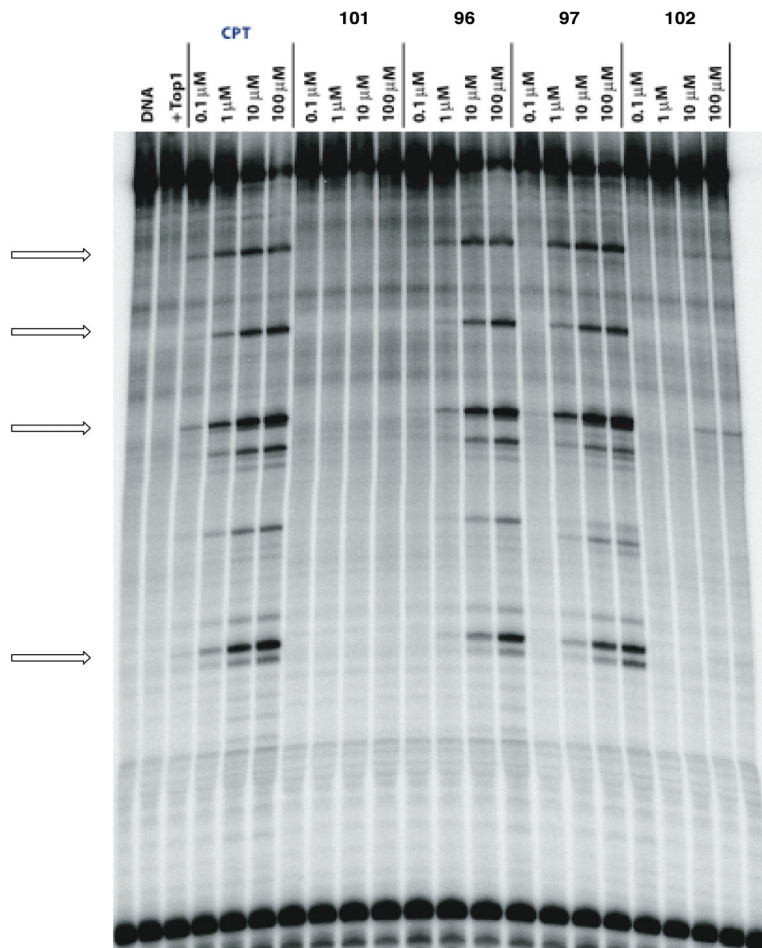


Figure 4.2 Results of Topo I Inhibitory Assay of Derivatives 96, 97, 101 & 102

We next studied the stability of the hydrazides at room temperature. Two portions (of arbitrary amounts) of hydrazide **96**, one as a solution in DMSO and the other as a solid sample, were allowed to stand at room temperature. It was learned that **96**, as a solution of DMSO, closes to the lactone generating camptothecin. However, it is quite stable on the bench top as a solid sample as indicated by ^1H NMR spectrum. When the ^1H NMR spectrum of **96** was recorded after it was present as a solution in DMSO for 20 days, the spectrum showed a complete conversion of the hydrazide to camptothecin. The hydrazide **96** is, however, stable as a solid at room

temperature for at least six months with no traces of camptothecin formed as indicated by ^1H NMR.

The hydrazone samples were checked for conversion to CPT after they had been tested for topo I inhibitory activity. The ^1H NMR spectrum showed a ratio of 2:1 of CPT/hydrazone **96**. It is still unclear if the activity displayed by the hydrazones originates from the *in situ* generated CPT in DMSO. More experimentation is required to confirm unambiguously the nature of the species in the assay contributing to the biological activity. If CPT is determined responsible for the observed activity, then these hydrazones can serve as prodrug analogs that can potentially undergo reconversion to CPT *in vivo*.

The open form analogs of CPT were also studied in a cell growth inhibition assay. The plot of the percentage of cells remaining (y-axis) versus the concentration of the CPT analog (x-axis) is shown in Figure 4.3. The first two entries are the CPT (blue) and DB67 (pink, see Figure 1.5, Chapter 1) controls. The other four entries are **101** (green), **96** (cyan), **97** (purple) and **102** (brown). The SRB assay, done in the cell growth inhibition studies, measures the amount of protein attached to a well. This amount is proportional to the number of cells still attached to the well. The cells used, MDA-MB-435S+ are no longer viable if they lose their attachment after exposure to CPT or its analogs.

The cells were plated onto 24 well plates 24 h before they were exposed to CPT analogs. After the CPT derivative was added, cells were allowed to grow for 72 h (full cell cycle arrest was observed around 48 h after exposure to CPT analog). Thus the cells grew for 96 h, with CPT analog present for 72 h. The cells were then gently washed with PBS buffer and fixed with trichloroacetic acid. The plates were dried and stained with sulforhodamine blue (SRB) and excess

dye was washed off with 1% acetic acid. Plates were dried again. SRB dye was then mobilized with 10 mM tris base and measured with a spectrophotometer set at 490 nm.

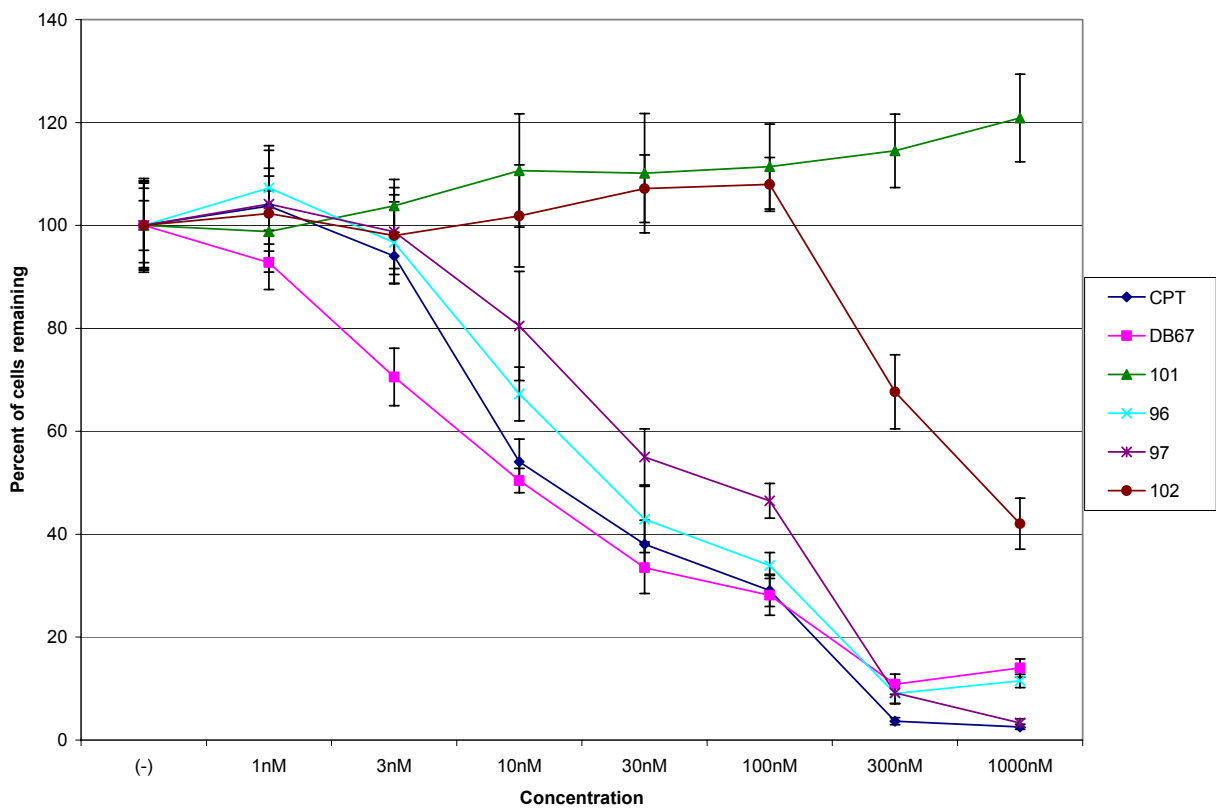


Figure 4.3 Results of the Cell Growth Inhibition SRB Assay of Derivatives 96, 97, 101 and 102

The results of the SRB assay were in agreement with those of the topo I inhibitory assay (see Figure 4.2). Hydrazides **96** and **97** inhibited the growth of cells with an approximate $GI_{50} = 20$ nM and 100 nM respectively. These values are comparable to those of CPT and DB67 which are in the 10 nM range. Acids **101** and **102**, on the other hand, showed no growth inhibition of cells.

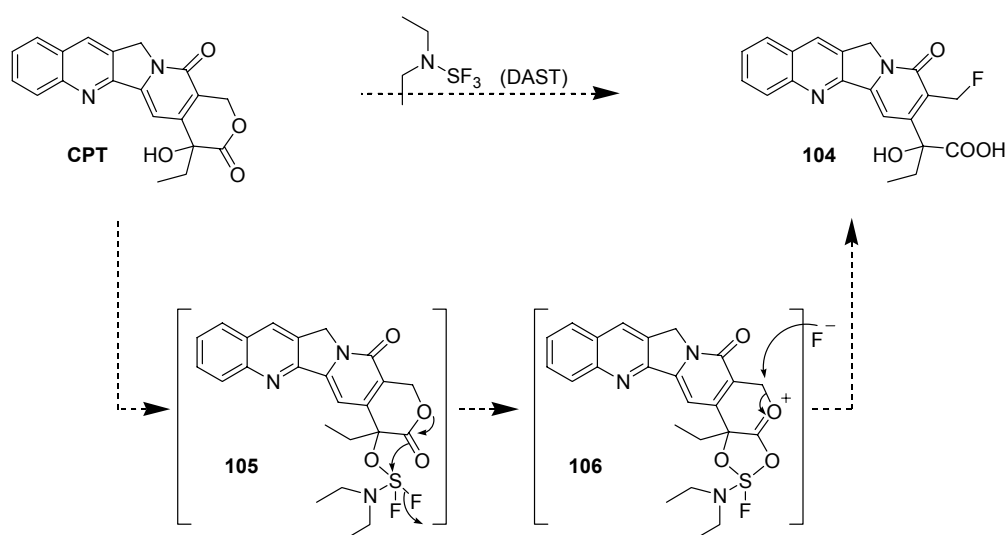
4.4. Summary

This chapter described the synthesis of a small assortment of E-ring open form analogs of camptothecin. This analog synthesis evolved from an interesting report of the X-ray crystal structure of the topo I-DNA-topotecan ternary complex by Stewart and co-workers which revealed that the open carboxylate form of CPT contributed to its biological activity. The analogs were synthesized using semi-synthetic approaches commencing from CPT and DB67, a well-studied CPT analog. The different substitution patterns of the analogs were designed based on the findings of the report. All the analogs synthesized were biologically tested and the hydrazides showed good activity in the topoisomerase inhibitory assay. Additional experimentation is needed to confirm that these hydrazides remain in the open form under the assay conditions. Further development in this nascent field of open form CPT analogs is necessary to understand the implications of this report.

5. 20-FLUOROCAMPTOTHECINS: AN ACCIDENTAL DISCOVERY

5.1. Introduction

During the course of our studies of E-ring open form derivatives of CPT, we became interested in studying open form analogs which have fluorine incorporated such as **104** (Scheme 5.1). We envisioned that such primary fluorides could be synthesized in a semi-synthetic fashion starting from CPT or its analog using diethylamine sulfurtrifluoride (DAST). Based on a related literature precedent by Kirihara and coworkers,⁶⁴ we envisioned a plausible mechanism for the desired transformation as shown in Scheme 5.1.

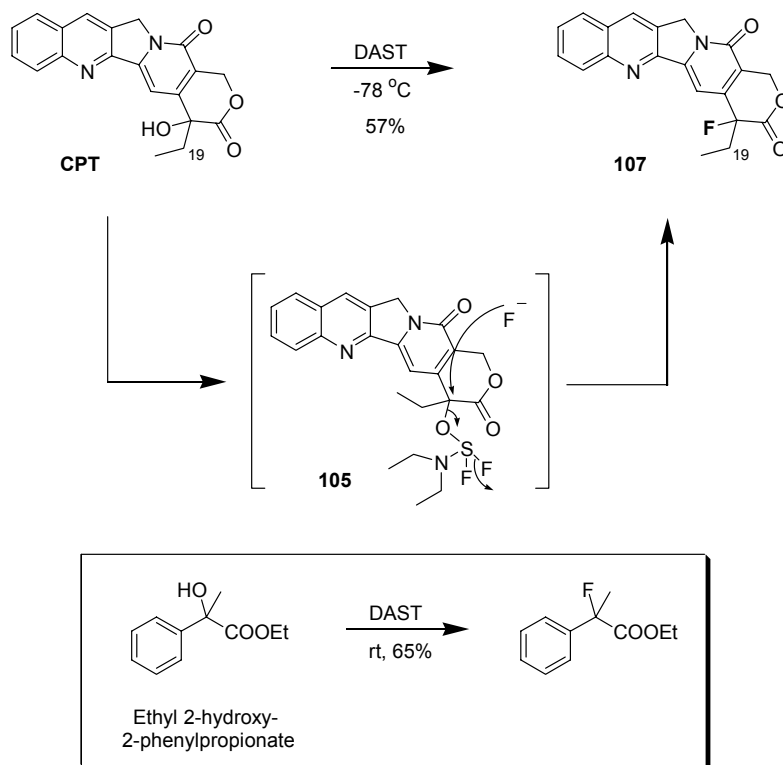


Scheme 5.1 Proposed Synthesis of **104** from CPT

Thus, CPT could react with DAST via the nucleophilic displacement of the fluoride on sulfur by the oxygen of the 3° alcohol in CPT to afford **105**. Intermediate **105** could then displace a second fluoride in an intramolecular fashion to give the oxonium ion intermediate **106**.

Attack of fluoride ion at the benzylic position in **106** could afford the desired fluorinated derivative **104**.

When CPT was treated with DAST at $-78\text{ }^{\circ}\text{C}$ and the reaction mixture was stirred overnight followed by an aqueous workup, a clean monofluorinated product was isolated in 54% yield after purification by flash column chromatography (99.0:0.5:0.5 dichloromethane/methanol/acetonitrile). Based on a detailed spectroscopic analysis, we concluded that the product was not the fluorinated derivative **104** but rather 20-fluorocamptothecin **107** (Scheme 5.2). The best precedent for this fluorination was reported by Takeuchi and coworkers⁶⁵ where ethyl 2-hydroxy-2-phenylpropionate was reacted with DAST to the corresponding fluorinated derivative (boxed in Scheme 5.2).



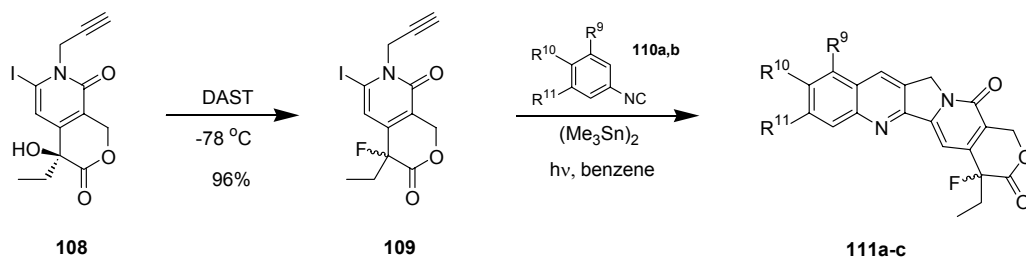
Scheme 5.2 Reaction of CPT with DAST

The ^1H NMR spectrum of **107** showed a doublet of quartets ($J = 7.4$ Hz, 22.2 Hz) for the C19 methylene protons of the ethyl chain. The large 22 Hz coupling constant for the doublet indicated that the methylene protons were coupled to a fluorine atom consistent with a $\text{CH}_3\text{CH}_2\text{CFR}_2$ fragment. The product shows a triplet at -163 ppm ($J = 22.6$ Hz) in ^{19}F NMR spectrum, which is consistent with a fluorine atom with no geminal protons rather than the expected primary fluoride **104** with two geminal protons. An HMBC ($^1\text{H} - ^{13}\text{C}$ correlation, greater than one bond coupling) spectrum of the product displayed crosspeaks between the C19 methylene protons and the carbon bearing the fluorine atom. In addition, no crosspeaks between the benzyl protons (protons geminal to F in **104** in Scheme 5.1) and F were observed. The ^{13}C NMR spectrum showed a doublet at 89.5 ppm with a coupling constant of 193.7 Hz consistent with a C-F one bond coupling. MS analysis showed an m/z value of 350 also consistent with a monofluorinated product. All these data support structure **107**.

The proposed mechanism of the formation of 20-fluorocamptothecin **107** is shown in Scheme 5.2. The formation of the intermediate **105** is followed a nucleophilic substitution of the oxygen leaving group by a fluoride ion to give a tertiary fluoride **107**. 20-Chloro and 20-bromocamptothecins have been reported⁶⁶ to stabilize the covalent topo I-DNA binary complex fully despite lacking hydrogen bond donors. Interestingly, 20-fluorocamptothecin contains a hydrogen bond acceptor (a fluorine atom) in place of a hydrogen bond donor (a hydroxy moiety) at the C20 position. Also from the standpoint of the importance of fluorine functionality in medicinal chemistry,⁶⁷ we decided to test the viability of **107** and its analogs as drug candidates. During the preparation of this thesis, Toru and co-workers reported the synthesis of 20-fluorocamptothecin starting from 20-deoxyCPT⁶⁸ by the electrophilic fluorination of 20-deoxycamptothecin using selectfluor (not shown).

5.2. Synthesis and Biological Evaluation of Analogs of 20-Fluorocamptothecin

Beginning with the known propargylated pyridone **108** (see Scheme 1.3, Chapter 1, $R^7 = H$), we synthesized a few analogs of **107** (Scheme 5.3). Thus, **108** was treated with DAST at -78°C to afford fluoropyridone **109** in 96% yield. Pyridone **109** was reacted with *p*-fluoro (**110a**) and 3,4-methylenedioxy isonitriles (**110b**) under the standard radical cyclization conditions to afford the corresponding camptothecins **111a-c** in moderate yields. The reaction with isonitrile **110b** produces a separable mixture of the 9,10- (**111b**) and the 10,11-substituted (**111c**) fluorocamptothecins in the ratio of 1:2.5 respectively. The assignment of the isomers was made based on the splitting pattern in the aromatic region of the ^1H NMR spectrum.

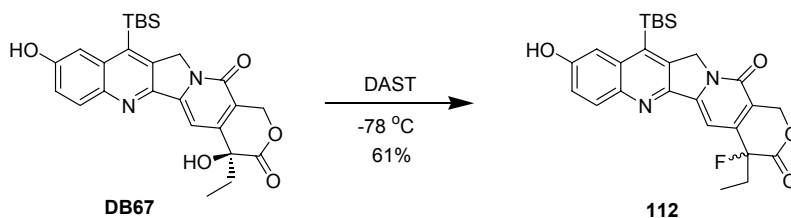


Isonitrile	Product	R^9	R^{10}	R^{11}	Yield, %
110a	111a	H	F	H	23
110b	111b		H	H	27
110b	111c	H		H	26

Scheme 5.3 Synthesis of Analogs of 20F-CPT

20F-DB67 **112** was synthesized in a semi-synthetic fashion from DB67 upon treatment with DAST at -78°C in a 61% yield (Scheme 5.4). Fortunately, the TBS group at the C7

position remained unaffected under these conditions. The structure of **112** was confirmed by NMR and MS techniques.



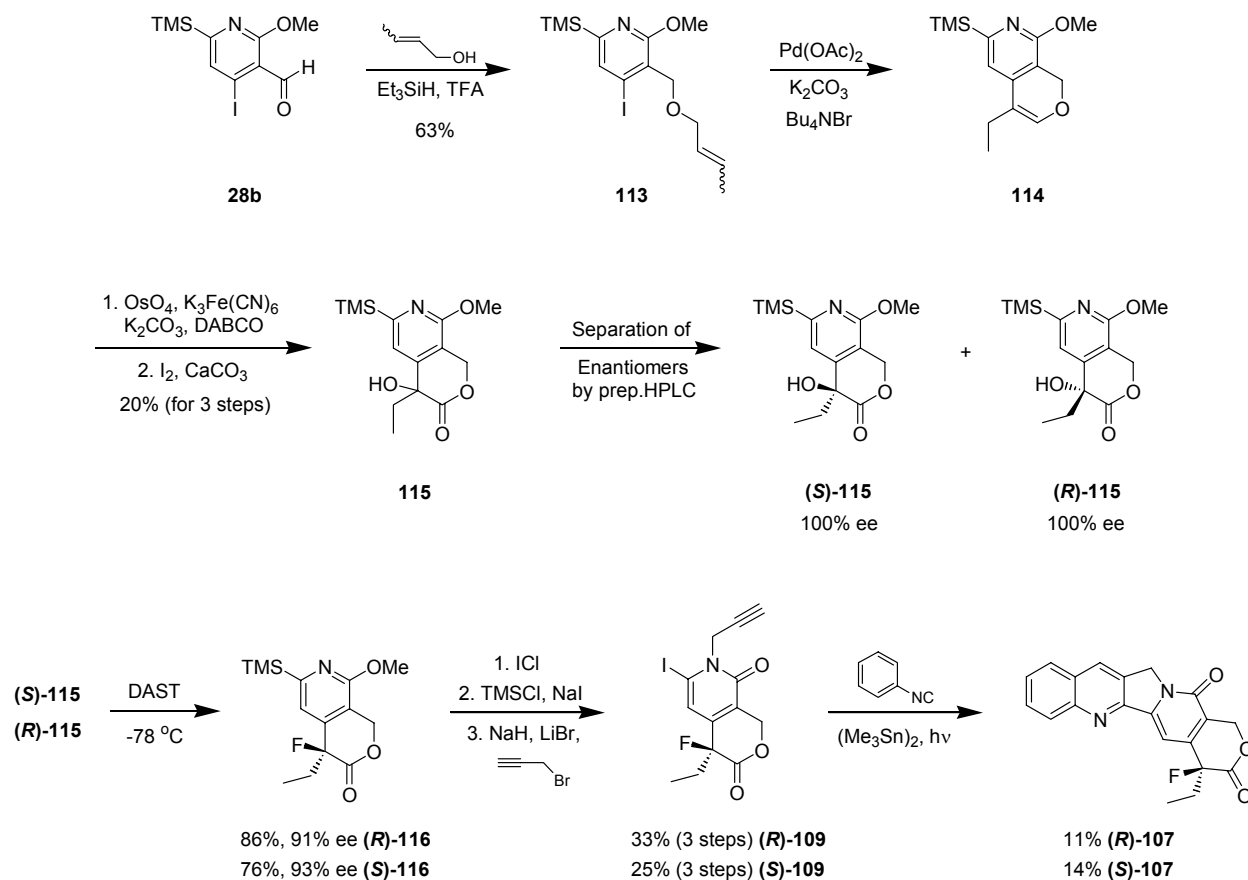
Scheme 5.4 Reaction of DAST with DB67

Fluorocamptothecins **107**, **111a-c** and **112** were sent for biological tests in the topoisomerase inhibitory assay. The assay conditions were identical to those described in previous chapters. The results of the assay showed that compounds **111a-c** were not active at concentrations ranging from 0.1 μM to 100 μM . However, compounds **107** and **112** showed only traces of activity at 100 μM . We hypothesized that the lack of activity was due to the “*R*” stereochemistry of the C20 stereocenter. If the fluorination reaction proceeded with inversion of configuration at C20, then the resulting (*20R*)-fluorocamptothecin would be inactive. A total synthesis of both the enantiomers and the racemate of **107** was undertaken to confirm the hypothesis.

5.3. Stereoselective Total Synthesis of *20S* and *20R*-Fluorocamptothecin

The synthesis of (*20R*)- and (*20S*)-fluorocamptothecins commences with the previously introduced aldehyde **28b** (see Scheme 2.7, Chapter 2) as shown in Scheme 5.5. A reductive etherification reaction⁶⁹ of **28b** with crotyl alcohol, Et_3SiH and TFA provided the crotyl ether **113** in 63% yield. Iodide **113** was subjected to an intramolecular Heck reaction in the presence of

$\text{Pd}(\text{OAc})_2$, K_2CO_3 and Bu_4NBr to afford the enol ether **114**. After an aqueous workup, the crude enol ether **114** was subjected to dihydroxylation under Sharpless' conditions but with DABCO in place of the chiral ligand⁷⁰ to afford the corresponding racemic diol (not shown).

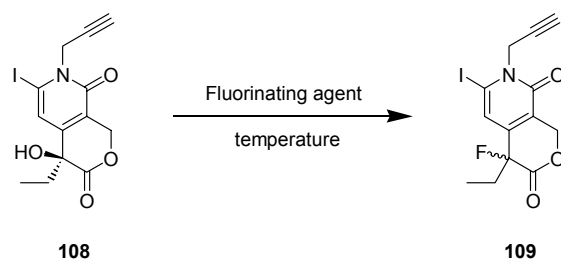


Scheme 5.5 Synthesis of 20-Fluorocamptothecin 107

After purification by column chromatography, this diol was oxidized to the lactone **115** on treatment with I_2 and CaCO_3 in an overall yield of 20% for the three steps. To access both the enantiomers of **115**, racemic alcohol **115** was separated into its constituent enantiomers **(S)-115** and **(R)-115** in 100% ee as determined by semi-preparative HPLC using (S,S) WHELK O 1 chiral column under isocratic elution (95:5 hexanes/isopropanol) conditions. The retention time of **(S)-115** under these conditions at the rate of 1 mL/min was 7.5 min and that of **(R)-115** was

10.5 min. When 68 mg of the racemic alcohol **115** was loaded on the HPLC with semi-preparative column in three injections, 21 mg each of the *R* and *S* enantiomers could be isolated.

The key fluorination reactions of (*S*)-**115** and (*R*)-**115** with DAST were carried out at -78 °C to afford the fluoropyridines (*R*)-**116** and (*S*)-**116** respectively in 86% and 76% yields with good chiral transfer in 91% and 93% ee respectively as shown by HPLC analysis using (S,S)-WHELK O 1 chiral column under isocratic elution (95:5 hexanes/isopropanol) conditions. The retention time of (*S*)-**116** under these conditions at the rate of 1 mL/min was 10.6 min and that of (*R*)-**116** was 18.0 min. The stereochemical assignment of fluoropyridines **116** will be described later. Pyridine lactone **115** was identified as a suitable intermediate for performing the fluorination reaction after it provided the best yield and cleaner reaction in comparison to other intermediates in the synthesis.⁷¹ In a comparison study between DAST and the other well-known fluorinating agent Deoxofluor $[(\text{CH}_3\text{OCH}_2\text{CH}_2)_2\text{NSF}_3]$,⁷² in which the temperature, time of the reaction and the equivalents of the fluorinating agent were varied, we discovered that the reactions with DAST afforded cleaner products, better yields and conversions and were completed in shorter times (Table 5.1).

Table 5.1 Comparison of DAST and Deoxofluor for the Fluorination of 108

Entry	Temperature	Rxn. time	Fluorinating Agent	
			DAST (pdt. yield)	Deoxofluor (pdt. yield)
1.	Room temp.	30 min	109 (25%)	109 (23%)
2.	-40 °C	1.5 h	109 (67%)	109 (60%)
3.	-78 °C	5 h	109 (96%)	109/108 (3:2, 25%)

Pyridine lactones **116** were converted to the pyridones **109** in three steps. First, an iododesilylation reaction using ICl afforded the corresponding enantiomeric iodides. Second, a demethylation reaction of these iodides with *in situ* generated TMSI gave the corresponding pyridones. Third, the pyridones were alkylated with propargyl bromide in the presence of NaH and LiBr to give both enantiomers of **109** in overall yields of 33% and 25% for three steps. We were pleased to observe good yields with the iododesilylation reaction of **116** (59% and 65%) which, with most other similar substrates, was a low-yielding step.

The key radical cyclization was carried out with the propargylated pyridones **109** and phenyl isonitrile in the presence of (Me₃Sn)₂ under photo-irradiation conditions to give both the enantiomers of 20-fluorocamptothecin (**R**)-**107** and (**S**)-**107** in 11% and 14% yields after purification by flash column chromatography. The purity of fluorocamptothecins **107** was

confirmed by NMR and MS techniques. Also, the ^1H and ^{13}C NMR spectra of these samples matched with that of **107** made via the semisynthesis route (see Scheme 5.2). Racemic **107** was synthesized following the reaction sequences described in Scheme 5.3 starting from racemic **108**. The three samples, (*R*)-**107**, (*S*)-**107** and (\pm)-**107**, were sent for the preliminary biological evaluation and the results from this are shown in Figure 5.1.

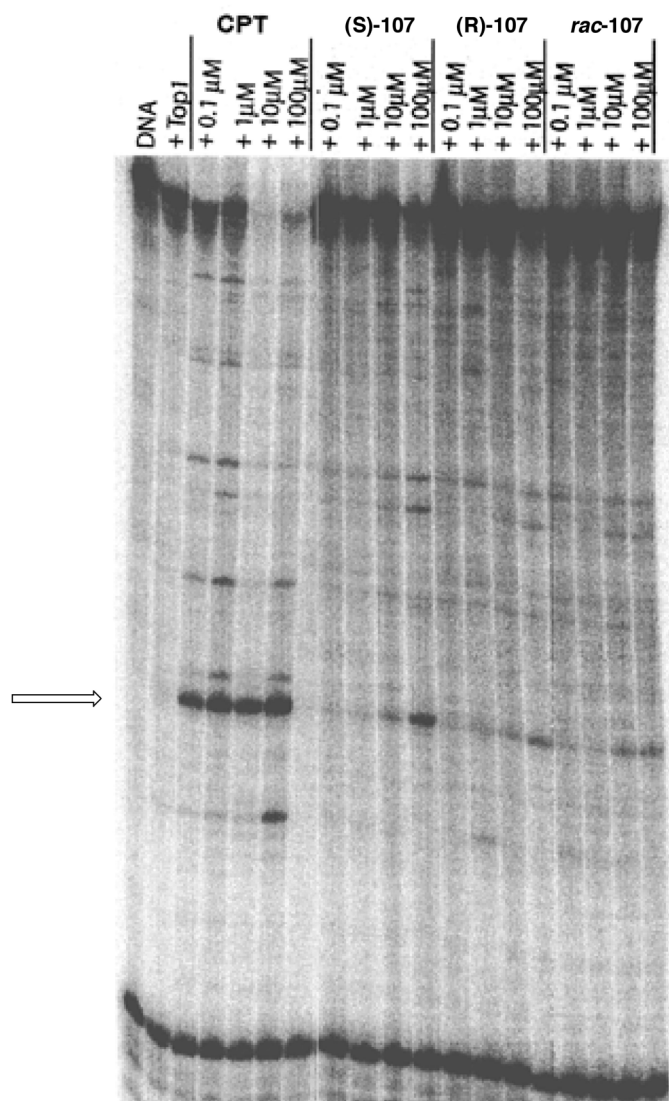


Figure 5.1 Results of the Topo I Inhibitory DNA Cleavage Assay of Derivatives (*S*)-**107**, (*R*)-**107** and *rac*-**107**

The first two lanes in the gel display show the controls DNA and topo I in the absence of CPT. As expected, no cleavage products were observed. The next set of four lanes shows CPT control and the cleavage products are clearly observed. Each of these four lanes refers to the concentrations 0.1 μM , 1 μM , 10 μM and 100 μM respectively. The next three sets of lanes show the assay results of **(S)-107**, **(R)-107** and **(±)107** in that order. The DNA cleavage products are indicated by the arrow in Figure 5.1.

The electrophoresis experiments showed that both the enantiomers of **107** showed activity at a concentration of 10 μM . We assigned the compound with the highest intensity to be **(S)-107** and the less intense one **(R)-107** based on the known premise that only (*S*)-camptothecins are biologically active (see Section 1.3, Chapter 1). Tracing backwards in the reaction sequence, we determined that **(S)-107** was obtained from **(S)-116** which in turn was obtained from the fluorination of **(R)-115**. Thus, the reaction with DAST had occurred with an inversion of configuration. Racemic **107** also showed some weak activity at 10 μM concentration. The small selection of analogs presented in Section 5.2 had, therefore, been synthesized in the “wrong” configuration. Resynthesis and biological reevaluation of these analogs is currently in progress in our laboratories to confirm the configuration of the biologically active enantiomer of **107**.

The fluorocamptothecins can also be envisioned as good substrates for the determination of the function of the lactone moiety in DNA/Topo I interactions by using high-field ^{19}F NMR spectroscopy. This allows the study of the dynamics of the ternary complex possible without isotopic labeling the protein. Studies using this technique in combination with computational modeling are currently in progress.

5.4. Summary

This chapter described the accidental discovery of the 20-fluorocamptothecins (20F-CPTs) that were synthesized from their alcohol counterparts upon reaction with DAST. A small assortment of analogs of 20F-CPT was synthesized. However, these compounds showed no activity in the topoisomerase inhibitory assay. The two enantiomers of **107** have also been synthesized and submitted for biological testing. It was found that (**S**)-**107** displayed activity at 10 μ M concentration while the *R* enantiomer showed no activity. Further research in the synthesis and biological studies of additional analogs of 20F-CPT with *S* configuration at the C20 position is underway.

6. TOTAL SYNTHESIS OF LUOTONIN A AND ITS ANALOGS USING CASCADE RADICAL CYCLIZATION

6.1. Introduction

In 1997, Nomura and coworkers reported the isolation of a pyrroloquinazolinoquinoline alkaloid, luotonin A, extracted from the Chinese medicinal plant *Peganum nigellastrum*.⁷³ The structure of luotonin A bears striking similarities to the well-studied topo I poison, camptothecin (Figure 6.1).

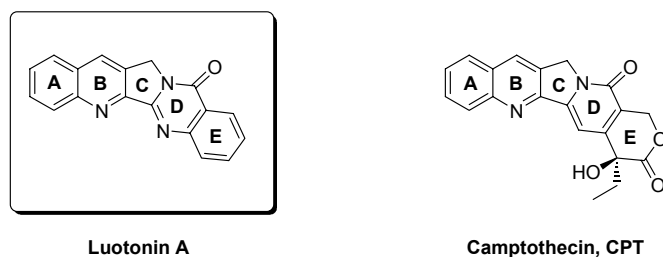


Figure 6.1 Structures of Luotonin A and Camptothecin

The structural similarities are in the rings A-C which are identical in luotonin A and CPT. The differences are in the D-ring in which pyrimidone moiety replaces the pyridone in CPT and the E-ring in which the lactone moiety, thought to be crucial for the biological activity of CPT, is absent in luotonin A. The lack of any functionality in the E-ring of luotonin A is interesting in light of several reports that modifications in the E-ring resulted in either diminishing or destroying CPT's activity (see Section 1.3, Chapter 1).

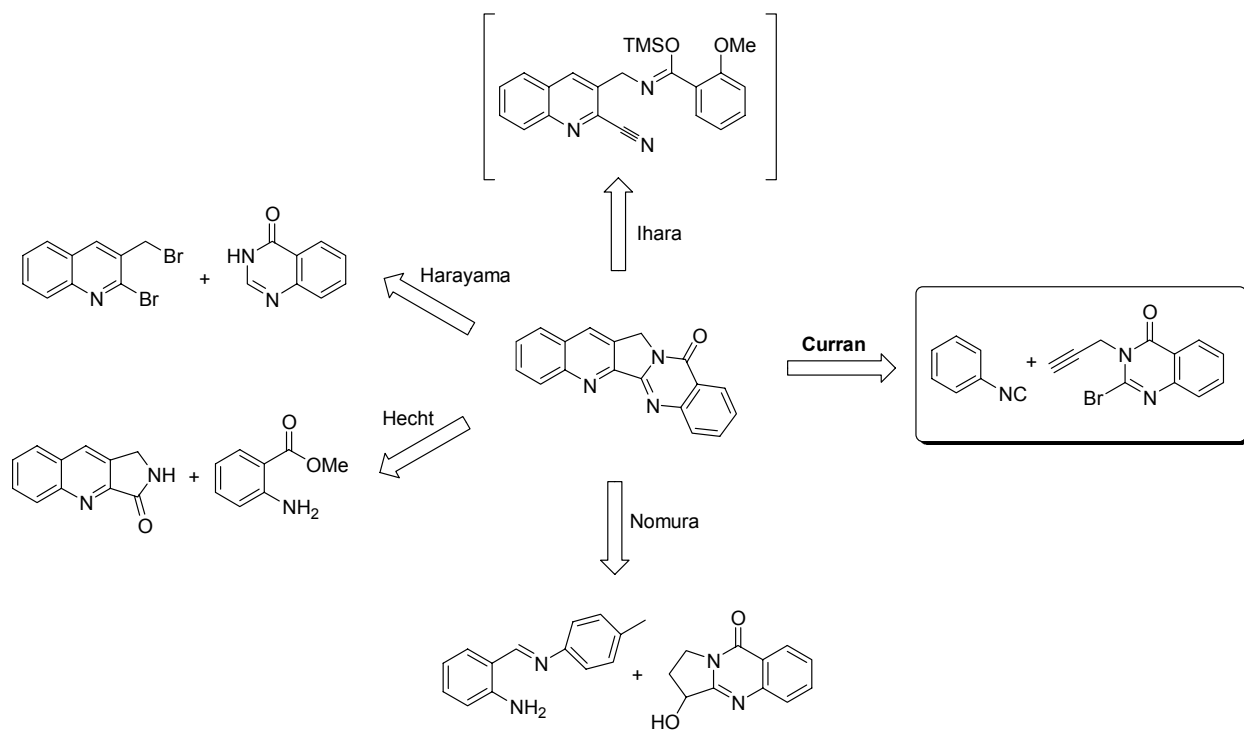
Furthermore, recently Hecht and coworkers reported that luotonin A mediates topoisomerase I-dependent cytotoxicity much like CPT. It was demonstrated that despite the lack of lactone moiety and the tertiary alcohol stereocenter in the E-ring, luotonin A stabilizes the

human DNA- topo I covalent binary complex forming a ternary complex. Luotonin A was found to be cytotoxic towards the murine leukemia P-388 cell line with an IC₅₀ of 1.8 µg/mL. It was also observed that luotonin A displays identical sequence selectivity of DNA cleavage by topo I to that of CPT in the electrophoresis experiments. With its similarities in structure and function to CPT, luotonin A was an attractive synthetic target to many research groups.

6.2. Synthetic Approaches to Luotonin A

A brief summary of the five distinct synthetic approaches to luotonin A reported thus far is shown in Scheme 6.1. Ihara reported a synthesis employing an intramolecular hetero Diels-Alder reaction⁷⁴ with a suitable aza-diene and cyano group as the dienophile. Harayama used an alkylation followed by an intramolecular Pd-assisted biaryl coupling in the presence of tricyclohexylphosphine as the ligand and KOAc as the base to afford the desired luotonin A.⁷⁵

The classical Friedlander condensation of the dihydropyrroloquinolinone with 2-aminobenzoate was the method of choice of Hecht.⁷⁶ Several other research groups employed the Friedlander condensation in their synthesis of luotonin A.⁷⁷ The key difference in these syntheses is the choice of the aniline derivative for the condensation. Nomura reported the reaction of the pyrroloquinazoline derivative with *N*-(2-aminobenzylidene)-*p*-toluidine in the presence of *p*TsOH.⁶⁸



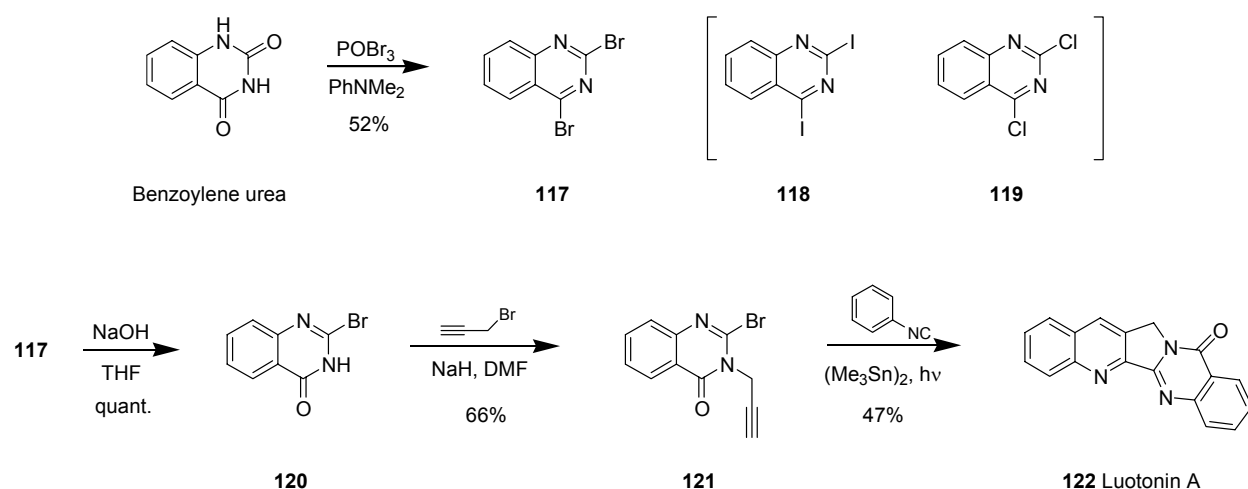
Scheme 6.1 Synthetic Approaches to Luotonin A

While many of these syntheses are elegant, they are not sufficiently flexible to allow the ready functionalization of the parent luotonin A. Our approach (shown in the box in Scheme 6.1), on the other hand, is modular in nature and facilitates quick access to several derivatives of luotonin A, particularly the A,B-ring analogs. In addition, the mild conditions of the radical reaction make it possible to tolerate a wide variety of functional groups.

6.3. Total Synthesis of Luotonin A

The synthesis of luotonin A commenced with the synthesis of dibromoquinazoline **117** as shown in Scheme 6.2. Commercially available benzoylene urea was treated with POBr_3 and *N,N*-dimethylaniline under solvent-free conditions at 105 °C to afford the quinazoline **117** in 52% yield. This use of solvents (such as CH_2Cl_2 , CH_3CN) in the dibromination reaction led to either

poor yields of the desired product or recovery of starting material. Diiodoquinazoline **118** is a better substrate in this synthetic scheme that could be carried over to luotonin A since iodides are better radical precursors than bromides. Despite several attempts at the synthesis of **118**, we were unsuccessful starting either from benzoylene urea (using PPh_3 , I_2 , Et_3N) or from the dichloride **119** ($\text{Bu}_4\text{NI}/\text{THF}$; $\text{NaI}/\text{CH}_3\text{CN}$; aq. HI) or any of its derivatives due to either the formation of multiple products or unreactive starting material.



Scheme 6.2 Total Synthesis of Luotonin A

Dibromoquinazoline **117** was then subjected to monohydrolysis on treatment with 1N NaOH to afford the bromoquinazolinone **120** as the sole product in quantitative yield as indicated by ^1H NMR, ^{13}C NMR and MS analysis. A short reaction time (~ 2 h) is essential to avoid nonselective hydrolysis resulting in a complex mixture. Quinazolinone **120** was next treated with propargyl bromide in the presence of NaH to effect *N*-alkylation affording propargylated quinazolinone **121** in 66% yield. Under these reaction conditions, no *O*-alkylation product was observed as indicated by ^1H and ^{13}C NMR analysis. Bromide **121** was then converted to luotonin A **122** under photoirradiation conditions upon treatment with phenyl

isonitrile in the presence of $(\text{Me}_3\text{Sn})_2$ in 47% yield after purification by flash column chromatography. The structure of **122** was confirmed by NMR and MS techniques and the data matched that reported in the literature.⁶⁸

6.4. Synthesis of Analogs of Luotonin A

Although luotonin A has been the subject of many syntheses, there is very limited knowledge about the effect of different substitution patterns in terms of the biological activity. Recently, Hecht reported a series of E-ring derivatives of luotonin A and evaluated them for topo I inhibitory activity (Figure 6.2). E-ring analogs **124**, **125** and **127** have shown good DNA-topo I stabilization. Among luotonins **123**, 17-chloroluotonin A ($\text{R}^1 = \text{R}^3 = \text{H}$, $\text{R}^2 = \text{Cl}$) displayed good biological activity.

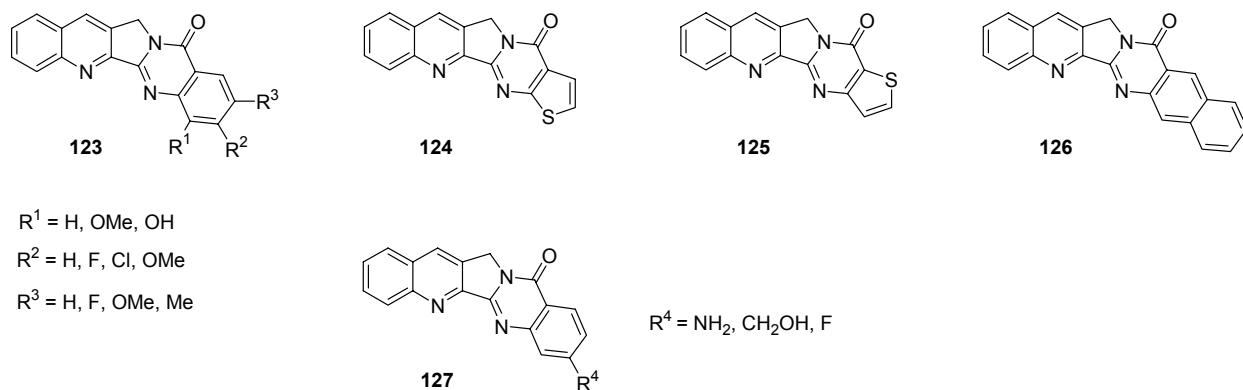
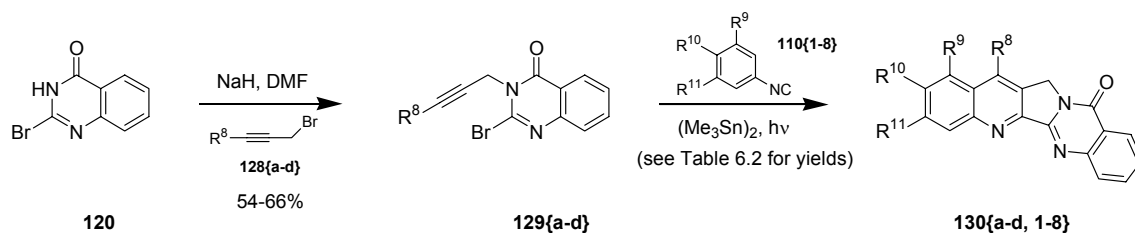


Figure 6.2 Hecht's E-ring Analogs of Luotonin A

The modular nature of our synthesis, in addition to its conciseness, presents a good opportunity to synthesize several analogs in a quick manner. In a complementary fashion to Hecht's synthesis of E-ring derivatives, our strategy could be used to synthesize a library of A,

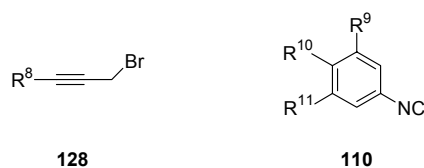
B-ring derivatives thus building a more complete SAR profile of luotonin A. The planned synthesis of the 4 x 8 library of luotonins is shown in Scheme 6.3.



Scheme 6.3 Synthesis of Library of Luotonin A Analogs

Prior to undertaking the library synthesis, 1.4 g of the key bromoquinazolinone intermediate **120** was synthesized according to the chemistry described in Scheme 6.2. All the reactions leading to the final luotonins were performed using standard laboratory techniques in a serial fashion. The requisite building blocks for the library synthesis are shown in Table 6.1. Four propargyl bromides **128{a-d}**, that were chosen based on previous experience in our laboratories, were synthesized according to literature procedures.⁵²

The isonitriles were chosen based on their electron-withdrawing character (**110{2}** and **110{3}**), electron-donating character (**110{4}**, **110{5}** and **110{8}**) and hydrogen bond donor capacity (**110{6}** and **110{7}**). All the isonitriles were synthesized following previously reported procedures.⁴⁴

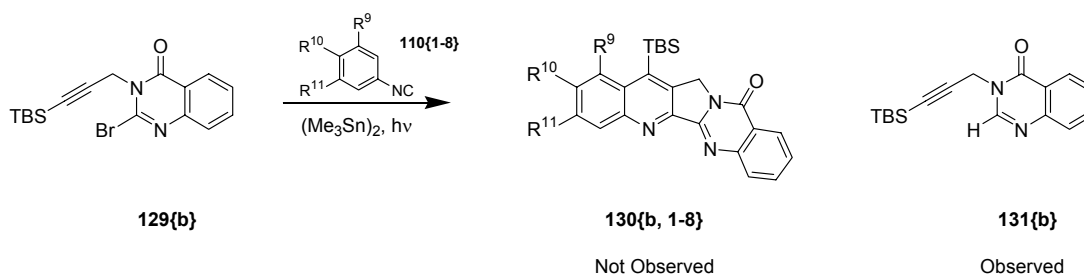
Table 6.1 Building Blocks for the Luotonin Library

Propargyl bromides		Isonitriles			
R^8	Entry	R^9	R^{10}	R^{11}	Entry
		H	H	H	110{1}
		H	F	H	110{2}
H	128{a}	H	CF ₃	H	110{3}
TBS	128{b}	H	Me	H	110{4}
Et	128{c}	H	OMe	H	110{5}
CH ₂ CH ₂ TMS	128{d}	H	OAc	H	110{6}
		H	NHBoc	H	110{7}
		H	OCH ₂ CH ₂ O	--	110{8}

Quinazolinone **120** was reacted with four propargyl bromides **128{a-d}** to afford four propargylated quinazolinones **129{a-d}** in 54-66% yields. Each of the four bromides **129{a-d}** was subjected to the radical cascade cyclization with eight isonitriles **110{1-8}** under photoirradiation conditions in the presence of (Me₃Sn)₂ to afford 32 products **130{a-d, 1-8}** in moderate to good yields (see Table 6.2). For the final radical cyclizations, groups of four reactions were irradiated simultaneously and each crude product was purified by a quick column chromatography to separate the excess tin and isonitrile derivatives from the desired product. In the case of the reaction of **129** with 3,4-ethylenedioxy isonitrile **110{8}**, two regioisomeric products, 9,10-ethylenedioxy luotonin and the 10,11-ethylenedioxy luotonin,⁶⁵ were obtained

and could be separated only by a semi-preparative HPLC, the details of which are discussed later in this chapter.

The compounds obtained after purification by column chromatography were analyzed by ^1H NMR spectroscopy and the structures of some of the compounds were confirmed. This ^1H NMR analysis, however, revealed an unexpected problem with some of the products of the radical cyclization. Compounds **130{b,1-6}** and **130{b,8}**, expected to be luotonins, displayed fewer than expected aromatic resonances. The proton signals of the substituent R^{10} (see Scheme 6.3) were completely absent in all the ^1H NMR spectra. Also, an additional singlet proton resonance was observed at 9.79 ppm in addition to only four aromatic resonances (two doublets and two triplets). Based on this analysis by ^1H NMR and MS techniques, it was concluded that the products **130{b,1-6}** and **130{b,8}** were all the same compound **131{b}** obtained by the direct reduction of the bromide **129{b}** under the reaction conditions (Scheme 6.4). The additional proton signal at 9.79 ppm is explained by the newly formed pyrimidinyl proton. 7-TBS-10-NHBoc luotonin, **130{b,7}** was the only luotonin recovered among **130{b,1-8}**. The same reduction behavior was also observed with a few products formed from **129{d}** (not shown). The reason for this premature reduction of the bromides **129{b}** is still unclear especially because all the 32 radical cyclizations were conducted at the same concentration.



Scheme 6.4 Unexpected Side Reaction of 129{b}

Table 6.2 Luotonin Library - Compound Numbers and Isolated Yields from Column Chromatography

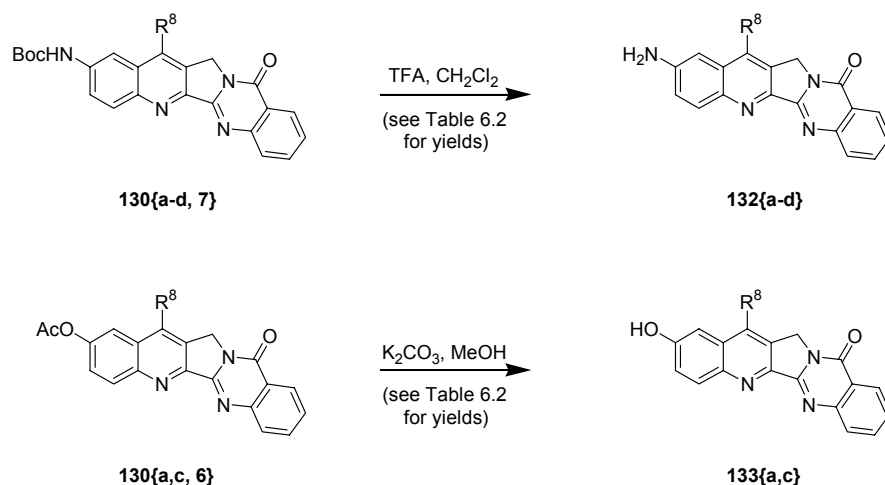
R^{10} \ R^8	H	TBS	Et	CH ₂ CH ₂ TMS
H	130{a,1} 47%	130{b,1} Red	130{c,1} 68%	130{d,1} Uidf
F	130{a,2} 65%	130{b,2} Red	130{c,2} 75%	130{d,2} Red
CF ₃	130{a,3} 71%	130{b,3} Uidf	130{c,3} 62%	130{d,3} Uidf
Me	130{a,4} 57%	130{b,4} Red	130{c,4} 33%	130{d,4} Uidf
OMe	130{a,5} 63%	130{b,5} Red	130{c,5} 86%	130{d,5} 74%
OAc	130{a,6} 62%	130{b,6} Red	130{c,6} 39%	130{d,6} Red
NHBoc	130{a,7} 52%	130{b,7} 31%	130{c,7} 94%	130{d,7} 37%
OCH ₂ CH ₂ O (9,10 & 10,11)	130{a,8} Uidf	130{b,8} Red	130{c,8} 86%	130{d,8} 94%

- Red - Reduced product (e.g., **131{b}**, see Scheme 6.4)
- Uidf - Unidentifiable product from ¹H NMR analysis

Studies in the field of camptothecins and homocamptothecins have shown that hydrogen bond donor substitution at the C¹⁰ (i.e., R¹⁰) has been beneficial to their biological activity. Owing to the similarities of luotonin A to CPT in its function as a topo I poison, we decided to

synthesize luotonin derivatives (possessing OH and NH₂ functionalities) that would address the effects of hydrogen bonding on the drug's biological activity.

To synthesize 10-hydroxy and 10-amino luotonins (**130**, R¹⁰ = OH and NH₂ respectively, Scheme 6.3), deprotections of the previously synthesized 10-acetoxy and 10-Boc protected aminoluotonins were undertaken (Scheme 6.5).



Scheme 6.5 Synthesis of 10-hydroxy and 10-aminoluotonins

Four Boc-protected amines **130** {a-d,7} were treated with TFA in CH₂Cl₂ (1:2 v/v) at room temperature for 12 h allowing for the cleavage of the Boc group. The two acetates **130**{a,c,6} were also cleaved upon treatment with 4 equiv of K₂CO₃ in a 1:1 MeOH/H₂O at room temperature for about 5 h. Unfortunately only one carbamate, **130**{d,7}, could be successfully deprotected to afford amine **132**{d} in 85% yield after purification by flash column chromatography. None of the other carbamates **130**{a-c,7} or the acetates **130**{a,c,6} the corresponding amines and alcohols as indicated by TLC. ¹H NMR analysis showed only traces of the desired amines and alcohols.

Ultimately, 22 luotonins were analyzed by HPLC with an analytical Novapak silica column employing isocratic elution with EtOAc/CH₂Cl₂ (2:98, 5:95, 8:92 or 15:85 depending upon the polarity of the luotonin). Nineteen compounds displayed good to excellent purities ranging from 75% to 95%. However, to guarantee high purity of the luotonins for biological testing, the products isolated from column chromatography were further purified by semi-preparative HPLC using a Novapak silica column under solvent elution conditions employed for the analytical HPLC study. Following the purification by HPLC, all the luotonins were characterized by LC-MS using XTerra C18 reverse phase column for LC and EI detection for MS. Fourteen luotonins showed high purities ranging from 90-100% and the remaining five displayed purities ranging from 75%-85%. They also displayed the expected molecular ions (M⁺) along with higher peaks (i.e. M + H, M + Na).

While the structures and purities of all the luotonins were confirmed by ¹H NMR and LC-MS, complete characterization of four of the luotonins, **130{a,1}**, **130{c,8}**, **130{a,3}** and **130{a,4}**, was also carried out and is described in the experimental section. A table of the structures, amounts and purities of the final fourteen luotonins is shown in Figure 6.3. These luotonins are currently in the course of being tested for topoisomerase I inhibitory activity.

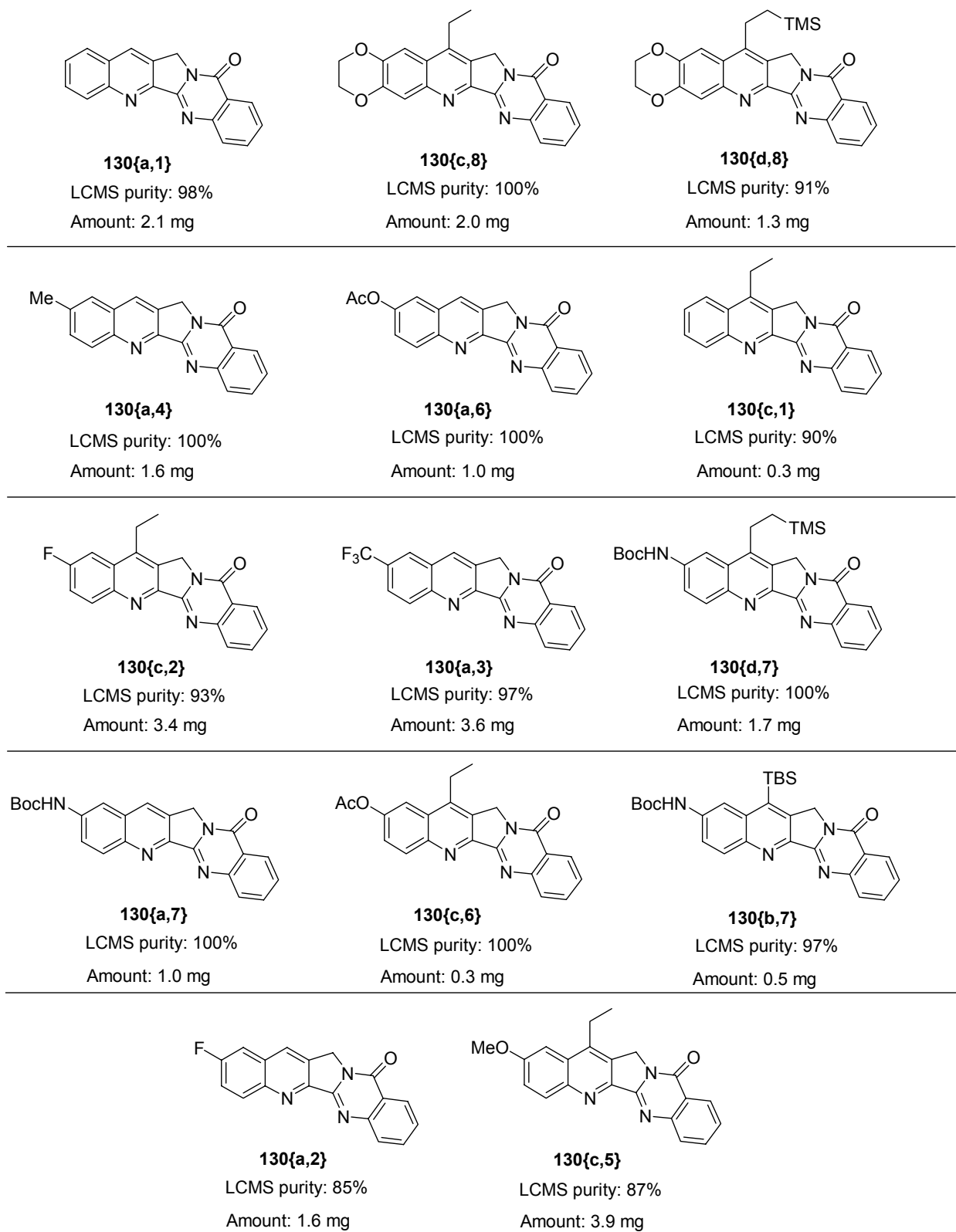


Figure 6.3 Structures, Amounts and LCMS Purities of Luotonins

6.5. Summary

This chapter described the synthesis of a recently isolated topo I poison, luotonin A and its analogs. The striking similarities in structure and biological function of luotonin A to those of CPT made luotonin A an attractive target in the synthetic community. A concise, modular and a rapid synthesis of several analogs of luotonin A was also described. Biological evaluation of these analogs, currently underway, will provide more insight into the structure-activity relationships of luotonin A that could lead to a promising chemotherapeutic drug.

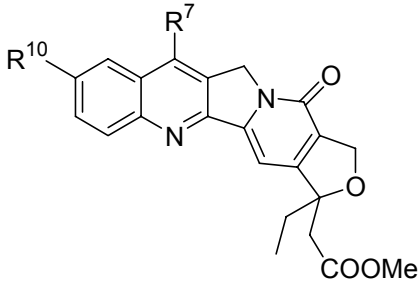
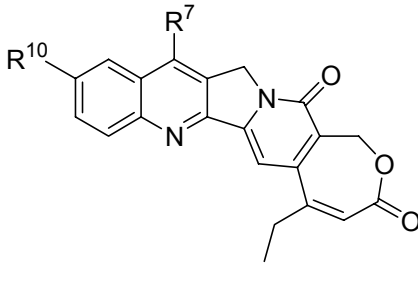
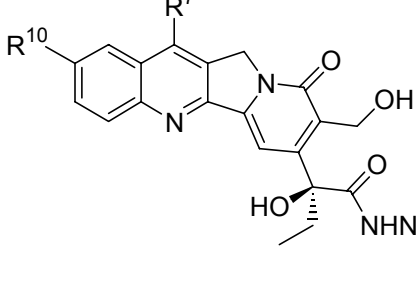
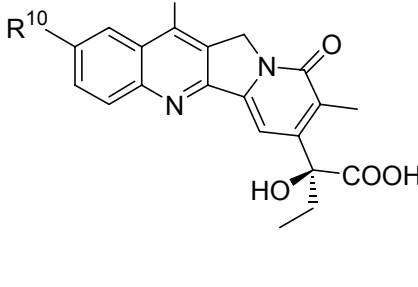
7. SUMMARY AND CONCLUSIONS

The central theme of the research presented in this thesis revolved around the synthesis of analogs of camptothecin differing mainly in the D and E rings of the pentacyclic skeleton. Accordingly, homocamptothecin, cyclic ether and enelactone derivatives, open-form analogs, fluorocamptothecins and luotonins were synthesized. Within each of these five modifications, the analogs differed in their A, B-ring substitution patterns.

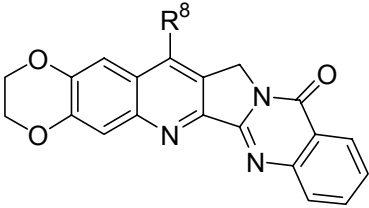
The biological activity of all these analogs was tested in two assays: topoisomerase I inhibitory DNA cleavage assay and the cell growth inhibition SRB assay. The topo I inhibitory assays revealed that non-lactone analogs (cyclic ethers) were not biologically active and enelactones **95a** and **95b** showed cleavage products only at a concentration of about 100 μM . The fluorocamptothecins, on the other hand, were weakly active. Among the parent fluorocamptothecin enantiomers, (*S*)-**107** and (*R*)-**107** showed cleavage products at 10 μM and 100 μM concentrations and thus were weakly active. The racemate (\pm)-**107** showed some weak activity. Luotonins are currently being biologically evaluated.

With regards to the biological activity, the most interesting analogs in this research have been the E-ring open form analogs. Hydrazides **96** and **97** have shown DNA cleavage profiles comparable to that of camptothecin. Also, the cell growth inhibition studies indicated that the GI_{50} values of **96** and **97** were about 20 nM and 100 nM respectively. These values are comparable to those of CPT and DB67 which are about 10 nM. These compounds show promise and further development of these analogs is needed to understand the implications of open form analogs in the broad picture of analog development of camptothecin. The following is a tabular summary of all the biological results.

Table 7.1 Summary of the Biological Results

Entry	Structure of the Analog	Compd.no.	GI ₅₀ (nM)	DNA clvg. assay activity
1.		92a , R ⁷ = H, R ¹⁰ = H 92b , R ⁷ = H, R ¹⁰ = F 92c , R ⁷ = TBS, R ¹⁰ = H 92d , R ⁷ = TBS, R ¹⁰ = F	- - - -	- - - -
2.		95a , R ⁷ = H, R ¹⁰ = H 95b , R ⁷ = H, R ¹⁰ = F 95c , R ⁷ = TBS, R ¹⁰ = H 95d , R ⁷ = TBS, R ¹⁰ = F	- - - -	+ + - -
3.		96 , R ⁷ = H, R ¹⁰ = H 97 , R ⁷ = TBS, R ¹⁰ = OH	20 100	++ ++
4.		101 , R ⁷ = H, R ¹⁰ = H 102 , R ⁷ = TBS, R ¹⁰ = OH	- -	- -

Entry	Structure of the Analog	Compd.no.	GI ₅₀ (nM)	DNA clvg. assay activity
5.		rac-107 (R)-107 (S)-107	- - -	+ + +
6.		111a , R ⁹ = R ¹¹ = H 111b , R ⁹ , R ¹⁰ = OCH ₂ O, R ¹¹ = H 111c , R ⁹ = H, R ¹⁰ , R ¹¹ = OCH ₂ O	- - -	- - -
7.		112	-	-
8.		130{a,1} , R ⁸ = R ¹⁰ = H 130{a,4} , R ⁸ = H, R ¹⁰ = Me 130{a,6} , R ⁸ = H, R ¹⁰ = OAc 130{c,1} , R ⁸ = Et, R ¹⁰ = H 130{c,2} , R ⁸ = Et, R ¹⁰ = F 130{a,3} , R ⁸ = H, R ¹⁰ = CF ₃ 130{d,7} , R ⁸ = CH ₂ CH ₂ TMS, R ¹⁰ = BocNH 130{a,7} , R ⁸ = H, R ¹⁰ = BocNH 130{c,6} , R ⁸ = Et, R ¹⁰ = OAc 130{b,7} , R ⁸ = TBS, R ¹⁰ = BocNH	To be determined	To be determined

Entry	Structure of the Analog	Compd.no.	GI ₅₀ (nM)	DNA clvg. assay activity
9.		130{c,8} , R ⁸ = Et 130{d,8} , R ⁸ = CH ₂ CH ₂ TMS	To be determined	To be determined

- No or negligible activity
- + Weakly active
- ++ Moderate to good activity

8. EXPERIMENTAL

General Procedures

All reactions were performed under argon atmosphere unless otherwise noted. Air and moisture sensitive chemicals were handled by using standard syringe techniques. THF and diethyl ether were either distilled from sodium/benzophenone under argon or were dried by activated alumina according to literature procedure.⁷⁸ Dichloromethane was distilled from calcium hydride under argon or dried by activated alumina according to the above reference. DMSO and acetonitrile were used from a Sure/SealTM bottle purchased from Aldrich. Diisopropylamine was distilled from NaOH under argon immediately prior to use. LiCl was predried under vacuum at 120 °C for 24 h before use. 4Å molecular sieves were predried under vacuum at 150 °C for 24 h before use. All other chemicals and solvents were purchased from chemical companies and used without purification unless otherwise stated.

Experimental procedures and spectroscopic data for new compounds other than the library members are reported in this experimental section. All library compounds have been characterized by ¹H NMR and MS or LCMS. ¹H, ¹⁹F and ¹³C spectra were recorded on Bruker models Avance DPX 300 (300 MHz), Avance DRX 500 (500 MHz) NMR spectrometers. ¹⁹F spectra were recorded with CFCl₃ as the reference solvent. Chemical shifts (δ) are reported in ppm. In reporting data, the following abbreviations were used: s = singlet, br s = broad singlet, d = doublet, t = triplet, q = quartet, dd = doublet of doublet, ddd = doublet of doublet of doublet, dt = doublet of triplet, dq = doublet of quartet, tq = triplet of quartet, tt = triplet of triplet and m = multiplet. Coupling constants (J) are reported in Hertz (Hz). IR spectra were recorded as thin films on NaCl plates (unless otherwise noted) on an ATI Mattson Genesis Series FTIR spectrometer. The peaks are reported in wavenumbers (cm⁻¹). Low resolution mass spectra were

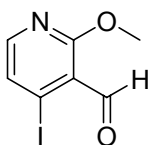
obtained on a Fisions Autospec in EI mode at 70 eV and are reported in m/z units. High resolution mass spectra were taken on a VG-Autospec double focusing spectrometer. Optical rotations were measured on a Perkin-Elmer 241 polarimeter at the Na D-line ($\lambda = 589$ nm) using a 1 dm cell. Analytical chiral HPLC analyses were conducted using either a Chiralcel-OD column (Daicel Chemical Industries) or an (S,S)-WHELK O 1 (Regis Technologies Inc.) column with a Waters model 440 UV detector at wavelengths 254 and 210 nm.

Thin layer chromatography (TLC) was performed on silica gel 60 F₂₅₄ glass backed plates with a layer thickness of 0.25 mm manufactured by E. Merck. TLC visualization was performed by illumination with a 254 nm UV lamp or by staining with phosphomolybdic acid or permanganate solution and subsequent heating. Flash chromatography was performed on silica gel (230 – 400 mesh ASTM) purchased from Sorbtech or Bodman.

Caution: Camptothecin and its derivatives can be toxic. All experiments must be done in a well-ventilated hood. Gloves and goggles must be worn at all times.

Chapter 2

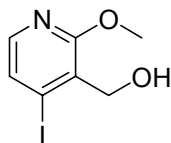
4-Iodo-2-methoxypyridine-3-carbaldehyde (28a):



Methylolithium in diethyl ether (1.4 M, 24 mL, 33 mmol) was added to a solution of 2-methoxypyridine (1.9 mL, 18 mmol) in THF (120 mL) at -40 °C. Diisopropylamine (0.13 mL, 0.90 mmol) was added and the color changed from colorless to yellow-orange. After warming to 0 °C and stirring for 3 h, the mixture was cooled to -78 °C and *N,N,N'*-trimethyl-*N'*-formylethylenediamine (2.6 g, 20 mmol) was added slowly. The reaction was allowed to warm

to $-40\text{ }^{\circ}\text{C}$ immediately. *n*BuLi in hexanes (1.6 M, 23 mL, 37 mmol) was added dropwise through a syringe and the mixture was stirred for 3 h at $-30\text{ }^{\circ}\text{C}$. A solution of I_2 (11 g, 44 mmol) in THF (70 mL) kept at $0\text{ }^{\circ}\text{C}$ in a jacketed dropping funnel was then added dropwise at $-78\text{ }^{\circ}\text{C}$ with vigorous stirring. After 30 min, the resulting mixture was allowed to warm slowly to $0\text{ }^{\circ}\text{C}$ (1 h), poured into 5% Na_2SO_3 (250 mL) and extracted with Et_2O (3 x 150 mL). The residue obtained after removal of the solvents was purified by flash column chromatography (95:5 hexanes/ethyl acetate) to provide **28a** as a yellow oil (1.9 g, 40%): ^1H NMR (300 MHz, CDCl_3) δ 4.06 (s, 3H), 7.54 (d, $J = 5.3$ Hz, 1H), 7.86 (d, $J = 5.3$ Hz, 1H), 10.21 (s, 1H); ^{13}C NMR (75 MHz, CDCl_3) δ 54.6, 108.7, 119.4, 130.5, 151.0, 164.4, 190.4; IR (CH_2Cl_2 , NaCl, cm^{-1}) 1703, 1551, 1462, 1368, 1298, 1265, 1017, 847, 736; HRMS (EI) m/z calcd for $\text{C}_7\text{H}_6\text{INO}_2$ (M^+) 262.9443, found 262.9431; LRMS (EI) m/z 263 (M^+ , 100), 234 (80), 205 (30), 127 (30), 93 (28), 78 (72).

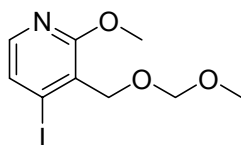
(4-Iodo-2-methoxypyridin-3-yl)methanol (29a):



A solution of NaBH_4 (0.14 g, 3.6 mmol) in EtOH (20 mL) was added slowly to a solution of **28a** (1.9 g, 7.1 mmol) in EtOH (20 mL) at $0\text{ }^{\circ}\text{C}$. After stirring for 4 h at $0\text{ }^{\circ}\text{C}$, the reaction mixture was carefully quenched with an ice-cold brine solution and extracted with Et_2O (3 x 30 mL). The combined organic extracts were dried over MgSO_4 and solvents were removed under reduced pressure to afford **29a** as a pale yellow oil (1.8 g, 97%). The crude product was used crude for the subsequent reaction: ^1H NMR (300 MHz, CDCl_3) δ 2.43 (t, $J = 7.0$ Hz, 1H), 3.99 (s, 3H), 4.82 (d, $J = 7.0$ Hz, 2H), 7.35 (d, $J = 5.4$ Hz, 1H), 7.70 (d, $J = 5.4$ Hz, 1H); ^{13}C NMR (75 MHz, CDCl_3) δ 54.3, 64.9, 112.1, 126.5, 128.1, 146.6, 161.7; IR (CH_2Cl_2 , NaCl, cm^{-1}) 3391, 2946,

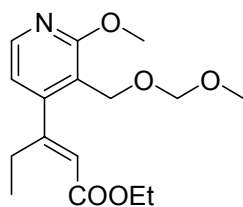
1561, 1459, 1380, 1019, 805; HRMS (EI) m/z calcd for $C_7H_8NO_2I$ (M^+) 264.9600, found 264.9598; LRMS (EI) m/z 265 (M^+ , 53), 250 (84), 138 (30), 84 (100), 78 (30).

4-Iodo-2-methoxy-3-methoxymethylpyridine (**30a**):



Chloromethylmethyl ether (1.5 mL, 20 mmol) was added dropwise through a syringe to a solution of **29a** (1.8 g, 6.7 mmol) and i -Pr₂EtN (3.5 mL, 20 mmol) in dry CH₂Cl₂ (40 mL) kept in an ice-bath at 0 °C. The resulting mixture was allowed to warm to room temperature and stirred for 22 h at room temperature. The reaction was then quenched with 5% NaHCO₃ solution and extracted with CH₂Cl₂ (3 x 30 mL). The combined organic extracts were washed with brine, dried over MgSO₄ and concentrated under reduced pressure to afford **30a** as an orange-yellow oil (2.1 g, 100%). The crude product was used for the subsequent reaction: ¹H NMR (300 MHz, CDCl₃) δ 3.45 (s, 3H), 3.96 (s, 3H), 4.72 (s, 2H), 4.75 (s, 2H), 7.35 (d, J = 5.4 Hz, 1H), 7.71 (d, J = 5.4 Hz, 1H); ¹³C NMR (75 MHz, CDCl₃) δ 54.3, 55.8, 67.9, 96.7, 114.2, 124.0, 128.1, 147.1, 162.4; IR (CH₂Cl₂, NaCl, cm⁻¹) 2949, 1561, 1459, 1380, 1265, 1039, 741; HRMS (EI) m/z calcd for $C_9H_{12}NO_3I$ (M^+) 308.9862, found 308.9860; LRMS (EI) m/z 309 (M^+ , 19), 277 (20), 264 (45), 248 (100), 218 (68), 152 (39), 92 (50), 79 (35).

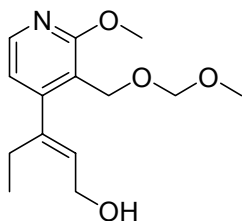
(E)-3-(2-Methoxy-3-methoxymethylpyridin-4-yl)-pent-2-enoic acid ethyl ester
(32a):



A round bottomed flask was charged with LiCl (0.82 g, 19 mmol) and dried with a heatgun under vacuum. After cooling to room temperature, CuCl (1.6 g, 16 mmol) and Pd(PPh₃)₄ (0.19 g, 0.16 mmol) were added. The reaction vessel was then degassed (4 times) under vacuum with an argon purge. Dry DMSO (35 mL) was added with concomitant stirring, followed by addition of **30a** (1.0 g, 3.2 mmol) and ethyl (*E*)-3-(tributylstannyl)-2-pentenoate **31** (1.6 g, 3.9 mmol). The resulting mixture was degassed (3 times) by a freeze-thaw process. The reaction mixture was stirred at room temperature for 1 h and then at 60 °C for 17 h. This was then cooled to room temperature, diluted with Et₂O (200 mL) and washed with a mixture of brine (265 mL) and 5% NH₄OH (55 mL). The aqueous layer was further extracted with Et₂O (2 x 100 mL). The combined organic layers were washed with water (2 x 250 mL) and then with brine (2 x 250 mL), dried over MgSO₄ and concentrated under reduced pressure. The crude product was purified by flash chromatography (95:5 hexanes/ethyl acetate) to afford **32a** as a yellow oil (0.82 g, 82%): ¹H NMR (300 MHz, CDCl₃) δ 0.99 (t, *J* = 7.6 Hz, 3H), 1.30 (t, *J* = 7.1 Hz, 3H), 2.99 (q, *J* = 7.6 Hz, 2H), 3.43 (s, 3H), 4.01 (s, 3H), 4.21 (q, *J* = 7.0 Hz, 2H), 4.49 (s, 2H), 4.73 (s, 2H), 5.81 (s, 1H), 6.69 (d, *J* = 5.0 Hz, 1H), 8.11 (d, *J* = 5.0 Hz, 1H); ¹³C NMR (75 MHz, CDCl₃) δ 12.5, 14.4, 26.6, 54.0, 55.6, 60.3, 62.0, 97.0, 116.3, 116.8, 120.0, 146.4, 153.3, 159.4, 163.4, 165.9; IR (CH₂Cl₂, NaCl, cm⁻¹) 2982, 1713, 1640, 1593, 1560, 1453, 1392, 1266, 1186, 1040,

743; HRMS (EI) m/z calcd for $C_{16}H_{23}NO_5$ (M^+) 309.1576, found 309.1587; LRMS (EI) m/z 309 (M^+ , 32), 277 (42), 236 (100), 190 (84), 174 (73), 160 (22), 77 (10).

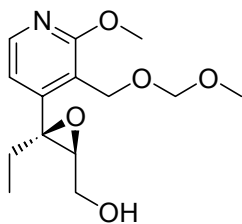
(E)-3-(2-Methoxy-3-methoxymethoxymethylpyridin-4-yl)-pent-2-en-1-ol (33a):



LAH in diethyl ether (1 M, 9.7 mL, 9.7 mmol) was slowly added to a solution of **32a** (1.2 g, 3.9 mmol) in Et_2O (35 mL) kept in a dry ice-acetone bath at -78 °C. The resulting mixture was allowed to warm to 0 °C (~ 2 h) and quenched by adding an ice-cold solution of satd. aqueous sodium potassium tartrate. The aqueous layer was extracted with Et_2O (3 x 25 mL). The combined organic extracts were washed with water (20 mL) and brine (20 mL), dried over $MgSO_4$ and concentrated under reduced pressure to afford **33a** as a pale yellow oil (0.84 g, 81%). The crude product was used for the subsequent reaction: 1H NMR (300 MHz, $CDCl_3$) δ 0.92 (t, $J = 7.6$ Hz, 3H), 2.44 (q, $J = 7.6$ Hz, 2H), 3.44 (s, 3H), 4.00 (s, 3H), 4.33 (dd, $J = 5.6$ Hz, 6.7 Hz, 2H), 4.55 (s, 2H), 4.70 (s, 2H), 5.63 (t, $J = 6.8$ Hz, 1H), 6.68 (d, $J = 5.2$ Hz, 1H), 8.07 (d, $J = 5.2$ Hz, 1H); ^{13}C NMR (75 MHz, $CDCl_3$) δ 13.2, 15.5, 25.4, 54.0, 55.6, 59.0, 61.8, 96.2, 117.3, 129.4, 142.0, 146.1, 154.6, 163.6; IR (CH_2Cl_2 , NaCl, cm^{-1}) 3383, 2945, 1594, 1555, 1452, 1391, 1320, 1268, 1148, 1038, 739, 541; HRMS (EI) m/z calcd for $C_{13}H_{18}NO_3$ 236.1287, found 236.1292; LRMS (EI) m/z 268 ($M + H$, 38), 249 (31), 236 (62), 190 (48), 176 (100), 160 (35), 91 (16), 77 (15). Copies of spectral data can be found in the appendix section.

(2*S*,3*S*)-(+)-[3-Ethyl-3-(2-methoxy-3-methoxymethylpyridin-4-yl)-oxiranyl]

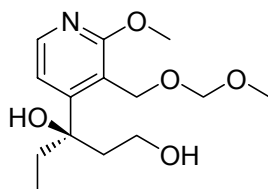
methanol (34a):



(*L*)-(+)-Diethyltartrate (0.1 mL, 0.6 mmol) and $\text{Ti}(\text{O}^i\text{Pr})_4$ (0.14 mL, 0.48 mmol) were added to a suspension of **33a** (0.16 g, 0.60 mmol) and 4Å molecular sieves (48 mg) in dry CH_2Cl_2 (5.0 mL) kept in a dry ice-acetone bath at -20°C and the mixture was stirred for 1 h. Then $^t\text{BuOOH}$, pre-dried over 4Å molecular sieves for 1 h (0.19 mL, 5.0-6.0 M in decane), was added and stirred at -20°C for 24 h. The resulting mixture was then diluted with Et_2O (1.0 mL) and quenched with satd. Na_2SO_4 solution (0.5 mL). The resulting heterogenous mixture was stirred until it warmed to room temperature (2 h). This was then filtered through a celite pad washing with hot ethyl acetate several times. The combined filtrates were concentrated under vacuum. The residue was dissolved in Et_2O (2.5 mL) at 0°C and a 1 N NaOH solution saturated with NaCl (1.6 mL) was added. The two-phase mixture was vigorously stirred at 0°C for 1 h and then transferred to a separatory funnel. The aqueous layer was separated and extracted with EtOAc (3 x 5 mL). The combined organic extracts were dried over MgSO_4 and concentrated under reduced pressure to afford **34a** as a yellow oil (0.14 g, 84%) with 96% ee. The crude product was used for the subsequent reaction. However, for HPLC analysis, the crude product was filtered over a silica plug to remove solvent front and baseline impurities. Epoxide **34a** was then analyzed for enantiomeric purity using a Chiralcel OD column with 98:2 hexane/ $^i\text{PrOH}$ as the eluent using the racemate as the standard. The desired (2*S*,3*S*) enantiomer elutes first, ($R_t = 23.1$ min): $^1\text{H NMR}$ (300 MHz, CDCl_3) δ 0.92 (t, $J = 7.6$ Hz, 3H), 1.81 (dq, $J = 7.4$ Hz, 14.8 Hz, 1H), 2.01 (dq, $J =$

7.6 Hz, 15.0 Hz, 1H), 3.24 (t, $J = 5.8$ Hz, 1H), 3.46 (s, 3 H), 3.90 (m, 2H), 3.99 (s, 3H), 4.71 (s, 2H), 4.73 (s, 2H), 6.93 (d, $J = 5.2$ Hz, 1H), 8.12 (d, $J = 5.2$ Hz, 1H) (-OH proton resonance not detected); ^{13}C NMR (75 MHz, CDCl_3) δ 9.4, 25.7, 26.0, 54.1, 55.8, 60.8, 61.3, 63.7, 64.7, 96.7, 116.5, 116.8, 146.6, 151.0, 163.1; IR (CH_2Cl_2 , NaCl, cm^{-1}) 3408, 2980, 1765, 1607, 1457, 1410, 1393, 1266, 1040, 742, 546; HRMS (EI) m/z calcd for $\text{C}_{14}\text{H}_{22}\text{NO}_5$ (M+H) 284.1498, found 284.1507; LRMS (EI) m/z 284 (M + H, 58), 190 (100), 178 (73), 162 (27), 148 (27), 77 (13); $[\alpha]_{\text{D}}^{23} = +65.6$ (c = 0.25, CH_2Cl_2).

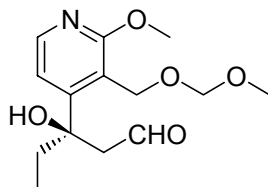
(R)-(+)-3-(2-Methoxy-3-methoxymethylpyridin-4-yl)-pentane-1,3-diol (35a):



LAH in diethyl ether (1 M, 2.5 mL, 2.5 mmol) was added to a solution of **34a** (0.71 g, 2.5 mmol) in Et_2O (50 mL) kept in an ice bath at 0°C and allowed to warm to room temperature and stirred for 24 h. The reaction was quenched with a chilled solution of sodium potassium tartrate at 0°C and the aqueous layer was extracted with Et_2O (3 x 40 mL). The combined organic extracts were washed with water (2 x 25 mL) and brine (2 x 25 mL), dried over MgSO_4 and concentrated under reduced pressure to afford **35a** as a colorless oil (0.54 g, 76%). The crude product was sufficiently pure for the subsequent reaction: ^1H NMR (300 MHz, CDCl_3) δ 0.79 (t, $J = 7.3$ Hz, 3H), 1.91 (q, $J = 7.3$ Hz, 2H), 2.15 (m, 2H), 3.42 (s, 3H), 3.60 (m, 1H), 3.74 (m, 1H), 3.98 (s, 3H), 4.71 (s, 2H), 4.89 (d, $J = 10.7$ Hz, 1H), 5.10 (d, $J = 10.7$ Hz, 1H), 6.77 (d, $J = 5.5$ Hz, 1H), 8.05 (d, $J = 5.5$ Hz, 1H); ^{13}C NMR (75 MHz, CDCl_3) δ 7.8, 36.6, 43.8, 54.1, 55.9, 60.2, 61.1, 80.9, 96.5, 116.3, 117.9, 146.2, 156.4, 163.8; IR (CH_2Cl_2 , NaCl, cm^{-1}) 3391, 3056, 2984, 1593,

1446, 1382, 1265, 1037, 743, 546; HRMS (EI) m/z calcd for $C_{14}H_{24}NO_5$ (M+H) 286.1654, found 286.1658; LRMS (EI) m/z 286 (M + H, 39), 235 (23), 222 (86), 205 (52), 194 (74), 178 (100), 150 (49), 92 (30), 77 (15); $[\alpha]_D^{23} = +0.185$ ($c = 1.08$, CH_2Cl_2).

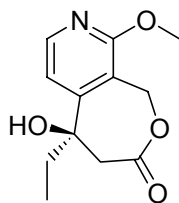
(R)-(-)-3-Hydroxy-3-(2-methoxy-3-methoxymethoxymethylpyridin-4-yl)pentanal (36a):



Dess-Martin periodinane (1.2 g, 2.9 mmol) was added to a solution of **35a** (0.50 g, 1.8 mmol) in CH_2Cl_2 (20 mL). The mixture was stirred at room temperature for 3 h and then poured into a well-stirred mixture of satd. $Na_2S_2O_3$ (10 mL) and satd. $NaHCO_3$ (10 mL). After 30 min, the layers were separated and the aqueous layer was extracted with diethyl ether (3 x 15 mL). The combined organic extracts were washed with satd. $NaHCO_3$ and brine, dried over $MgSO_4$, and concentrated under vacuum to give the crude aldehyde **36a** (0.47 g, 89%) as pale yellow oil. The crude product was used for the subsequent reaction: 1H NMR (300 MHz, $CDCl_3$) δ 0.82 (t, $J = 7.4$ Hz, 3H), 1.91 (2 overlapping dqs, 2H), 2.85 (dd, $J = 2.1$ Hz, 16.4 Hz, 1H), 3.10 (dd, $J = 2.2$ Hz, 16.3 Hz, 1H), 3.41 (s, 3H), 3.96 (s, 3H), 4.74 (s, 2H), 4.98 (q, $J = 10.9$ Hz, 2H), 6.74 (d, $J = 5.5$ Hz, 1H), 8.06 (d, $J = 5.5$ Hz, 1H), 9.73 (t, $J = 2$ Hz, 1H); ^{13}C NMR (75 MHz, $CDCl_3$) δ 7.9, 36.4, 54.2, 55.3, 56.0, 60.9, 77.9, 96.4, 115.8, 117.4, 146.5, 155.6, 163.8, 202.2; IR (CH_2Cl_2 , $NaCl$, cm^{-1}) 3380, 3057, 2982, 1763, 1655, 1596, 1422, 1264, 895, 735, 547; HRMS (EI) m/z calcd for $C_{14}H_{22}NO_5$ (M+H) 284.1498, found 284.1498; LRMS (EI) m/z 284 (M + H, 15), 265 (25), 192 (20), 178 (72), 148 (24), 84 (100), 57 (26); $[\alpha]_D^{23} = -11.5$ ($c = 0.125$, CH_2Cl_2).

(R)-(+)-5-Ethyl-5-hydroxy-1-methoxy-5,6-dihydro-9H-8-oxa-2-aza-benzocyclohepten-7-one

[(R)-18]:



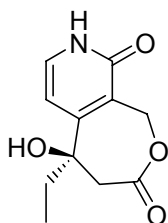
2-methyl-2-butene (2.1 mL) was added to a solution of the aldehyde **36a** (0.13 g, 0.46 mmol) in *tert*-butyl alcohol (7.1 mL). A solution of sodium chlorite (0.37 g, 4.1 mmol) and sodium dihydrogen phosphate (0.44 g, 3.2 mmol) in H₂O (3.8 mL) was added dropwise to this mixture through a syringe. The resulting mixture was stirred at room temperature for 36 h. Then the crude mixture was extracted with ethyl acetate (2 x 10 mL). The aqueous layer was then acidified (pH ~ 3.5) by dropwise addition of 5% HCl and subsequently washed with ethyl acetate (2 x 10 mL). If a yellow coloration was observed, the mixture was washed with 5% sodium sulfite solution prior to this ethyl acetate extraction. The combined organic extracts were washed with brine, dried over sodium sulfate and concentrated under vacuum to give the crude product **37a** (0.12 g, 84%) as a light green oil which was used immediately after the workup.

TFA (8.0 mL) was added to **37a** (0.11 g, 0.38 mmol) at room temperature via a syringe. After stirring for 24 h, the mixture was neutralized with satd. NaHCO₃ (pH ~ 8) and extracted with diethyl ether (3 x 6 mL). The combined organic extracts were dried over MgSO₄ and concentrated under reduced pressure to afford **(R)-18** as a yellow-brown oil (72 mg, 80%) which was used crude for the subsequent reaction. When necessary, the crude product was purified by column chromatography (75:25 hexanes/ethyl acetate): ¹H NMR (300 MHz, CD₃OD) δ 0.84 (t, *J* = 7.4 Hz, 3H), 1.85 (q, *J* = 7.4 Hz, 2H), 3.01 (d, *J* = 13.9 Hz, 1H), 3.41 (d, *J* = 13.9 Hz, 1H), 3.94 (s, 3H), 5.29 (d, *J* = 15.2 Hz, 1H), 5.44 (d, *J* = 15.2 Hz, 1H), 7.15 (d, *J* = 5.5 Hz, 1H), 8.13

(d, $J = 5.5$ Hz, 1H); ^{13}C NMR (75 MHz, CD_3OD) δ 9.0, 38.5, 43.8, 55.0, 61.4, 62.7, 74.7, 117.1, 147.8, 156.0, 161.9, 173.1; IR (MeOH, NaCl, cm^{-1}) 3390, 2958, 1725, 1683, 1596, 1377, 1204, 1140, 1041; HRMS (EI) m/z calcd for $\text{C}_{12}\text{H}_{15}\text{NO}_4$ (M^+) 237.1001, found 237.0996; LRMS (EI) m/z 237 (M^+ , 75), 208 (22), 166 (100), 136 (25), 106 (7), 77 (7); $[\alpha]_{\text{D}}^{23} = +3.0$ ($c = 0.1$, MeOH).

(R)-(+)-5-Ethyl-5-hydroxy-2,5,6,9-tetrahydro-8-oxa-2-aza-benzocycloheptene-1,7-dione

[(R)-19]:

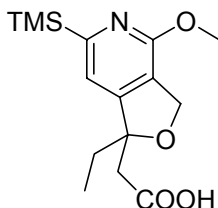


Sodium iodide (0.070 g, 0.49 mmol) was added to a solution of lactone **(R)-18** (0.070 g, 0.30 mmol) in dry acetonitrile (1.0 mL) followed by chlorotrimethylsilane (0.060 mL, 0.49 mmol). The resulting mixture was stirred at room temperature for 15 min. Then H_2O (2.7 μL , 0.15 mmol) was added and the reaction mixture was heated to 60 $^\circ\text{C}$ for 7 h. The mixture was then poured into a 1:1 solution of 5% sodium sulfite/brine (7.0 mL) and then quickly extracted with ethyl acetate (4 x 5 mL). The organic layer was dried over MgSO_4 and concentrated under reduced pressure. The crude product was subjected to flash chromatography (5:95 MeOH/ CH_2Cl_2) to afford pure **(R)-19** as pale yellow oil (10 mg, 16%): ^1H NMR (300 MHz, CD_3OD) δ 0.91 (t, $J = 7.5$ Hz, 3H), 1.82 (m, 2H), 3.10 (d, $J = 13.8$ Hz, 1H), 3.40 (d, $J = 13.8$ Hz, 1H), 5.30 (d, $J = 15.2$ Hz, 1H), 5.46 (d, $J = 15.2$ Hz, 1H), 6.57 (d, $J = 7.0$ Hz, 1H), 7.35 (d, $J = 7.0$ Hz, 1H); ^{13}C NMR (75 MHz, $\text{CDCl}_3/\text{CD}_3\text{OD}$) δ 6.8, 35.2, 41.5, 61.0, 72.4, 105.9, 122.4, 132.8, 156.3, 161.6, 172.6; IR (MeOH, NaCl, cm^{-1}) 3370(br), 1655, 1049, 1025, 823, 768; HRMS (EI) m/z calcd for $\text{C}_{11}\text{H}_{13}\text{NO}_4$ (M^+) 223.0845, found 223.0851; LRMS (EI) m/z 224 ($\text{M} +$

H, 32), 195 (21), 163 (43), 153 (100), 91 (40), 77 (19), 55 (24); $[\alpha]_D^{23} = +35.0$ ($c = 0.08$, MeOH). Copies of spectral data can be found in the appendix section.

Chapter 3

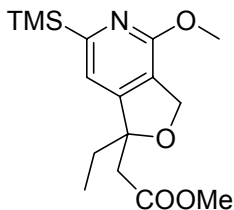
(1-Ethyl-4-methoxy-6-trimethylsilylanyl-1,3-dihydro-furo[3,4-*c*]pyridin-1-yl)acetic acid (**87**):



H₂O₂ (30% w/w, 1.8 mL, 16 mmol) was added to a solution of **71** (0.30 g, 1.0 mmol) in MeOH (10.5 mL) kept at 0 °C in an ice bath. A solution of NaOH (6 N, 0.55 mL, 3.3 mmol) was added dropwise to this mixture via a syringe at 0 °C. After the addition was complete (5 min), the reaction mixture was warmed to room temperature and stirred for 6 h. Water (15 mL) was added, the layers were separated and the aqueous layer washed with CH₂Cl₂ (2 x 15 mL). The aqueous layer was then acidified (pH ~ 3) by dropwise addition of 1 N HCl via a Pasteur pipet and subsequently washed with CH₂Cl₂ (2 x 10 mL). The combined organic extracts were dried over MgSO₄ and concentrated under reduced pressure to afford **87** as a colorless oil (0.28 g, 88%). The crude product was sufficiently pure for the subsequent reaction: ¹H NMR (300 MHz, CDCl₃) δ 0.29 (s, 9H), 0.77 (t, *J* = 7.3 Hz, 3H), 1.87 (dq, *J* = 14.7 Hz, 7.4 Hz, 1H), 2.01 (dq, *J* = 7.4 Hz, 14.6 Hz, 1H), 2.79 (d, *J* = 15.2 Hz, 1H), 2.81 (d, *J* = 15.2 Hz, 1H), 4.00 (s, 3H), 5.10 (d, *J* = 12.7 Hz, 1H), 5.12 (d, *J* = 12.8 Hz, 1H), 6.88 (s, 1H); ¹³C NMR (75 MHz, CDCl₃) δ -1.8, 7.9, 32.2, 44.4, 52.9, 71.1, 89.6, 115.1, 120.1, 151.8, 158.2, 165.6, 173.9; IR (CH₂Cl₂, NaCl, cm⁻¹) 2950, 2858, 1705, 1582, 1449, 1352, 1239, 1029; HRMS (EI) *m/z* calcd for C₁₅H₂₃NO₄Si (M⁺)

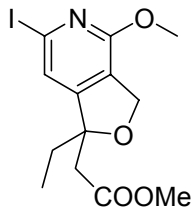
309.1396, found 309.1382; LRMS (EI) m/z 309 (M^+ , 17), 294 (27), 280 (62), 249 (65), 208 (20), 162 (9), 117 (10), 89 (37), 73 (100).

(1-Ethyl-4-methoxy-6-trimethylsilyl-1,3-dihydrofuro[3,4-*c*]pyridin-1-yl)acetic acid methyl ester:



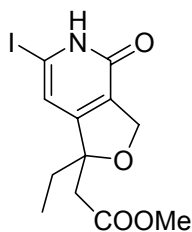
TMSCHN₂ (2 M solution in hexanes, 0.55 mL, 1.09 mmol) was added to a solution of **87** (0.26 g, 0.84 mmol) in a mixture of methanol (1.5 mL) and benzene (5.3 mL) at room temperature. After stirring for 30 min at room temperature, the reaction mixture was concentrated under reduced pressure to afford the ester as a yellow oil (0.26 g, 98%). The crude product was sufficiently pure for the subsequent reaction: ¹H NMR (300 MHz, CDCl₃) δ 0.29 (s, 9H), 0.76 (t, $J = 7.3$ Hz, 3H), 1.88 (dq, $J = 7.4$ Hz, 14.8 Hz, 1H), 2.01 (dq, $J = 7.4$ Hz, 14.7 Hz, 1H), 2.78 (d, $J = 14.4$ Hz, 1H), 2.80 (d, $J = 14.4$ Hz, 1H), 3.59 (s, 3H), 4.00 (s, 3H), 5.03 (d, $J = 12.7$ Hz, 1H), 5.05 (d, $J = 12.7$ Hz, 1H), 6.89 (s, 1H); ¹³C NMR (75 MHz, CDCl₃) δ -1.8, 7.8, 32.5, 44.5, 51.4, 52.8, 70.9, 89.7, 115.5, 120.8, 152.4, 158.2, 165.0, 170.2; IR (CH₂Cl₂, NaCl, cm⁻¹) 2955, 2858, 1777, 1741, 1593, 1460, 1362, 1034; HRMS (EI) m/z calcd for C₁₆H₂₅NO₄Si (M^+) 323.1553, found 323.1563; LRMS (EI) m/z 323 (M^+ , 43), 308 (40), 294 (65), 250 (100), 234 (42), 208 (46), 84 (82). Copies of spectral data can be found in the appendix section.

(1-Ethyl-6-iodo-4-methoxy-1,3-dihydrofuro[3,4-c]pyridin-1-yl)acetic acid methyl ester:



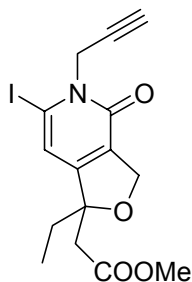
A solution of ICl (0.42 g, 2.6 mmol) in CCl₄ (1.82 mL) was added to a solution of the above ester (0.21 g, 0.65 mmol) in CH₂Cl₂ (2.6 mL) kept at 0 °C in an ice bath and allowed to warm to room temperature. After stirring for 14 h, the reaction mixture was poured into a chilled solution of 5% Na₂SO₃/brine (1:1, 40 mL) and extracted the mixture with ethyl acetate (3 x 30 mL). The combined organic extracts were dried over MgSO₄ and concentrated under reduced pressure. The crude product was purified by flash chromatography (5:95 ethyl acetate/hexanes) to afford the iodide as a pale yellow oil (0.1 g, 41%): ¹H NMR (300 MHz, CDCl₃) δ 0.60 (t, *J* = 7.2 Hz, 3H), 1.73 (m, 2H), 2.60 (d, *J* = 15.0 Hz, 1H), 2.62 (d, *J* = 15.0 Hz, 1H), 3.44 (s, 3H), 3.79 (s, 3H), 4.80 (d, *J* = 12.9 Hz, 1H), 4.82 (d, *J* = 12.9 Hz, 1H), 7.00 (s, 1H); ¹³C NMR (75 MHz, CDCl₃) δ 7.6, 32.6, 51.5, 54.1, 70.5, 89.0, 111.3, 121.1, 121.4, 156.2, 157.5, 169.8; IR (CH₂Cl₂, NaCl, cm⁻¹) 2950, 2853, 2356, 2330, 1741, 1593, 1460, 1362, 1035, 850; HRMS (EI) *m/z* calcd for C₁₃H₁₆INO₄ (M⁺) 377.0124, found 377.0129; LRMS (EI) *m/z* 377 (M⁺, 32), 348 (35), 303 (100), 288 (23), 162 (28), 77 (20).

**(1-Ethyl-6-iodo-4-oxo-1,3,4,5-tetrahydro-furo[3,4-c]pyridin-1-yl)acetic acid methyl ester
(90):**



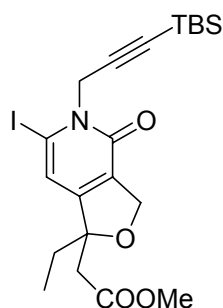
Sodium iodide (29 mg, 0.20 mmol) was added to a solution of the above iodide (46 mg, 0.12 mmol) in dry acetonitrile (1.2 mL) at room temperature. Chlorotrimethylsilane (25 μ L, 0.20 mmol) was then added and the reaction mixture was stirred for 15 min at room temperature. H₂O (1.0 μ L, 0.061 mmol) was added and the reaction mixture was heated at 60 $^{\circ}$ C for 22 h. The mixture was then poured into a solution of 5% Na₂SO₃/brine (1:1, 7.8 mL) and quickly extracted with ethyl acetate (4 x 10 mL). The combined organic extracts were dried over MgSO₄ and concentrated under reduced pressure. The crude product was purified by flash chromatography (2:3 ethyl acetate/hexanes) to afford **90** as a pale yellow solid (30 mg, 68%): ¹H NMR (300 MHz, CDCl₃) δ 0.80 (t, J = 7.2 Hz, 3H), 1.86 (m, 2H), 2.75 (q, J = 14.8 Hz, 2H), 3.61 (s, 3H), 5.01 (s, 2H), 6.66 (s, 1H); ¹³C NMR (75 MHz, CDCl₃) δ 7.7, 32.2, 43.8, 51.7, 71.8, 90.2, 94.0, 113.2, 127.4, 155.8, 161.0, 169.8; IR (CH₂Cl₂, NaCl, cm⁻¹); HRMS (EI) m/z calcd for C₁₂H₁₄INO₄ (M⁺) 362.9968, found 362.9961; LRMS (EI) m/z 363 (M⁺, 22), 334 (31), 289 (100), 274 (15), 163 (23), 78 (21).

(1-Ethyl-6-iodo-4-oxo-5-prop-2-ynyl-1,3,4,5-tetrahydrofuro[3,4-*c*]pyridin-1-yl)acetic acid methyl ester (91a):



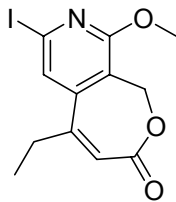
NaH in mineral oil (60%, 1.5 mg, 0.036 mmol) was added to a solution of **90** (12 mg, 0.033 mmol) in a mixture of DME (0.25 mL) and DMF (0.10 mL) at 0 °C under argon. After stirring this mixture for 10 min at 0 °C, LiBr (5.8 mg, 0.066 mmol) was added. The reaction mixture was allowed to warm to room temperature and stirred for 15 min. Propargyl bromide (80% w/w in toluene, 15 µL, 0.13 mmol) was then added via a syringe and the reaction mixture was heated in the dark at 65 °C for 7 h. The final solution was poured into brine (5 mL) and extracted with ethyl acetate (3 x 5 mL). The combined organic extracts were dried over MgSO₄ and concentrated under reduced pressure. The crude product was purified by flash chromatography (2:3 ethyl acetate/hexanes) to give **91a** as a pale yellow foam (7.0 mg, 54%): ¹H NMR (300 MHz, CDCl₃) δ 0.82 (t, *J* = 7.4 Hz, 3H), 1.78 (dq, *J* = 7.4 Hz, 14.7 Hz, 1H), 1.92 (dq, *J* = 7.4 Hz, 14.7 Hz, 1H), 2.45 (t, *J* = 2.4 Hz, 1H), 2.75 (q, *J* = 14.8 Hz, 2H), 3.63 (s, 3H), 4.97 (s, 2H), 5.11 (dd, *J* = 2.4 Hz, 17.2 Hz, 1H), 5.13 (dd, *J* = 2.5 Hz, 17.1 Hz, 1H), 6.77 (s, 1H); ¹³C NMR (75 MHz, CDCl₃) δ 7.8, 32.0, 43.4, 43.7, 51.8, 71.9, 73.2, 90.2, 98.8, 114.6, 128.4, 153.8, 157.4, 170.0; IR (CH₂Cl₂, NaCl, cm⁻¹) 3288, 2970, 2852, 2356, 2335, 1736, 1649, 1521, 1198, 1024; HRMS (EI) *m/z* calcd for C₁₅H₁₆INO₄ (M⁺) 401.0124, found 401.0135; LRMS (EI) *m/z* 401 (M⁺, 31), 372 (24), 345 (13), 327 (100), 245 (18), 206 (20), 162 (36), 77 (17). Copies of spectral data can be found in the appendix section.

(5-[3-*tert*-Butyldimethylsilyl]prop-2-ynyl]-1-ethyl-6-iodo-4-oxo-1,3,4,5-tetrahydrofuro[3,4-*c*]pyridin-1-yl)acetic acid methyl ester (91b**):**



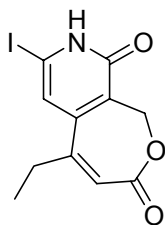
Following the above procedure, **90** (19 mg, 0.051 mmol) was alkylated with 3-*tert*-butyldimethylsilyl propargyl bromide (24 mg, 0.10 mmol) in the presence of NaH in mineral oil (60%, 2.3 mg, 0.056 mmol) and LiBr (8.9 mg, 0.10 mmol) in a mixture of DME (0.39 mL) and DMF (0.15 mL). The crude product was purified by flash chromatography (1:4 ethyl acetate/hexanes) to afford **91b** as a colorless oil (12 mg, 45%): ^1H NMR (300 MHz, CDCl_3) δ 0.10 (s, 6H), 0.82 (t, $J = 7.4$ Hz, 3H), 0.93 (s, 9H), 1.78 (dq, $J = 7.4$ Hz, 14.7 Hz, 1H), 1.92 (dq, $J = 7.3$ Hz, 14.7 Hz, 1H), 2.75 (q, $J = 14.7$ Hz, 2H), 3.62 (s, 3H), 4.98 (s, 2H), 5.12 (d, $J = 17.3$ Hz, 1H), 5.15 (d, $J = 17.3$ Hz, 1H), 6.76 (s, 1H); ^{13}C NMR (75 MHz, CDCl_3) δ -4.9, 7.7, 16.6, 26.0, 32.1, 43.8, 51.7, 72.0, 89.0, 90.2, 98.8, 99.3, 114.5, 128.2, 153.5, 157.3, 170.0; IR (CH_2Cl_2 , NaCl, cm^{-1}) 2950, 2924, 2852, 2356, 2330, 1736, 1654, 1526, 1198, 1034; HRMS (EI) m/z calcd for $\text{C}_{21}\text{H}_{30}\text{INO}_4\text{Si}$ (M^+) 515.0989, found 515.0999; LRMS (EI) m/z 515 (M^+ , 25), 458 (100), 441 (58), 420 (22), 384 (54), 356 (17), 258 (11), 162 (12), 96 (58), 73(57). Copies of spectral data can be found in the appendix section.

5-Ethyl-3-iodo-1-methoxy-9*H*-8-oxa-2-azabenzocyclohepten-7-one:



ICl (1 M in dichloromethane, 10 mL, 10 mmol) was added to a solution of **71** (0.73 g, 2.5 mmol) in CH₂Cl₂ (12 mL) kept at 0 °C in an ice bath and then allowed to warm to room temperature. After stirring for 16 h, the reaction mixture was poured into a chilled solution of 5% Na₂SO₃/brine (1:1, 150 mL) and extracted the mixture with ethyl acetate (3 x 120 mL). The combined organic extracts were dried over MgSO₄ and concentrated under reduced pressure. The crude product was purified by flash chromatography (5:95 ethyl acetate/hexanes) to afford the iodide as a pale yellow oil (0.32 g, 38%): ¹H NMR (300 MHz, CDCl₃) δ 1.17 (t, *J* = 7.3 Hz, 3H), 2.62 (dq, *J* = 1.3 Hz, 7.4 Hz, 2H), 4.02 (s, 3H), 5.06 (br s, 2H), 6.38 (s, 1H), 7.38 (s, 1H); ¹³C NMR (75 MHz, CDCl₃) δ 12.4, 28.9, 54.9, 60.2, 114.6, 116.4, 122.5, 124.4, 148.2, 149.4, 160.3, 167.3; IR (CH₂Cl₂, NaCl, cm⁻¹) 2955, 2924, 2847, 1736, 1618, 1454, 1362, 1045; HRMS (EI) *m/z* calcd for C₁₂H₁₂INO₃ (M⁺) 344.9862, found 344.9868; LRMS (EI) *m/z* 345 (M⁺, 100), 316 (58), 302 (74), 288 (54), 218 (22), 188 (35), 159 (43), 130 (55), 77 (36).

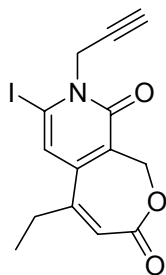
5-Ethyl-3-iodo-2,9-dihydro-8-oxa-2-azabenzocycloheptene-1,7-dione (**93**):



Sodium iodide (0.15 g, 1.0 mmol) was added to a solution of the above iodide (0.12 g, 0.33 mmol) in dry acetonitrile (3.3 mL) at room temperature. Chlorotrimethylsilane (0.13 mL, 1.0

mmol) was then added and the reaction mixture was stirred for 15 min at room temperature. H₂O (3.0 μL, 0.17 mmol) was next added and the reaction mixture was heated to 60 °C and stirred at that temperature for 21 h. The mixture was then poured into a solution of 5% Na₂SO₃/brine (1:1, 20 mL) and quickly extracted with ethyl acetate (4 x 20 mL). The combined organic extracts were dried over MgSO₄ and concentrated under reduced pressure. The crude product was purified by flash chromatography (1:4 acetone/dichloromethane) to afford **93** as a pale yellow solid (36 mg, 33%): ¹H NMR (300 MHz, CDCl₃) δ 1.13 (t, *J* = 7.4 Hz, 3H), 2.60 (q, *J* = 7.2 Hz, 2H), 4.99 (br s, 2H), 6.32 (s, 1H), 7.04 (s, 1H), 12.27 (br s, 1H); ¹³C NMR (75 MHz, CDCl₃) δ 12.0, 28.0, 29.0, 60.0, 122.2, 148.2, 149.3, 161.0, 166.7; IR (CH₂Cl₂, NaCl, cm⁻¹) 3344, 2955, 2837, 1710, 1629, 1583, 1444, 1014; HRMS (EI) *m/z* calcd for C₁₁H₁₀INO₃ (M⁺) 330.9705, found 330.9717; LRMS (EI) *m/z* 331 (M⁺, 100), 302 (82), 288 (92), 274 (65), 174 (17), 160 (26), 146 (18).

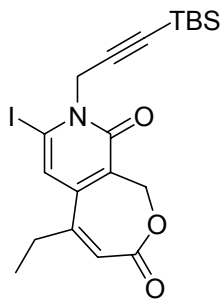
5-Ethyl-3-iodo-2-prop-2-ynyl-2,9-dihydro-8-oxa-2-azabenzocycloheptene-1,7-dione (94a):



NaH in mineral oil (60%, 7.2 mg, 0.18 mmol) was added to a solution of **93** (30 mg, 0.091 mmol) in a mixture of DME (0.70 mL) and DMF (0.30 mL) at 0 °C under argon. After stirring this mixture for 10 min at 0 °C, LiBr (32 mg, 0.36 mmol) was added. The reaction mixture was allowed to warm to room temperature and stirred for 15 min. Propargyl bromide (80% w/w in toluene, 80 μL, 0.72 mmol) was then added via a syringe and the reaction mixture was heated in

the dark at 65 °C for 14 h. The final solution was poured into brine (10 mL) and extracted with ethyl acetate (3 x 10 mL). The combined organic extracts were dried over MgSO₄ and concentrated under reduced pressure. The crude product was purified by flash chromatography (3:7 ethyl acetate/hexanes) to give **94a** as a pale yellow oil (12 mg, 37%): ¹H NMR (300 MHz, CDCl₃) δ 1.17 (t, *J* = 7.3 Hz, 3H), 2.39 (t, *J* = 2.5 Hz, 1H), 2.55 (q, *J* = 7.4 Hz, 2H), 5.11 (s, 2H), 6.41 (s, 1H), 6.88 (s, 1H); ¹³C NMR (75 MHz, CDCl₃) δ 12.4, 28.4, 44.7, 61.1, 73.5, 101.1, 116.8, 123.8, 125.0, 148.0, 149.2, 159.8, 167.3; IR (CH₂Cl₂, NaCl, cm⁻¹) 2909, 2842, 2361, 2330, 1710, 1644, 1506, 1454, 1045; HRMS (EI) *m/z* calcd for C₁₄H₁₂INO₃ (M⁺) 368.9862, found 368.9866; LRMS (EI) *m/z* 369 (M⁺, 37), 340 (35), 326 (12), 256 (12), 149 (30), 129 (30), 73 (66), 57 (100). Copies of spectral data can be found in the appendix section.

2-[3-(*tert*-Butyldimethylsilyl)prop-2-ynyl]-5-ethyl-3-iodo-2,9-dihydro-8-oxa-2-azabenzocycloheptene-1,7-dione (94b**):**



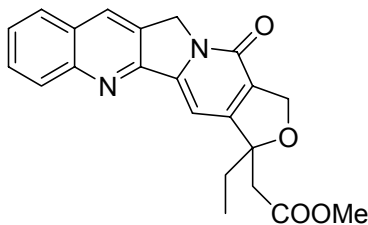
Following the above procedure, **93** (32 mg, 0.097 mmol) was alkylated with 3-*tert*-butyldimethylsilyl propargyl bromide (0.18 g, 0.77 mmol) in the presence of NaH in mineral oil (60%, 7.7 mg, 0.19 mmol) and LiBr (34 mg, 0.39 mmol) in a mixture of DME (0.75 mL) and DMF (0.31 mL). The crude product was purified by flash chromatography (1:4 ethyl acetate/hexanes) to afford **94b** as a colorless oil (20 mg, 43%): ¹H NMR (300 MHz, CDCl₃) δ 0.10 (s, 6H), 0.91 (s, 9H), 1.17 (t, *J* = 7.4 Hz, 3H), 2.55 (q, *J* = 7.6 Hz, 2H), 5.13 (s, 2H), 6.41 (s,

1H), 6.88 (s, 1H); ¹³C NMR (75 MHz, CDCl₃) δ -4.9, 12.4, 16.6, 26.1, 28.4, 45.1, 61.3, 89.5, 98.5, 101.2, 116.7, 123.6, 124.9, 147.9, 149.4, 159.8, 167.4; IR (CH₂Cl₂, NaCl, cm⁻¹) 2955, 2847, 2248, 2176, 1726, 1649, 1511, 1265, 1035; HRMS (EI) *m/z* calcd for C₁₆H₁₇INO₃Si (M - ^tBu) 426.0022, found 426.0023; LRMS (EI) *m/z* 426 (M - ^tBu, 25), 398 (19), 382 (22), 223 (10), 127 (56), 96 (100), 75 (91). Copies of spectral data can be found in the appendix section.

General procedure 3A: Radical Cascade Cyclization towards the Synthesis of Non-lactone Analogs 92a-d, 95a-d.

A solution of iodopyridone (~ 6-11 mg) in benzene was taken up in a 15 x 45 mm cylindrical screw-cap glass vial and kept at room temperature. A solution of isonitrile (1 M in benzene) and then hexamethylditin were added at room temperature. The vial was capped and the reaction mixture was irradiated with a 275W GE sunlamp for 4 h. The solvent was then evaporated and the residue was purified by preparative thin layer chromatography (1:9 acetone/dichloromethane).

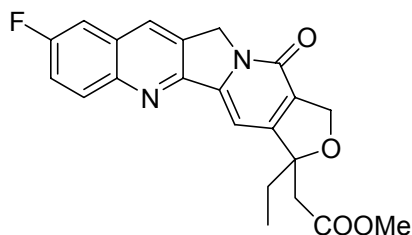
Methyl(3-ethyl-13-oxo-11,13-dihydro-1*H*,3*H*-furo[3',4':6,7]indolizino[1,2-*b*]quinolin-3-yl)acetate (92a):



Following general procedure 3A, iodopyridone **91a** (7.6 mg, 0.019 mmol) was reacted with phenyl isonitrile (1 M, 76 μ L, 0.076 mmol) and hexamethylditin (11 μ L, 0.028 mmol) in benzene (0.32 mL) to afford **92a**, after purification, as a yellow solid (2.1 mg, 30%): ¹H NMR

(500 MHz, CDCl₃) δ 0.86 (t, J = 7.3 Hz, 3H), 1.94 (dq, J = 7.2 Hz, 14.5 Hz, 1H), 2.05 (dq, J = 7.5 Hz, 14.7 Hz, 1H), 2.89 (d, J = 14.7 Hz, 1H), 2.90 (d, J = 14.8 Hz, 1H), 3.63 (s, 3H), 5.17 (d, J = 13.5 Hz, 1H), 5.18 (d, J = 13.4 Hz, 1H), 5.30 (s, 2H), 7.21 (s, 1H), 7.66 (t, J = 7.2 Hz, 1H), 7.83 (t, J = 7.1 Hz, 1H), 7.94 (d, J = 8.1 Hz, 1H), 8.21 (d, J = 8.4 Hz, 1H), 8.39 (s, 1H); ¹³C NMR (151 MHz, CDCl₃) δ 7.9, 32.9, 44.4, 49.7, 51.8, 72.5, 90.8, 95.4, 127.8, 128.2, 128.3, 129.1, 129.2, 129.7, 130.6, 131.1, 147.2, 148.9, 152.9, 154.3, 157.1, 170.1; IR (CH₂Cl₂, NaCl, cm⁻¹) 2919, 2842, 2356, 2325, 1731, 1654, 1603, 1439, 1224, 1024; HRMS (EI) m/z calcd for C₂₂H₂₀N₂O₄ (M⁺) 376.1423, found 376.1417; LRMS (EI) m/z 376 (M⁺, 6), 347 (6), 302 (39), 261 (5), 137 (13), 97 (18), 81 (45), 69 (100). Copies of spectral data can be found in the appendix section.

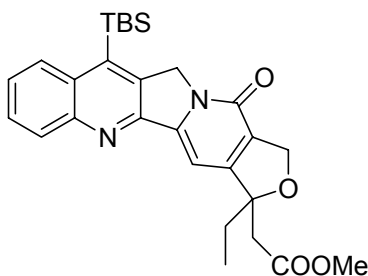
Methyl(3-ethyl-8-fluoro-13-oxo-11,13-dihydro-1*H*,3*H*-furo[3',4':6,7]indolizino[1,2-*b*]quinolin-3-yl)acetate (92b):



Following general procedure 3A, iodopyridone **91a** (6.5 mg, 0.016 mmol) was reacted with *p*-fluorophenyl isonitrile (1 M, 65 μ L, 0.065 mmol) and hexamethylditin (9.0 μ L, 0.024 mmol) in benzene (0.27 mL) to afford **92b**, after purification, as a yellow solid (3.5 mg, 55%): ¹H NMR (300 MHz, CDCl₃) δ 0.86 (t, J = 7.3 Hz, 3H), 1.94 (dq, J = 7.5 Hz, 14.6 Hz, 1H), 2.05 (dq, J = 7.8 Hz, 15.1 Hz, 1H), 2.89 (d, J = 14.7 Hz, 1H), 2.91 (d, J = 14.7 Hz, 1H), 3.63 (s, 3H), 5.17 (s, 2H), 5.30 (s, 2H), 7.17 (s, 1H), 7.54-7.64 (m, 2H), 8.21 (dd, J = 5.3 Hz, 9.2 Hz, 1H), 8.33 (s,

1H); ^{13}C NMR (75 MHz, CDCl_3) δ 7.8, 32.8, 44.3, 49.5, 51.8, 72.4, 90.7, 95.2, 111.3 (d, $J_{\text{CF}} = 20.0$ Hz), 121.0, 128.8 (d, $J_{\text{CF}} = 11.3$ Hz), 129.1, 130.2 (d, $J_{\text{CF}} = 46.3$ Hz), 132.0 (d, $J_{\text{CF}} = 7.5$ Hz), 145.9, 146.8, 152.4, 154.3, 157.0, 170.1; IR (CH_2Cl_2 , NaCl, cm^{-1}) 2909, 2847, 2351, 2340, 1721, 1654, 1593, 1501, 1449, 1234, 1024; HRMS (EI) m/z calcd for $\text{C}_{22}\text{H}_{19}\text{FN}_2\text{O}_4$ (M^+) 394.1329, found 394.1326; LRMS (EI) m/z 394 (M^+ , 18), 365 (15), 337 (10), 320 (100), 293 (14), 171 (20), 105 (30), 83 (33), 69 (52).

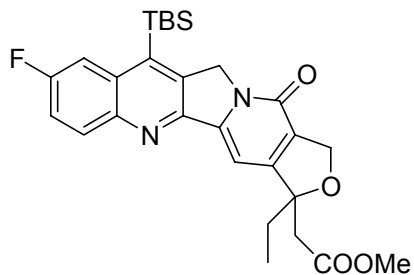
Methyl{10-[*tert*-butyl(dimethyl)silyl]-3-ethyl-13-oxo-11,13-dihydro-1*H*,3*H*-furo[3',4':6,7]indolizino[1,2-*b*]quinolin-3-yl}acetate (92c**):**



Following general procedure 3A, iodopyridone **91b** (8.3 mg, 0.016 mmol) was reacted with phenyl isonitrile (1 M, 64 μL , 0.064 mmol) and hexamethylditin (9.0 μL , 0.024 mmol) in benzene (0.27 mL) to afford **92c**, after purification, as a yellow solid (5.6 mg, 71%): ^1H NMR (500 MHz, CDCl_3) δ 0.71 (s, 6H), 0.86 (t, $J = 7.3$ Hz, 3H), 1.01 (s, 9H), 1.94 (dq, $J = 7.3$ Hz, 14.6 Hz, 1H), 2.05 (dq, $J = 7.3$ Hz, 14.7 Hz, 1H), 2.89 (d, $J = 14.7$ Hz, 1H), 2.90 (d, $J = 14.7$ Hz, 1H), 3.63 (s, 3H), 5.16 (d, $J = 13.4$ Hz, 1H), 5.18 (d, $J = 13.4$ Hz, 1H), 5.32 (s, 2H), 7.19 (s, 1H), 7.61 (t, $J = 7.3$ Hz, 1H), 7.78 (t, $J = 7.3$ Hz, 1H), 8.20 (d, $J = 8.2$ Hz, 1H), 8.24 (d, $J = 8.5$ Hz, 1H); ^{13}C NMR (75 MHz, CDCl_3) δ -0.5, 7.7, 19.2, 27.1, 32.7, 44.3, 51.7, 52.0, 72.5, 90.6, 94.7, 126.7, 128.5, 129.5, 130.5, 132.7, 136.6, 143.0, 147.0, 148.0, 151.0, 154.1, 155.2, 156.8, 170.0; IR (CH_2Cl_2 , NaCl, cm^{-1}) 2960, 2852, 2361, 2340, 1741, 1659, 1598, 1557, 1214, 1024; HRMS

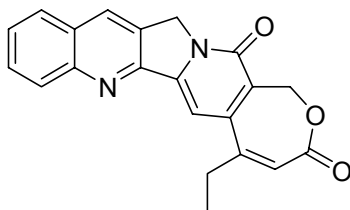
(EI) m/z calcd for $C_{28}H_{34}N_2O_4Si$ (M^+) 490.2288, found 490.2293; LRMS (EI) m/z 490 (M^+ , 27), 461 (15), 434 (10), 416 (100), 359 (14), 331 (7), 73 (8).

Methyl{10-[*tert*-butyl(dimethyl)silyl]-3-ethyl-8-fluoro-13-oxo-11,13-dihydro-1*H*,3*H*-furo[3',4':6,7]indolizino[1,2-*b*]quinolin-3-yl}acetate (92d**):**



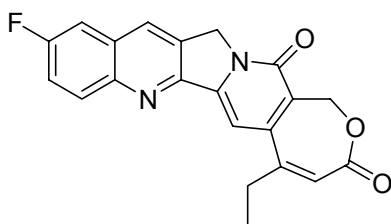
Following general procedure 3A, iodopyridone **91b** (7.7 mg, 0.015 mmol) was reacted with *p*-fluorophenyl isonitrile (1 M, 60 μ L, 0.060 mmol) and hexamethylditin (9.0 μ L, 0.022 mmol) in benzene (0.25 mL) to afford **92d**, after purification, as a yellow solid (5.0 mg, 66%): 1H NMR (300 MHz, $CDCl_3$) δ 0.71 (s, 6H), 0.85 (t, $J = 7.3$ Hz, 3H), 1.01 (s, 9H), 1.94 (dq, $J = 7.2$ Hz, 14.4 Hz, 1H), 2.05 (dq, $J = 7.5$ Hz, 14.9 Hz, 1H), 2.89 (d, $J = 14.7$ Hz, 1H), 2.90 (d, $J = 14.7$ Hz, 1H), 3.63 (s, 3H), 5.16 (s, 2H), 5.31 (s, 2H), 7.16 (s, 1H), 7.56 (ddd, $J = 2.7$ Hz, 7.6 Hz, 10.1 Hz, 1H), 7.87 (dd, $J = 2.7$ Hz, 11.1 Hz, 1H), 8.20 (dd, $J = 6.0$ Hz, 9.2 Hz, 1H); ^{13}C NMR (75 MHz, $CDCl_3$) δ -0.7, 7.8, 19.2, 27.1, 32.8, 44.3, 51.8, 52.0, 72.5, 90.7, 94.8, 113.5 (d, $J_{CF} = 24.0$ Hz), 120.0 (d, $J_{CF} = 25.0$ Hz), 128.6, 133.2 (d, $J_{CF} = 96.2$ Hz), 137.5, 142.2, 145.1, 146.8, 150.7, 154.2, 156.8, 170.1; IR (CH_2Cl_2 , NaCl, cm^{-1}) 2955, 2929, 2852, 2366, 2335, 1736, 1664, 1593, 1501, 1219; HRMS (EI) m/z calcd for $C_{28}H_{33}FN_2O_4Si$ (M^+) 508.2194, found 508.2199; LRMS (EI) m/z 508 (M^+ , 22), 479 (14), 452 (10), 434 (100), 393 (13), 349 (6), 73 (5). Copies of spectral data can be found in the appendix section.

5-Ethyl-1,13-dihydro-3*H*,15*H*-oxepino[3',4':6,7]indolizino[1,2-*b*]quinoline-3,15-dione (95a):



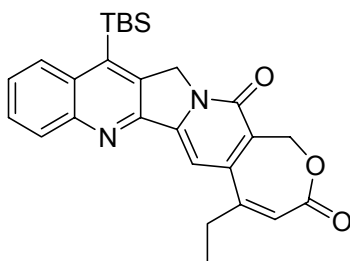
Following general procedure 3A, iodopyridone **94a** (7.2 mg, 0.020 mmol) was reacted with phenyl isonitrile (1 M, 78 μ L, 0.078 mmol) and hexamethylditin (11 μ L, 0.029 mmol) in benzene (0.33 mL) to afford **95a**, after purification, as a yellow solid (2.0 mg, 41%): ^1H NMR (300 MHz, CDCl_3) δ 1.25 (t, $J = 7.3$ Hz, 3H), 2.81 (q, $J = 7.3$ Hz, 2H), 5.36 (s, 4H), 6.51 (t, $J = 1.4$ Hz, 1H), 7.49 (s, 1H), 7.71 (t, $J = 7.4$ Hz, 1H), 7.88 (t, $J = 6.9$ Hz, 1H), 7.98 (d, $J = 8.2$ Hz, 1H), 8.30 (d, $J = 8.7$ Hz, 1H), 8.47 (s, 1H); ^{13}C NMR (151 MHz, CDCl_3) δ 12.8, 29.3, 50.5, 61.0, 123.1, 125.8, 128.3, 128.4, 128.9, 130.9, 149.0, 151.3, 159.6, 167.8; IR (CH_2Cl_2 , NaCl, cm^{-1}) 2914, 2847, 2361, 2335, 1710, 1644, 1598, 1444, 1035; HRMS (EI) m/z calcd for $\text{C}_{21}\text{H}_{16}\text{N}_2\text{O}_3$ (M^+) 344.1161, found 344.1161; LRMS (EI) m/z 344 (M^+ , 55), 315 (70), 301 (45), 285 (35), 271 (20), 242 (32), 129 (17), 91 (46), 55 (100). Copies of spectral data can be found in the appendix section.

5-Ethyl-10-fluoro-1,13-dihydro-3*H*,15*H*-oxepino[3',4':6,7]indolizino[1,2-*b*]quinoline-3,15-dione (95b):



Following general procedure 3A, iodopyridone **94a** (7.8 mg, 0.021 mmol) was reacted with *p*-fluorophenyl isonitrile (1 M, 85 μ L, 0.085 mmol) and hexamethylditin (12 μ L, 0.032 mmol) in benzene (0.35 mL) to afford **95b**, after purification, as a yellow solid (3.5 mg, 55%): ^1H NMR (300 MHz, CDCl_3) δ 1.25 (t, $J = 7.3$ Hz, 3H), 2.80 (q, $J = 7.3$ Hz, 2H), 5.34 (s, 4H), 6.51 (s, 1H), 7.35 (s, 1H), 7.58 (dd, $J = 2.5$ Hz, 8.6 Hz, 1H), 7.61-7.65 (m, 1H), 8.24 (dd, $J = 5.3$ Hz, 9.2 Hz, 1H), 8.38 (s, 1H); ^{13}C NMR (125 MHz, CDCl_3) δ 12.7, 29.1, 50.3, 60.8, 97.8, 111.3 (d, $J_{\text{CF}} = 22.5$ Hz), 121.2 (d, $J_{\text{CF}} = 25.0$ Hz), 123.1, 125.7, 129.0 (d, $J_{\text{CF}} = 10.0$ Hz), 129.6, 130.5, 132.3, 146.0, 146.3, 149.0, 151.1, 152.0, 159.5, 160.3, 162.3, 167.7; IR (CH_2Cl_2 , NaCl, cm^{-1}) 2914, 2852, 2356, 2340, 1695, 1654, 1588, 1454, 1188, 1034; HRMS (EI) m/z calcd for $\text{C}_{21}\text{H}_{15}\text{FN}_2\text{O}_3$ (M^+) 362.1067, found 362.1068; LRMS (EI) m/z 362 (M^+ , 22), 333 (30), 319 (19), 289 (7), 236 (7), 199 (12), 111 (25), 97 (46), 69 (75), 55 (100).

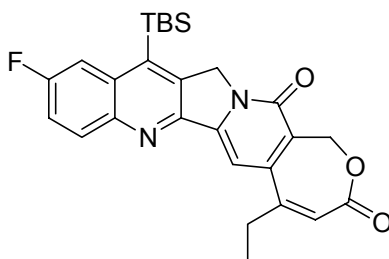
12-[*tert*-Butyl(dimethyl)silyl]-5-ethyl-1,13-dihydro-3*H*,15*H*-oxepino[3',4':6,7]indolizino[1,2-*b*]quinoline-3,15-dione (95c**):**



Following general procedure 3A, iodopyridone **94b** (11 mg, 0.023 mmol) was reacted with phenyl isonitrile (1 M, 91 μ L, 0.091 mmol) and hexamethylditin (13 μ L, 0.034 mmol) in benzene (0.38 mL) to afford **95c**, after purification, as a yellow solid (4.0 mg, 39%): ^1H NMR (300 MHz, CDCl_3) δ 0.72 (s, 6H), 1.01 (s, 9H), 1.25 (t, $J = 7.4$ Hz, 3H), 2.81 (dq, $J = 1.3$ Hz, 7.4 Hz, 2H), 5.36 (s, 4H), 6.50 (t, $J = 1.4$ Hz, 1H), 7.37 (s, 1H), 7.64 (ddd, $J = 1.5$ Hz, 6.8 Hz, 8.4

Hz, 1H), 7.80 (ddd, $J = 1.3$ Hz, 6.8 Hz, 8.2 Hz, 1H), 8.24 (t, $J = 8.6$ Hz, 2H); ^{13}C NMR (75 MHz, CDCl_3) δ -0.5, 12.7, 19.3, 27.2, 29.2, 52.8, 61.0, 97.5, 122.9, 125.1, 127.1, 129.6, 129.8, 130.7, 133.0, 136.3, 143.4, 146.7, 148.1, 149.0, 150.6, 151.4, 159.4, 167.9; IR (CH_2Cl_2 , NaCl, cm^{-1}) 2914, 2842, 2351, 2335, 1726, 1649, 1598, 1465, 1045; HRMS (EI) m/z calcd for $\text{C}_{27}\text{H}_{30}\text{N}_2\text{O}_3\text{Si}$ (M^+) 458.2026, found 458.2028; LRMS (EI) m/z 458 (M^+ , 100), 429 (58), 401 (47), 373 (63), 357 (46), 343 (16), 299 (7), 255 (7), 91 (8), 73 (15).

12-[*tert*-Butyl(dimethyl)silyl]-5-ethyl-10-fluoro-1,13-dihydro-3*H*,15*H*-oxepino[3',4':6,7]indolizino[1,2-*b*]quinoline-3,15-dione (95d):

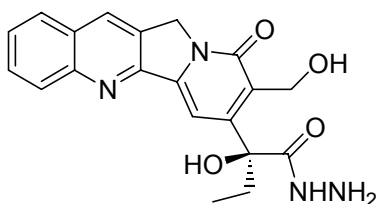


Following general procedure 3A, iodopyridone **94b** (9.0 mg, 0.019 mmol) was reacted with *p*-fluorophenyl isonitrile (1 M, 75 μL , 0.075 mmol) and hexamethylditin (11 μL , 0.028 mmol) in benzene (0.31 mL) to afford **95d**, after purification, as a yellow solid (3.0 mg, 34%): ^1H NMR (300 MHz, CDCl_3) δ 0.72 (s, 6H), 1.01 (s, 9H), 1.25 (t, $J = 7.4$ Hz, 3H), 2.81 (dq, $J = 1.3$ Hz, 7.4 Hz, 2H), 5.35 (s, 4H), 6.50 (t, $J = 1.4$ Hz, 1H), 7.34 (s, 1H), 7.59 (ddd, $J = 2.7$ Hz, 7.5 Hz, 9.3 Hz, 1H), 7.89 (dd, $J = 2.6$ Hz, 11.0 Hz, 1H), 8.23 (dd, $J = 6.0$ Hz, 9.3 Hz, 1H); ^{13}C NMR (125 MHz, CDCl_3) δ -0.7, 12.7, 19.2, 27.1, 29.2, 52.8, 60.9, 97.4, 113.2 (d, $J_{\text{CF}} = 23.8$ Hz), 120.0 (d, $J_{\text{CF}} = 25.0$ Hz), 123.0, 125.2, 133.0 (d, $J_{\text{CF}} = 102.5$ Hz), 137.0, 142.5, 145.2, 146.4, 149.0, 150.3, 151.2, 159.3, 159.7 (d, $J_{\text{CF}} = 26.2$ Hz), 161.6, 167.8; IR (CH_2Cl_2 , NaCl, cm^{-1}) 2955, 2914, 2842, 2361, 2330, 1716, 1659, 1593, 1214, 1040; HRMS (EI) m/z calcd for $\text{C}_{27}\text{H}_{29}\text{FN}_2\text{O}_3\text{Si}$ (M^+)

476.1932, found 476.1929; LRMS (EI) m/z 476 (M^+ , 100), 447 (66), 433 (36), 419 (40), 391 (57), 375 (42), 361 (15), 273 (7), 98 (10), 73 (18). Copies of spectral data can be found in the appendix section.

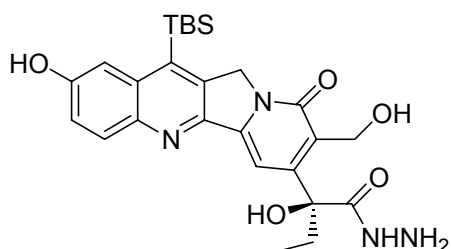
Chapter 4

(*S*)-2-Hydroxy-2-[8-(hydroxymethyl)-9-oxo-9,11-dihydroindolizino[1,2-*b*]quinolin-7-yl]butanohydrazide (**96**):



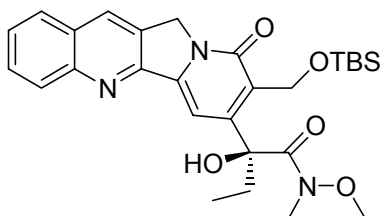
Hydrazine monohydrate (45 μ L, 0.93 mmol) was added to a suspension of camptothecin (54 mg, 0.15 mmol) in MeOH (0.62 mL) at room temperature. After stirring at the same temperature for 8 h, the reaction mixture was concentrated under reduced pressure to afford **96** as a pale yellow solid (59 mg, 100%) which was sufficiently pure for further analysis: ^1H NMR (300 MHz, CD_3SOCD_3) δ 0.85 (t, $J = 7.0$ Hz, 3H), 2.17 (d, $J = 6.8$ Hz, 2H), 4.29 (br s, 2H), 4.75 (dd, $J = 5.7$ Hz, 11.5 Hz, 1H), 4.77 (dd, $J = 5.5$ Hz, 11.6 Hz, 1H), 5.00 (t, $J = 5.6$ Hz, 1H), 5.23 (s, 2H), 6.40 (br s, 1H), 7.46 (s, 1H), 7.69 (t, $J = 7.4$ Hz, 1H), 7.84 (t, $J = 7.1$ Hz, 1H), 8.10 (d, $J = 8.1$ Hz, 1H), 8.17 (d, $J = 8.5$ Hz, 1H), 8.65 (s, 1H), 9.25 (br s, 1H); ^{13}C NMR (75 MHz, CD_3SOCD_3) δ 7.8, 31.8, 50.1, 55.3, 79.3, 99.3, 127.4, 127.7, 128.4, 128.8, 128.9, 129.7, 130.2, 131.3, 142.6, 147.9, 152.8, 152.9, 160.9, 171.7; HRMS (EI) m/z calcd for $\text{C}_{20}\text{H}_{16}\text{N}_2\text{O}_4$ ($M - \text{N}_2\text{H}_4$) 348.1110, found 348.1100; LRMS (EI) m/z 378 ($M^+ - 2$, 31), 348 (100), 319 (30), 289 (22), 248 (38), 219 (34), 140 (15). Copies of spectral data can be found in the appendix section.

(S)-2-[12-[*tert*-Butyl(dimethyl)silyl]-2-hydroxy-8-(hydroxymethyl)-9-oxo-9,11-dihydroindolizino[1,2-b]quinolin-7-yl]-2-hydroxybutanohydrazide (97):



Following the above procedure, 7-*tert*-butyldimethylsilyl-10-hydroxycamptothecin (24 mg, 0.050 mmol) was reacted with hydrazine monohydrate (24 μ L, 0.50 mmol) in MeOH (0.20 mL) to afford **97** as a yellow solid (25 mg, 99%) which was sufficiently pure for subsequent analysis: ^1H NMR (300 MHz, CD_3SOCD_3) δ 0.64 (s, 6H), 0.84 (t, J = 6.8 Hz, 1H), 0.93 (s, 9H), 2.15 (d, J = 6.9 Hz, 1H), 4.27 (br s, 2H), 4.67 (d, J = 11.6 Hz, 1H), 4.81 (d, J = 11.7 Hz, 1H), 5.16 (s, 2H), 7.35-7.38 (m, 2H), 7.54 (d, J = 2.2 Hz, 1H), 8.02 (d, J = 9.1 Hz, 1H); ^{13}C NMR (75 MHz, CD_3SOCD_3) δ -1.1, 7.9, 18.8, 27.1, 31.8, 48.6, 52.3, 79.3, 98.1, 110.8, 122.4, 127.5, 131.3, 133.9, 137.1, 138.2, 142.1, 143.1, 147.8, 153.2, 156.9, 160.7, 171.9; HRMS (EI) m/z calcd for $\text{C}_{26}\text{H}_{30}\text{N}_2\text{O}_5\text{Si}$ ($\text{M}^+ - \text{N}_2\text{H}_4$) 478.1924, found 478.1906; LRMS (EI) m/z 478 ($\text{M}^+ - \text{N}_2\text{H}_4$, 22), 434 (59), 421 (23), 377 (100), 320 (11), 291 (13), 235 (6), 73 (17).

(S)-2-[8-({*tert*-Butyl(dimethyl)silyl}oxy)methyl]-9-oxo-9,11-dihydroindolizino[1,2-b]quinolin-7-yl]-2-hydroxy-*N*-methoxy-*N*-methylbutanamide (99):

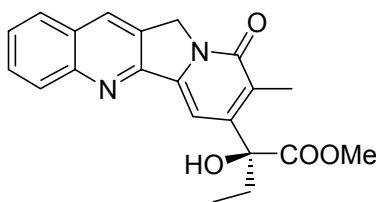


Trimethylaluminum (2 M in heptane, 0.52 mL, 1.0 mmol) was added dropwise via a syringe over 3 - 4 min to a suspension of *N,O*-dimethylhydroxylamine hydrochloride (0.10 g, 1.0 mmol) in CH₂Cl₂ (5.4 mL) at -10 °C accompanied by the evolution of gas. The resulting colorless solution was stirred at room temperature for 30 min and recooled to 0 °C. A suspension of camptothecin (0.12 g, 0.34 mmol) in CH₂Cl₂ (1.5 mL) was then added and the resulting clear brown solution was stirred at room temperature for 22 h. NaHSO₄ (1 M, 1.2 mL) was carefully added and the resulting mixture was extracted with CH₂Cl₂ (3 x 10 mL). The combined organic extracts were washed with brine (10 mL), dried over MgSO₄ and concentrated under reduced pressure to afford **98** as a yellow solid (96 mg, 68%). The crude product was used in the subsequent reaction immediately after the workup.

Alcohol **98** (95 mg, 0.23 mmol) was added to a solution of *tert*-butylchlorodimethylsilane (53 mg, 0.35 mmol) and imidazole (44 mg, 0.64 mmol) in DMF (0.19 mL). The reaction mixture was heated to 35 °C and stirred for 24 h. The reaction mixture was diluted with water (5 mL) and then extracted with ethyl acetate (3 x 5 mL). The combined organic extracts were washed with brine, dried over MgSO₄ and concentrated under reduced pressure to afford the Weinreb amide **99** as a pale yellow solid (0.11 g, 92%). The crude product was sufficiently pure for subsequent analysis. However, an analytical sample of **99** was prepared by purification of the crude product by flash column chromatography (step gradient elution 1:49, 1:19, 1:9 acetone/dichloromethane): ¹H NMR (300 MHz, CDCl₃) δ 0.19 (s, 3H), 0.22 (s, 3H), 0.96 (s, 9H), 0.97 (t, *J* = 7.3 Hz, 3H), 2.18 (dq, *J* = 7.4 Hz, 14.1 Hz, 1H), 2.44 (dq, *J* = 7.3 Hz, 13.9 Hz, 1H), 3.22 (s, 3H), 3.24 (s, 3H), 5.01 (d, *J* = 10.6 Hz, 1H), 5.02 (d, *J* = 10.7 Hz, 1H), 5.26 (d, *J* = 19.0 Hz, 1H), 5.30 (d, *J* = 19.0 Hz, 1H), 5.41 (br s, 1H), 7.37 (s, 1H), 7.65 (ddd, *J* = 1.1 Hz, 6.9 Hz, 8.1 Hz, 1H), 7.82 (ddd, *J* = 1.4 Hz, 6.9 Hz, 8.4 Hz, 1H), 7.92 (d, *J* = 8.1 Hz, 1H), 8.22 (d, *J* = 8.5 Hz, 1H), 8.37 (s, 1H); ¹³C

NMR (75 MHz, CDCl₃) δ -5.4, -5.2, 7.6, 18.5, 26.0, 31.4, 33.3, 50.1, 56.5, 59.9, 80.0, 99.4, 127.5, 127.7, 128.0, 128.1, 128.8, 129.6, 130.4, 130.9, 143.8, 148.8, 152.9, 154.4, 161.3, 172.9; IR (CH₂Cl₂, NaCl, cm⁻¹) 3370, 2929, 2847, 1659, 1603, 1465, 1398, 1250, 1055; HRMS (EI) m/z calcd for C₂₈H₃₇N₃O₅Si (M⁺) 523.2502, found 523.2477; LRMS (EI) m/z 523 (M⁺, 18), 508 (28), 466 (100), 377 (98), 363 (28), 303 (60), 275 (15), 191 (7), 75(72). Copies of spectral data can be found in the appendix section.

(S)-2-Hydroxy-2-(8-methyl-9-oxo-9,11-dihydroindolizino[1,2-*b*]quinolin-7-yl)butanoic acid methyl ester (103):

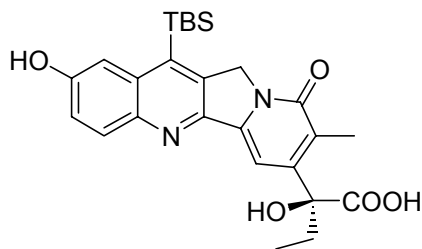


Triethylamine (0.17 mL, 1.2 mmol) was added to a solution of camptothecin (27 mg, 0.078 mmol) in DMF (1.7 mL) under argon. Dry 10% palladium on activated carbon (5 mg) was carefully added to the reaction mixture and the dissolved oxygen was removed under vacuum. Then a balloon of hydrogen was mounted and the mixture was stirred vigorously for 24 h. The catalyst was removed by filtration of the reaction mixture through a pad of Celite. The filtrate was concentrated under reduced pressure to remove solvents and excess reagents. The crude product was purified by semipreparative HPLC using Symmetry C18 column under isocratic elution conditions (30:70 MeOH/H₂O + 0.1% HCOOH) to afford acid **101** as a yellow solid (11 mg, 40%). This was used immediately in the subsequent reaction.

TMSCHN₂ (2 M solution in hexanes, 20 μ L, 0.041 mmol) was added to a solution of **101** (11 mg, 0.031 mmol) in a mixture of methanol (0.10 mL) and benzene (0.21 mL) at room

temperature. After 30 min, the reaction mixture was concentrated under reduced pressure. The crude product was purified by flash column chromatography (gradient elution 1:4 to 7:3 acetone/dichloromethane) to afford the ester **103** as a pale yellow solid (8.6 mg, 76%): $^1\text{H NMR}$ (300 MHz, CDCl_3) δ 1.05 (t, $J = 7.3$ Hz, 3H), 2.31 (s, 3H), 2.37 (q, $J = 7.5$ Hz, 2H), 3.79 (s, 3H), 5.24 (s, 2H), 7.57 (s, 1H), 7.58 (t, $J = 7.4$ Hz, 1H), 7.78 (t, $J = 8.4$ Hz, 1H), 7.82 (d, $J = 8.2$ Hz, 1H), 8.17 (d, $J = 8.5$ Hz, 1H), 8.27 (s, 1H); HRMS (EI) m/z calcd for $\text{C}_{21}\text{H}_{20}\text{N}_2\text{O}_4$ (M^+) 364.1423, found 364.1406; LRMS (EI) m/z 364 (M^+ , 67), 346 (19), 305 (100), 276 (65), 248 (35), 219 (45), 140 (13), 75 (15).

(S)-2-{12-[*tert*-Butyl(dimethyl)silyl]-2-hydroxy-8-methyl-9-oxo-9,11-dihydroindolizino[1,2-*b*]quinolin-7-yl}-2-hydroxybutanoic acid (102**):**

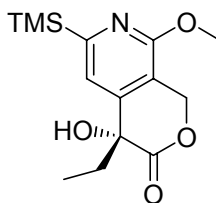


Triethylamine (98 μL , 0.70 mmol) was added to a solution of 7-*tert*-butyldimethylsilyl-10-hydroxy camptothecin (21 mg, 0.044 mmol) in MeOH (0.98 mL) under argon. Dry 10% palladium on activated carbon (4 mg) was carefully added to the reaction mixture and the dissolved oxygen was removed under vacuum. Then a balloon of hydrogen was mounted and the mixture was stirred vigorously for 14 h. The catalyst was removed by filtration of the reaction mixture through a pad of Celite. The filtrate was concentrated under reduced pressure to remove solvents and excess reagents. The crude product was purified by preparative TLC under isocratic elution conditions (95:5:5 dichloromethane/methanol/water) to afford **102** as a yellow solid (17

mg, 83%): ^1H NMR (300 MHz, CD_3SOCD_3) δ 0.68 (s, 6H), 0.88 (t, $J = 6.8$ Hz, 3H), 0.98 (s, 9H), 1.88-2.09 (m, 2H), 2.24 (s, 3H), 5.10 (s, 2H), 7.33 (dd, $J = 2.4$ Hz, 9.0 Hz, 1H), 7.45 (s, 1H), 7.53 (d, $J = 2.4$ Hz, 1H), 7.99 (d, $J = 9.1$ Hz, 1H); ^{13}C NMR (75 MHz, CD_3SOCD_3) δ -1.1, 8.9, 13.9, 18.9, 27.1, 31.1, 52.1, 78.7, 99.1, 110.9, 121.8, 125.9, 131.3, 133.5, 137.0, 138.4, 140.6, 142.3, 148.9, 153.7, 155.9, 161.1, 175.4. Copies of spectral data can be found in the appendix section.

Chapter 5

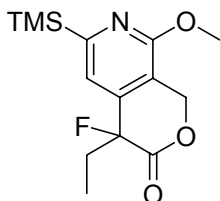
(*R*)-(-)-4-Ethyl-4-hydroxy-8-methoxy-6-(trimethylsilyl)-1,4-dihydro-3*H*-pyrano[3,4-*c*]pyridine-3-one [(*R*)-115]:



Enol ether **114** (1.1 g, 4.0 mmol) was added to a vigorously stirred solution of $\text{K}_3\text{Fe}(\text{CN})_6$ (4.0 g, 12 mmol), K_2CO_3 (1.7 g, 12 mmol), $\text{CH}_3\text{SO}_2\text{NH}_2$ (74 mg, 7.8 mmol), $(\text{DHQ})_2\text{-PYR}$ (89 mg, 0.20 mmol) and OsO_4 (0.25 mL of a 2.5w% in $t\text{BuOH}$, 0.5 mol%) in a 1:1 mixture of $t\text{BuOH}/\text{H}_2\text{O}$ (40 mL) at 0 °C. After stirring at room temperature for 18 h, Na_2SO_3 (4.0 g) was slowly added and the resulting suspension stirred for a further 30 min. CH_2Cl_2 (50 mL) and H_2O (50 mL) were added and the aqueous layer was further extracted with CH_2Cl_2 (3 x 25 mL). The combined organic extracts were dried over Na_2SO_4 and concentrated under reduced pressure. The crude product was purified by flash chromatography (5:1 dichloromethane/ethyl acetate) to afford the α -hydroxylactol as a white solid (0.96 g, 85%).

N-Iodosuccinimide (3.3 g, 15 mmol) and tetrabutylammonium iodide (1.1 g, 3.0 mmol) were added to a solution of the α -hydroxylactol (0.88 g, 3.0 mmol) in CH₂Cl₂ (6.0 mL). The reaction mixture was stirred at room temperature in the dark for 3 h, 5% Na₂SO₄ (50 mL) was added and the biphasic solution further diluted with CH₂Cl₂ (50 mL). The organic phase was washed with H₂O (3 x 30 mL), dried over Na₂SO₄ and concentrated under reduced pressure. The crude product was purified by flash chromatography (1:4 ethyl acetate/hexanes) to afford the lactone (**R**)-**115** as a clear oil (0.79 g, 90%, 96% ee); [α]_D²³ = -83.0 (c = 0.5, CHCl₃). For this lactone, all spectral data matched that previously reported for the corresponding (*S*)-lactone.⁶⁵

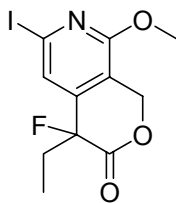
(R)-(-)- **and** **(S)-(+)-4-Ethyl-4-fluoro-8-methoxy-6-trimethylsilyl-1,4-dihydro-3H-pyrano[3,4-c]pyridin-3-one (116):**



Diethylamino sulfurtrifluoride (15 μ L, 0.11 mmol) was added dropwise via a syringe to a solution of (**R**)-**115** (31 mg, 0.10 mmol) in CH₂Cl₂ (0.27 mL) at -78 °C. After stirring for 2 h at -78 °C, the reaction mixture was quenched with water (1.0 mL) and warmed to room temperature. The resulting suspension was extracted with CH₂Cl₂ (3 x 5 mL). The combined organic extracts were dried over MgSO₄ and concentrated under reduced pressure to afford (**S**)-**116** as a yellow solid (22 mg, 76%). The crude product was sufficiently pure for subsequent reaction. Pyridine lactone (**S**)-**116** was analyzed for enantiomeric purity using (S,S) WHELK O 1 chiral column under isocratic elution with 5% isopropanol in hexanes. The enantiomeric excess (ee) was determined to be 93%. Following the same procedure, (**S**)-**115** (36 mg, 0.12 mmol) was

reacted with diethylamino sulfurtrifluoride (18 μ L, 0.13 mmol) in CH_2Cl_2 (0.31 mL) to afford the product **(R)-116** as a yellow solid (31 mg, 86%, 91% ee): ^1H NMR (300 MHz, CDCl_3) δ 0.31 (s, 9H), 1.03 (t, $J = 7.4$ Hz, 3H), 2.01 (m, 2H), 4.01 (s, 3H), 5.21 (d, $J = 15.9$ Hz, 1H), 5.54 (d, $J = 15.9$ Hz, 1H), 7.25 (s, 1H); ^{19}F NMR (282 MHz, CDCl_3) δ -164.3 (t, $J = 22.6$ Hz); ^{13}C NMR (75 MHz, CDCl_3) δ -2.0, 7.2 (d, $J = 4.2$ Hz), 30.3 (d, $J = 27.0$ Hz), 53.5, 65.5, 90.1 (d, $J = 191$ Hz), 110.8 (d, $J = 5.5$ Hz), 116.9 (d, $J = 5.3$ Hz), 142.8 (d, $J = 24.0$ Hz), 157.9, 167.0, 167.9 (d, $J = 22.0$ Hz); IR (CHCl_3 , NaCl, cm^{-1}) 2950, 2893, 1767, 1577, 1449, 1357, 1244, 1096; HRMS (EI) m/z calcd for $\text{C}_{14}\text{H}_{20}\text{FNO}_3\text{Si}$ (M^+) 297.1197, found 297.1202; LRMS (EI) m/z 297 (M^+ , 32), 282 (100), 269 (30), 254 (32), 238 (32), 213 (27), 162 (10), 84 (27), 77 (38); For “R” $[\alpha]_{\text{D}}^{23} = -57.2$ ($c = 0.50$, CH_2Cl_2), for “S” $[\alpha]_{\text{D}}^{23} = +59.5$ ($c = 0.64$, CH_2Cl_2). Copies of spectral data including the HMBC spectrum can be found in the appendix section.

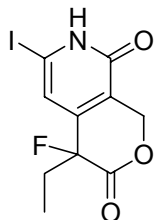
(R)-(-)- and (S)-(+)-4-Ethyl-4-fluoro-6-iodo-8-methoxy-1,4-dihydro-3H-pyrano[3,4-c]pyridin-3-one:



ICl (1 M in dichloromethane, 1.2 mL, 1.2 mmol) was added to a solution of **(S)-116** (92 mg, 0.31 mmol) in CH_2Cl_2 (1.5 mL) at 0°C in an ice bath and then allowed to warm to room temperature. After stirring for 16 h, the reaction mixture was poured into a chilled solution of 5% Na_2SO_3 /brine (1:1, 24 mL) and extracted the mixture with ethyl acetate (3 x 30 mL). The combined organic extracts were dried over MgSO_4 and concentrated under reduced pressure. The crude product was purified by flash chromatography (step gradient elution 1:9 to 1:4 ethyl

acetate/hexanes) to afford the corresponding (*S*)-iodide as a pale yellow oil (63 mg, 59%). Following the same procedure, (***R***)-**116** (0.10 g, 0.35 mmol) was reacted with ICl (1.4 mL, 1.4 mmol) in CH₂Cl₂ (1.8 mL) to afford the corresponding (*R*)-iodide as a pale yellow oil (80 mg, 65%): ¹H NMR (300 MHz, CDCl₃) δ 1.02 (t, *J* = 7.3 Hz, 3H), 1.99 (m, 2H), 3.99 (s, 3H), 5.13 (d, *J* = 15.8 Hz, 1H), 5.46 (d, *J* = 15.9 Hz, 1H), 7.50 (s, 1H); ¹⁹F NMR (282 MHz, CDCl₃) δ -164.3 (t, *J* = 22.6 Hz); ¹³C NMR (75 MHz, CDCl₃) δ 7.2, 30.1 (d, *J* = 26.3 Hz), 54.8, 64.8, 89.4 (d, *J* = 192.9 Hz), 111.0 (d, *J* = 5.6 Hz), 113.3, 122.7 (d, *J* = 6.6 Hz), 146.0 (d, *J* = 23.6 Hz), 157.7, 167.0 (d, *J* = 21.6 Hz); IR (CHCl₃, NaCl, cm⁻¹) 2980, 2950, 1772, 1582, 1460, 1362, 1096; HRMS (EI) *m/z* calcd for C₁₁H₁₁FINO₃ (M⁺) 350.9768, found 350.9769; LRMS (EI) *m/z* 351 (M⁺, 100), 323 (6), 307 (55), 292 (44), 224 (27), 180 (45), 137 (24), 109 (19), 77 (13); For “*R*” [α]_D²³ = -39.3 (c = 0.70, CH₂Cl₂), for “*S*” [α]_D²³ = +38.9 (c = 2.80, CH₂Cl₂).

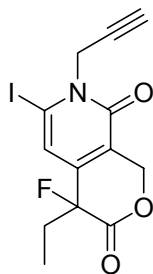
(*R*)-(-)- and (*S*)-(+)-4-Ethyl-4-fluoro-6-iodo-1*H*-pyrano[3,4-*c*]pyridine-3,8(4*H*,7*H*)-dione:



Sodium iodide (81 mg, 0.54 mmol) was added to a solution of the above (*S*)-iodide (63 mg, 0.18 mmol) in dry acetonitrile (2.4 mL) at room temperature. Chlorotrimethylsilane (68 μL, 0.54 mmol) was then added and the reaction mixture was stirred for 15 min at room temperature. H₂O (2.0 μL, 0.090 mmol) was next added and the reaction mixture was heated to 60 °C and stirred at that temperature for 14 h. The mixture was then poured into a solution of 5% Na₂SO₃/brine (1:1, 17 mL) and quickly extracted with ethyl acetate (3 x 20 mL). The combined organic extracts were dried over MgSO₄ and concentrated under reduced pressure. The crude product was

purified by flash chromatography (1:4 ethyl acetate/hexanes) to afford the corresponding (*S*)-iodopyridone as a pale yellow solid (43 mg, 71%). Following the same procedure, (*R*)-iodide (80 mg, 0.23 mmol) was reacted with sodium iodide (0.10 g, 0.68 mmol), chlorotrimethylsilane (87 μ L, 0.68 mmol) and H₂O (2.0 μ L, 0.11 mmol) in dry acetonitrile (3.0 mL) to afford the corresponding (*R*)-iodopyridone as a pale yellow solid (58 mg, 76%): ¹H NMR (300 MHz, CDCl₃) δ 1.06 (t, *J* = 7.2 Hz, 3H), 2.02 (dq, *J* = 7.2 Hz, 21.4 Hz, 2H), 5.11 (d, *J* = 16.2 Hz, 1H), 5.54 (d, *J* = 16.3 Hz, 1H), 6.95 (s, 1H); ¹⁹F NMR (282 MHz, CDCl₃) δ -164.2 (t, *J* = 22.6 Hz); ¹³C NMR (75 MHz, CDCl₃) δ 7.3, 30.0 (d, *J* = 26.2 Hz), 65.3, 89.0 (d, *J* = 193.2 Hz), 95.4, 114.1 (d, *J* = 5.3 Hz), 118.5, 147.2 (d, *J* = 23.4 Hz), 161.2, 166.5 (d, *J* = 21.8 Hz); IR (CHCl₃, NaCl, cm⁻¹) 3431, 3098, 2919, 2842, 1762, 1649, 1547, 1454, 1152; HRMS (EI) *m/z* calcd for C₁₀H₉FINO₃ (M⁺) 336.9611, found 336.9613; LRMS (EI) *m/z* 337 (M⁺, 100), 309 (7), 293 (94), 278 (56), 266 (23), 166 (38), 138 (28), 91 (35); For “*R*” [α]_D²³ = -45.2 (c = 0.21, CH₂Cl₂), for “*S*” [α]_D²³ = +46.7 (c = 0.15, CH₂Cl₂).

(*R*)-(-)- and (*S*)-(+)-4-Ethyl-4-fluoro-6-iodo-7-prop-2-ynyl-1*H*-pyrano[3,4-*c*]pyridine-3,8(4*H*,7*H*)-dione (109):



NaH in mineral oil (95%, 3.5 mg, 0.14 mmol) was added to a solution of the above (*S*)-iodopyridone (43 mg, 0.13 mmol) in a mixture of DME (0.40 mL) and DMF (0.13 mL) at 0 °C under argon. After stirring this mixture for 10 min at 0 °C, LiBr (22 mg, 0.25 mmol) was added.

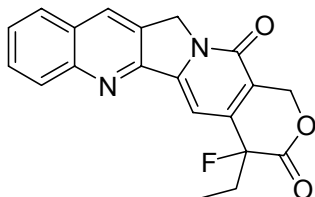
The reaction mixture was allowed to warm to room temperature and stirred for 15 min. Propargyl bromide (80% w/w in toluene, 42 μ L, 0.38 mmol) was then added via a syringe and the reaction mixture was heated in the dark at 65 $^{\circ}$ C for 6 h. The final solution was poured into brine (5 mL) and extracted with ethyl acetate (3 x 5 mL). The combined organic extracts were dried over MgSO_4 and concentrated under reduced pressure. The crude product was purified by flash chromatography (1:9 ethyl acetate/dichloromethane) to give (**S**)-**109** as a white solid (28 mg, 60%). Following the same procedure, (*R*)-iodopyridone (58 mg, 0.17 mmol) was alkylated with propargyl bromide (58 μ L, 0.52 mmol) in the presence of NaH (4.8 mg, 0.19 mmol) and LiBr (30 mg, 0.34 mmol) in a mixture of DME (0.54 mL) and DMF (0.18 mL) to afford (**R**)-**109** as a white solid (42 mg, 66%): ^1H NMR (300 MHz, CDCl_3) δ 1.05 (t, $J = 7.5$ Hz, 3H), 2.00 (m, 2H), 2.40 (t, $J = 2.5$ Hz, 1H), 5.08 (dd, $J = 1.4$ Hz, 14.3 Hz, 1H), 5.11 (s, 2H), 5.48 (dd, $J = 1.2$ Hz, 16.9 Hz, 1H), 7.06 (s, 1H); ^{19}F NMR (282 MHz, CDCl_3) δ -164.4 (t, $J = 22.6$ Hz); ^{13}C NMR (75 MHz, CDCl_3) δ 7.3, 30.0 (d, $J = 26.5$ Hz), 44.1, 65.9, 73.7, 88.6 (d, $J = 192.7$ Hz), 100.5, 115.1 (d, $J = 7.8$ Hz), 119.3, 145.2 (d, $J = 23.6$ Hz), 157.5, 166.4 (d, $J = 21.8$ Hz); IR (CHCl_3 , NaCl, cm^{-1}) 3257, 3083, 2909, 2115, 1762, 1654, 1419, 1526, 1132; HRMS (EI) m/z calcd for $\text{C}_{13}\text{H}_{11}\text{FINO}_3$ (M^+) 374.9768, found 374.9771; LRMS (EI) m/z 375 (M^+ , 100), 346 (8), 331 (20), 248 (5), 122 (8), 75 (13); For “*R*” $[\alpha]_{\text{D}}^{23} = -29.6$ (c = 0.50, CH_2Cl_2), for “*S*” $[\alpha]_{\text{D}}^{23} = +32.0$ (c = 0.35, CH_2Cl_2). Copies of spectral data can be found in the appendix section.

General procedure 5A: Radical Cascade Cyclization towards the Synthesis of 20-Fluorocamptothecins.

A solution of iodopyridone **109** in benzene was taken up in a 15 x 45 mm cylindrical screw-cap glass vial and kept at room temperature. A solution of isonitrile and then

hexamethylditin were added at room temperature. The vial was capped and the reaction mixture was irradiated with a 275W GE sunlamp for 5 h. The solvent was then evaporated and the residue was purified by flash column chromatography (1:9 acetone/dichloromethane).

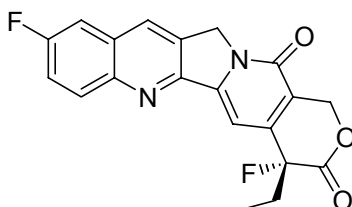
(R)-(-)- and (S)-(+)-20-Fluoro camptothecin (107):



Following general procedure 5A, iodopyridone (**S**)-**109** (10 mg, 0.027 mmol) was reacted with phenyl isonitrile (1 M in benzene, 0.13 mL, 0.13 mmol) and hexamethylditin (15 μ L, 0.040 mmol) in benzene (0.44 mL) to afford (**S**)-**107**, after purification, as a yellow solid (1.0 mg, 11%). Following the same procedure, iodopyridone (**R**)-**109** (12 mg, 0.033 mmol) was reacted with phenyl isonitrile (1 M in benzene, 0.17 mL, 0.17 mmol) and hexamethylditin (19 μ L, 0.050 mmol) in benzene (0.55 mL) to afford (**R**)-**107**, after purification, as a yellow solid (1.6 mg, 14%): ^1H NMR (300 MHz, CDCl_3) δ 1.12 (t, $J = 7.4$ Hz, 3H), 2.14 (dq, $J = 7.4$ Hz, 22.2 Hz, 2H), 5.28 (dd, $J = 1.4$ Hz, 15.3 Hz, 1H), 5.32 (s, 2H), 5.72 (dd, $J = 1.2$ Hz, 16.7 Hz, 1H), 7.54 (s, 1H) 7.69 (ddd, $J = 1.2$ Hz, 6.9 Hz, 8.1 Hz, 1H), 7.86 (ddd, $J = 1.5$ Hz, 6.9 Hz, 8.4 Hz, 1H), 7.95 (d, $J = 8.2$ Hz, 1H), 8.24 (d, $J = 8.3$ Hz, 1H), 8.42 (s, 1H); ^{19}F NMR (282 MHz, CDCl_3) δ -163.2 (t, $J = 22.6$ Hz); ^{13}C NMR (75 MHz, CDCl_3) δ 7.4, 30.1 (d, $J = 14.7$ Hz), 50.2, 66.1, 89.5 (d, $J = 193.7$ Hz), 96.6 (d, $J = 3.7$ Hz), 119.5, 128.2, 128.4, 129.8, 130.8, 131.2, 146.4 (d, $J = 14.3$ Hz), 146.9, 149.0, 152.1, 157.3, 167.3 (d, $J = 11.3$ Hz); IR (CHCl_3 , NaCl, cm^{-1}) 2914, 2842, 2356, 2335, 1767, 1649, 1603, 1454, 1157; HRMS (EI) m/z calcd for $\text{C}_{20}\text{H}_{15}\text{FN}_2\text{O}_3$ (M^+) 350.1067, found 350.1055; LRMS (EI) m/z 350 (M^+ , 45), 307 (10), 291 (25), 266 (10), 129 (17), 97 (40),

83 (50), 69 (69), 57 (100); For “*R*” $[\alpha]_D^{23} = -76.2$ ($c = 0.08$, CH_2Cl_2), for “*S*” $[\alpha]_D^{23} = +74.4$ ($c = 0.10$, CH_2Cl_2). Copies of spectral data can be found in the appendix section.

(*R*)-(-)-10,20-Difluorocamptothecin (111a):

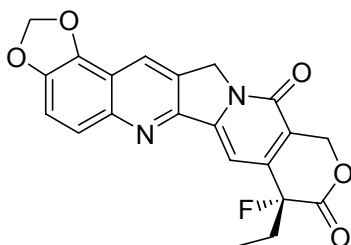


Following the general procedure 5A, iodopyridone (**(*R*)-109**) (9.0 mg, 0.024 mmol) was reacted with *p*-fluorophenyl isonitrile (1 M in benzene, 0.12 mL, 0.12 mmol) and hexamethylditin (14 μL , 0.036 mmol) in benzene (0.40 mL) to afford (**(*R*)-111a**), after purification, as a pale yellow solid (2.0 mg, 23%): ^1H NMR (300 MHz, CDCl_3) δ 1.13 (t, $J = 7.4$ Hz, 3H), 2.14 (dq, $J = 7.6$ Hz, 22.0 Hz, 2H), 5.28 (d, $J = 17.3$ Hz, 1H), 5.33 (s, 2H), 5.73 (d, $J = 16.7$ Hz, 1H), 7.53 (s, 1H), 7.56-7.67 (m, 2H), 8.26 (dd, $J = 5.4$ Hz, 9.3 Hz, 1H), 8.38 (s, 1H); ^{19}F NMR (282 MHz, CDCl_3) δ -108.7 (dd, $J = 8.5$ Hz, 14.1 Hz), -161.6 (t, $J = 22.6$ Hz); IR (CH_2Cl_2 , NaCl, cm^{-1}) 3354, 2924, 2858, 1762, 1664, 1603, 1495, 1465, 1229, 1060; HRMS (EI) m/z calcd for $\text{C}_{20}\text{H}_{14}\text{F}_2\text{N}_2\text{O}_3$ (M^+) 368.0972, found 368.0973; LRMS (EI) m/z 368 (M^+ , 100), 340 (16), 325 (35), 309 (67), 297 (72), 261 (19), 158 (19), 131 (17), 75 (20); $[\alpha]_D^{23} = -10.0$ ($c = 0.005$, CH_2Cl_2).

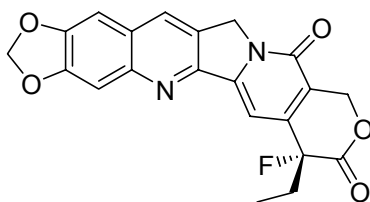
(*R*)-(-)-20-Fluoro-9,10-methylenedioxy camptothecin (111b) and 20-Fluoro-10,11-methylenedioxcamptothecin (111c):

Following the general procedure 5A, iodopyridone (**(*R*)-109**) (25 mg, 0.024 mmol) was reacted with 3,4-methylenedioxyphenyl isonitrile (49 mg, 0.33 mmol) and hexamethylditin (39 μL , 0.10 mmol) in benzene (1.1 mL) to afford a separable 1:2.5 mixture of 9,10- and 10,11-

methylenedioxy isomers (**R**)-111b and (**R**)-111c, after purification, as a pale yellow solids (2.0 and 5.0 mg respectively, 26%):

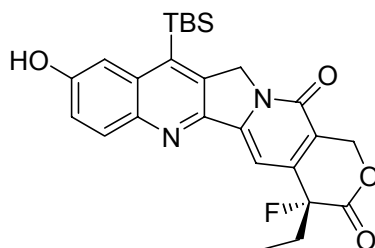


^1H NMR (300 MHz, CDCl_3) δ 1.12 (t, $J = 7.4$ Hz, 3H), 2.13 (dq, $J = 7.4$ Hz, 21.6 Hz, 2H), 5.27 (d, $J = 16.5$ Hz, 1H), 5.30 (s, 2H), 5.73 (d, $J = 16.6$ Hz, 1H), 6.29 (s, 2H), 7.49 (s, 1H), 7.53 (d, $J = 8.8$ Hz, 1H), 7.86 (d, $J = 9.0$ Hz, 1H), 8.38 (s, 1H); ^{19}F NMR (282 MHz, CDCl_3) δ -163.5 (t, $J = 22.0$ Hz); IR (CH_2Cl_2 , NaCl, cm^{-1}) 3354, 2919, 2852, 2345, 2325, 1659, 1629, 1460, 1050; HRMS (EI) m/z calcd for $\text{C}_{21}\text{H}_{15}\text{FN}_2\text{O}_5$ (M^+) 394.0965, found 394.0954; LRMS (EI) m/z 394 (M^+ , 100), 365 (13), 323 (36), 310 (17), 153 (5); $[\alpha]_{\text{D}}^{23} = -14.2$ ($c = 0.06$, CH_2Cl_2).



^1H NMR (300 MHz, CDCl_3) δ 1.12 (t, $J = 7.4$ Hz, 3H), 2.13 (m, 2H), 5.25 (s, 2H), 5.27 (d, $J = 16.4$ Hz, 1H), 5.73 (d, $J = 16.4$ Hz, 1H), 6.21 (s, 2H), 7.17 (s, 1H), 7.45 (s, 1H), 7.50 (s, 1H), 8.21 (s, 1H); ^{19}F NMR (282 MHz, CDCl_3) δ -163.6 (t, $J = 22.0$ Hz); IR (CH_2Cl_2 , NaCl, cm^{-1}) 2919, 2842, 1654, 1465, 1255, 1157, 1111; HRMS (EI) m/z calcd for $\text{C}_{21}\text{H}_{15}\text{FN}_2\text{O}_5$ (M^+) 394.0965, found 394.0964; LRMS (EI) m/z 394 (M^+ , 100), 365 (13), 351 (17), 335 (60), 323 (54), 310 (25), 207 (10), 105 (19), 64 (42); $[\alpha]_{\text{D}}^{23} = -8.3$ ($c = 0.17$, CH_2Cl_2). Copies of spectral data of both isomers can be found in the appendix section.

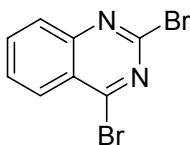
(R)-(-)-7-tert-Butyldimethylsilyl-20-fluoro-10-hydroxy camptothecin (112):



Diethylamino sulfurtrifluoride (9.0 μL , 0.070 mmol) was added dropwise via a syringe to a solution of **DB67** (31 mg, 0.064 mmol) in CH_2Cl_2 (0.21 mL) at $-78\text{ }^\circ\text{C}$. After stirring for 2 h at $-78\text{ }^\circ\text{C}$, the reaction mixture was quenched with water (1.0 mL) and warmed to room temperature. The resulting suspension was extracted with CH_2Cl_2 (3 x 5 mL). The combined organic extracts were dried over MgSO_4 and concentrated under reduced pressure to afford **112** as a yellow solid (19 mg, 61%). The crude product was sufficiently pure for subsequent analysis: ^1H NMR (300 MHz, CD_3SOCD_3) δ 0.64 (s, 6H), 0.94 (s, 9H), 0.96 (t, $J = 7.5$ Hz, 3H), 2.07-2.22 (m, 2H), 5.22 (s, 2H), 5.47 (d, $J = 16.7$ Hz, 1H), 5.50 (d, $J = 16.4$ Hz, 1H), 7.10 (s, 1H), 7.38 (dd, $J = 2.4$ Hz, 9.1 Hz, 1H), 7.56 (d, $J = 2.5$ Hz, 1H), 8.03 (d, $J = 9.1$ Hz, 1H); ^{19}F NMR (282 MHz, CDCl_3) δ -163.5; ^{13}C NMR (150 MHz, CD_3OD) δ -0.8, 7.7, 19.8, 27.6, 30.2 (d, $J = 25.6$ Hz), 53.8, 66.7, 91.2 (d, $J = 191.0$ Hz), 95.7 (d, $J = 8.4$ Hz), 112.0, 119.2 (d, $J = 4.5$ Hz), 123.3, 132.4, 135.6, 138.1, 140.9, 143.8, 147.3 (d, $J = 24.0$ Hz), 148.4 (d, $J = 36.0$ Hz), 157.6, 158.2, 168.5 (d, $J = 21.0$ Hz); IR (CH_2Cl_2 , NaCl, cm^{-1}) 3380, 3242, 2929, 2858, 1767, 1659, 1588, 1552, 1413, 1301, 1106; HRMS (EI) m/z calcd for $\text{C}_{26}\text{H}_{29}\text{FN}_2\text{O}_4\text{Si}$ (M^+) 480.1881, found 480.1876; LRMS (EI) m/z 480 (M^+ , 31), 423 (40), 379 (20), 264 (43), 199 (12), 136 (13), 91 (100), 73 (52); $[\alpha]_{\text{D}}^{23} = -15.0$ (c = 0.08, CH_2Cl_2).

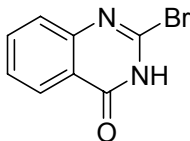
Chapter 6

2,4-Dibromoquinazoline (117):



A two-necked round bottomed flask charged with benzoylene urea (1.9 g, 12 mmol) was fitted with an overhead mechanical stirrer. Addition of phosphorus oxybromide (23 g, 80 mmol) was followed by a dropwise addition of *N,N*-dimethylaniline (0.75 mL, 5.9 mmol) via a syringe at room temperature. This mixture was heated to 105 °C in an oil bath and vigorously stirred for 4 h. At this temperature, the reaction mixture forms a pale yellow slurry which, after the reaction is done, turns bright yellow. The reaction was then cooled to 0 °C in an ice bath and carefully quenched with chilled water. The resulting mixture was extracted with CH₂Cl₂ (3 x 100 mL). The combined organic extracts were dried over MgSO₄ and concentrated under reduced pressure. The crude product was immediately purified by column chromatography using basic alumina as the immobile phase (gradient elution 15:85 to 3:2 ethyl acetate/hexanes) to afford **117** as a white solid (1.8 g, 52%): ¹H NMR (300 MHz, CD₃OD) δ 7.78 (ddd, *J* = 1.2 Hz, 7.0 Hz, 8.3 Hz, 1H), 7.89 (dd, *J* = 0.5 Hz, 8.4 Hz, 1H), 8.01 (ddd, *J* = 1.4 Hz, 6.9 Hz, 8.4 Hz, 1H), 8.19 (dd, *J* = 1.3 Hz, 8.4 Hz, 1H); ¹³C NMR (75 MHz, CDCl₃) δ 124.8, 128.0, 128.3, 129.5, 136.0, 145.7, 151.8, 157.6; HRMS (EI) *m/z* calcd for C₈H₄⁷⁹Br₂N₂ (*M*⁺ - 2) 285.8741, found 285.8750; LRMS (EI) *m/z* 286 (*M*⁺ - 2, 55), 288 (*M*⁺, 85), 290 (*M*⁺ + 2, 54), 207 (100), 209 (100), 128 (75), 102 (75), 75 (50).

2-Bromoquinazolin-4(3H)-one (**120**):



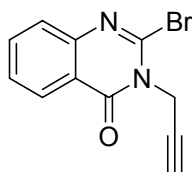
Aqueous NaOH (1 N, 37 mL, 37 mmol) was added to a solution of **117** (1.8 g, 6.1 mmol) in THF (12 mL) at room temperature and the reaction mixture was stirred for 2 h. The reaction mixture was then acidified (pH ~ 5) with glacial acetic acid and extracted with CH₂Cl₂ (3 x 40 mL). The combined organic extracts were concentrated under reduced pressure. Small amounts of water were azeotropically removed by coevaporation with MeOH to afford **120** as a tan solid (1.4 g, 100%): ¹H NMR (300 MHz, CD₃OD) δ 7.46 (ddd, *J* = 1.1 Hz, 7.2 Hz, 8.1 Hz, 1H), 7.54 (d, *J* = 8.1 Hz, 1H), 7.73 (ddd, *J* = 1.5 Hz, 7.1 Hz, 8.5 Hz, 1H), 8.13 (dd, *J* = 1.5 Hz, 8.0 Hz, 1H); ¹³C NMR (75 MHz, CD₃SOCD₃) δ 114.4, 115.5, 122.5, 127.0, 135.1, 141.0, 150.4, 163.0; IR (CH₂Cl₂, NaCl, cm⁻¹) 3385, 2909, 2847, 1700, 1669, 1593, 1449, 1296; HRMS (EI) *m/z* calcd for C₈H₅⁷⁹BrN₂O (*M*⁺ - 2) 223.9585, found 223.9582; LRMS (EI) *m/z* 224 (*M*⁺ - 2, 27), 226 (*M*⁺, 27), 203 (37), 183 (10), 145 (60), 91 (47), 71 (100). Copies of spectral data can be found in the appendix section.

General Procedure 6A: *N*-Propargylation of Quinazolinone **120**.

NaH (95% in mineral oil) was added to a solution of **120** in DMF at 0 °C under argon. After stirring this mixture for 10 min at 0 °C, propargyl bromide (80% w/w in toluene) was then added via a syringe and the reaction mixture was stirred at room temperature for 6.5 h. The final solution was poured into brine (10 mL) and extracted with ethyl acetate (3 x 10 mL). The combined organic extracts were dried over MgSO₄ and concentrated under reduced pressure. The

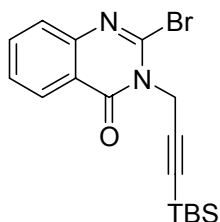
crude product was purified by flash chromatography (1:4 ethyl acetate/hexanes) to give *N*-propargylated quinazolinones in good yields.

2-Bromo-3-prop-2-ynylquinazolin-4(3*H*)-one (121):



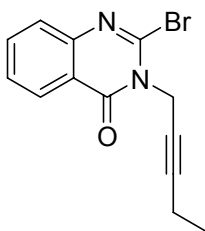
Following general procedure 6A, **120** (0.11 g, 0.47 mmol) was reacted with propargyl bromide (62 μ L, 0.56 mmol) in the presence of NaH (13 mg, 0.51 mmol) in DMF (2.3 mL) to give **121** as a pale yellow solid (81 mg, 66%): ^1H NMR (300 MHz, CDCl_3) δ 2.35 (t, $J = 2.5$ Hz, 1H), 5.08 (d, $J = 2.5$ Hz, 2H), 7.50 (ddd, $J = 1.2$ Hz, 7.4 Hz, 8.1 Hz, 1H), 7.62 (dd, $J = 0.6$ Hz, 8.2 Hz, 1H), 7.75 (ddd, $J = 1.6$ Hz, 7.2 Hz, 8.3 Hz, 1H), 8.24 (dd, $J = 1.2$ Hz, 8.0 Hz, 1H); ^{13}C NMR (75 MHz, CDCl_3) δ 38.2, 72.9, 76.8, 120.3, 126.9, 127.4, 127.7, 134.6, 135.1, 147.0, 160.5; IR (CH_2Cl_2 , NaCl, cm^{-1}) 3267, 2980, 2361, 2125, 1690, 1577, 1557, 1332, 1152; HRMS (EI) m/z calcd for $\text{C}_{11}\text{H}_7\text{BrN}_2\text{O}$ ($\text{M}^+ - 1$) 261.9742, found 261.9747; LRMS (EI) m/z 262 ($\text{M}^+ - 1$, 46), 262 ($\text{M}^+ + 1$, 46), 183 (100), 155 (20), 129 (31), 102 (19), 63 (14). Copies of spectral data can be found in the appendix section.

2-Bromo-3-{3-[*tert*-butyl(dimethyl)silyl]prop-2-ynyl}quinazolin-4(3*H*)-one (129{b}):



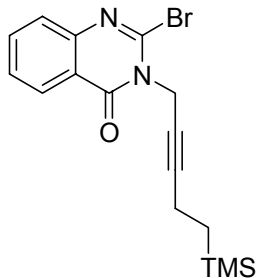
Following general procedure 6A, **120** (0.31 g, 1.4 mmol) was reacted with 3-*tert*-butyldimethylsilyl propargyl bromide (0.38 g, 1.6 mmol) in the presence of NaH (38 mg, 1.5 mmol) in DMF (6.8 mL) to give **129{b}** as a tan solid (0.29 g, 56%): ^1H NMR (300 MHz, CDCl_3) δ 0.1 (s, 6H), 0.93 (s, 9H), 5.12 (s, 2H), 7.53 (ddd, $J = 1.3$ Hz, 7.1 Hz, 8.3 Hz, 1H), 7.65-7.69 (m, 1H), 7.78 (ddd, $J = 1.6$ Hz, 7.1 Hz, 8.6 Hz, 1H), 8.27 (ddd, $J = 0.6$ Hz, 1.5 Hz, 8.0 Hz, 1H); ^{13}C NMR (75 MHz, $\text{CDCl}_3 + \text{CD}_3\text{SOCD}_3$) δ -5.6, 15.5, 25.1, 29.7, 84.0, 100.0, 113.1, 114.6, 121.7, 126.9, 134.1, 138.6, 149.1, 160.8; IR (CH_2Cl_2 , NaCl, cm^{-1}) 2924, 2852, 1721, 1669, 1449, 1244, 1019. Copies of spectral data can be found in the appendix section.

2-Bromo-3-pent-2-ynylquinazolin-4(3*H*)-one (129{c}**):**



Following general procedure 6A, **120** (0.32 g, 1.4 mmol) was reacted with 1-bromopent-2-yne (0.18 mL, 1.7 mmol) in the presence of NaH (39 mg, 1.6 mmol) in DMF (7.1 mL) to give **129{c}** as a tan solid (0.23 g, 56%): ^1H NMR (300 MHz, CDCl_3) δ 1.11 (t, $J = 7.5$ Hz, 3H), 2.18 (tq, $J = 2.2$ Hz, 7.5 Hz, 2H), 5.03 (t, $J = 2.5$ Hz, 2H), 7.49 (ddd, $J = 1.2$ Hz, 7.2 Hz, 8.1 Hz, 1H), 7.61 (d, $J = 7.8$ Hz, 1H), 7.74 (ddd, $J = 1.5$ Hz, 7.2 Hz, 8.4 Hz, 1H), 8.23 (dd, $J = 1.3$ Hz, 8.0 Hz, 1H); ^{13}C NMR (75 MHz, $\text{CDCl}_3 + \text{CD}_3\text{SOCD}_3$) δ 11.7, 13.3, 29.6, 74.0, 83.0, 113.5, 115.1, 122.1, 127.2, 134.5, 139.1, 149.4, 161.1; IR (CH_2Cl_2 , NaCl, cm^{-1}) 3042, 2899, 1721, 1659, 1629, 1454, 1342, 1142; HRMS (EI) m/z calcd for $\text{C}_{13}\text{H}_{11}^{79}\text{BrN}_2\text{O}$ ($M - 1$) 290.0055, found 290.0065; LRMS (EI) m/z 290 ($M^+ - 1$, 12), 290 ($M^+ + 1$, 12), 277 ($M^+ - 1$, 46), 277 ($M^+ + 1$, 46), 213 (100), 146 (47), 119 (25). Copies of spectral data can be found in the appendix section.

2-Bromo-3-[5-(trimethylsilyl)pent-2-ynyl]quinazolin-4(3H)-one (129{d}):



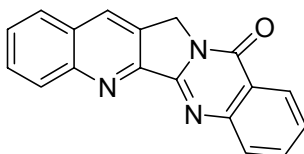
Following general procedure 6A, **120** (0.12 g, 0.54 mmol) was reacted with 5-trimethylsilyl propargyl bromide (0.14 g, 0.65 mmol) in the presence of NaH (15 mg, 0.60 mmol) in DMF (2.7 mL) to give **129{d}** as a pale yellow solid (0.10 g, 54%): ^1H NMR (300 MHz, CDCl_3) δ -0.02 (s, 9H), 0.77 (t, $J = 8.1$ Hz, 2H), 2.21 (tt, $J = 2.2$ Hz, 7.9 Hz, 2H), 5.05 (t, $J = 2.1$ Hz, 2H), 7.50 (dt, $J = 1.0$ Hz, 8.0 Hz, 1H), 7.64 (d, $J = 8.0$ Hz, 1H), 7.75 (dt, $J = 1.5$ Hz, 8.3 Hz, 1H), 8.26 (dd, $J = 1.4$ Hz, 8.0 Hz, 1H); ^{13}C NMR (75 MHz, CDCl_3) δ -1.8, 13.3, 15.8, 30.7, 73.5, 85.1, 114.6, 115.2, 123.5, 128.5, 135.1, 138.4, 151.4, 161.6; IR (CH_2Cl_2 , NaCl, cm^{-1}) 3057, 2950, 2909, 1726, 1664, 1618, 1449, 1270, 1239. Copies of spectral data can be found in the appendix section.

General procedure 6B: Radical Cascade Cyclization towards the Synthesis of Luotonins.

A solution of *N*-propargylated quinazolinone in benzene was taken up in a 15 x 45 mm cylindrical screw-cap glass vial and kept at room temperature. The appropriate isonitrile followed by hexamethylditin were added at room temperature. The vial was capped and the reaction mixture was irradiated with a 275W GE sunlamp for 8 h. The solvent was then evaporated and the residue was purified by column chromatography (1:9 acetone/dichloromethane or 1:9 ethyl acetate/dichloromethane) to give luotonins as pale yellow to tan solids.

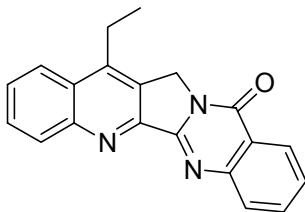
LC-MS analysis: All the luotonins were analyzed by LCMS using XTerra C18 analytical column at the wavelength of 254 nm under the following conditions: 5 μ L injection in CH_2Cl_2 , gradient $\text{CH}_3\text{CN}/\text{H}_2\text{O}$ (25:75) to $\text{CH}_3\text{CN}/\text{H}_2\text{O}$ (100:0) for 30 min, then isocratic CH_3CN (100%) for 10 min at the rate of 0.4 mL/min. The peaks were detected by ESI-MS for the corresponding m/z ratios.

Luotonin A (122):



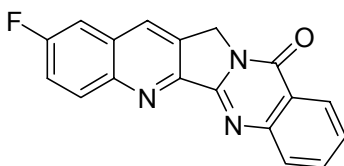
Following general procedure 6B, quinazolinone **121** (35 mg, 0.13 mmol) was reacted with phenyl isonitrile (1 M in benzene, 0.66 mL, 0.66 mmol) and hexamethylditin (77 μ L, 0.20 mmol) in benzene (2.2 mL) to afford **122** (18 mg, 47%): ^1H NMR (300 MHz, CDCl_3) δ 5.37 (s, 2H), 7.60 (dt, $J = 1.1$ Hz, 8.0 Hz, 1H), 7.71 (ddd, $J = 1.1$ Hz, 7.0 Hz, 8.1 Hz, 1H), 7.87 (dt, $J = 1.3$ Hz, 7.1 Hz, 2H), 7.98 (d, $J = 7.7$ Hz, 1H), 8.14 (d, $J = 8.1$ Hz, 1H), 8.47 (t, $J = 8.0$ Hz, 2H), 8.48 (s, 1H); ^{13}C NMR (75 MHz, CDCl_3) δ 47.3, 121.3, 126.4, 127.4, 128.0, 128.5, 128.8, 129.4, 130.7, 131.6, 134.6, 149.3, 149.4, 151.1, 152.5, 160.7; IR (CH_2Cl_2 , NaCl, cm^{-1}) 2919, 2842, 2351, 2335, 1669, 1623, 1454; HRMS (EI) m/z calcd for $\text{C}_{18}\text{H}_{11}\text{N}_3\text{O}$ (M^+) 285.0902, found 285.0900; LRMS (EI) m/z 285 (M^+ , 50), 218 (47), 200 (100), 184 (20), 146 (69), 119 (45), 92 (43); LCMS [Rt = 13.5 min; 286 ($\text{M} + \text{H}$)]. Copies of ^1H NMR spectrum and LCMS data can be found in the appendix section.

8-Ethylfluotonin A (130{c, 1}):



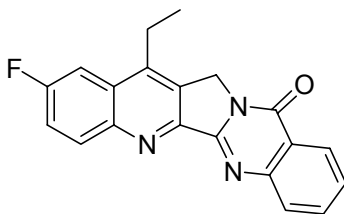
Following general procedure 6B, quinazolinone **129{c}** (13 mg, 0.043 mmol) was reacted with phenyl isonitrile (1 M in benzene, 0.26 mL, 0.26 mmol) and hexamethylditin (25 μ L, 0.064 mmol) in benzene (0.72 mL) to afford **130{c, 1}** (9.2 mg, 68%): ^1H NMR (300 MHz, CDCl_3) δ 1.47 (t, $J = 7.7$ Hz, 3H), 3.28 (q, $J = 7.7$ Hz, 2H), 5.34 (s, 2H), 7.60 (t, $J = 7.1$ Hz, 1H), 7.74 (dd, $J = 5.5$ Hz, 7.1 Hz, 1H), 7.83-7.90 (m, 2H), 8.13 (t, $J = 8.3$ Hz, 1H), 8.19 (d, $J = 8.0$ Hz, 1H), 8.46 (dd, $J = 1.9$ Hz, 8.1 Hz, 1H), 8.51 (d, $J = 8.6$ Hz, 1H); LCMS [$R_t = 16.8$ min; 314 (M + H)].

10-Fluoroluotonin A (130{a, 2}):



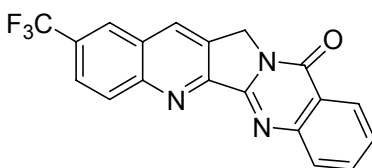
Following general procedure 6B, quinazolinone **121** (12 mg, 0.046 mmol) was reacted with *p*-fluorophenyl isonitrile (1 M in benzene, 0.23 mL, 0.23 mmol) and hexamethylditin (26 μ L, 0.068 mmol) in benzene (0.76 mL) to afford **130{a, 2}** (9.0 mg, 65%): ^1H NMR (300 MHz, CDCl_3) δ 5.37 (s, 2H), 7.57-7.66 (m, 3H), 7.88 (ddd, $J = 1.6$ Hz, 7.2 Hz, 8.6 Hz, 1H), 8.13 (d, $J = 8.3$ Hz, 1H), 8.43-8.53 (m, 3H); LCMS [$R_t = 14.6$ min; 304 (M + H)].

8-Ethyl-10-fluoroluotonin A (**130{c, 2}**):



Following general procedure 6B, quinazolinone **129{c}** (15 mg, 0.050 mmol) was reacted with *p*-fluorophenyl isonitrile (1 M in benzene, 0.25 mL, 0.25 mmol) and hexamethylditin (29 μ L, 0.075 mmol) in benzene (0.84 mL) to afford **130{c, 2}** (13 mg, 75%): ^1H NMR (300 MHz, CDCl_3) δ 1.45 (t, $J = 7.6$ Hz, 3H), 3.21 (q, $J = 7.7$ Hz, 2H), 5.33 (s, 2H), 7.57-7.65 (m, 2H), 7.76 (dd, $J = 2.7$ Hz, 9.9 Hz, 1H), 7.87 (dt, $J = 1.5$ Hz, 8.6 Hz, 1H), 8.12 (d, $J = 8.2$ Hz, 1H), 8.45 (dd, $J = 1.2$ Hz, 8.0 Hz, 1H), 8.50 (dd, $J = 5.6$ Hz, 9.3 Hz, 1H); LCMS [$R_t = 17.6$ min; 332 (M + H)]. Copies of ^1H NMR spectrum and LCMS data can be found in the appendix section.

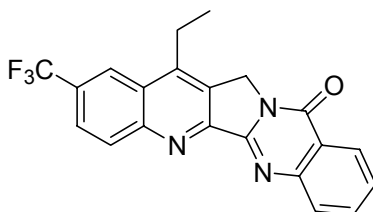
10-Trifluoromethyluotonin A (**130{a, 3}**):



Following general procedure 6B, quinazolinone **121** (11 mg, 0.043 mmol) was reacted with *p*-trifluoromethylphenyl isonitrile (1 M in benzene, 0.22 mL, 0.22 mmol) and hexamethylditin (25 μ L, 0.065 mmol) in benzene (0.72 mL) to afford **130{a, 3}** (11 mg, 71%): ^1H NMR (300 MHz, CDCl_3) δ 5.41 (s, 2H), 7.62 (t, $J = 7.2$ Hz, 1H), 7.89 (dt, $J = 1.4$ Hz, 8.4 Hz, 1H), 8.03 (dd, $J = 1.8$ Hz, 8.9 Hz, 1H), 8.14 (d, $J = 8.1$ Hz, 1H), 8.30 (s, 1H), 8.46 (dd, $J = 1.3$ Hz, 8.0 Hz, 1H), 8.58 (s, 1H), 8.61 (d, $J = 9.1$ Hz, 1H); ^{13}C NMR (75 MHz, CDCl_3) δ 47.3, 121.4, 125.4, 126.4, 126.5, 127.7, 127.9, 128.9, 130.6, 131.9, 132.7, 135.0, 149.2, 150.3, 152.0, 153.5, 160.5; IR

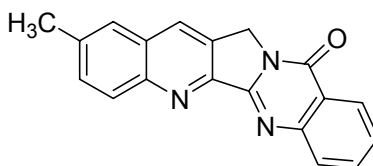
(CH₂Cl₂, NaCl, cm⁻¹) 2914, 2842, 2351, 1680, 1629, 1362, 1280, 1122; HRMS (EI) *m/z* calcd for C₁₉H₁₀F₃N₃O (M⁺) 353.0776, found 353.0779; LRMS (EI) *m/z* 353 (M⁺, 100), 325 (10), 284 (8), 140 (6), 77(25); LCMS [R_t = 17.9 min; 354 (M + H)]. Copies of ¹H NMR spectrum and LCMS data can be found in the appendix section.

8-Ethyl-10-trifluoromethyluotonin A (130{c, 3}):



Following general procedure 6B, quinazolinone **129{c}** (13 mg, 0.045 mmol) was reacted with *p*-trifluoromethylphenyl isonitrile (1 M in benzene, 0.23 mL, 0.23 mmol) and hexamethylditin (26 μL, 0.068 mmol) in benzene (0.76 mL) to afford **130{c, 3}** (11 mg, 62%): ¹H NMR (300 MHz, CDCl₃) δ 1.49 (t, *J* = 7.7 Hz, 3H), 3.32 (q, *J* = 7.7 Hz, 2H), 5.37 (s, 2H), 7.63 (t, *J* = 8.0 Hz, 1H), 7.89 (dt, *J* = 1.5 Hz, 8.3 Hz, 1H), 8.02 (dd, *J* = 1.8 Hz, 8.9 Hz, 1H), 8.15 (d, *J* = 8.3 Hz, 1H), 8.46 (s, 1H), 8.47 (dd, *J* = 1.5 Hz, 7.9 Hz, 1H), 8.62 (d, *J* = 8.8 Hz, 1H); LCMS [R_t = 20.4 min; 382 (M + H)].

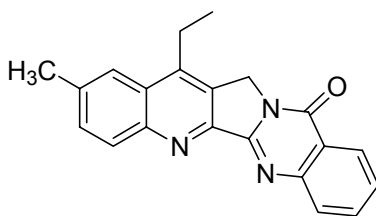
10-Methyluotonin A (130{a, 4}):



Following general procedure 6B, quinazolinone **121** (11 mg, 0.041 mmol) was reacted with *p*-methylphenyl isonitrile (1 M in benzene, 0.21 mL, 0.21 mmol) and hexamethylditin (24 μL,

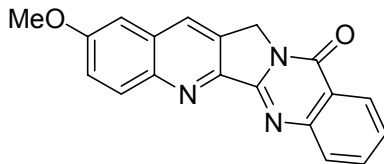
0.062 mmol) in benzene (0.68 mL) to afford **130{a, 4}** (7.0 mg, 57%): ^1H NMR (300 MHz, CDCl_3) δ 3.05 (s, 3H), 5.36 (s, 2H), 7.57-7.63 (m, 2H), 7.72 (d, $J = 7.0$ Hz, 1H), 7.82 (d, $J = 8.2$ Hz, 1H), 7.87 (dt, $J = 1.4$ Hz, 8.4 Hz, 1H), 8.11 (d, $J = 8.2$ Hz, 1H), 8.44-8.47 (m, 2H); ^{13}C NMR (75 MHz, CDCl_3) δ 20.1, 50.7, 129.5, 134.5, 135.0, 136.0, 137.1, 137.5, 137.6, 137.7, 138.0, 139.6, 140.6, 143.5, 148.5, 159.4; IR (CH_2Cl_2 , NaCl, cm^{-1}) 3272, 2919, 2852, 1680, 1629, 1598, 1460, 1311, 1096; HRMS (EI) m/z calcd for $\text{C}_{19}\text{H}_{13}\text{N}_3\text{O}$ (M^+) 299.1059, found 299.1053; LRMS (EI) m/z 299 (M^+ , 100), 150 (6), 77 (5); LCMS [$R_t = 16.8$ min; 300 (M + H)]. Copies of ^1H NMR spectrum and LCMS data can be found in the appendix section.

8-Ethyl-10-methyluotonin A (130{c, 4}):



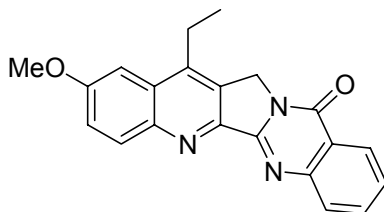
Following general procedure 6B, quinazolinone **129{c}** (11 mg, 0.037 mmol) was reacted with *p*-methylphenyl isonitrile (1 M in benzene, 0.18 mL, 0.18 mmol) and hexamethylditin (21 μL , 0.055 mmol) in benzene (0.61 mL) to afford **130{c, 4}** (4.0 mg, 33%): ^1H NMR (300 MHz, CDCl_3) δ 1.45 (t, $J = 7.6$ Hz, 3H), 3.05 (s, 3H), 3.25 (q, $J = 7.7$ Hz, 2H), 5.32 (s, 2H), 7.55-7.64 (m, 2H), 7.70 (d, $J = 5.8$ Hz, 1H), 7.87 (ddd, $J = 1.5$ Hz, 7.1 Hz, 8.4 Hz, 1H), 8.03 (d, $J = 8.3$ Hz, 1H), 8.10 (d, $J = 8.3$ Hz, 1H), 8.46 (dd, $J = 1.2$ Hz, 7.9 Hz, 1H); LCMS [$R_t = 20.0$ min; 328 (M + H)].

10-Methoxyluotonin A (130{a, 5}):



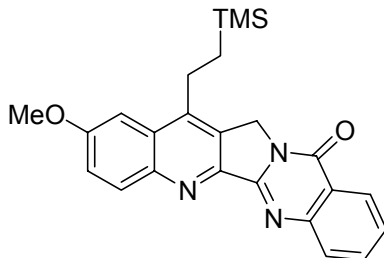
Following general procedure 6B, quinazolinone **121** (12 mg, 0.046 mmol) was reacted with *p*-methoxyphenyl isonitrile (1 M in benzene, 0.23 mL, 0.23 mmol) and hexamethylditin (26 μ L, 0.068 mmol) in benzene (0.76 mL) to afford **130{a, 5}** (9.1 mg, 63%): ^1H NMR (300 MHz, CDCl_3) δ 4.00 (s, 3H), 5.34 (s, 2H), 7.20 (d, $J = 2.6$ Hz, 3H), 7.51 (dd, $J = 2.7$ Hz, 9.4 Hz, 1H), 7.58 (t, $J = 7.9$ Hz, 1H), 7.85 (dt, $J = 1.4$ Hz, 8.3 Hz, 1H), 8.11 (d, $J = 8.3$ Hz, 1H), 8.33 (s, 1H), 8.38 (d, $J = 9.4$ Hz, 1H), 8.44 (d, $J = 8.0$ Hz, 1H); LCMS [Rt = 14.3 min; 316 (M + H)].

8-Ethyl-10-methoxyluotonin A (130{c, 5}):



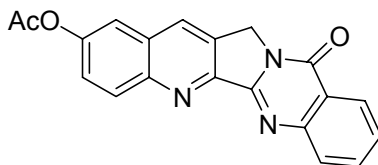
Following general procedure 6B, quinazolinone **129{c}** (14 mg, 0.048 mmol) was reacted with *p*-methoxyphenyl isonitrile (1 M in benzene, 0.24 mL, 0.24 mmol) and hexamethylditin (30 μ L, 0.072 mmol) in benzene (0.80 mL) to afford **130{c, 5}** (14 mg, 86%): ^1H NMR (300 MHz, CDCl_3) δ 1.44 (t, $J = 7.7$ Hz, 3H), 3.19 (q, $J = 7.7$ Hz, 2H), 4.00 (s, 3H), 5.27 (s, 2H), 7.31 (d, $J = 2.6$ Hz, 1H), 7.49 (dd, $J = 2.7$ Hz, 9.3 Hz, 1H), 7.56 (dt, $J = 1.1$ Hz, 8.1 Hz, 1H), 7.85 (ddd, $J = 1.5$ Hz, 7.2 Hz, 8.5 Hz, 1H), 8.10 (d, $J = 8.2$ Hz, 1H), 8.37 (d, $J = 9.3$ Hz, 1H), 8.42 (dd, $J = 1.3$ Hz, 8.0 Hz, 1H); LCMS [Rt = 17.6 min; 344 (M + H)].

8-Trimethylsilylethyl-10-methoxyluotonin A (130{d, 5}):



Following general procedure 6B, quinazolinone **129{d}** (12 mg, 0.033 mmol) was reacted with *p*-methoxyphenyl isonitrile (1 M in benzene, 0.16 mL, 0.16 mmol) and hexamethylditin (19 μ L, 0.050 mmol) in benzene (0.55 mL) to afford **130{d, 5}** (10 mg, 74%): ^1H NMR (300 MHz, CDCl_3) δ 0.21 (s, 9H), 0.95-1.01 (m, 2H), 3.07-3.13 (m, 2H), 4.00 (s, 3H), 5.28 (s, 2H), 7.35 (d, $J = 2.6$ Hz, 1H), 7.50 (dt, $J = 2.8$ Hz, 9.3 Hz, 1H), 7.58 (dt, $J = 1.0$ Hz, 8.0 Hz, 1H), 7.85 (ddd, $J = 1.5$ Hz, 7.2 Hz, 8.5 Hz, 1H), 8.11 (d, $J = 7.9$ Hz, 1H), 8.38 (dd, $J = 3.3$ Hz, 9.3 Hz, 1H), 8.45 (d, $J = 8.0$ Hz, 1H); LCMS [$R_t = 25.3$ min; 416 (M + H)].

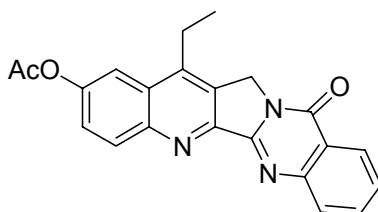
10-Acetoxyluotonin A (130{a, 6}):



Following general procedure 6B, quinazolinone **121** (15 mg, 0.056 mmol) was reacted with *p*-acetoxyphenyl isonitrile (1 M in benzene, 0.34 mL, 0.34 mmol) and hexamethylditin (33 μ L, 0.084 mmol) in benzene (0.94 mL) to afford **130{a, 6}** (12 mg, 62%): ^1H NMR (300 MHz, CDCl_3) δ 2.42 (s, 3H), 5.37 (s, 2H), 7.58-7.63 (m, 2H), 7.76 (d, $J = 2.5$ Hz, 1H), 7.88 (ddd, $J = 1.5$ Hz, 7.2 Hz, 8.5 Hz, 1H), 8.14 (d, $J = 7.9$ Hz, 1H), 8.44 (s, 1H), 8.46 (dd, $J = 1.3$ Hz, 8.0 Hz,

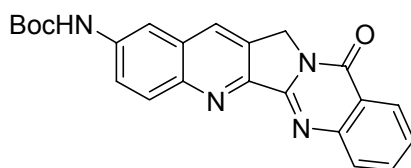
1H), 8.51 (d, $J = 9.2$ Hz, 1H); LCMS [Rt = 13.6 min; 344 (M + H)]. Copies of ^1H NMR spectrum and LCMS data can be found in the appendix section.

10-Acetoxy-8-ethyluotonin A (130{c, 6}):



Following general procedure 6B, quinazolinone **129{c}** (14 mg, 0.047 mmol) was reacted with *p*-acetoxyphenyl isonitrile (1 M in benzene, 0.28 mL, 0.28 mmol) and hexamethylditin (27 μL , 0.070 mmol) in benzene (0.78 mL) to afford **130{c, 6}** (6.7 mg, 39%): ^1H NMR (300 MHz, CDCl_3) δ 1.45 (t, $J = 7.6$ Hz, 3H), 2.43 (s, 3H), 3.22 (d, $J = 7.6$ Hz, 2H), 5.33 (s, 2H), 7.57-7.62 (m, 2H), 7.84-7.90 (m, 2H), 8.13 (d, $J = 8.2$ Hz, 1H), 8.46 (dd, $J = 1.3$ Hz, 8.0 Hz, 1H), 8.51 (d, $J = 9.2$ Hz, 1H); LCMS [Rt = 16.2 min; 372 (M + H)]. Copies of ^1H NMR spectrum and LCMS data can be found in the appendix section.

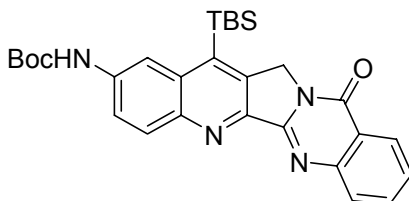
10-*tert*-Butyloxycarbonylamino luotonin A (130{a, 7}):



Following general procedure 6B, quinazolinone **121** (16 mg, 0.059 mmol) was reacted with *p*-*tert*-butyloxycarbonylamino phenyl isonitrile (65 mg, 0.30 mmol) and hexamethylditin (34 μL , 0.089 mmol) in benzene (0.99 mL) to afford **130{a, 7}** (12 mg, 52%): ^1H NMR (300 MHz, CDCl_3) δ 1.59 (s, 9H), 5.34 (s, 2H), 6.83 (br s, 1H), 7.54-7.61 (m, 2H), 7.86 (dt, $J = 1.5$ Hz, 8.5

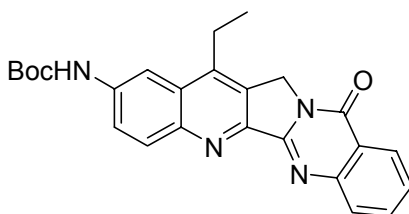
Hz, 1H), 8.11 (d, $J = 8.2$ Hz, 1H), 8.31-8.40 (m, 3H), 8.45 (d, $J = 7.9$ Hz, 1H); LCMS [Rt = 18.1 min; 401 (M + H)]. Copies of ^1H NMR spectrum and LCMS data can be found in the appendix section.

8-*tert*-Butyldimethylsilyl-10-*tert*-butyloxycarbonylamino luotonin A (130{b, 7}):



Following general procedure 6B, quinazolinone **129{b}** (13 mg, 0.033 mmol) was reacted with *p*-*tert*-butyloxycarbonylamino phenyl isonitrile (36 mg, 0.17 mmol) and hexamethylditin (20 μL , 0.050 mmol) in benzene (0.56 mL) to afford **130{b, 7}** (5.3 mg, 31%): ^1H NMR (300 MHz, CDCl_3) δ 0.77 (s, 6H), 1.03 (s, 9H), 1.58 (s, 9H), 5.36 (s, 2H), 6.73 (br s, 1H), 7.47 (dd, $J = 2.2$ Hz, 9.0 Hz, 1H), 7.57 (t, $J = 7.2$ Hz, 1H), 7.85 (dt, $J = 1.4$ Hz, 8.4 Hz, 1H), 8.12 (d, $J = 8.1$ Hz, 1H), 8.38 (d, $J = 9.1$ Hz, 1H), 8.45 (dd, $J = 1.3$ Hz, 8.0 Hz, 1H), 8.78 (d, $J = 1.5$ Hz, 1H); LCMS [Rt = 28.1 min; 515 (M + H)]. Copies of ^1H NMR spectrum and LCMS data can be found in the appendix section.

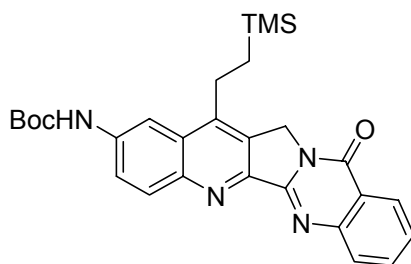
10-*tert*-Butyloxycarbonylamino-8-ethyl luotonin A (130{c, 7}):



Following general procedure 6B, quinazolinone **129{c}** (12 mg, 0.041 mmol) was reacted with *p*-*tert*-butyloxycarbonylamino phenyl isonitrile (45 mg, 0.21 mmol) and hexamethylditin (24 μL ,

0.062 mmol) in benzene (0.69 mL) to afford **130{c, 7}** (17 mg, 94%): ^1H NMR (300 MHz, CDCl_3) δ 1.46 (t, $J = 7.6$ Hz, 3H), 1.59 (s, 9H), 3.23 (d, $J = 7.4$ Hz, 2H), 5.31 (s, 2H), 6.83 (br s, 1H), 7.58-7.62 (m, 2H), 7.86 (dt, $J = 1.5$ Hz, 8.4 Hz, 1H), 8.11 (d, $J = 8.2$ Hz, 1H), 8.38-8.47 (m, 3H); LCMS [$R_t = 20.5$ min; 429 (M + H)].

10-tert-Butyloxycarbonylamino-8-trimethylsilylethyluotonin A (130{d, 7}):

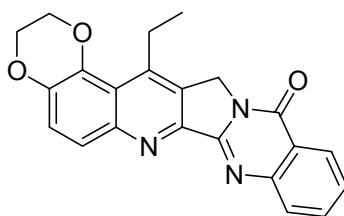


Following general procedure 6B, quinazolinone **129{d}** (21 mg, 0.056 mmol) was reacted with *p*-tert-butyloxycarbonylamino phenyl isonitrile (62 mg, 0.28 mmol) and hexamethylditin (33 μL , 0.085 mmol) in benzene (0.94 mL) to afford **130{d, 7}** (10 mg, 37%): ^1H NMR (300 MHz, CDCl_3) δ 0.22 (s, 9H), 0.95-1.01 (m, 2H), 1.58 (s, 9H), 3.09-3.15 (m, 2H), 5.28 (s, 2H), 6.80 (br s, 1H), 7.55-7.62 (m, 2H), 7.85 (dt, $J = 1.4$ Hz, 8.4 Hz, 1H), 8.11 (d, $J = 8.1$ Hz, 1H), 8.36-8.40 (m, 2H), 8.44 (dd, $J = 1.4$ Hz, 8.0 Hz, 1H); LCMS [$R_t = 27.9$ min; 501 (M + H)]. Copies of ^1H NMR spectrum and LCMS data can be found in the appendix section.

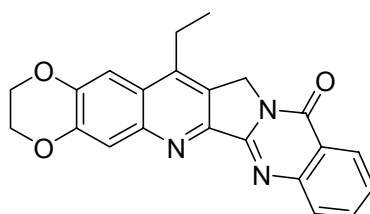
8-Ethyl-9,10-ethylenedioxyuotonin A and 8-Ethyl-10,11-ethylenedioxyuotonin A (130{c, 8}):

Following general procedure 6B, quinazolinone **129{c}** (18 mg, 0.063 mmol) was reacted with 3,4-ethylenedioxyphenyl isonitrile (50 mg, 0.31 mmol) and hexamethylditin (36 μL , 0.094 mmol) in benzene (1.0 mL) to afford a 2.5:1 mixture of 9,10- and 10,11-ethylenedioxy isomers

130{c, 8} (20 mg, 86%) which was separated using HPLC with a semipreparative column under the same conditions as described in the general procedure 6B:



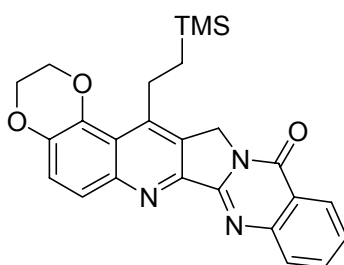
^1H NMR (300 MHz, CDCl_3) δ 1.39 (t, $J = 7.3$ Hz, 3H), 3.39 (q, $J = 7.4$ Hz, 2H), 4.45 (s, 4H), 5.29 (s, 2H), 7.41 (d, $J = 9.2$ Hz, 1H), 7.57 (t, $J = 7.2$ Hz, 1H), 7.84 (dt, $J = 1.3$ Hz, 8.4 Hz, 1H), 8.02 (d, $J = 9.2$ Hz, 1H), 8.10 (d, $J = 8.2$ Hz, 1H), 8.43 (d, $J = 7.9$ Hz, 1H); LCMS [$R_t = 17.1$ min; 372 (M + H)].



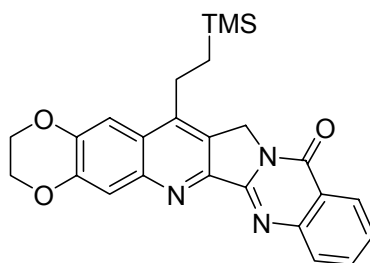
^1H NMR (300 MHz, CDCl_3) δ 1.41 (t, $J = 7.6$ Hz, 3H), 3.14 (q, $J = 7.6$ Hz, 2H), 4.45 (s, 4H), 5.26 (s, 2H), 7.51 (s, 1H), 7.57 (t, $J = 7.3$ Hz, 1H), 7.85 (dt, $J = 1.4$ Hz, 8.5 Hz, 1H), 7.91 (s, 1H), 8.10 (d, $J = 8.2$ Hz, 1H), 8.43 (dd, $J = 1.2$ Hz, 7.9 Hz, 1H); ^{13}C NMR (125 MHz, CDCl_3) δ 13.9, 22.9, 46.6, 64.5, 108.0, 109.5, 116.0, 121.2, 124.1, 126.2, 126.4, 127.1, 128.6, 134.5, 146.7, 149.5, 150.1, 160.8; IR (CH_2Cl_2 , NaCl, cm^{-1}) 2919, 2873, 2361, 2340, 1675, 1618, 1501, 1460, 1285, 1060; HRMS (EI) m/z calcd for $\text{C}_{22}\text{H}_{17}\text{N}_3\text{O}_3$ (M^+) 371.1270, found 371.1267; LRMS (EI) m/z 371 (M^+ , 100), 342 (20), 177 (26), 105 (43), 77 (58); LCMS [$R_t = 17.1$ min; 372 (M + H)].

9,10-Ethylenedioxy-8-trimethylsilylethylluotonin A and **10,11-Ethylenedioxy-8-trimethylsilylethylluotonin A (130{d, 8})**:

Following general procedure 6B, quinazolinone **129{d}** (15 mg, 0.041 mmol) was reacted with 3,4-ethylenedioxyphenyl isonitrile (33 mg, 0.21 mmol) and hexamethylditin (24 μ L, 0.062 mmol) in benzene (0.69 mL) to afford a 1:1 mixture of 9,10- and 10,11-ethylenedioxy isomers **130{d, 8}** (17 mg, 94%) which was separated using HPLC with a semipreparative column under the same conditions as described in the general procedure 6B:



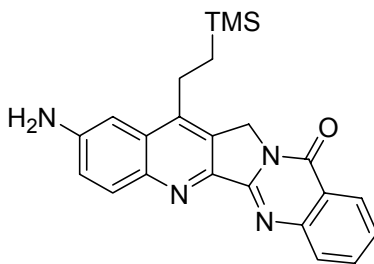
^1H NMR (300 MHz, CDCl_3) δ 0.16 (s, 9H), 0.91-0.97 (m, 2H), 3.29-3.34 (m, 2H), 4.44 (s, 4H), 5.26 (s, 2H), 7.41 (d, $J = 9.2$ Hz, 1H), 7.57 (dt, $J = 0.7$ Hz, 7.0 Hz, 1H), 7.85 (ddd, $J = 1.5$ Hz, 7.4 Hz, 8.4 Hz, 1H), 8.02 (d, $J = 9.2$ Hz, 1H), 8.10 (d, $J = 8.1$ Hz, 1H), 8.45 (dd, $J = 1.2$ Hz, 7.9 Hz, 1H); LCMS [$R_t = 25.7$ min; 444 (M + H)].



^1H NMR (300 MHz, CDCl_3) δ 0.19 (s, 9H), 0.91-0.97 (m, 2H), 3.01-3.07 (m, 2H), 4.45 (s, 4H), 5.24 (s, 2H), 7.43 (s, 1H), 7.57 (dt, $J = 1.1$ Hz, 8.0 Hz, 1H), 7.85 (dt, $J = 1.4$ Hz, 8.5 Hz, 1H), 7.91 (s, 1H), 8.11 (d, $J = 8.3$ Hz, 1H), 8.44 (dd, $J = 1.2$ Hz, 8.0 Hz, 1H); LCMS [$R_t = 24.7$ min;

444 (M + H)]. Copies of ^1H NMR spectrum and LCMS data can be found in the appendix section.

10-Amino-8-trimethylsilylethylluotonin A (132{d}):



TFA (0.30 mL) was added to a solution of **130{d, 7}** (5.0 mg, 0.010 mmol) in CH_2Cl_2 (0.60 mL) at room temperature. After stirring for 12 h, the reaction mixture was concentrated under reduced pressure and the residue was purified by flash column chromatography (1:9 acetone/dichloromethane) to afford **132{d}** as a light brown solid (3.4 mg, 85%): ^1H NMR (300 MHz, CDCl_3) δ 0.19 (s, 9H), 0.92-0.98 (m, 2H), 2.99-3.05 (m, 2H), 4.22 (br s, 2H), 5.23 (s, 2H), 7.05 (d, $J = 2.4$ Hz, 1H), 7.23-7.24 (m, 1H), 7.56 (t, $J = 7.5$ Hz, 1H), 7.84 (dt, $J = 1.3$ Hz, 8.3 Hz, 1H), 8.09 (d, $J = 8.1$ Hz, 1H), 8.28 (d, $J = 9.0$ Hz, 1H), 8.44 (d, $J = 8.0$ Hz, 1H); LCMS [$R_t = 20.9$ min; 401 (M + H)].

APPENDIX

NMR and LCMS Data of Representative Compounds

Figure A-1: ^1H and ^{13}C NMR spectra of compound 33a

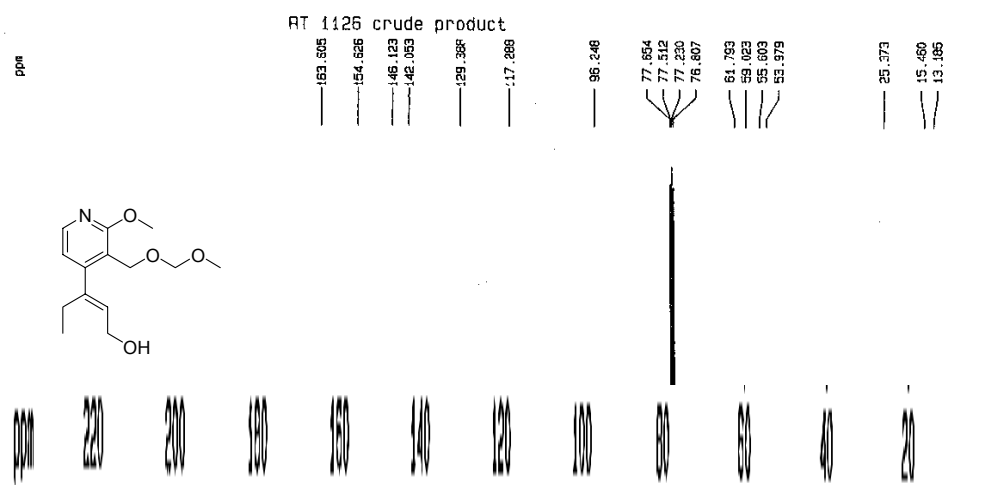
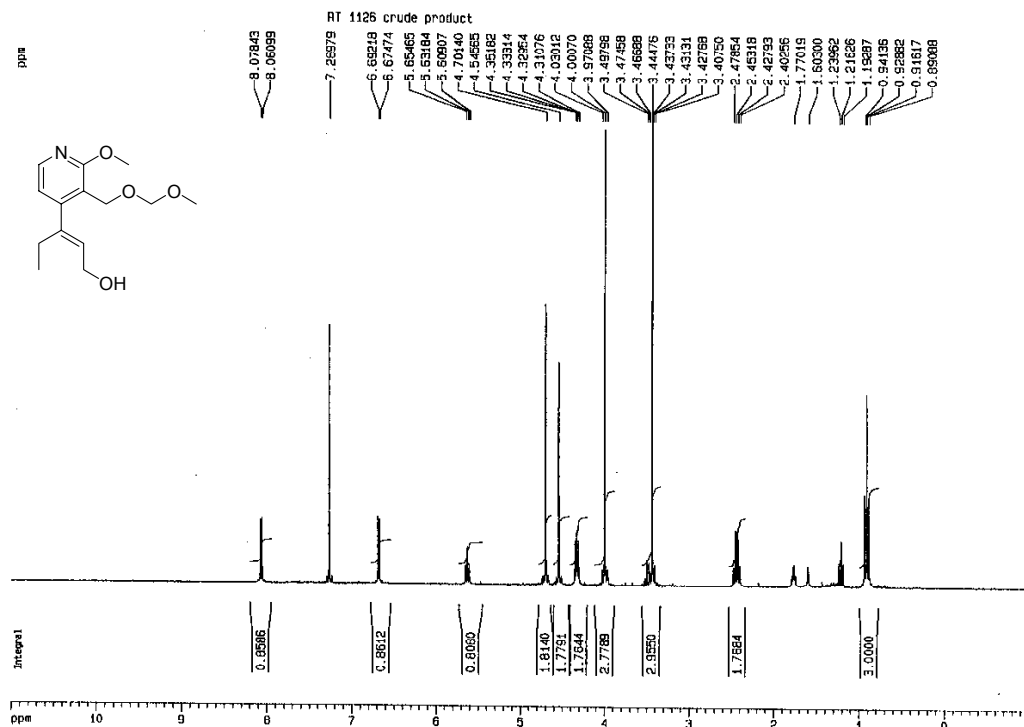


Figure A-2: ¹H and ¹³C NMR spectra of compound (R)-19

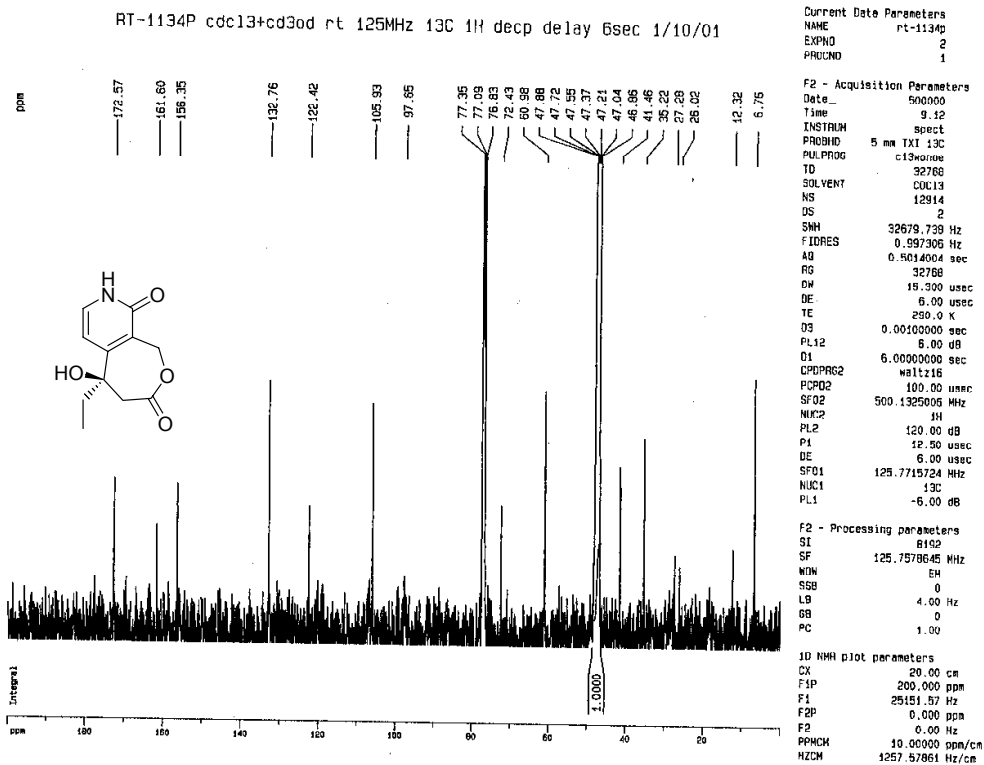
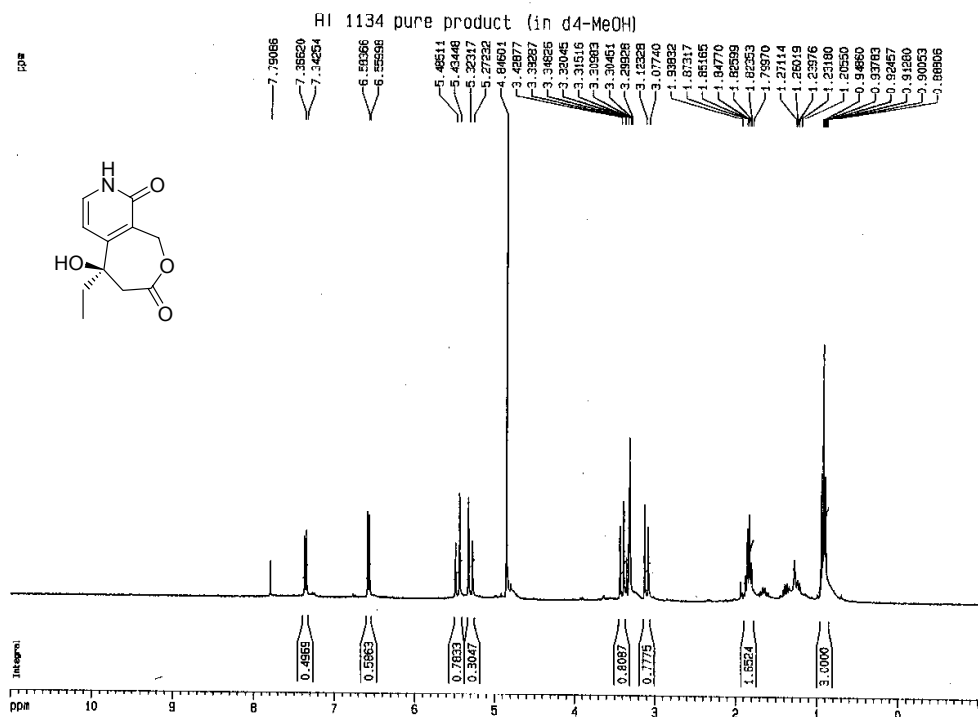
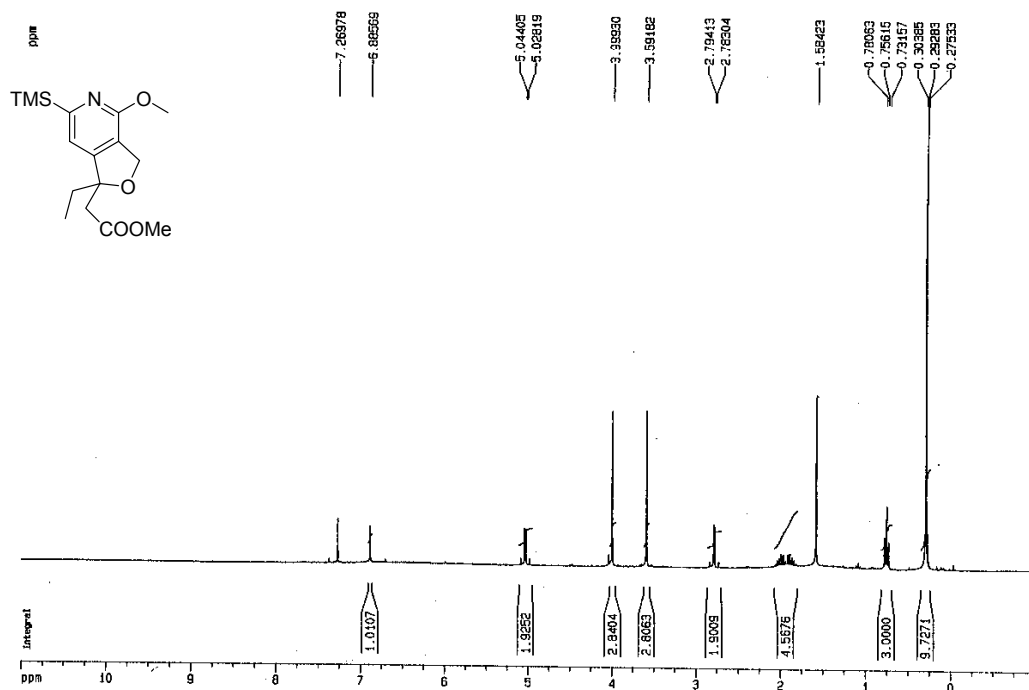


Figure A-3: ^1H and ^{13}C NMR spectra of compound "esterified 87"
RT 5006d crude product



RT 5009d starting material in CDCl₃ (RT-5006d)

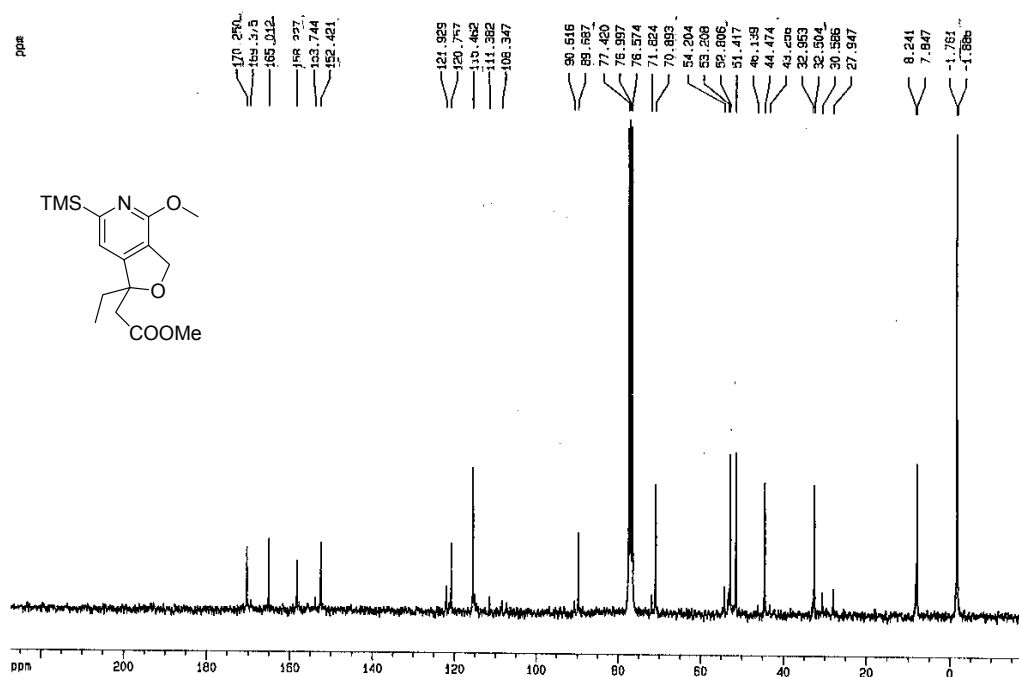


Figure A-4: ^1H and ^{13}C NMR spectra of compound 91a

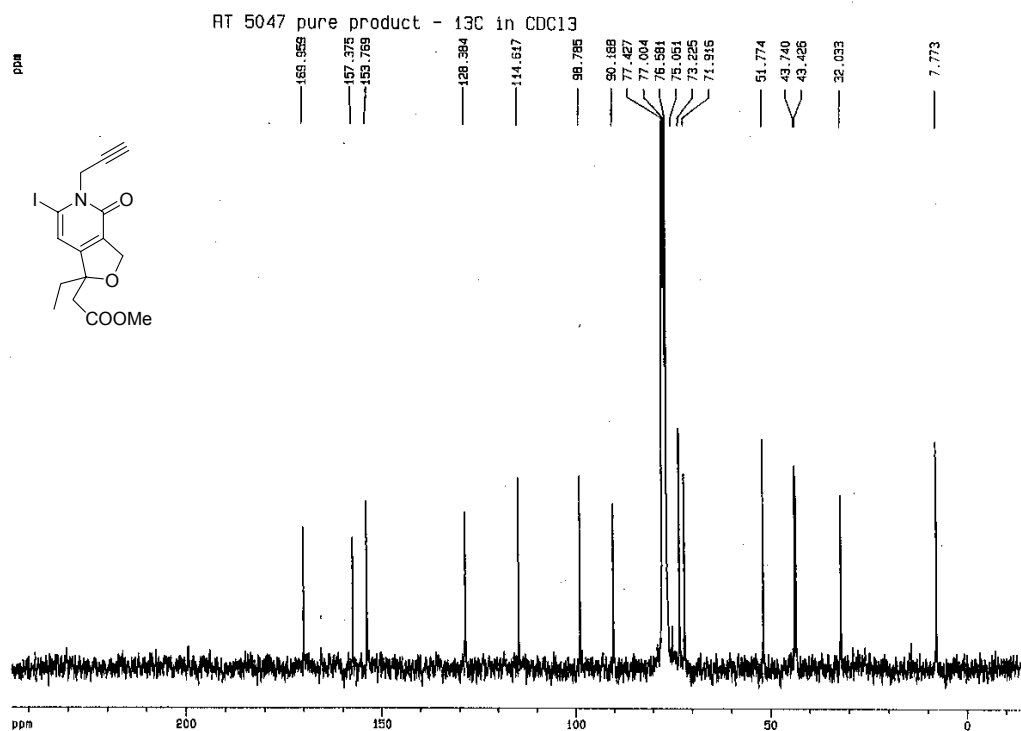
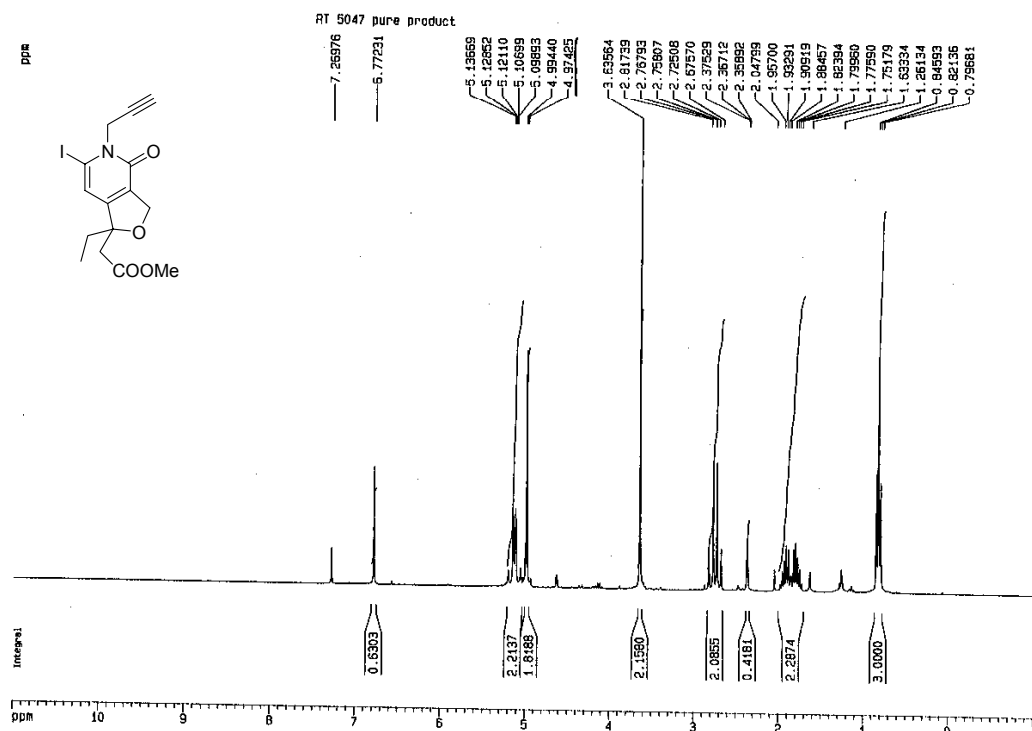


Figure A-5: ^1H and ^{13}C NMR spectra of compound 91b

RT 5047d pure product

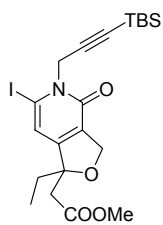
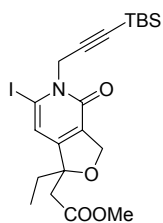


Figure A-6: ^1H and ^{13}C NMR spectra of compound 94a

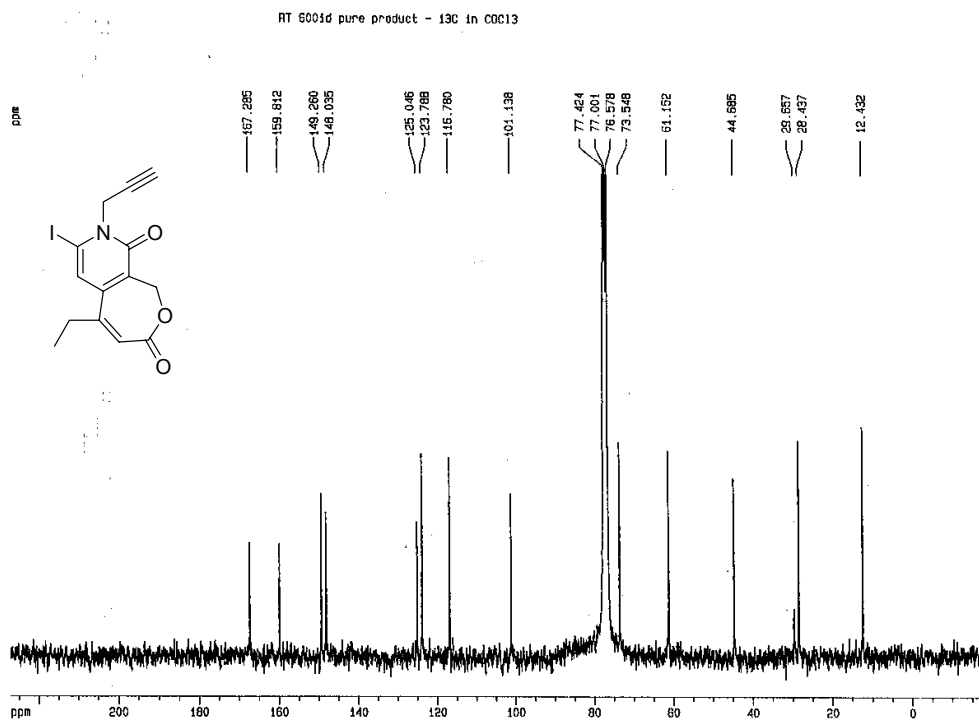
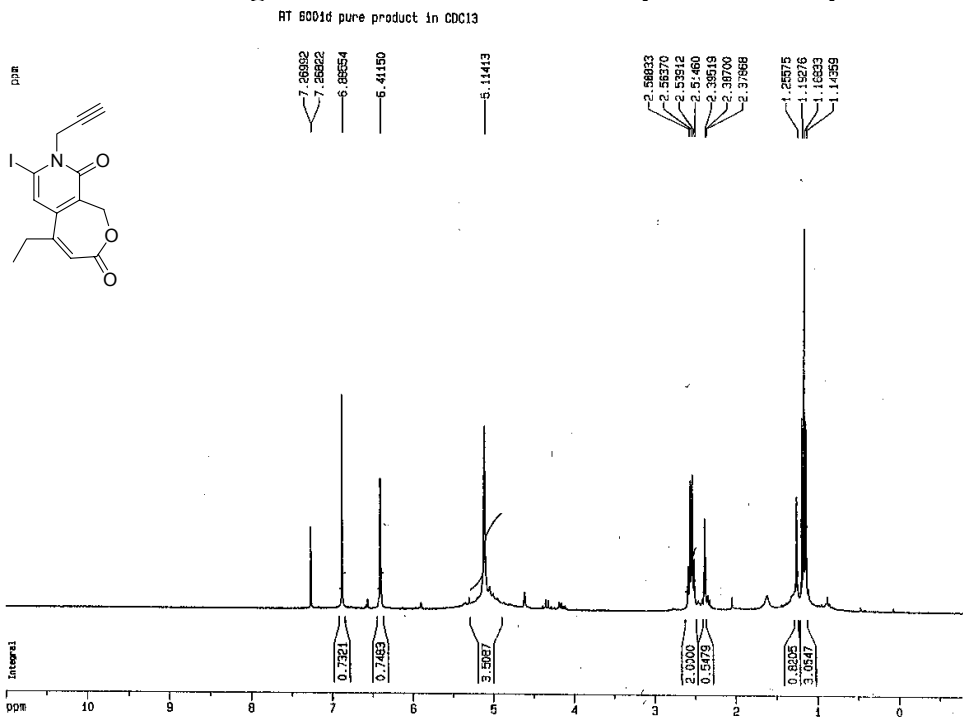


Figure A-7: ^1H and ^{13}C NMR spectra of compound 94b

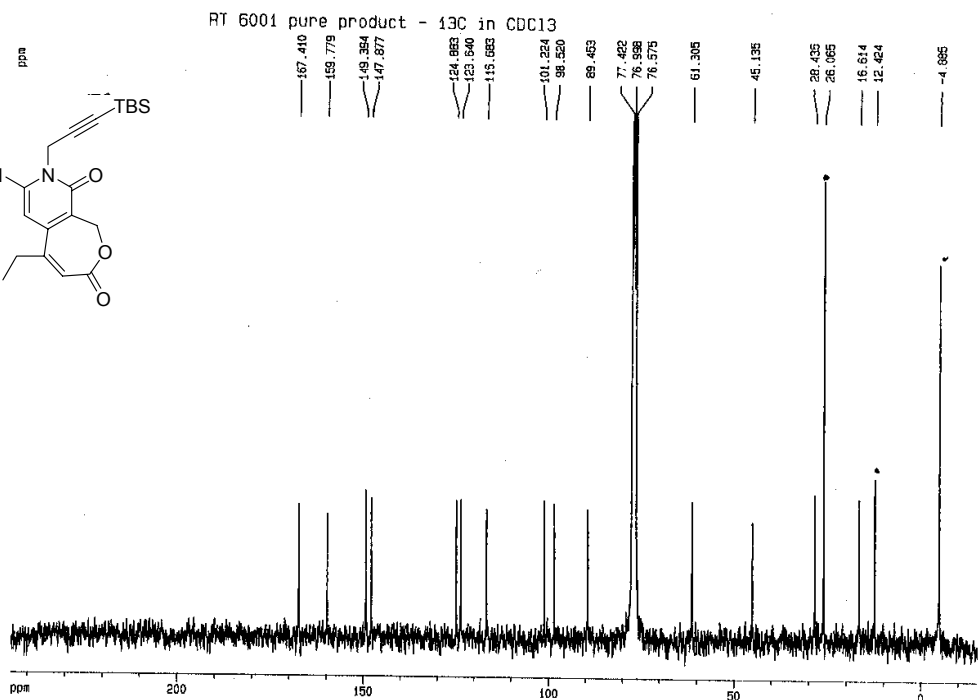
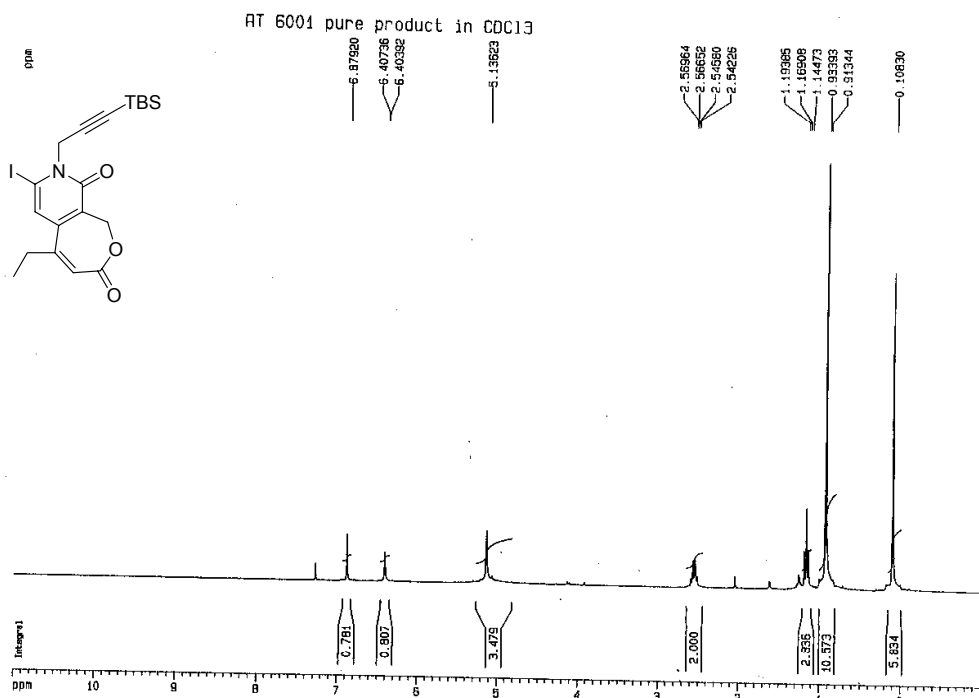


Figure A-8: ¹H and ¹³C NMR spectra of compound 92a

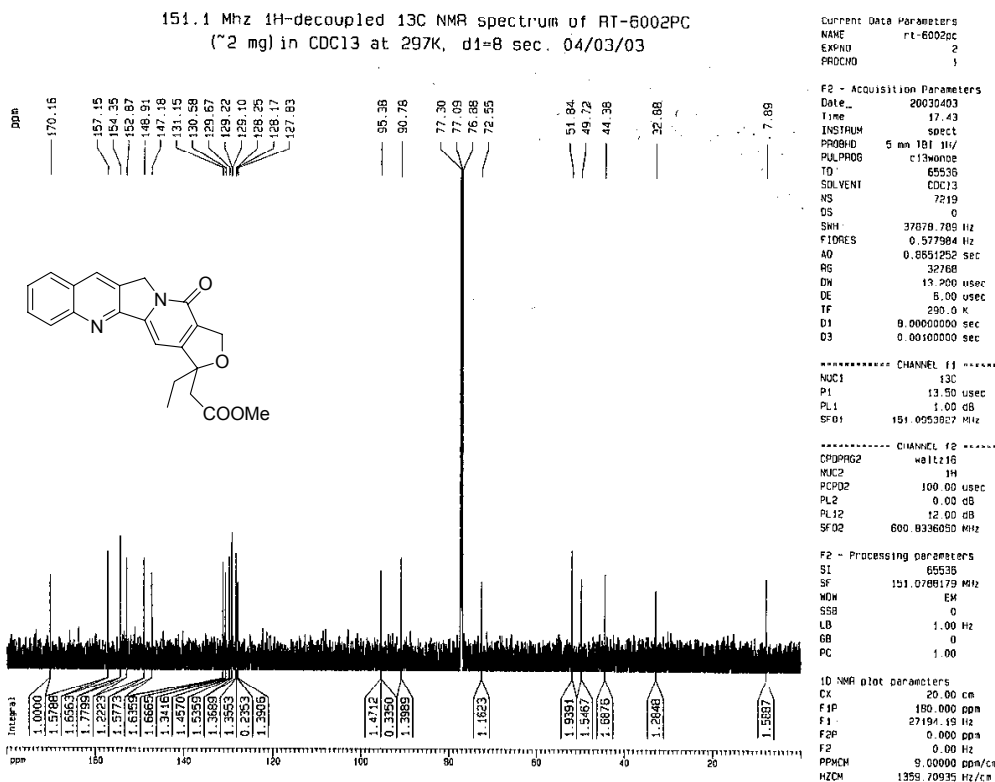
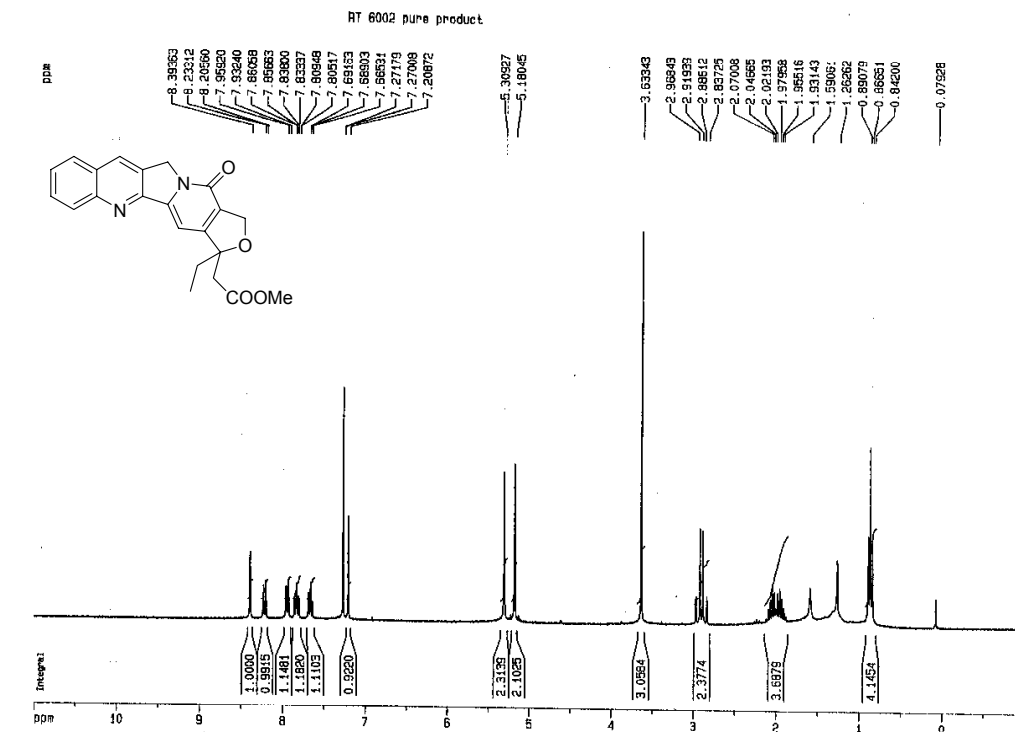


Figure A-9: ¹H and ¹³C NMR spectra of compound 92d

RT 6003d pure product.

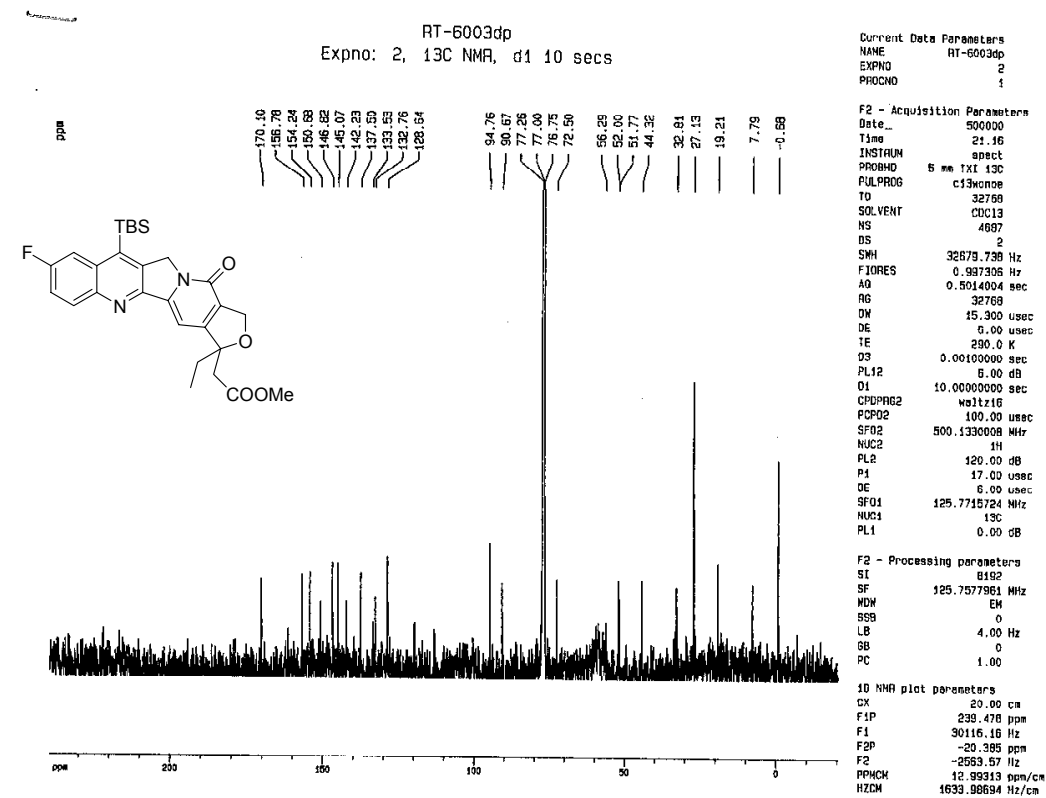
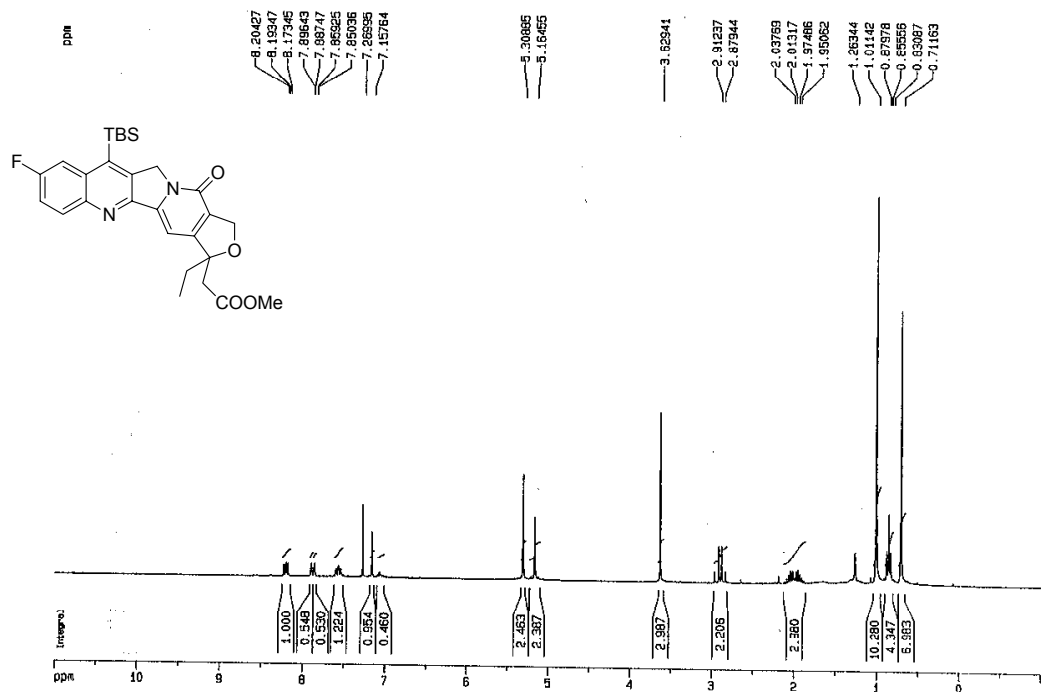
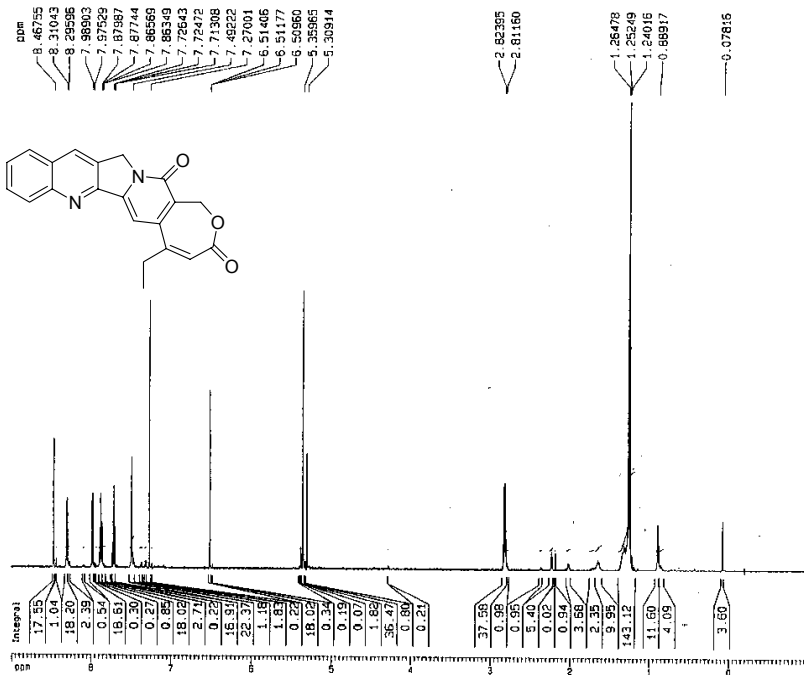


Figure A-10: ¹H and ¹³C NMR spectra of compound 95a

600.83 MHz ¹H NMR spectrum of RT-6021dp in 100% CDCl₃ at 297K, d1=12 sec., 4/17/03



Current Data Parameters
 NAME rt-6021dp
 EXPNO 1
 PROCNO 1

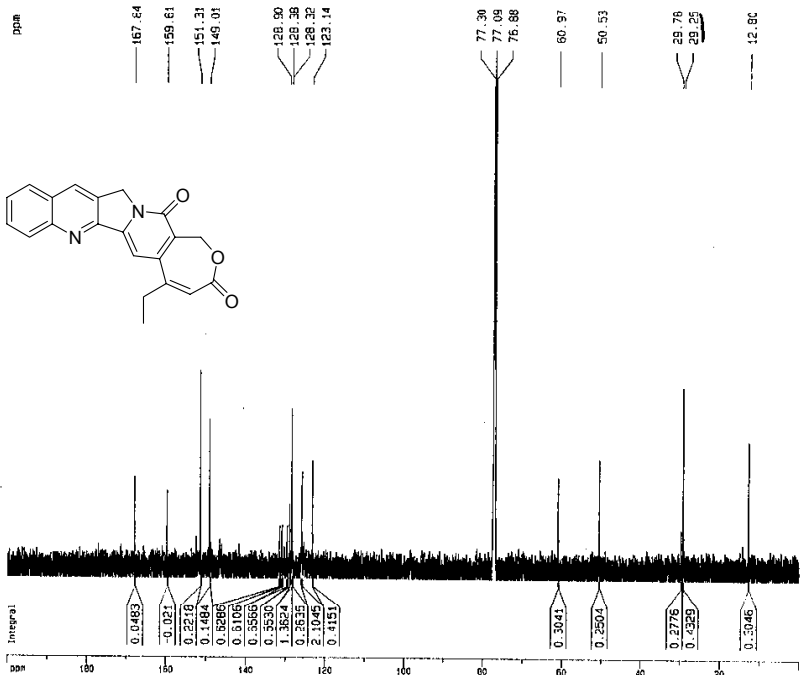
F2 - Acquisition Parameters
 Date_ 20030417
 Time 21.44
 INSTRUM spect
 PROBHD 5 mm TBI 1H/
 PULPROG zg
 TD 65536
 SOLVENT CDCl₃
 NS 16
 DS 0
 SWH 8992.806 Hz
 FIDRES 0.137219 Hz
 AQ 3.6438515 sec
 RG 10
 OW 55.600 usec
 OE 6.00 usec
 TE 290.0 K
 D1 12.00000000 sec

***** CHANNEL f1 *****
 NUC1 1H
 P1 9.60 usec
 PL1 0.00 dB
 SFO1 600.8336050 MHz

F2 - Processing parameters
 SI 65536
 SF 600.0300269 MHz
 MDW EM
 SSB 0
 LB 0.10 Hz
 GB 0
 PC 1.00

1D NMR plot parameters
 CX 20.00 cm
 FJP 9.000 ppr
 F1 5407.47 Hz
 F2P -1.000 ppr
 F2 -600.83 Hz
 PPNCH 0.50000 ppr
 HZCM 300.41501 Hz

151.1 Mhz ¹H-decoupled ¹³C NMR spectrum of RT-6021dp in 100% CDCl₃ at 297K, d1=8 sec., 04/21/03



Current Data Parameters
 NAME rt-6021dp
 EXPNO 2
 PROCNO 1

F2 - Acquisition Parameters
 Date_ 20030419
 Time 10.38
 INSTRUM spect
 PROBHD 5 mm TBI 1H/
 PULPROG c13wznoe
 TD 65536
 SOLVENT CDCl₃
 NS 34653
 DS 0
 SWH 37678.789 Hz
 FIDRES 0.577994 Hz
 AQ 0.8851252 sec
 RG 32789
 OW 13.200 usec
 OE 6.00 usec
 TE 290.0 K
 D1 8.00000000 sec
 D3 0.00100000 sec

***** CHANNEL f1 *****
 NUC1 13C
 P1 13.50 usec
 PL1 0.00 dB
 SFO1 151.0953827 MHz

***** CHANNEL f2 *****
 CPROPR2 waltz16
 NUC2 1H
 P2P2 100.00 usec
 PL2 0.00 dB
 PL12 12.00 dB
 SFO2 600.8336050 MHz

F2 - Processing parameters
 SI 65536
 SF 151.0788173 MHz
 MDW EM
 SSB 0
 LB 1.00 Hz
 GB 0
 PC 1.00

1D NMR plot parameters
 CX 20.00 cm
 FJP 200.000 ppr
 F1 30215.76 Hz
 F2P 0.000 ppr
 F2 0.00 Hz
 PPNCH 10.00000 ppr/cm
 HZCM 1510.78809 Hz/cm

Figure A-11: ¹H and ¹³C NMR spectra of compound 95d

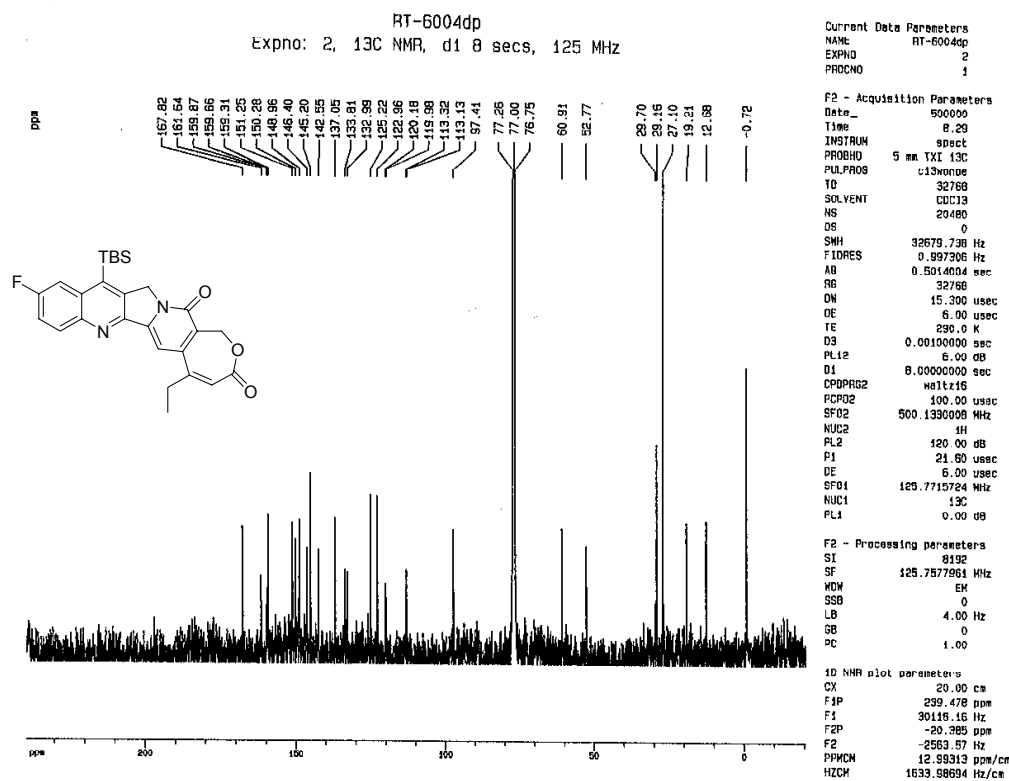
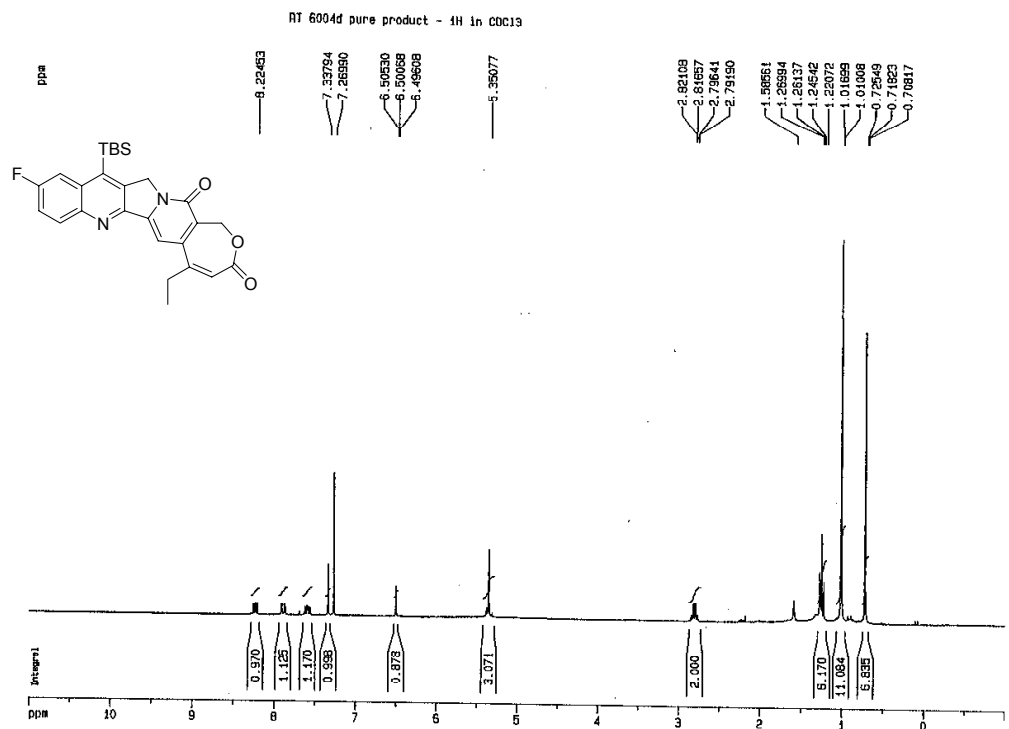


Figure A-12: ¹H and ¹³C NMR spectra of compound 96

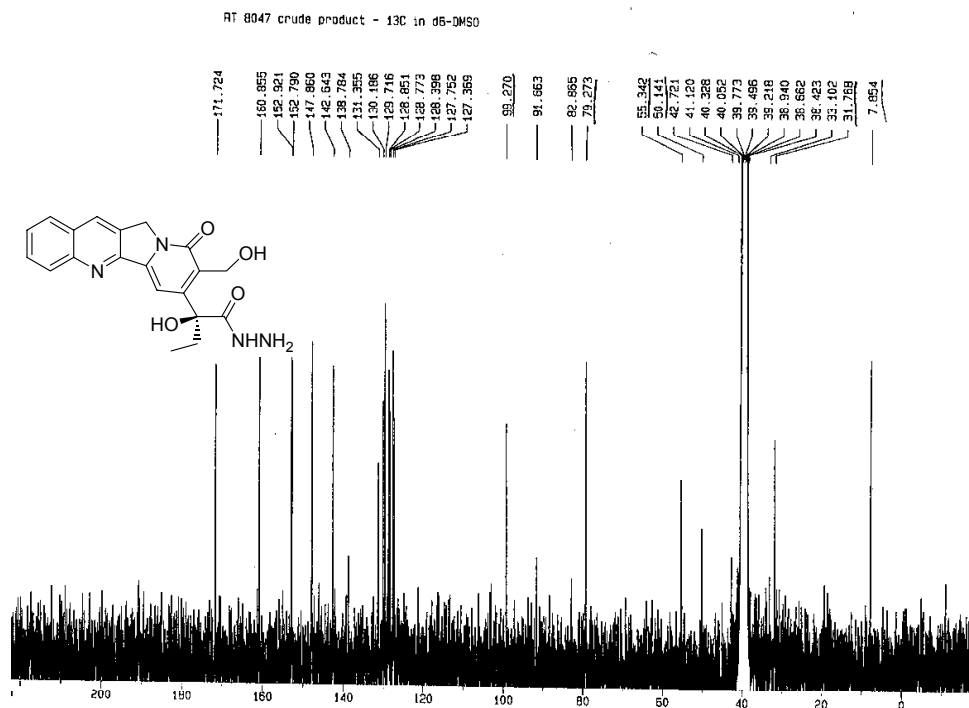
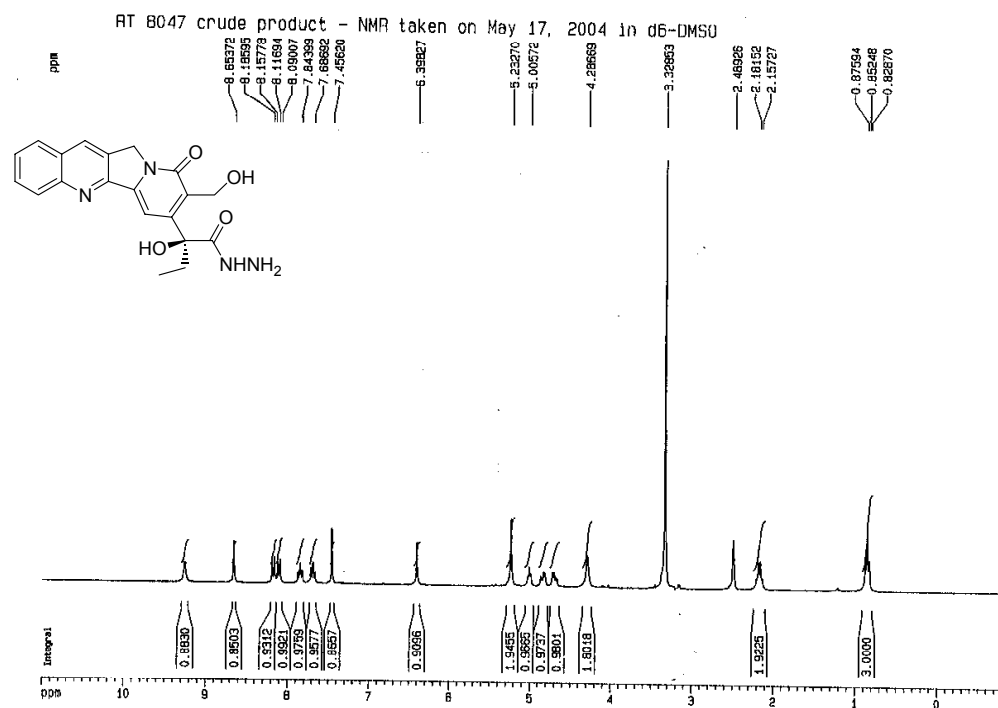


Figure A-13: ¹H and ¹³C NMR spectra of compound 99

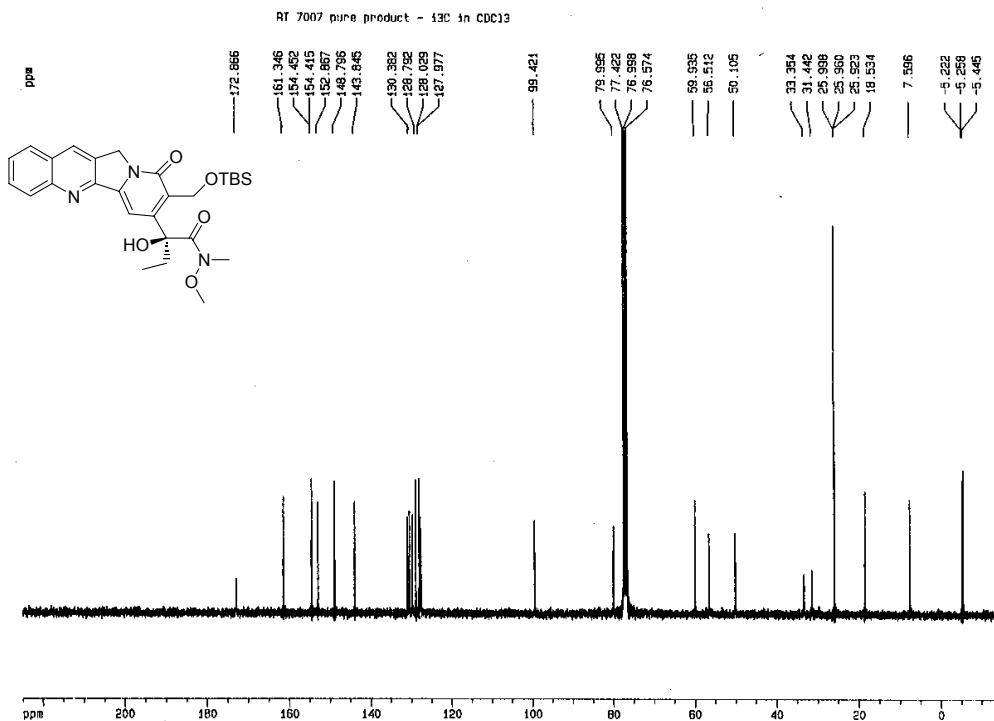
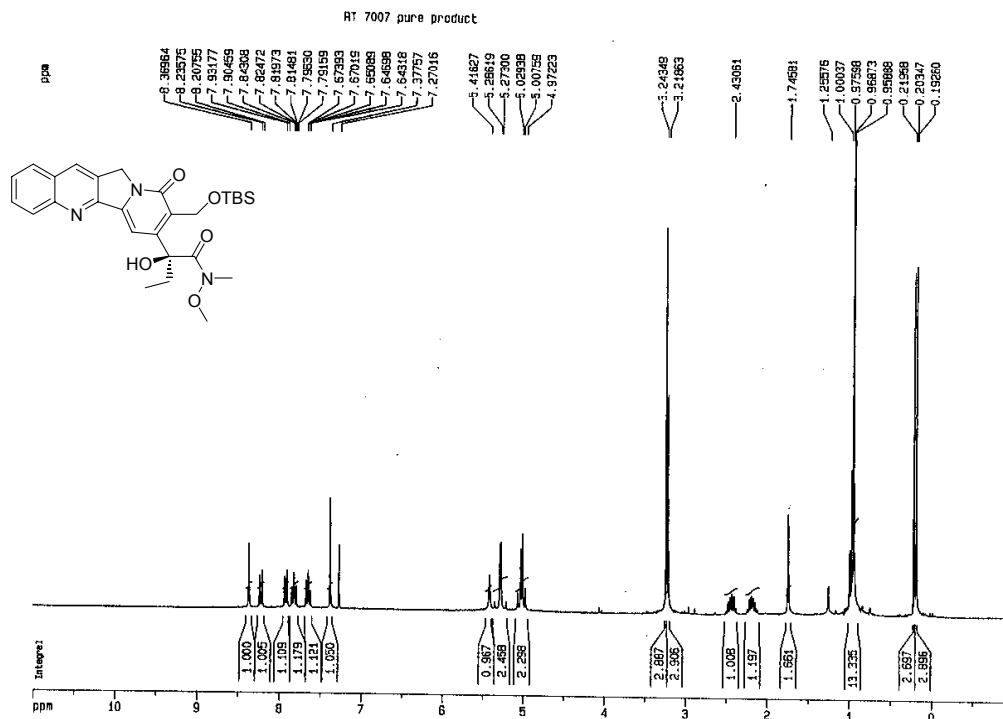


Figure A-14: ¹H and ¹³C NMR spectra of compound 102

RT B048d crude product recorded in d₆-DMSO on May 24, 2004

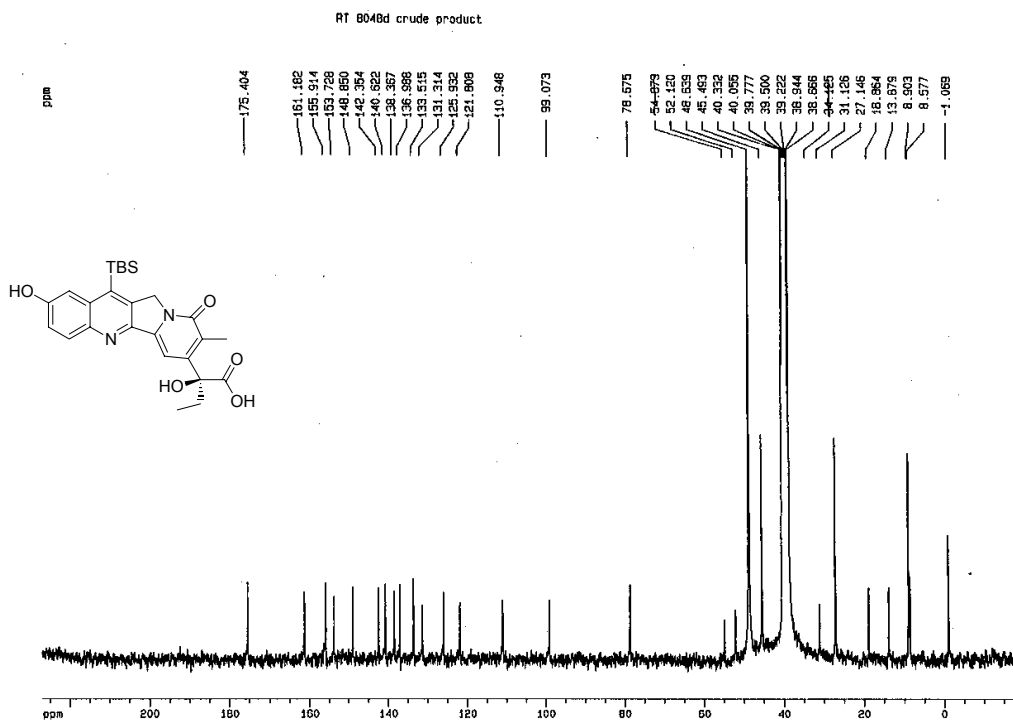
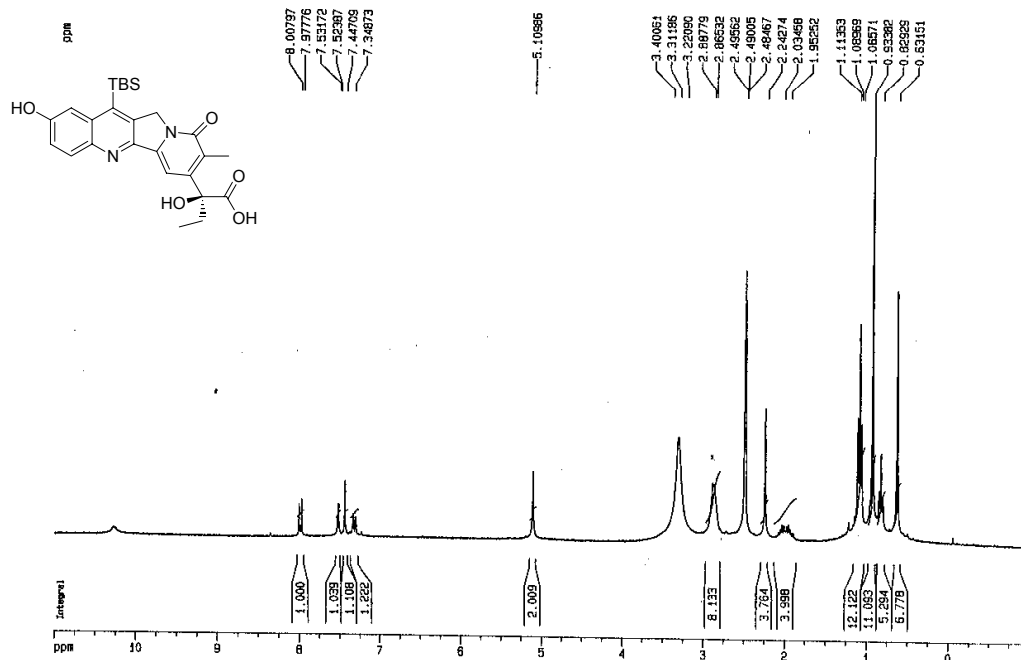


Figure A-15: ¹H and ¹³C NMR spectra of compound (S)-116

RT 7049 - the first elution peak (which comes from DAST rxn of "R"-DE lactone) from the HPLC purification

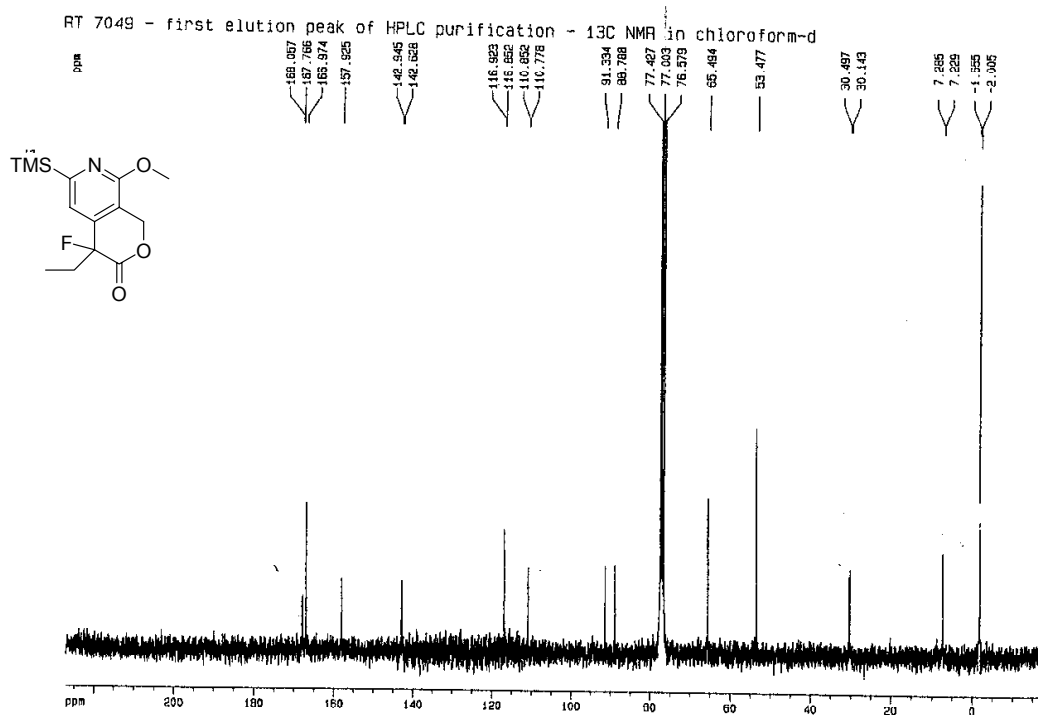


Figure A-16: ^1H and ^{13}C NMR spectra of compound (S)-109

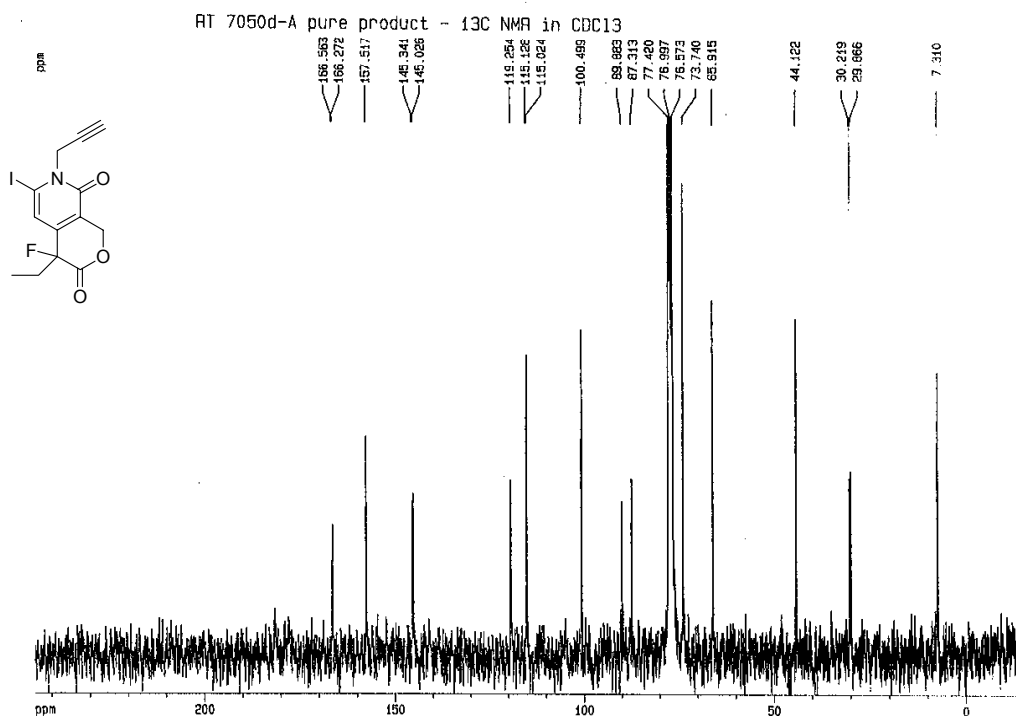
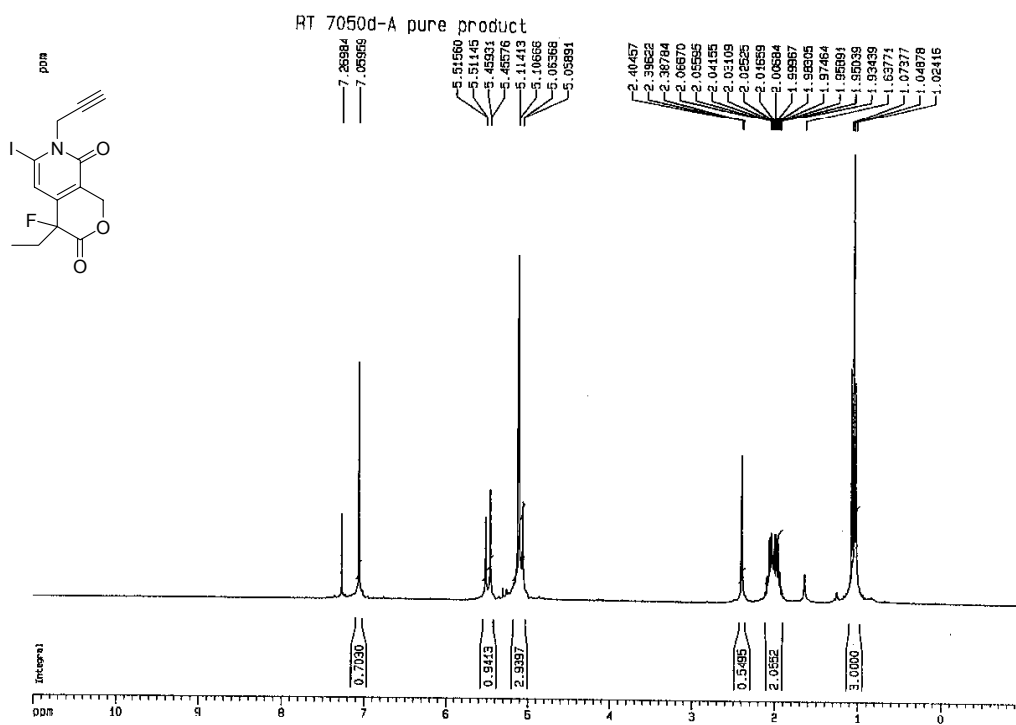


Figure A-17: ^1H and ^{13}C NMR spectra of compound (R)-107

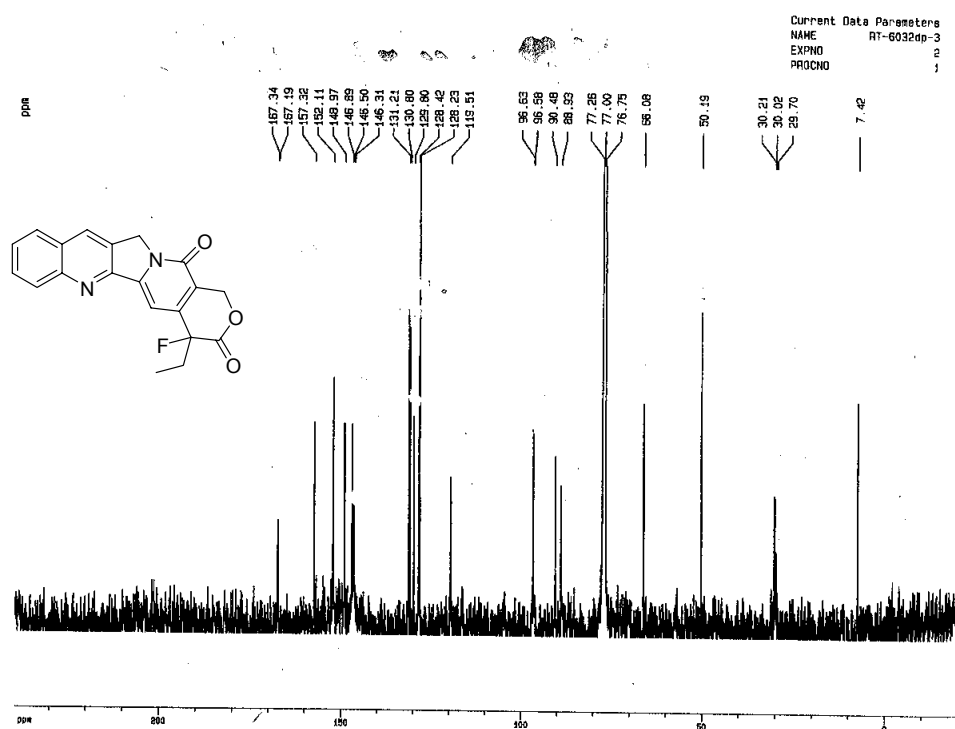
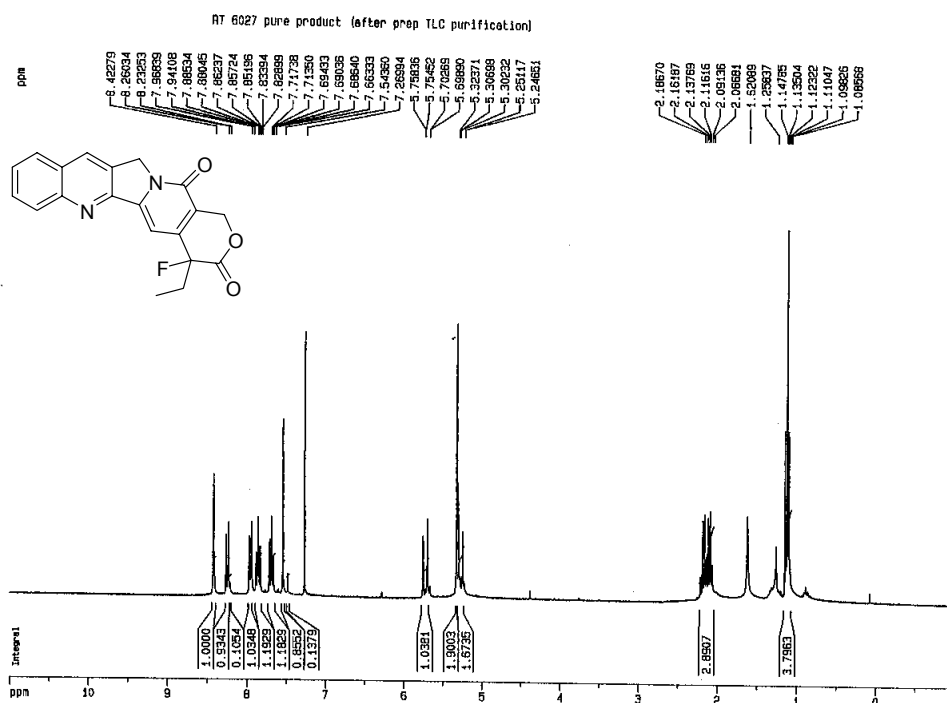


Figure A-18: HMBC spectrum of compound (R)-107

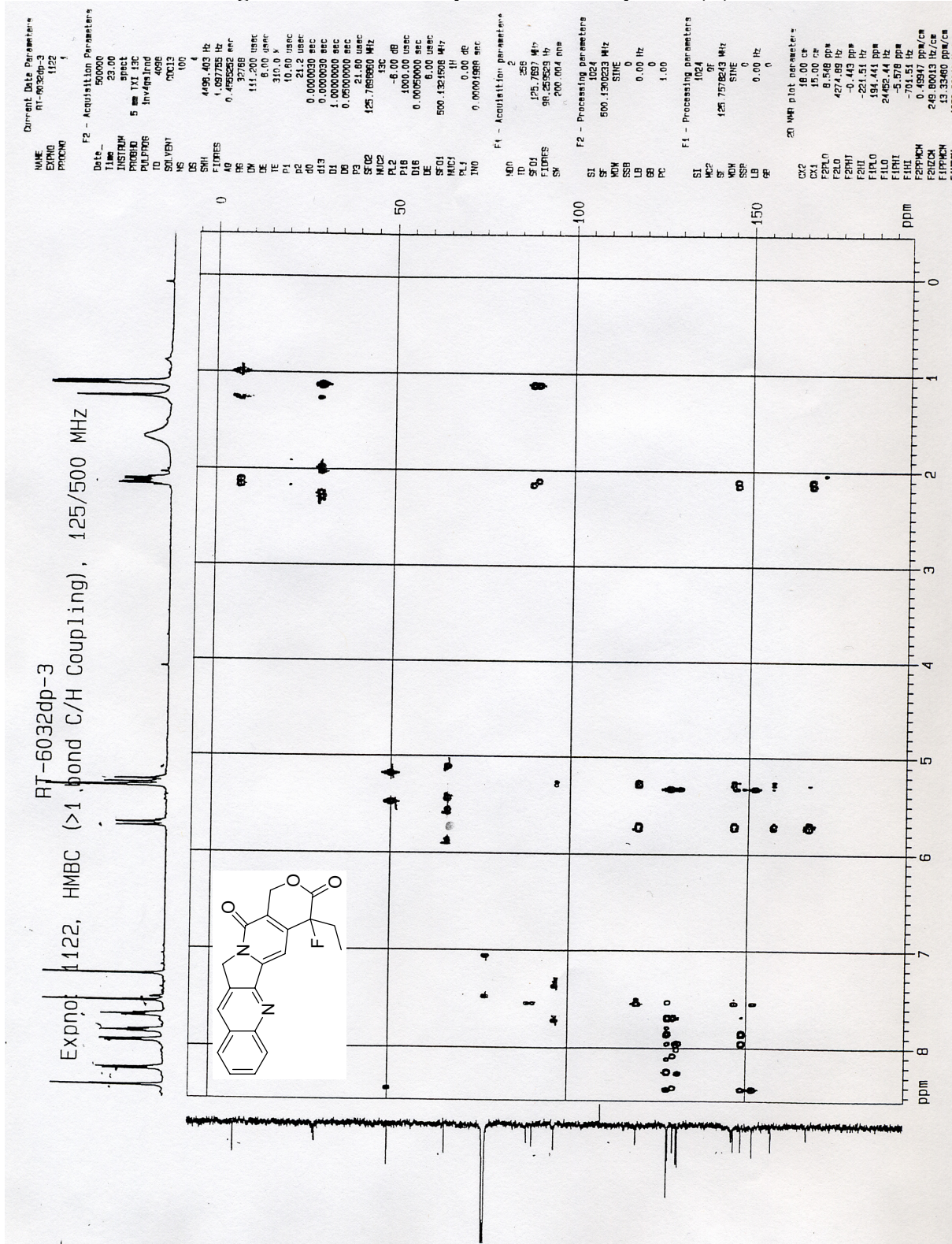


Figure A-19: ¹H NMR spectra of compounds 111b and 111c

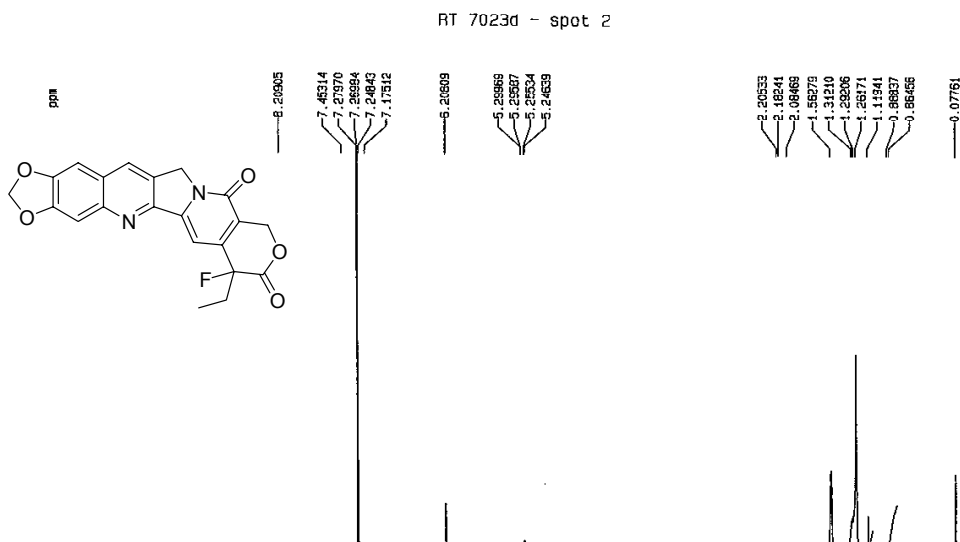
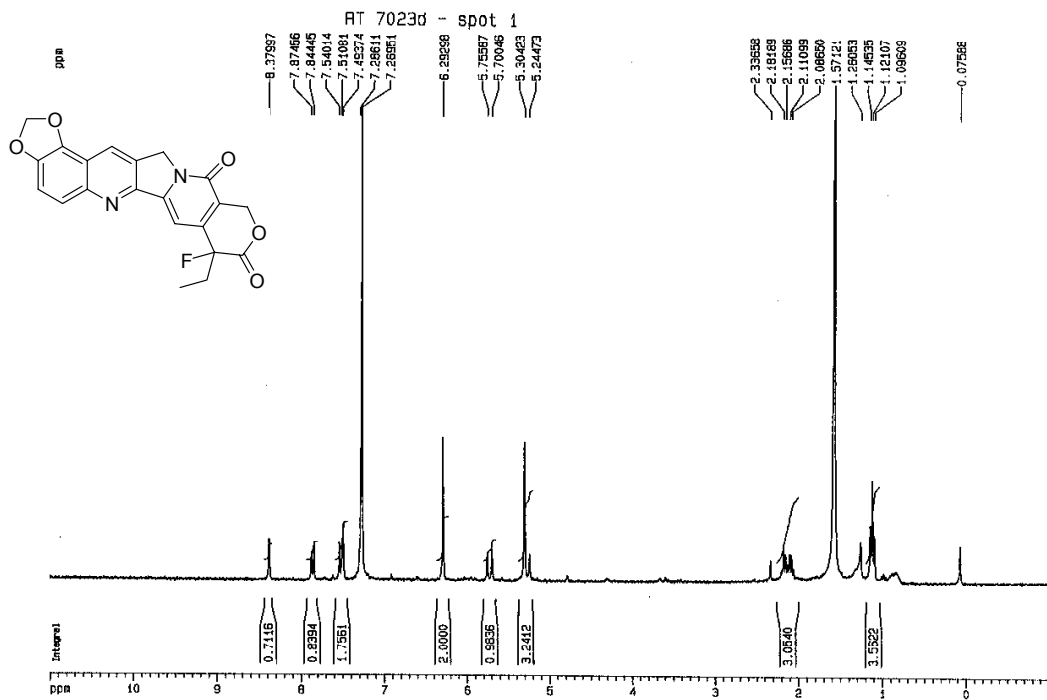


Figure A-20: ^1H and ^{13}C NMR spectra of compound 121

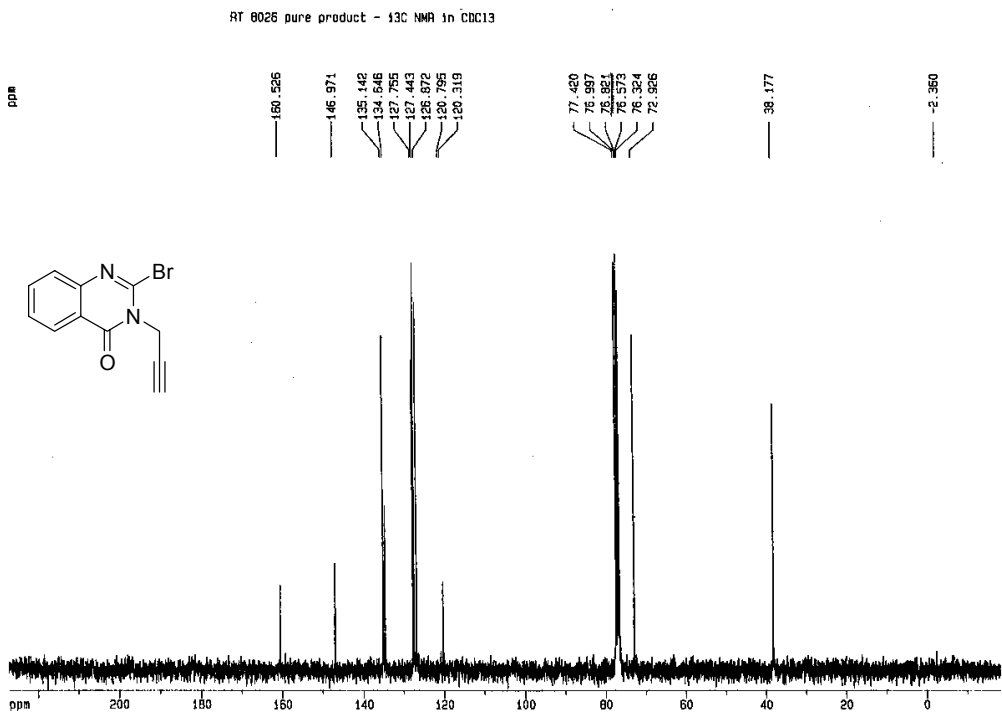
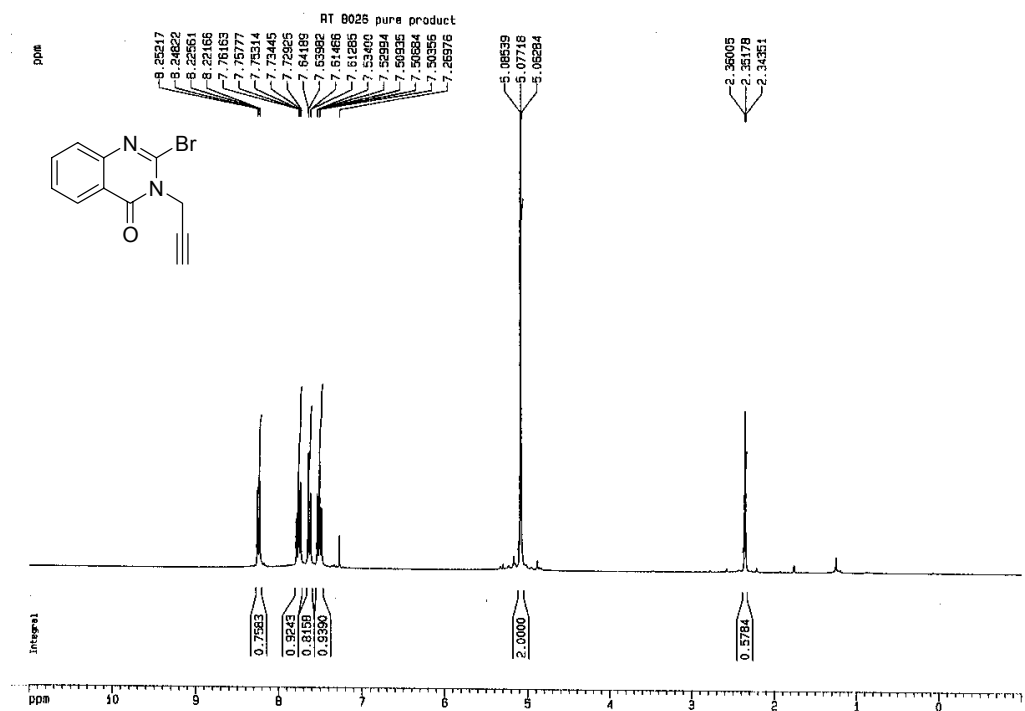


Figure A-21: ^1H and ^{13}C NMR spectra of compound 120

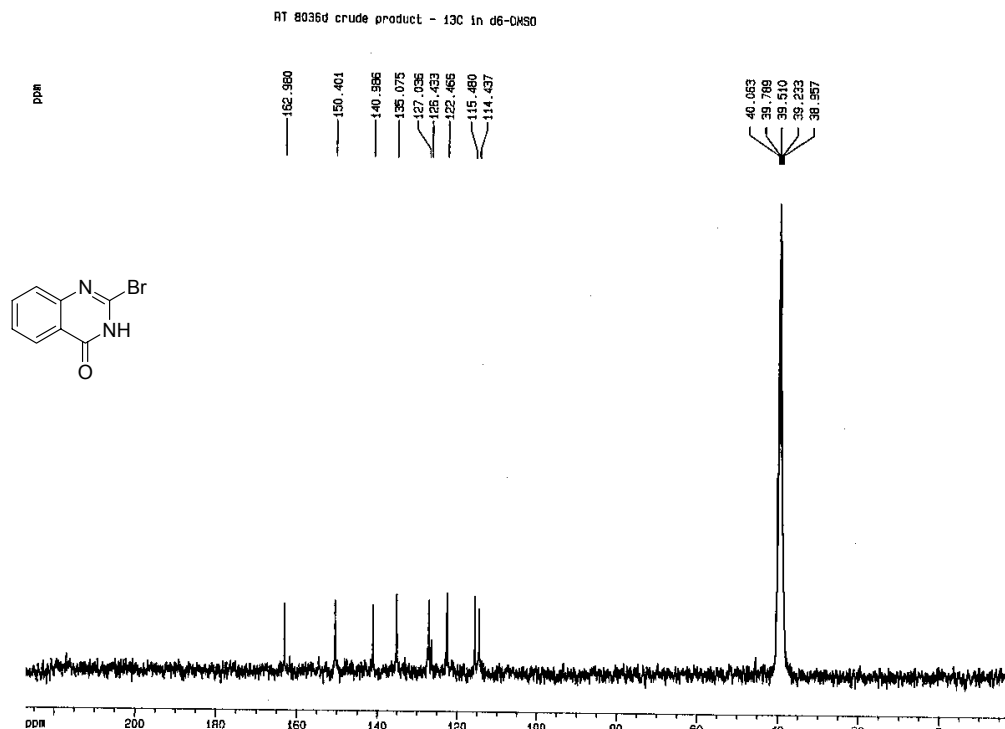
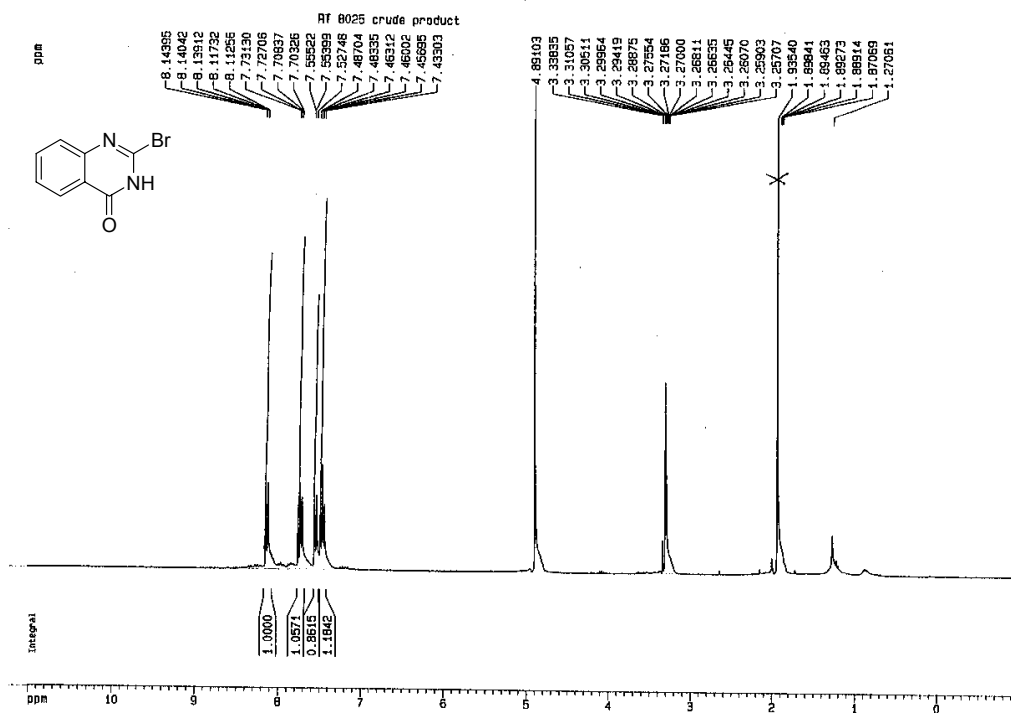


Figure A-22: ^1H and ^{13}C NMR spectra of compound 129{b}

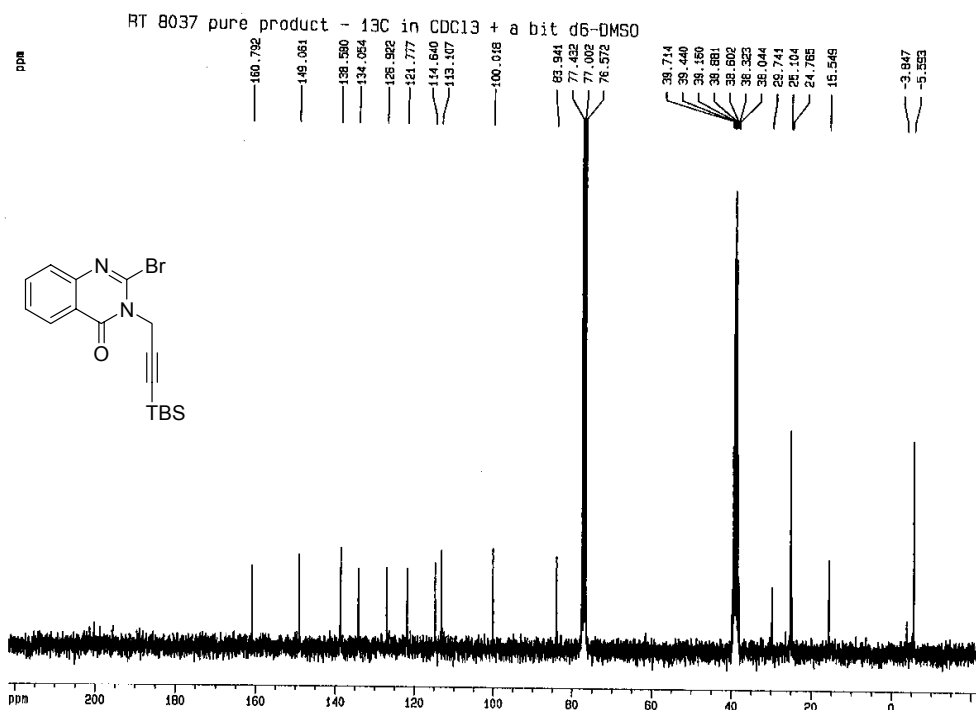
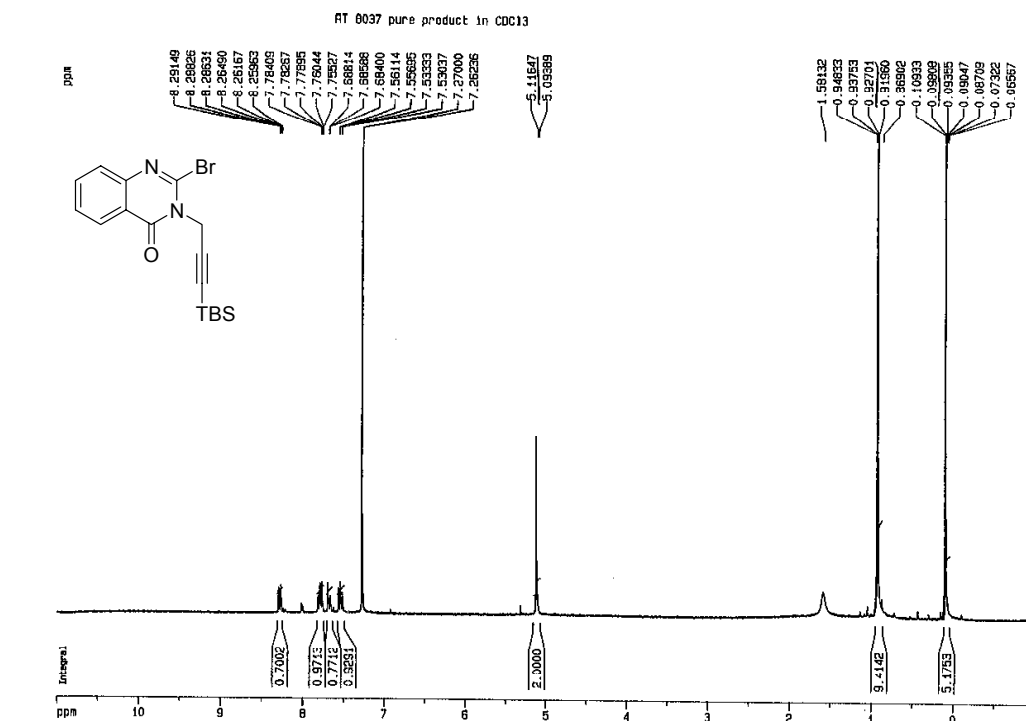


Figure A-23: ¹H and ¹³C NMR spectra of compound 129{c}

RT 8038d pure product

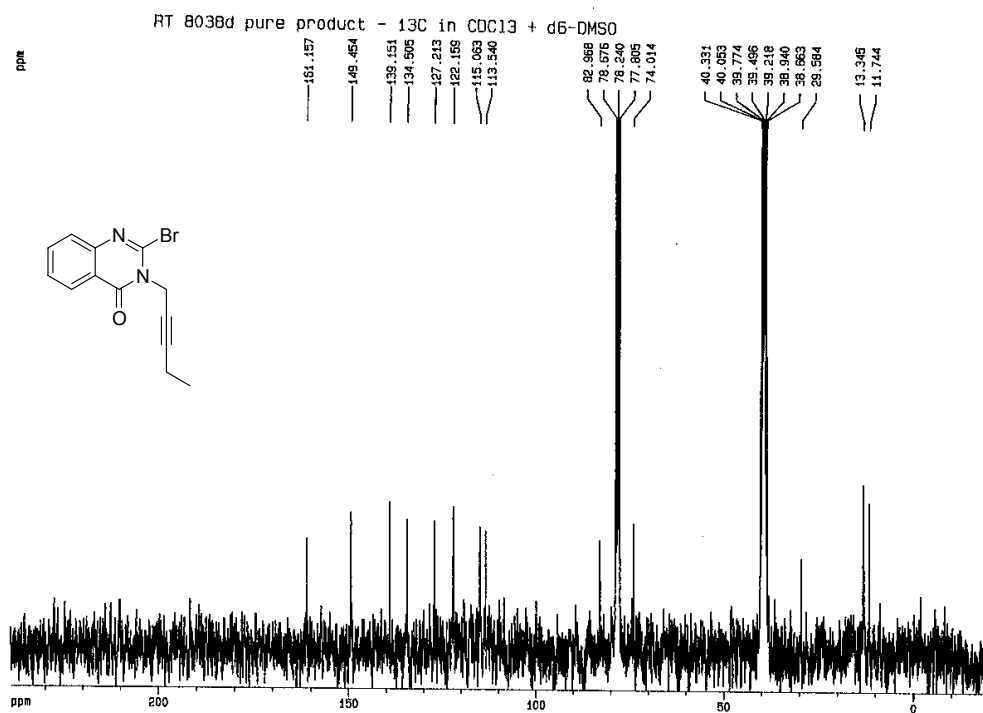
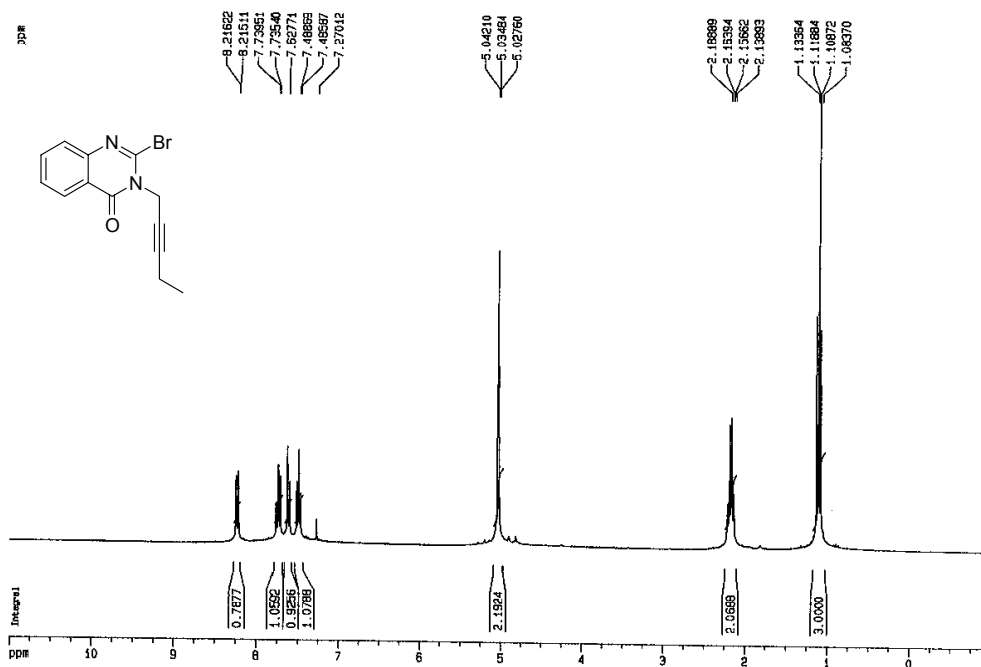


Figure A-24: ^1H and ^{13}C NMR spectra of compound 129{d}

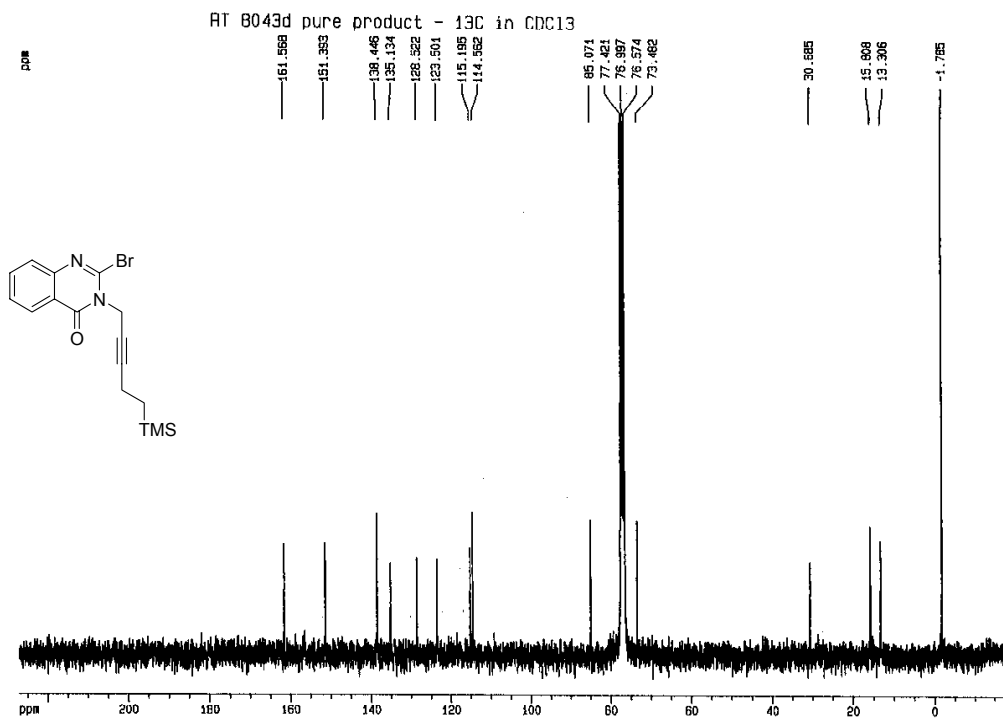
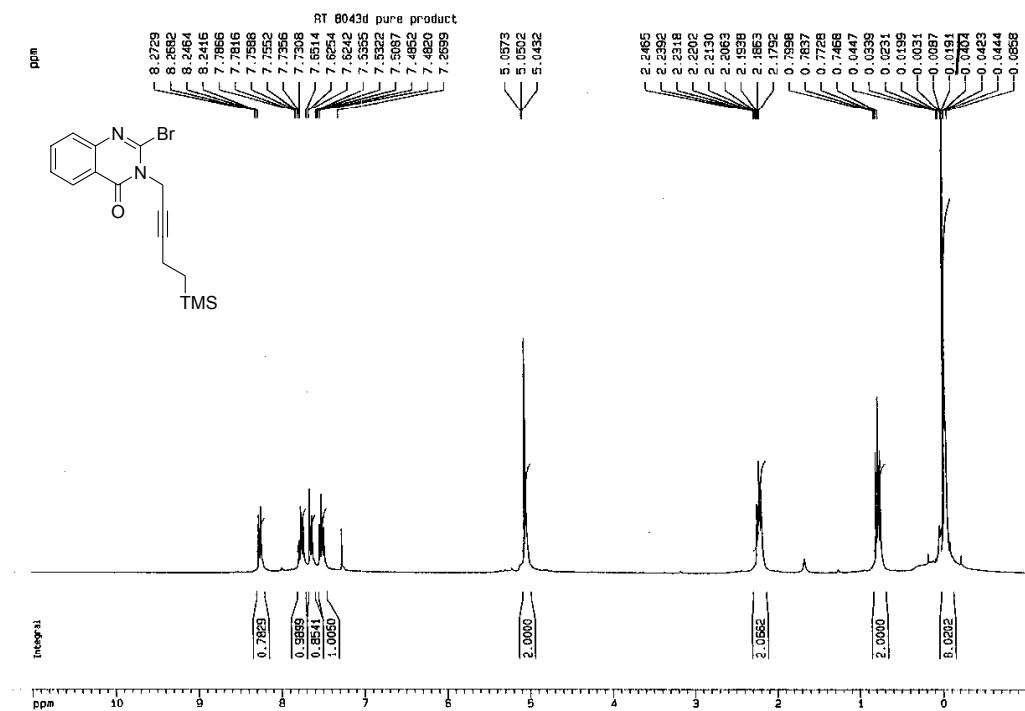


Figure A-25: ^1H spectrum of compound 122

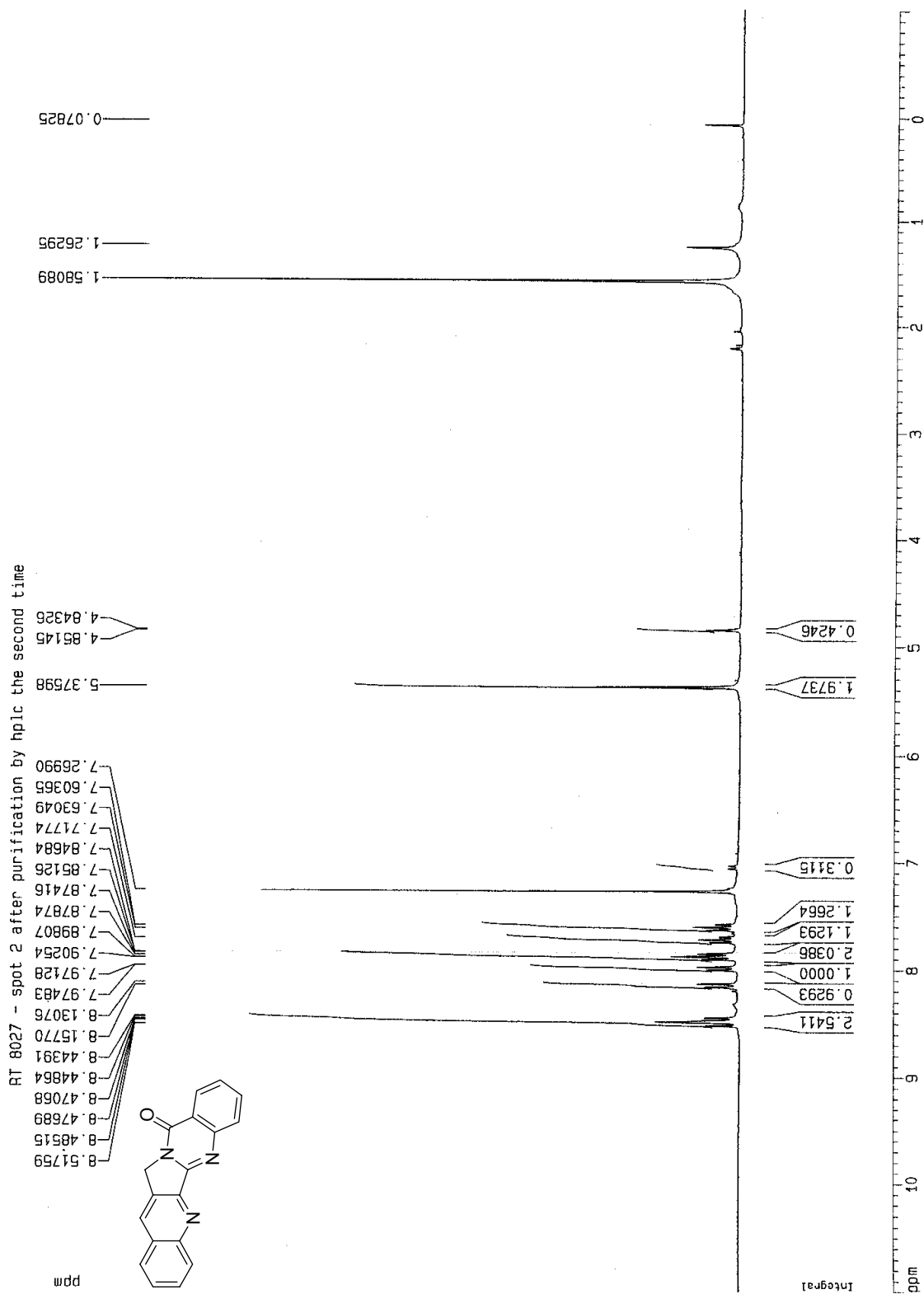
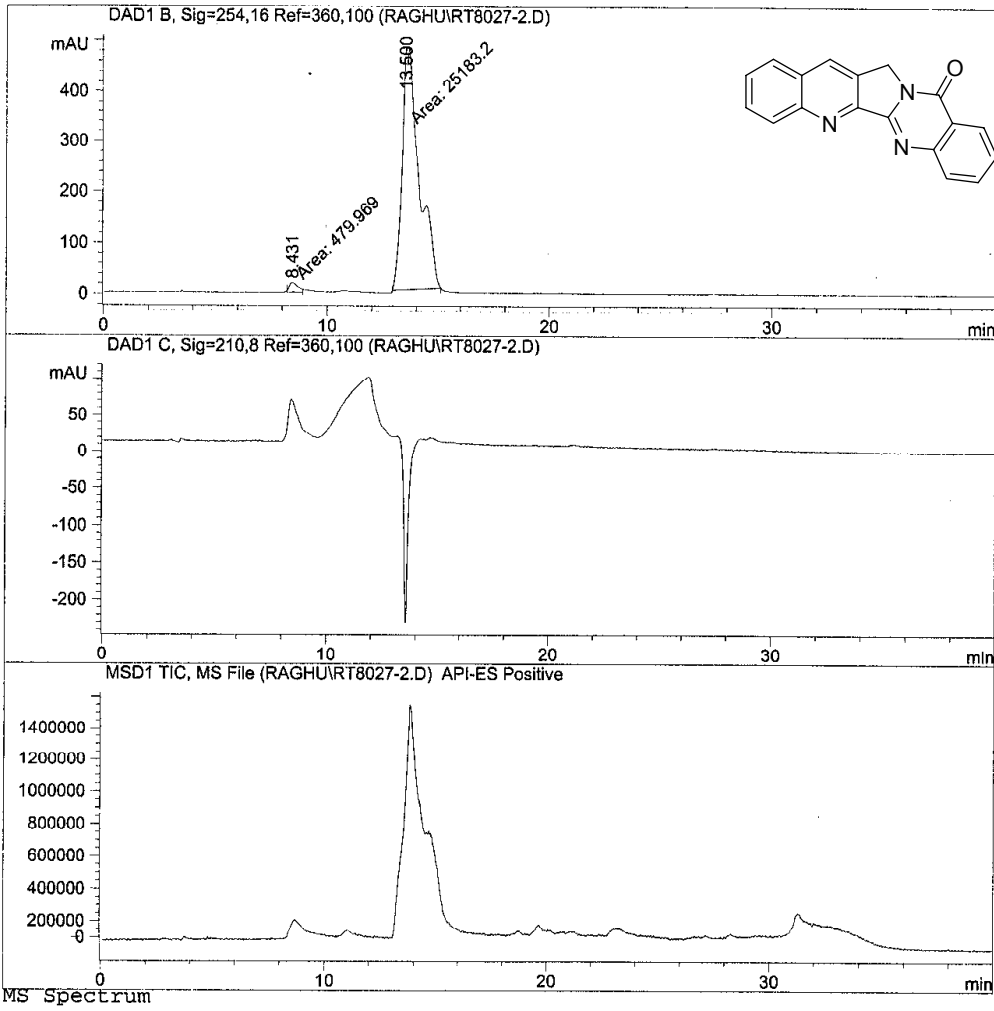


Figure A-26: LCMS data of compound 122

Current Chromatogram(s)



*MSD1 SPC, time=13.160:15.633 of RAGHU\RT8027-2.D API-ES Positive

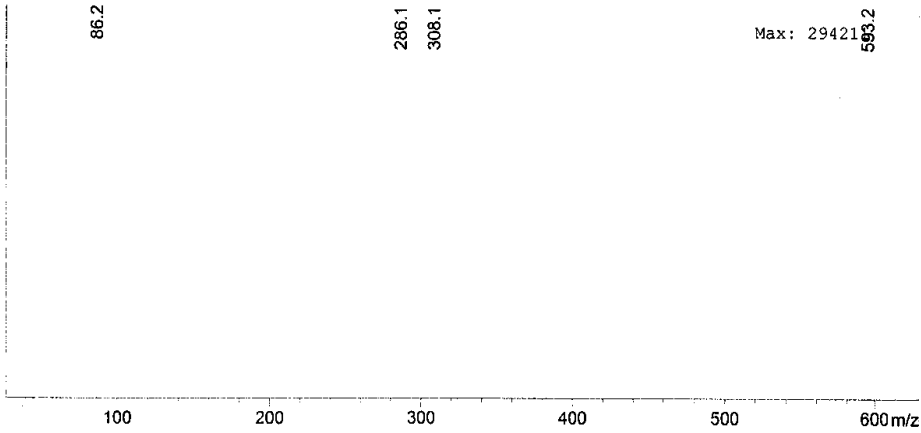


Figure A-27: ^1H spectrum of compound 130{c,2}

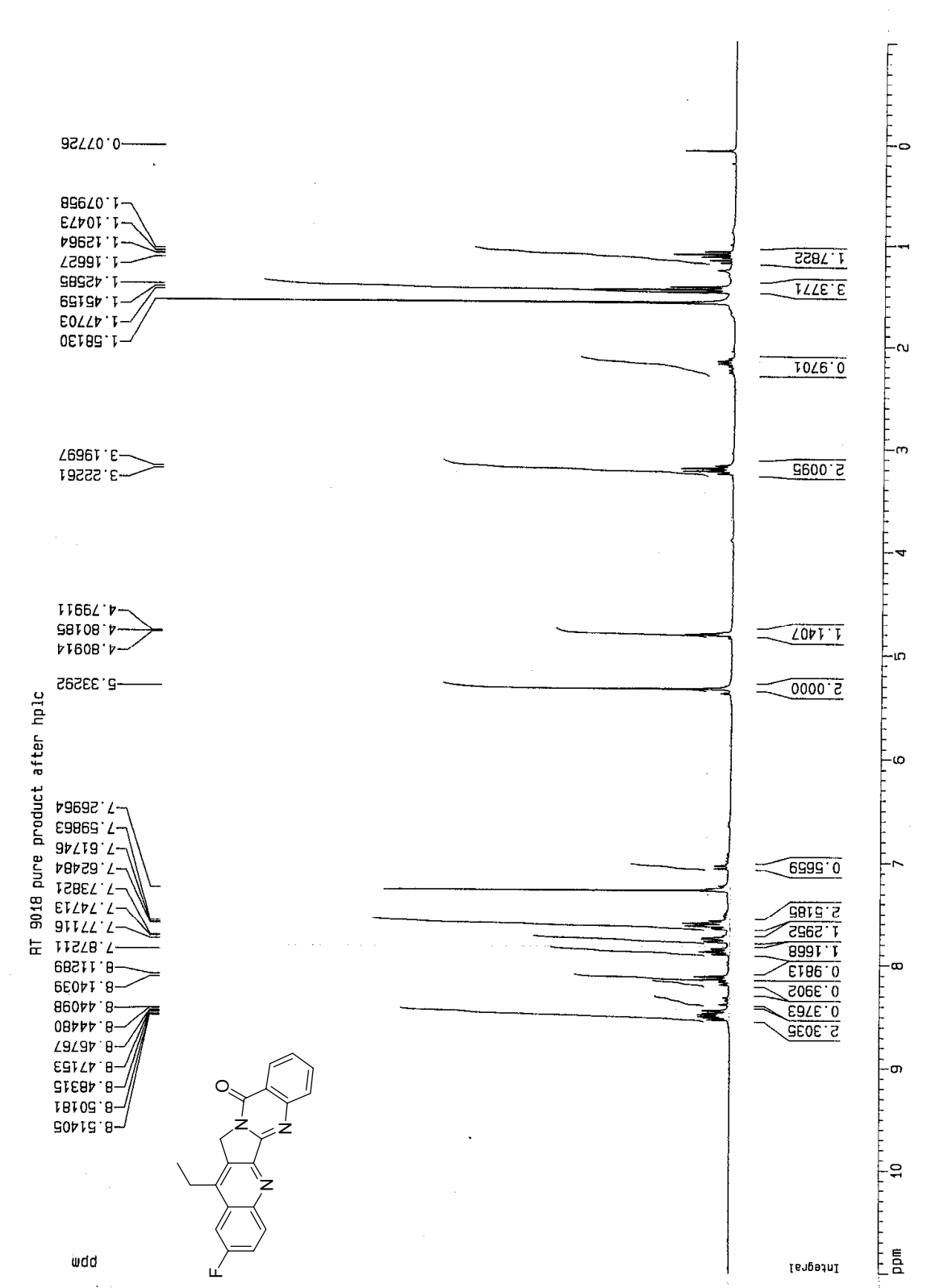
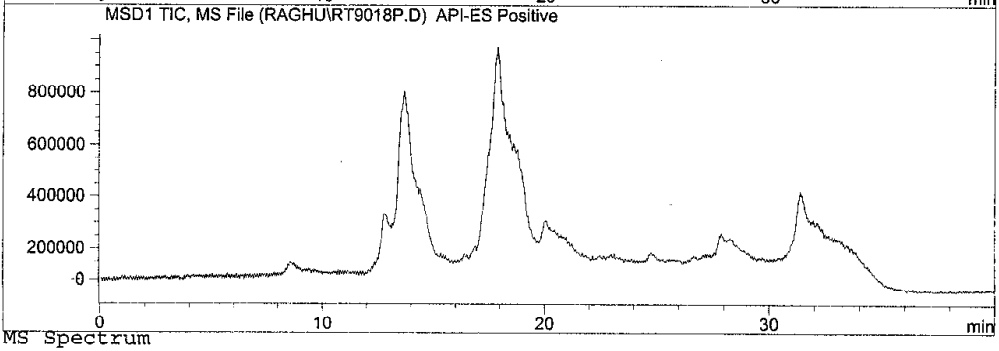
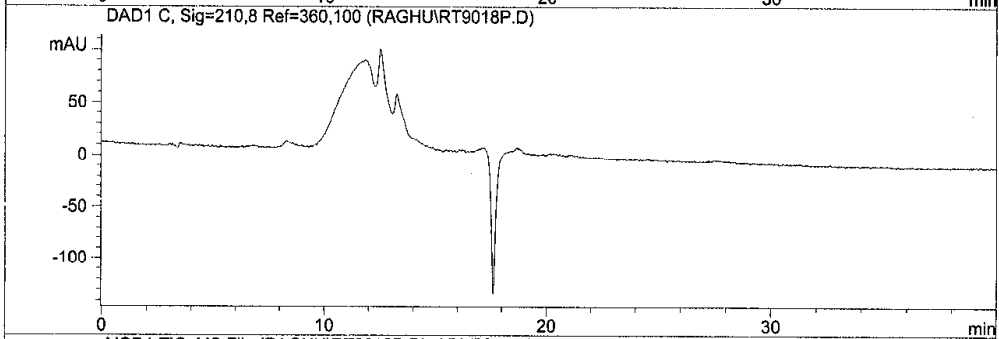
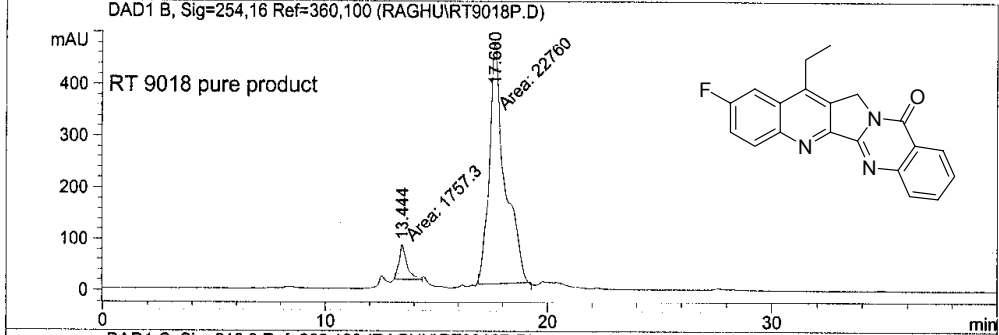


Figure A-28: LCMS data of compound 130{c,2}

Current Chromatogram(s)



*MSD1 SPC, time=16.988:19.650 of RAGHU\RT9018P.D API-ES Positive

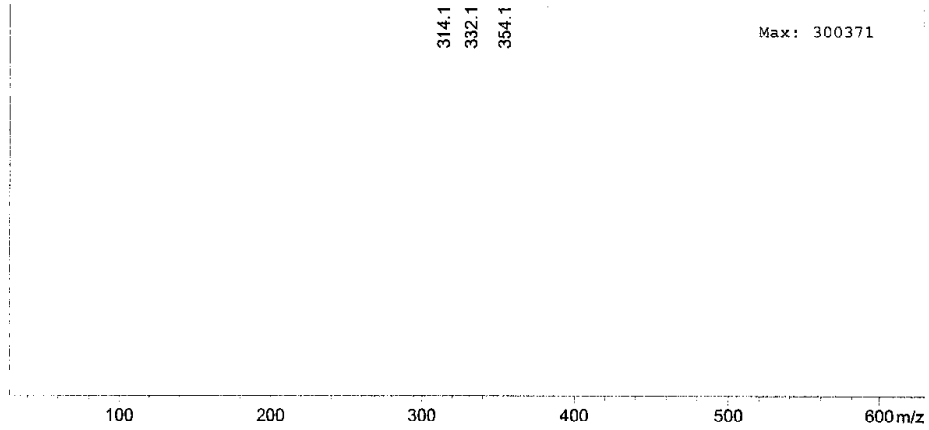


Figure A-29: ^1H spectrum of compound 130{a,3}

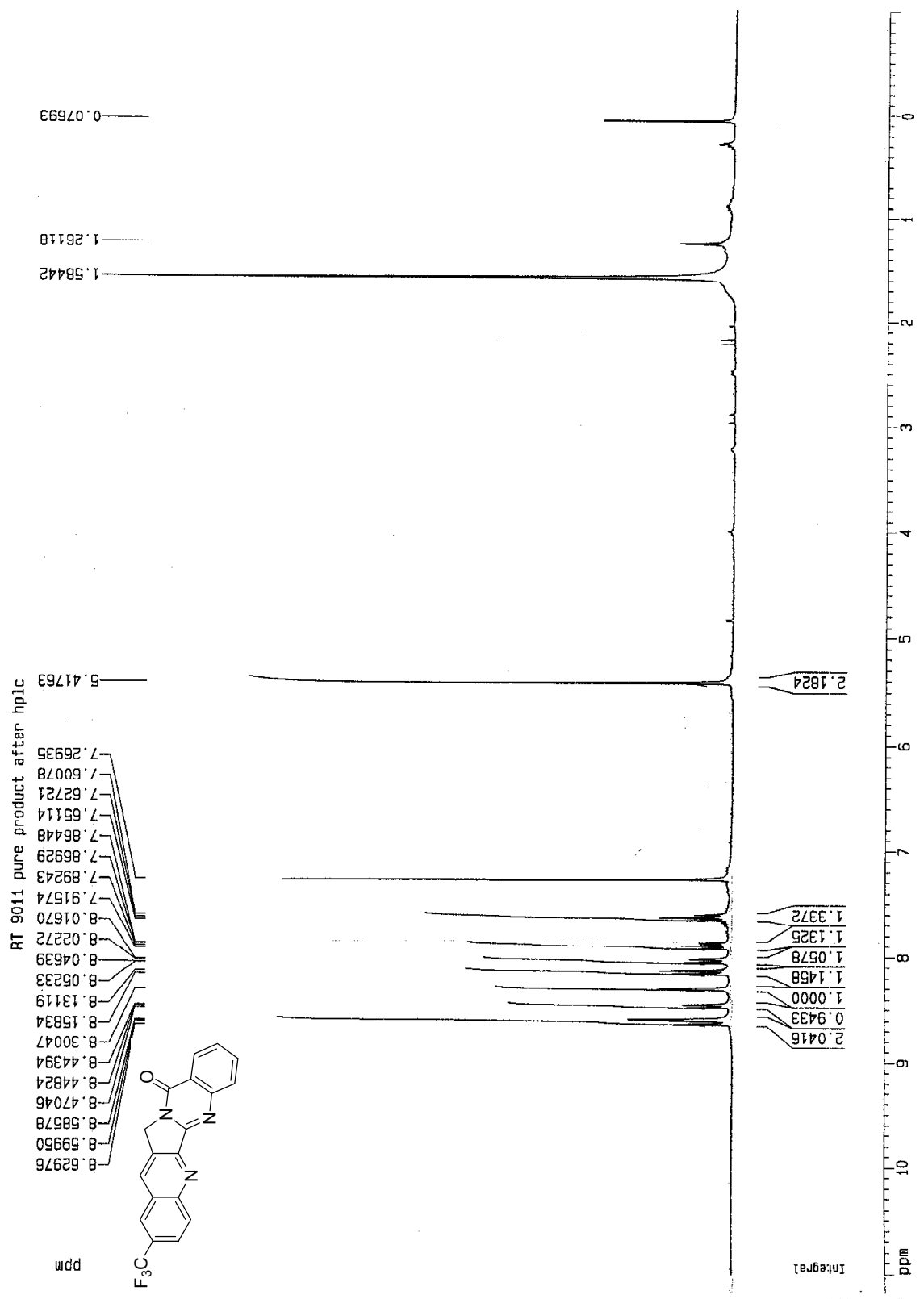


Figure A-30: LCMS data of compound 130{a,3}

Current Chromatogram(s)

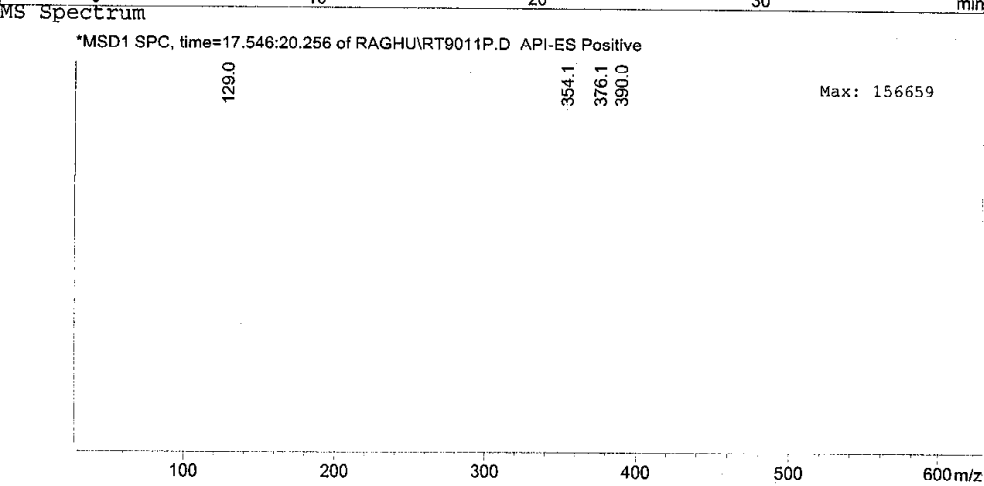
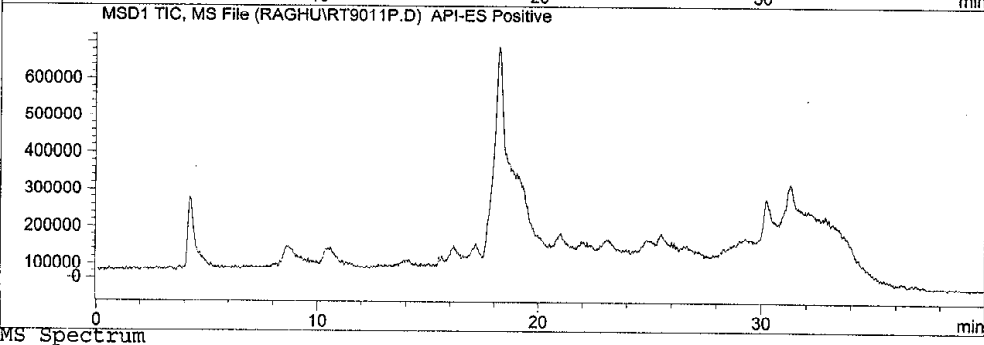
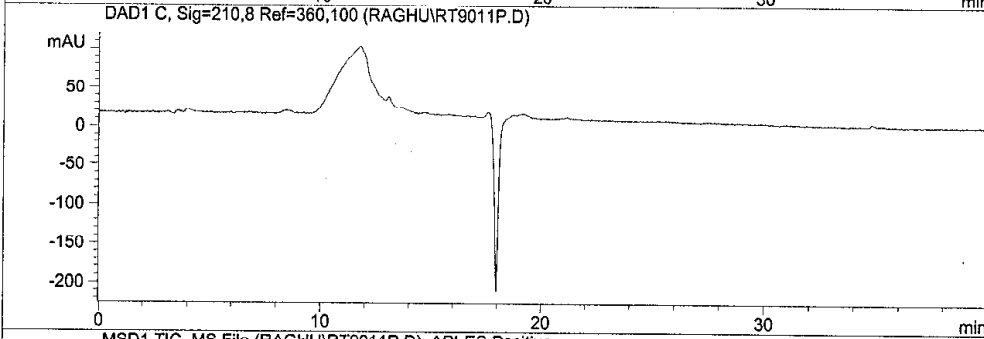
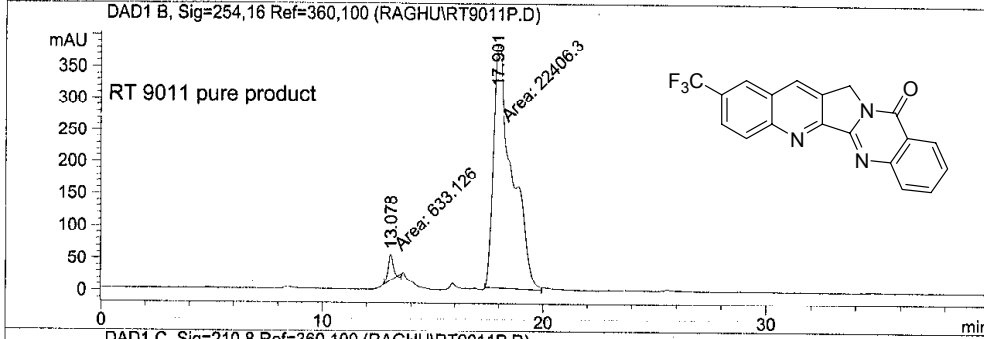


Figure A-31: ^1H spectrum of compound 130{a,4}

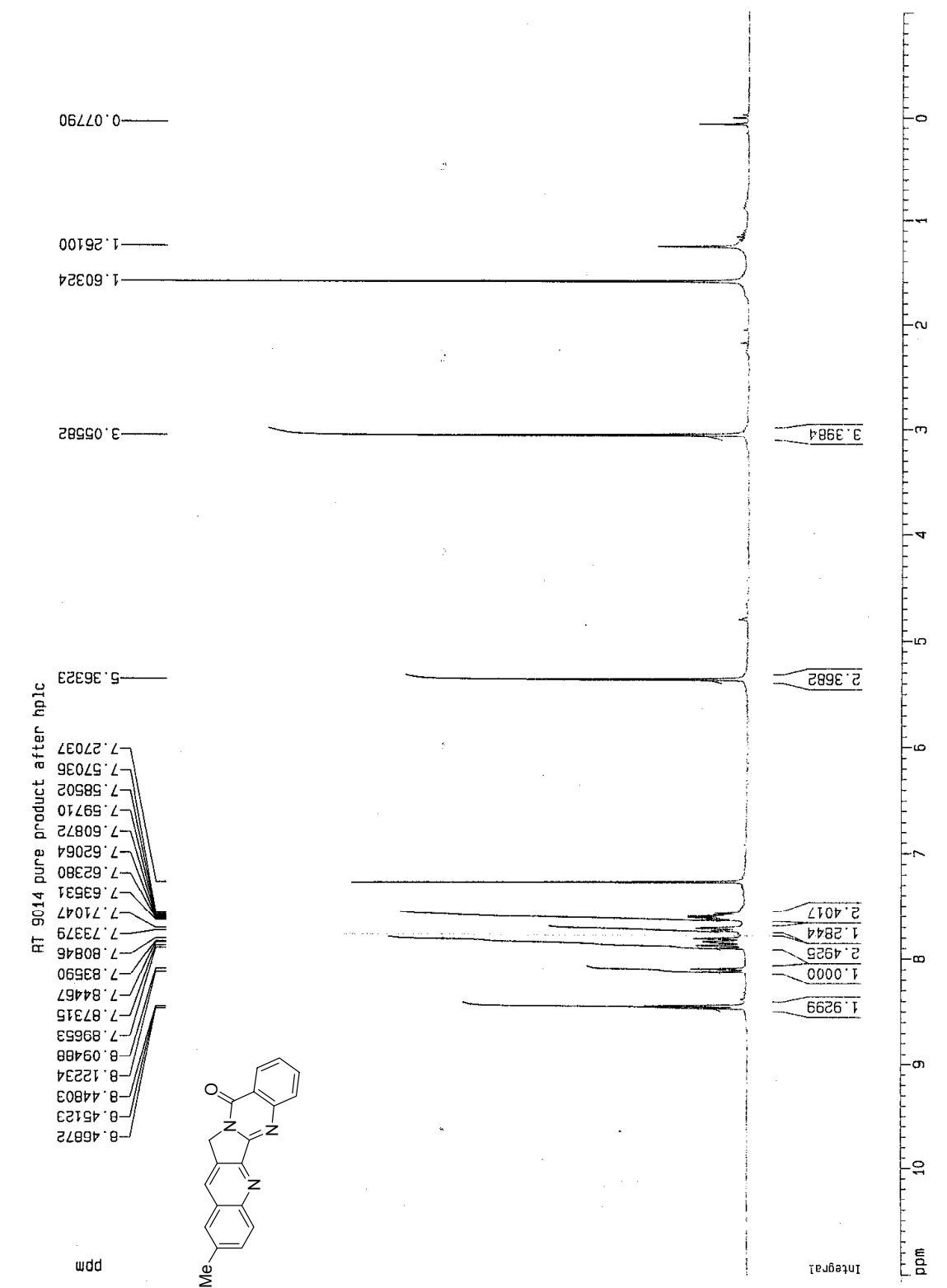


Figure A-32: LCMS data of compound 130{a,4}

Injection Date : 9/30/2004 3:52:39 AM Seq. Line : 13
Sample Name : rt9014p Vial : 18
Acq. Operator : Raghu Inj : 1
Inj Volume : 5 µl
Acq. Method : C:\HPCHEM\1\METHODS\TANGI.M
Last changed : 9/29/2004 6:02:25 PM by habay
Analysis Method : C:\HPCHEM\1\METHODS\SCHAFFM~1.M\A5_100QK.M
Last changed : 10/1/2004 2:23:38 PM by morgan
(modified after loading)
Water 0.1% formic acid/acetonitrile 5% to 95%. Do not change this method.
you need to make changes, save it as another file.

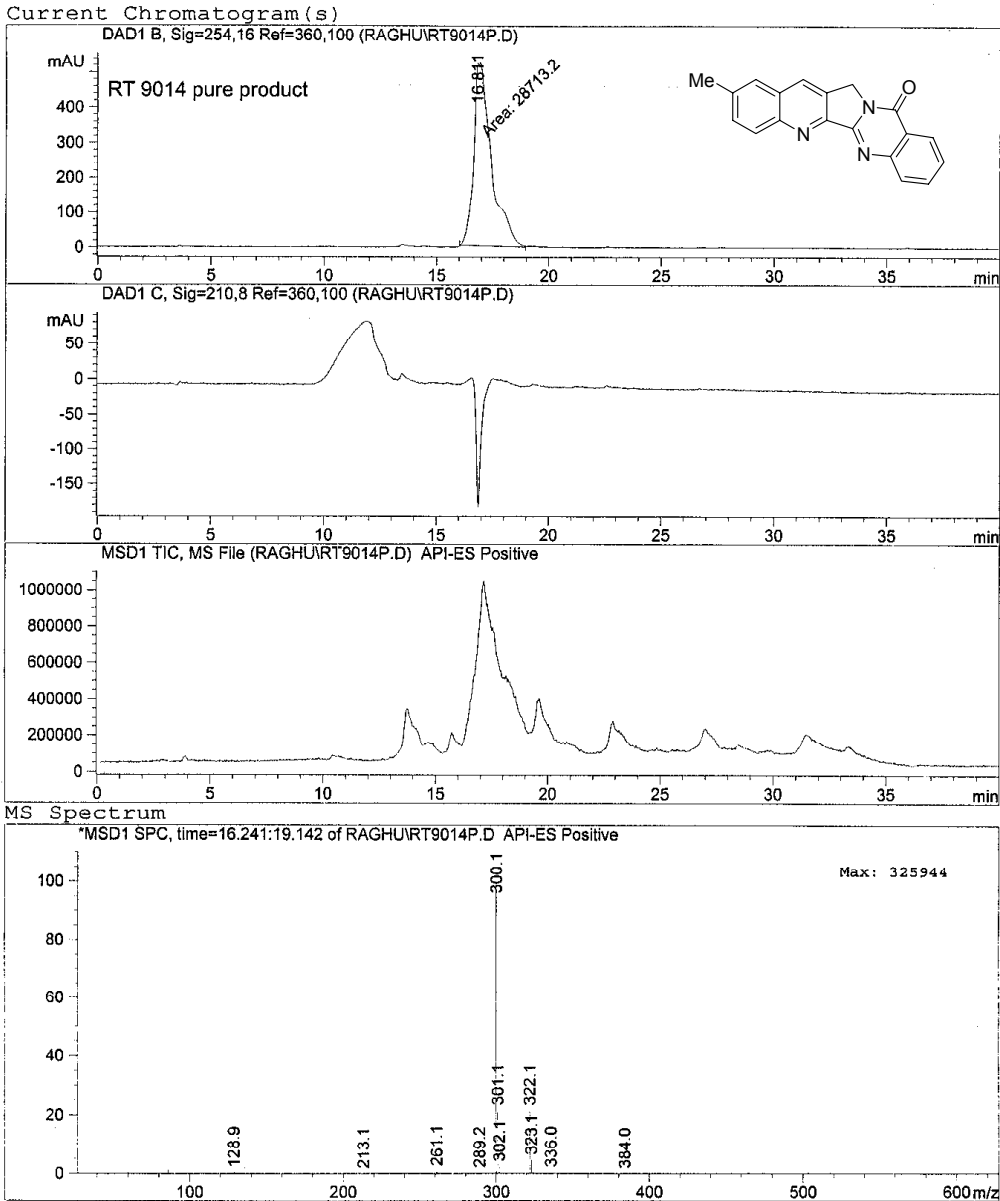


Figure A-33: ^1H spectrum of compound 130{a,6}

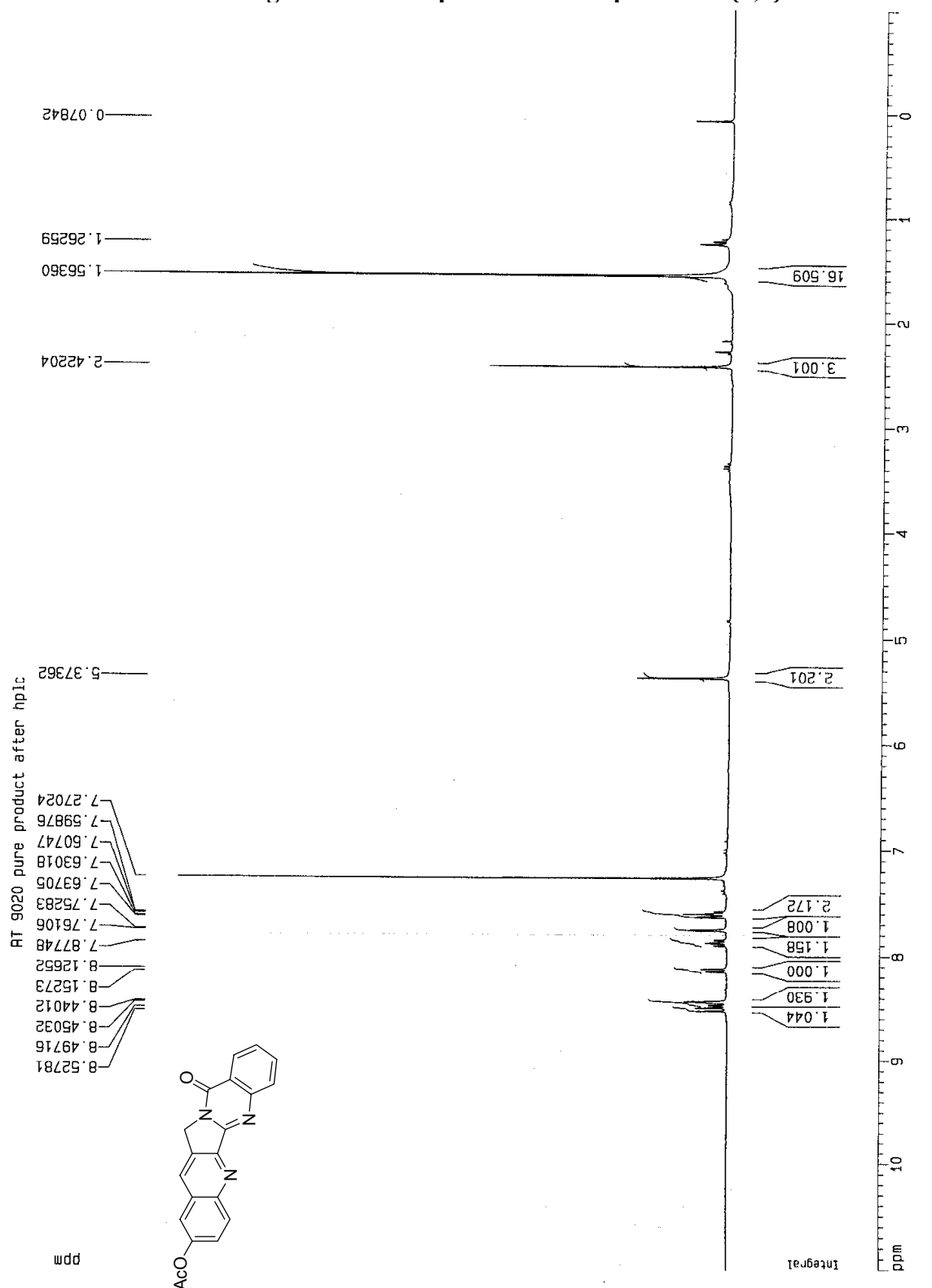


Figure A-34: LCMS data of compound 130{a,6}

```

=====
Injection Date   : 9/29/2004 8:57:18 PM          Seq. Line :    5
Sample Name     : rt9020p                        Vial       :    7
Acq. Operator  : Raghu                          Inj        :    1
                                                Inj Volume : 5 µl

Acq. Method    : C:\HPCHEM\1\METHODS\TANGI.M
Last changed   : 9/29/2004 6:02:25 PM by habay
Analysis Method : C:\HPCHEM\1\METHODS\SCHAFFM~1.M\A5_100QK.M
Last changed   : 10/1/2004 2:23:38 PM by morgan
                (modified after loading)

Water 0.1% formic acid/acetonitrile 5% to 95%. Do not change this method.
you need to make changes, save it as another file.
=====
    
```

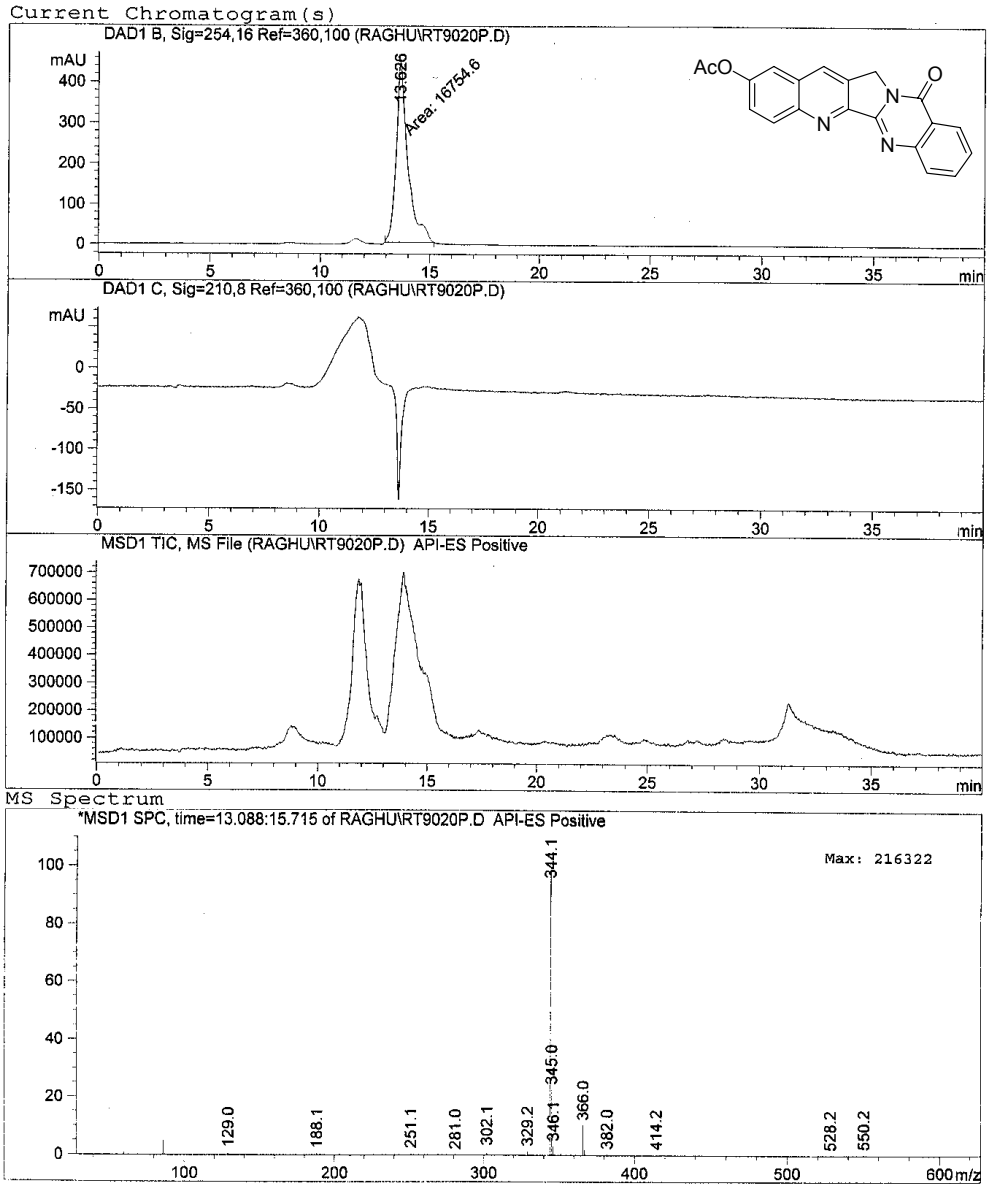


Figure A-35: ^1H spectrum of compound 130{c,6}

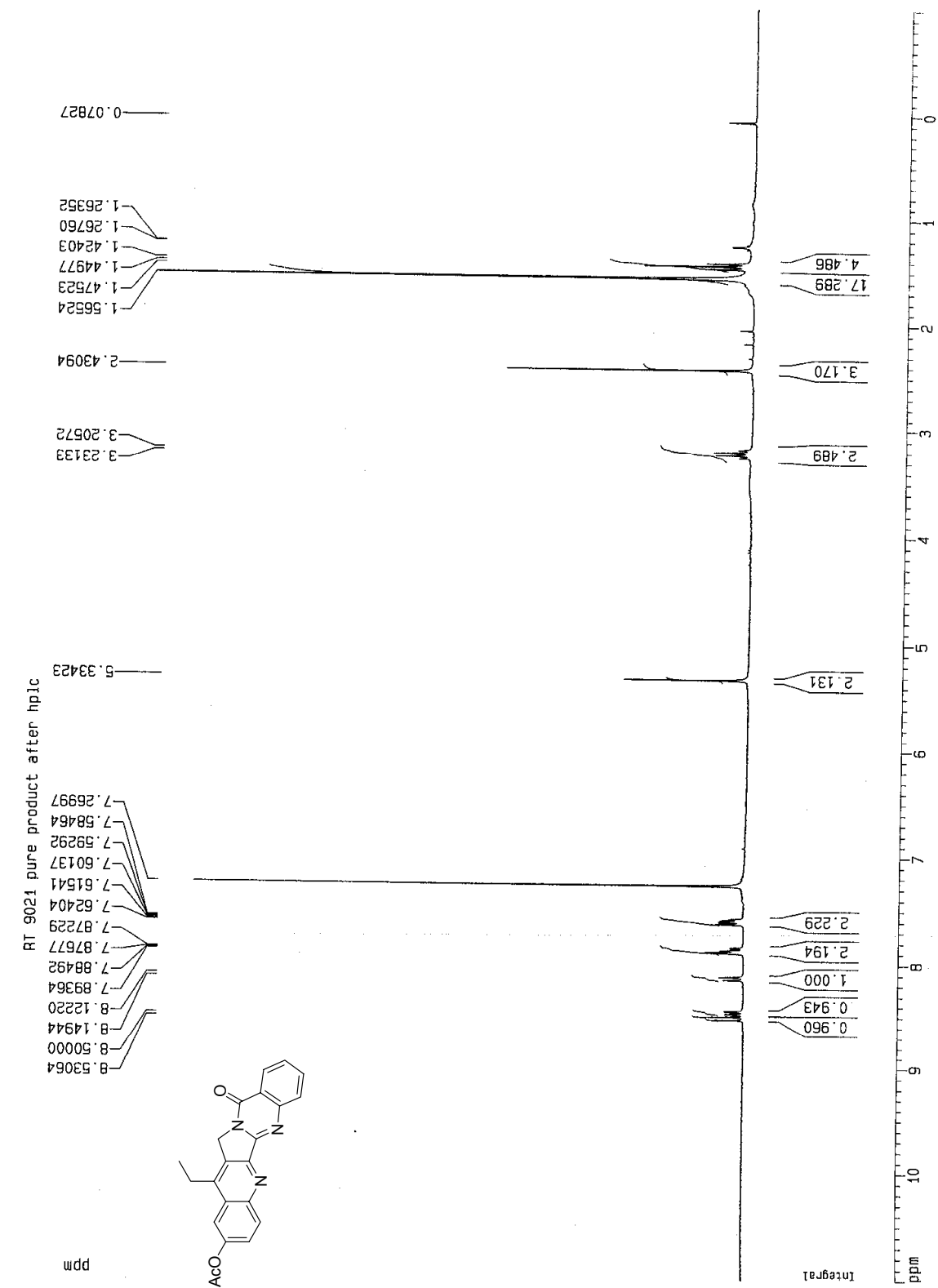


Figure A-36: LCMS data of compound 130{c,6}

Current Chromatogram (s)

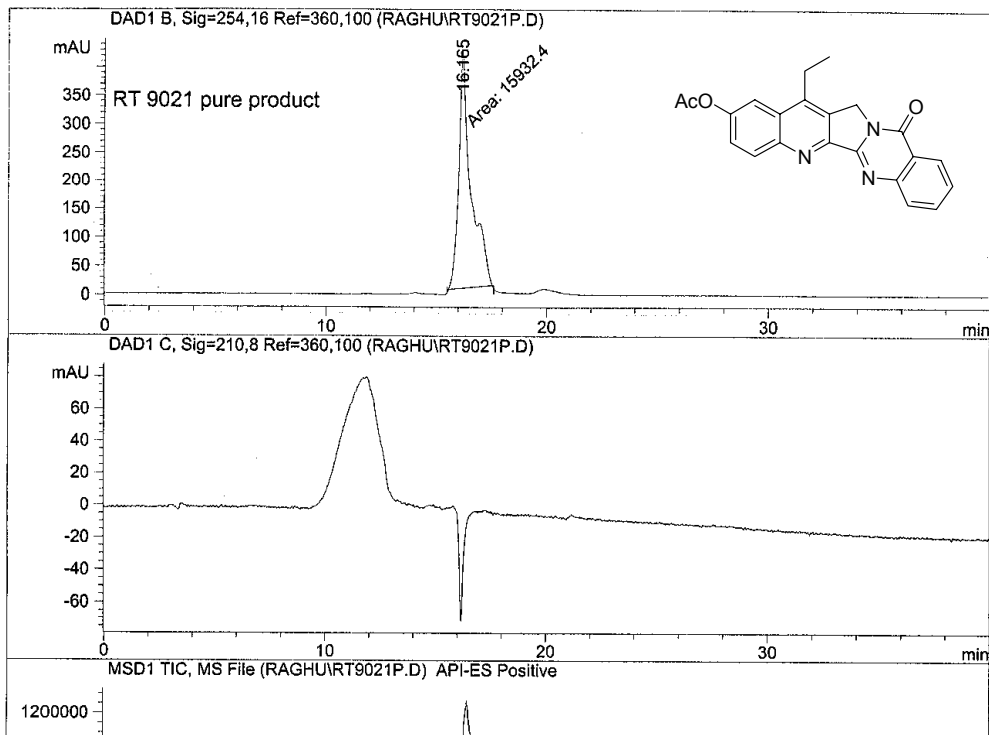


Figure A-37: ^1H spectrum of compound 130{a,7}

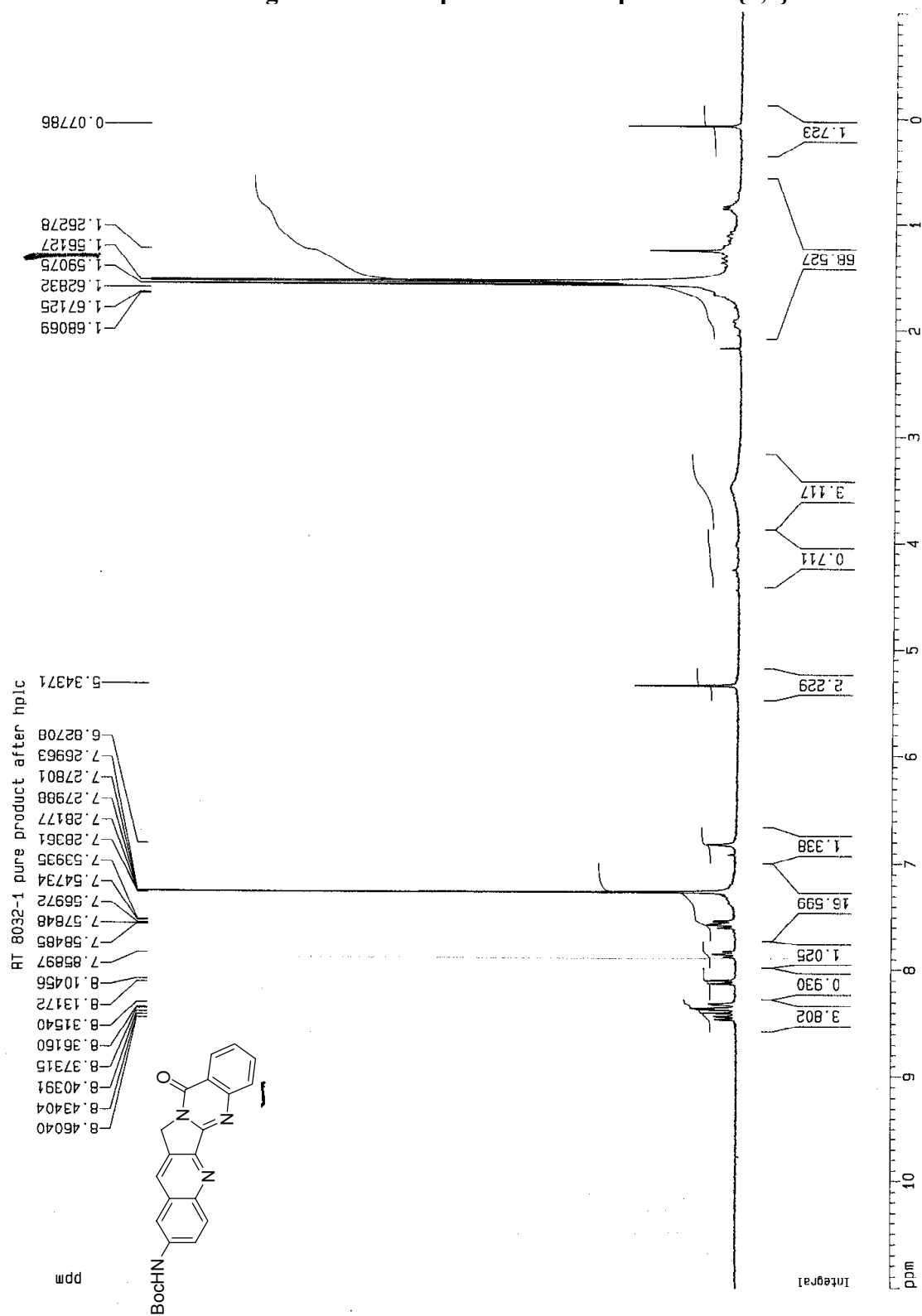
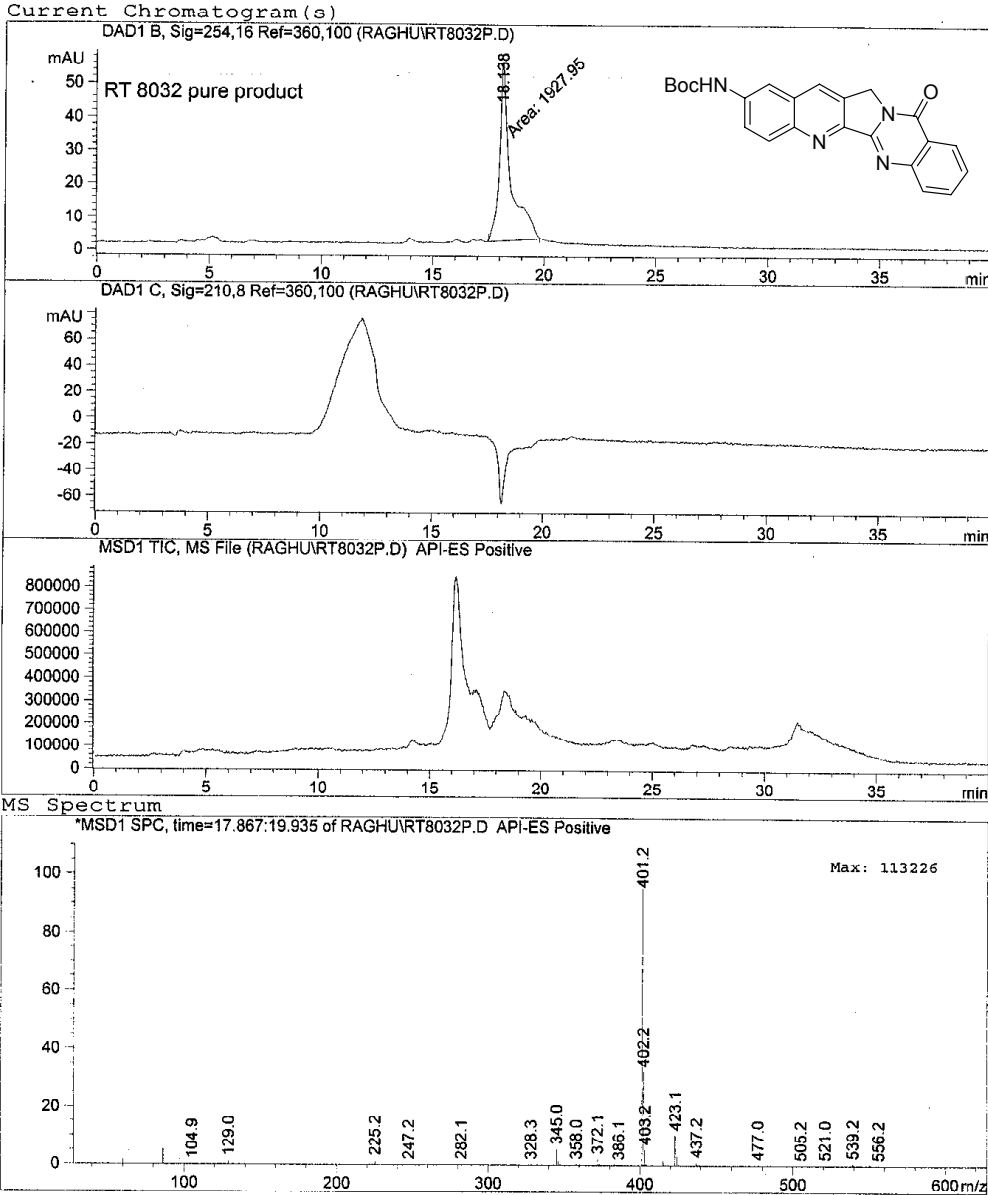


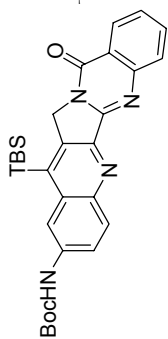
Figure A-38: LCMS data of compound 130{a,7}

Injection Date : 9/30/2004 1:16:56 AM Seq. Line : 10
Sample Name : rt8032p Vial : 15
Acq. Operator : Raghu Inj : 1
Inj Volume : 5 μ l

Acq. Method : C:\HPCHEM\1\METHODS\TANGI.M
Last changed : 9/29/2004 6:02:25 PM by habay
Analysis Method : C:\HPCHEM\1\METHODS\SCHAFFM~1.M\A5_100QK.M
Last changed : 10/1/2004 2:23:38 PM by morgan
(modified after loading)

Water 0.1% formic acid/acetonitrile 5% to 95%. Do not change this method.
you need to make changes, save it as another file.





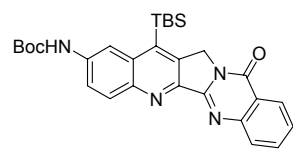


Figure A-41: ^1H spectrum of compound 130{d,7}

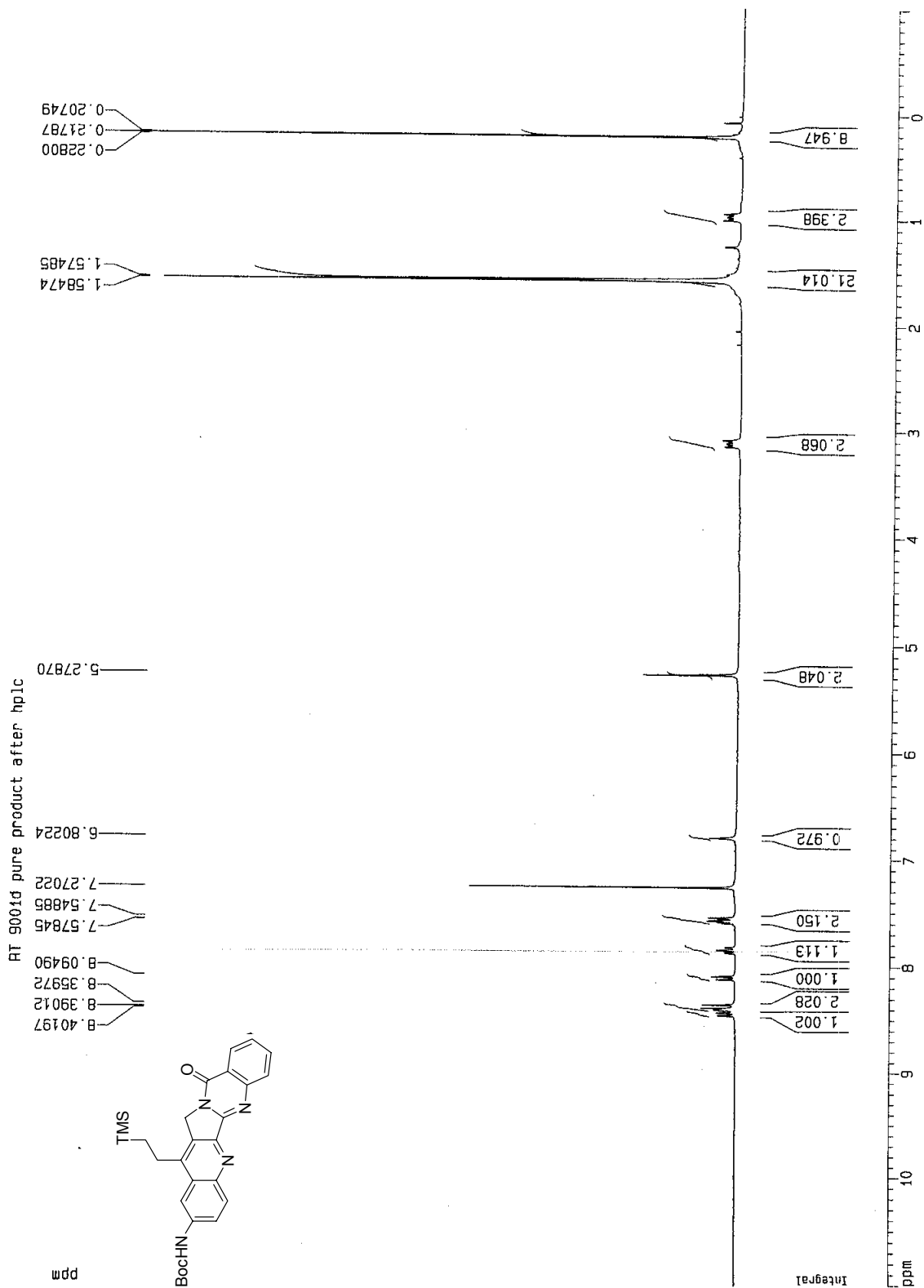
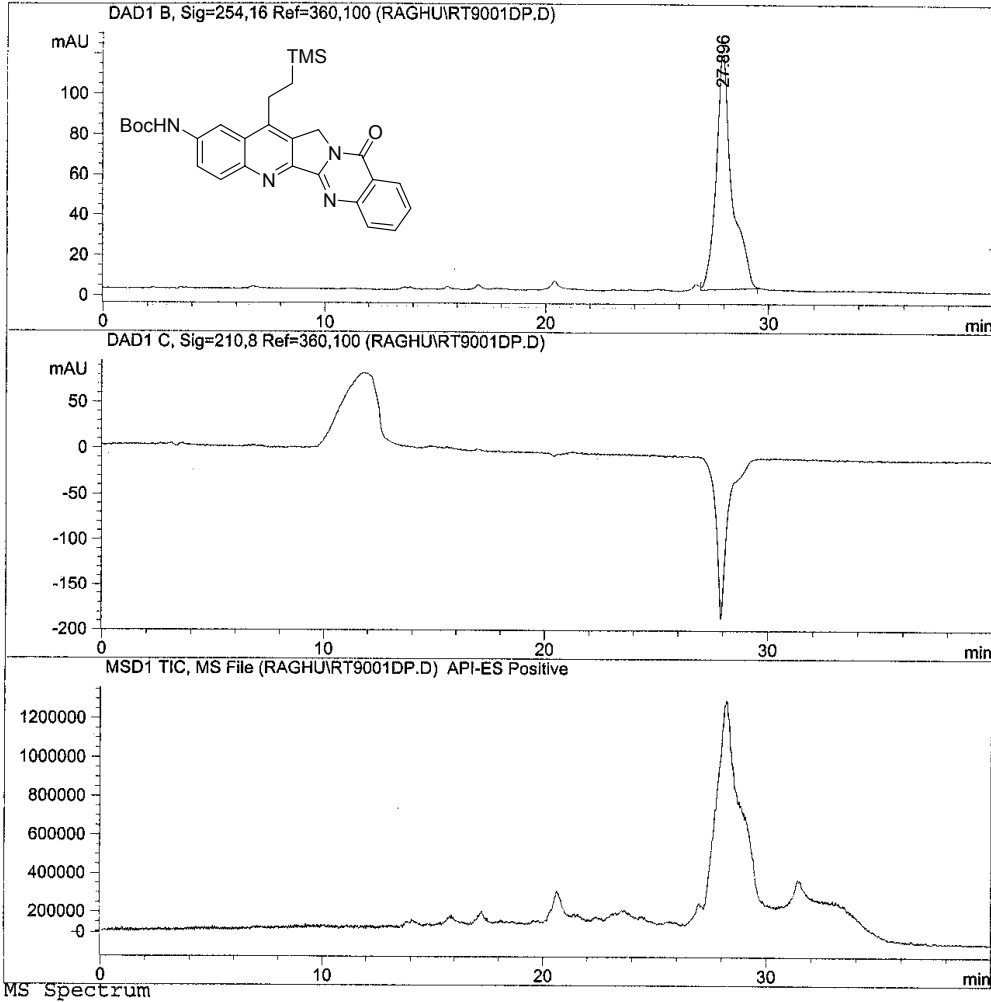


Figure A-42: LCMS data of compound 130{d,7}

Current Chromatogram (s)



*MSD1 SPC, time=27.209:29.907 of RAGHU\RT9001DP.D API-ES Positive

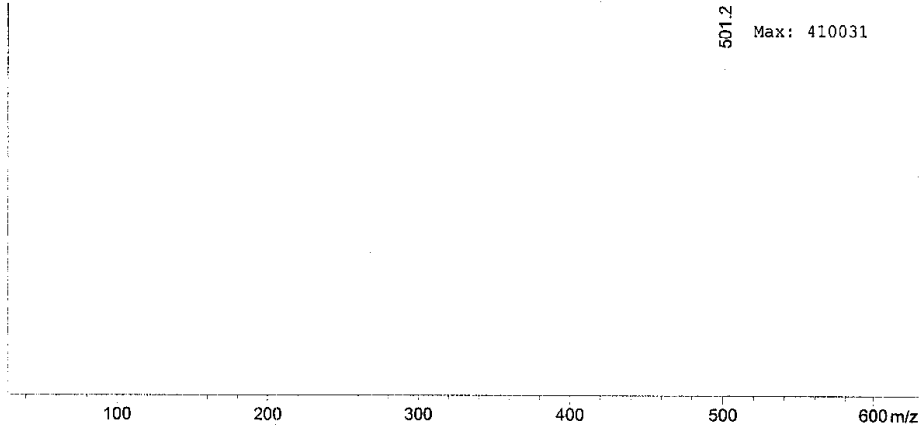


Figure A-43: ^1H spectrum of compound 130{d,8} (9,10 isomer)

RT 9002d pure product - spot 1 after hplc

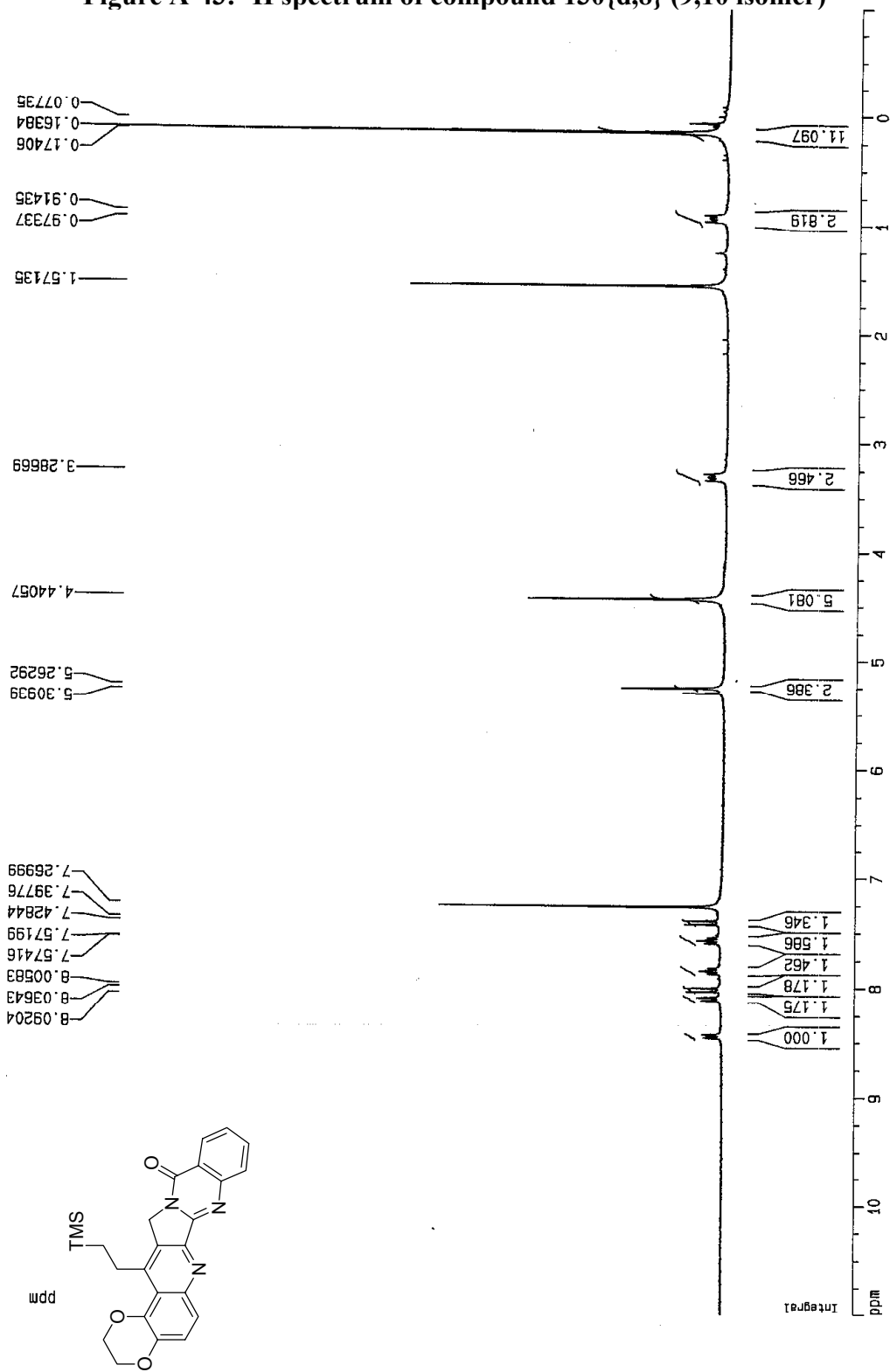
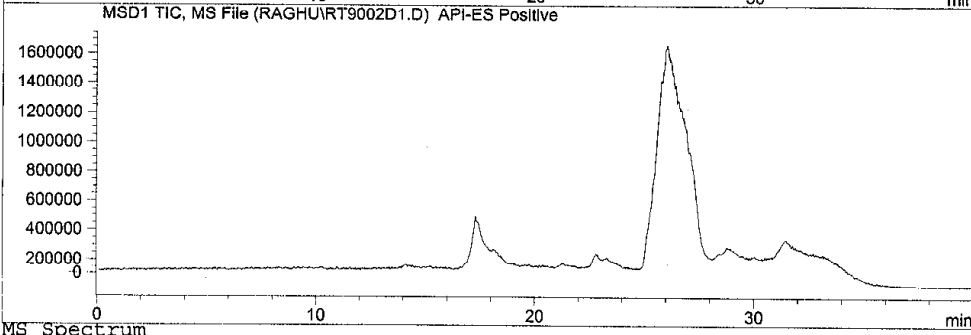
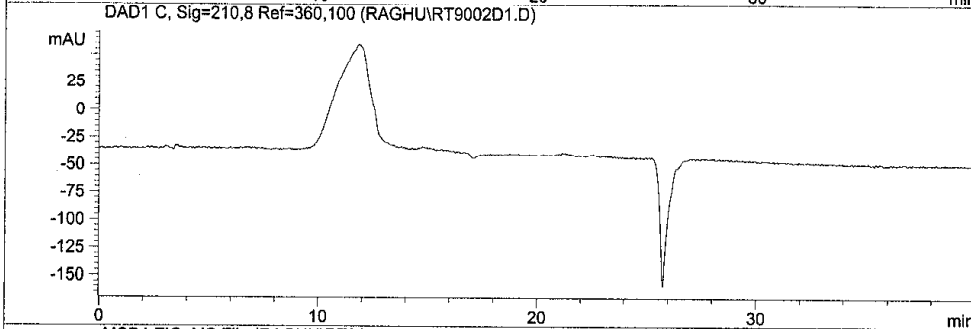
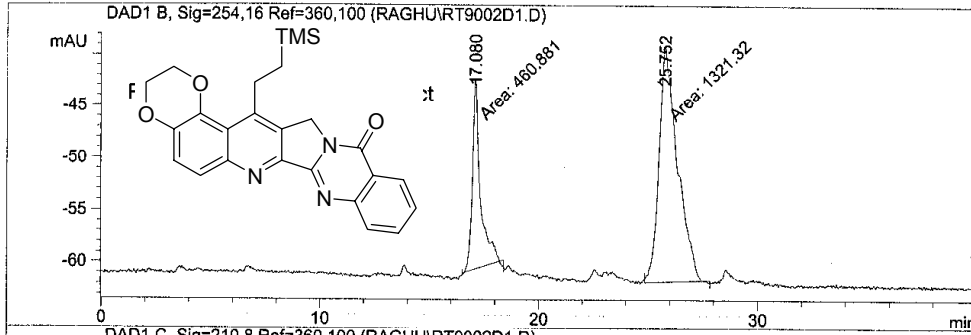


Figure A-44: LCMS data of compound 130{d,8} (9,10 isomer)

Current Chromatogram (s)



MS Spectrum

*MSD1 SPC, time=24.964:27.948 of RAGHU\RT9002D1.D API-ES Positive

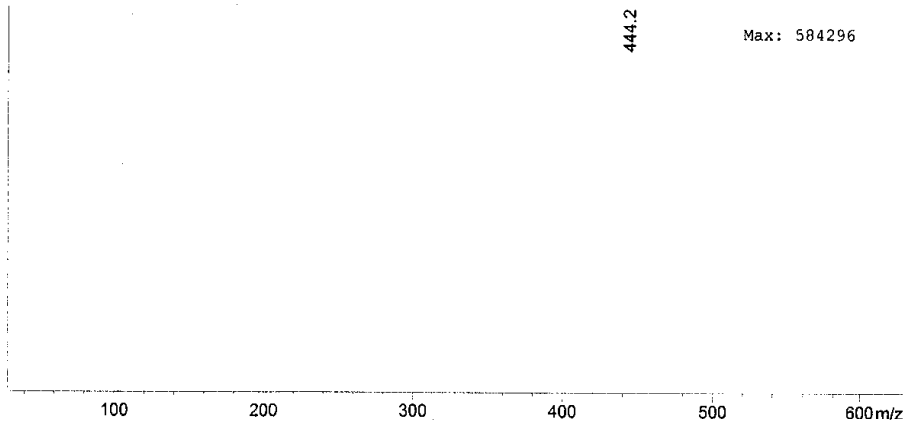


Figure A-45: ^1H spectrum of compound 130{d,8} (10,11 isomer)

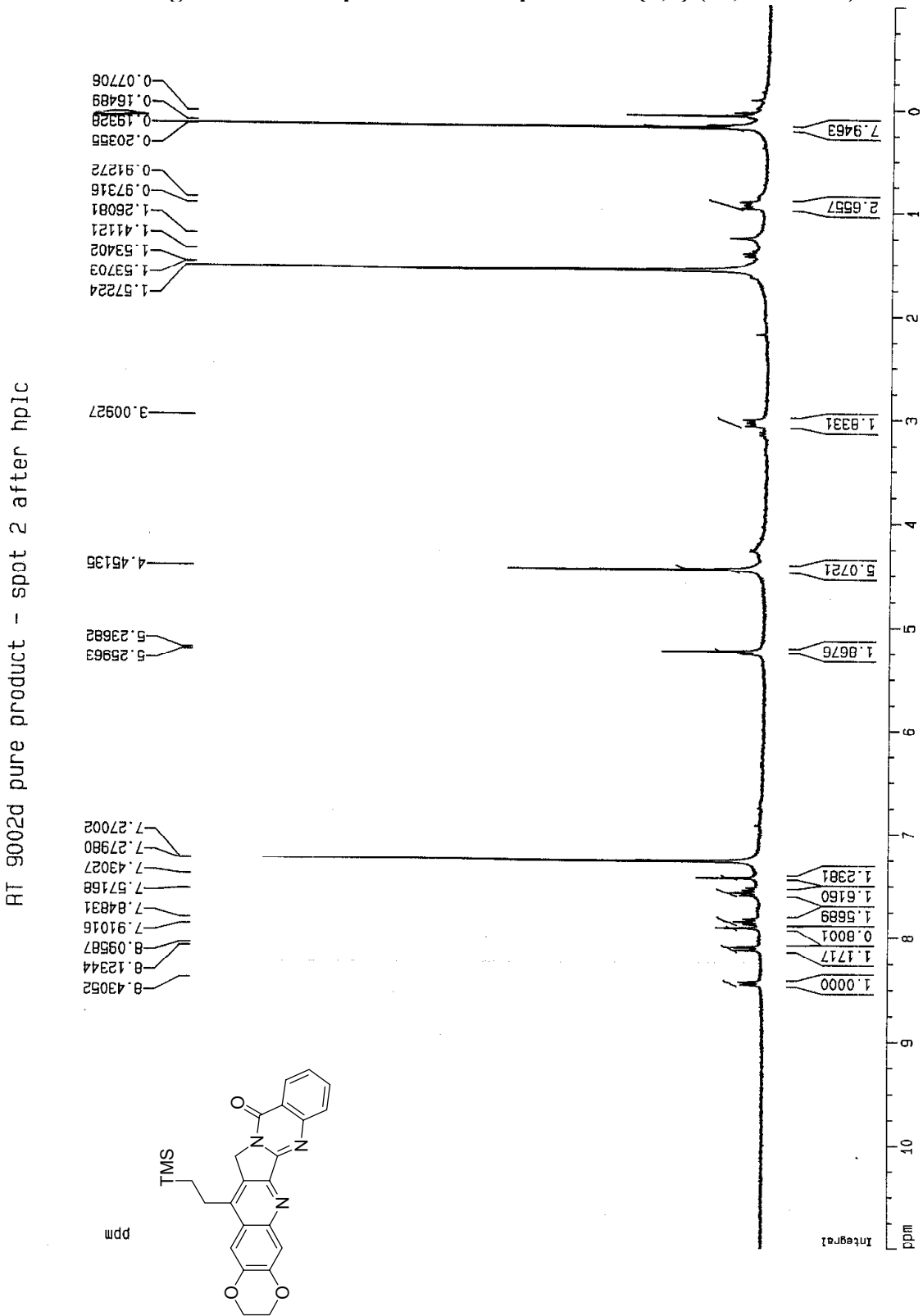
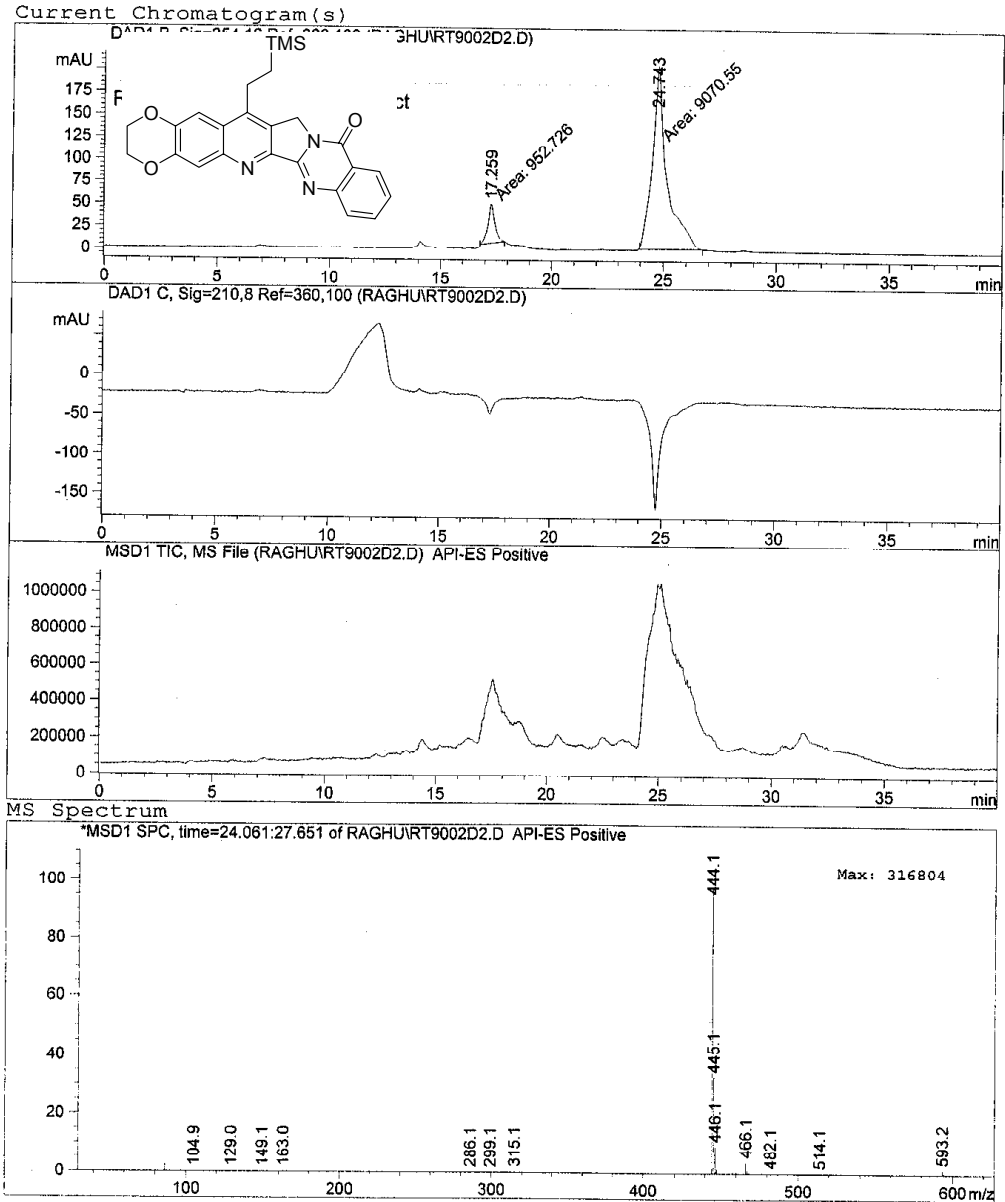


Figure A-46: LCMS data of compound 130{d,8} (10,11 isomer)

```

=====
Injection Date   : 9/29/2004 8:05:24 PM           Seq. Line   :    4
Sample Name     : rt9002dp-2                       Vial        :    6
Acq. Operator  : Raghu                             Inj         :    1
                                                    Inj Volume  : 5 µl

Acq. Method    : C:\HPCHEM\1\METHODS\TANGI.M
Last changed   : 9/29/2004 6:02:25 PM by habay
Analysis Method: C:\HPCHEM\1\METHODS\SCHAFFM-1.M\A5_100QK.M
Last changed   : 10/1/2004 2:23:38 PM by morgan
                (modified after loading)
Water 0.1% formic acid/acetonitrile 5% to 95%. Do not change this method.
you need to make changes, save it as another file.
    
```



BIBLIOGRAPHY

¹ *Cancer facts: A Concise Oncology Text*; Bishop, J. F., Ed.; Harwood Academic Publishers, Singapore, 1999.

² Wall, M. E.; Wani, M. C.; Cook, C. E.; Palmer, K. H.; McPhail, T. A.; Sim, G. A. *J. Am. Chem. Soc.* **1966**, *88*, 3888.

³ a) *Camptothecins: New Anticancer Agents*. Potmesil, H.; Pinedo, H. Eds.; CRC: Boca Raton, 1995. b) Takayama, H.; Kitajima, M.; Aimi, N. *J Syn Org Chem Jpn* **1999**, *57*, 181. c) Das, B.; Madhusudhan, P.; Reddy, P. V.; Anitha, Y. *Indian J Chem Sect B* **2001**, *40*, 453. d) Zunino, F.; Dallavalle, S.; Laccabue, D.; Beretta, G.; Merlini, L.; Pratesi, G. *Curr. Pharm. Design* **2002**, *8*, 2505. e) Lerchen, H.-G. *Drugs Fut.* **2002**, *29*, 869. f) Kim, D.-K.; Lee, N. *Mini Rev. Med. Chem.* **2002**, *2*, 611. g) Brezova, V.; Valko, M.; Breza, M.; Morris, H.; Telser, J.; Dvoranova, D.; Kaiserova, K.; Varecka, L.; Mazur, M.; Leibfritz, D. *J Phys Chem B* **2003**, *107*, 2415. h) Ulukan, H.; Swaan, P. *Drugs* **2002**, *62*, 2039. i) Du, W. *Tetrahedron* **2003**, *59*, 8649. j) Thomas, C. J.; Rahier, N. J.; Hecht, S. M. *Bioorg. Med. Chem.* **2004**, *12*, 1585.

⁴ a) *Twenty Years Later: Review of Clinical Trials With Camptothecin Sodium* Muggia, F. M.; In ref 3, pp 43-50. b) *Camptothecins: Dose-Limiting Toxicities and Their Management*. Burris, H. A.; Fields, S. M.; Kuhn, J. G.; Von Hoff, D. D.; In ref 3, pp 113-121. c) Abang, A. M.; *Semin. Hematol.* **1998**, *35*, 13.

⁵ a) Jaxel, C.; Kohn, K. W.; Wani, M. C. *et al*, *Cancer Res.* **1989**, *49*, 1465. b) Hertzberg, R. P.; Caranfa, M. J.; Holden, K. G.; Jakas, D. R.; Gallagher, G.; Mattern, M. R.; Mong, S.-M.; Bartus,

J. O.; Johnson, R. K. and Kingsbury, W.D. *J. Med. Chem.* **1989**, *32*, 715. c) Hsiang, Y. H.; Liu, L. F. *Cancer Res.* **1988**, *48*, 1722.

⁶ a) Hsiang, Y. H.; Hertzberg, R.; Hecht, S.; Liu, L. F. *J. Biol. Chem.* **1985**, *260*, 14873. b) Hsiang, Y. H.; Liu, L. F.; Wall, M. E.; Wani, M. C.; Nicholas, A. W.; Manikumar, G.; Kirschenbaum, S.; Silber, R.; Potmesil, M. *Cancer Res.* **1989**, *49*, 4385. c) Hertzberg, R. P.; Caranfa, M. J.; Hecht, S. M. *Biochemistry* **1989**, *28*, 4629. d) Wani, M. C.; Nicholas, A. W.; Manikumar, G.; Wall, M. E. *J. Med. Chem.* **1987**, *30*, 1774. e) Mi, Z. H.; Burke, T. G. *Biochemistry* **1994**, *33*, 10325. f) Gilbert, B. E.; Knight, V. *Sem. Ped. Infect. Dis.* **1996**, *7*, 148.

⁷ Redinbo, M. R.; Stewart, L.; Kuhn, P.; Champoux, J. J.; Hol, W. G. *Science* **1998**, *279*, 1504.

⁸ Hsiang, Y. H.; Lihou, M. G.; Liu, L. F. *Cancer Res.* **1989**, *49*, 5077.

⁹ Holm, C.; Covey, J. M.; Kerrigan, D.; Pommier, Y. *Cancer Res.* **1989**, *49*, 6365.

¹⁰ Sawada, S.; Yokokura, T. *Ann. N.Y. Acad. Sci.* **1996**, *803*, 13.

¹¹ a) Kingsbury, W. D.; Boehm, J. C.; Jakas, D. R.; Holden, K. G.; Hecht, S. M.; Gallagher, G.; Caranfa, M. J.; McCabe, F. L.; Faucette, L. F.; Johnson, R. K.; Hertzberg, R. P. *J. Med. Chem.* **1991**, *34*, 98. b) Sawada, S.; Okajima, S.; Aiyama, R.; Nokata, K.; Furuta, T.; Yokokura, T.; Sugino, E.; Yamaguchi, K.; Miyasaka, T. *Chem. Pharm. Bull.* **1991**, *39*, 1446. c) Luzzio, M. J.; Besterman, J. M.; Emerson, D. L.; Evans, M. G.; Lackey, K.; Leither, P. L.; McIntyre, G.; Morton, B.; Myers, P. L.; Peel, M.; Sisco, J. M.; Sternbach, D. D.; Tong, W.; Truesdale, A.; Uehling, D. E.; Vuong, A.; Yates, J. *J. Med. Chem.* **1995**, *38*, 395. d) Mitsui, I.; Kumazawa, E.; Hirota, Y.; Aonuma, M.; Sugimori, M.; Ohsuki, S.; Uoto, K.; Ejima, A.; Terasawa, H.; Sato, K. *Jpn. J. Cancer Res.* **1995**, *55*, 776. e) Pantazis, P.; Early, J. A.; Kozielski, A. J.; Mendoza, J. T.; Hinz, H. R.; Giovanella, B. C. *Cancer Res.* **1993**, *53*, 1577. f) Wani, M. C.; Nicholas, A. W.; Wall, M. E. *J. Med. Chem.* **1986**, *29*, 2358.

¹² Staker, B.L.; Hjerrild, K.; Feese, M. D.; Behnke, C. A.; Burgin, Jr. A. B.; Stewart, L. *Proc. Natl. Acad. Sci. USA* **2002**, *99*, 15387.

¹³ a) Stork, G.; Schultz, A. G. *J. Amer. Chem. Soc.* **1971**, *93*, 4074. b) Volkmann, R.; Danishefsky, S.; Eggler, J.; Solomon, D. M. *J. Amer. Chem. Soc.* **1971**, *93*, 5576. c) Tang, C.; Rapoport, H. *J. Amer. Chem. Soc.* **1972**, *94*, 8615. d) Meyers, A. I.; Nolen, R. L.; Collington, E. W.; Narwid, T. A.; Strickland, R. C. *J. Org. Chem.* **1973**, *38*, 1974. e) Ihara, M.; Noguchi, K.; Ohsawa, T.; Fukumoto, K.; Kametani, T. *Heterocycles* **1982**, *19*, 1835. f) Murata, N.; Sugihara, T.; Kondo, Y.; Sakamoto, T. *Synlett* **1997**, 298.

¹⁴ Corey, E. J.; Crouse, D. N.; Anderson, J. E. *J. Org. Chem.* **1975**, *40*, 2140.

¹⁵ a) Earl, R. A.; Volhardt, K. P. C. *J. Am. Chem. Soc.* **1983**, *105*, 6991. b) Wani, M. C.; Nicholas, A. W.; Wall, M. E. *J. Med. Chem.* **1987**, *30*, 2317. c) Ejima, A.; Terasawa, H.; Sugimori, M.; Tagawa, H. *Tetrahedron Lett.* **1989**, *30*, 2639. d) Ciufolini, M. A.; Roschangar, F. *Tetrahedron* **1997**, *53*, 11049. e) Comins, D. L.; Baevsky, M. F.; Hong, H. *J. Am. Chem. Soc.* **1992**, *114*, 10971. f) Fortunak, J. M. D.; Kitteringham, J.; Mastrocola, A. R.; Mellinger, M.; Sisti, N. J.; Wood, J. L.; Zhuang, Z.-P. *Tetrahedron Lett.* **1996**, *37*, 5683. g) Nguyen, T.; Wicki, M. A.; Snieckus, V. *J. Org. Chem.* **2004**, *69*, 7816.

¹⁶ a) Curran, D. P.; Liu, H. *J. Am. Chem. Soc.* **1992**, *114*, 5863. b) Curran, D. P.; Liu, H.; Josien, H.; Ko, S. B. *Tetrahedron* **1996**, *52*, 2763. c) Curran, D. P.; Josien, H.; Ko, S. B. *Angew. Chem. Int. Ed.* **1995**, *34*, 2683.

¹⁷ Yabu, K.; Masumoto, S.; Yamasaki, S.; Hamashima, Y.; Kanai, M.; Du, W.; Curran, D. P.; Shibasaki, M. *J. Am. Chem. Soc.* **2001**, *123*, 9908.

¹⁸ Rahier, N. J.; Eisenhauer, B. M.; Gao, R.; Jones, S. H.; Hecht, S. M. *Org. Lett.* **2004**, *6*, 321.

¹⁹ Thomas, O. P.; Dumas, C.; Zaparucha, A.; Husson, H. -P. *Eur. J. Org. Chem.* **2004**, 1128.

-
- ²⁰ Bom, D. C.; Curran, D. P.; Chavan, A. J.; Kruszewski, S.; Zimmer, S. G.; Fraley, K. A.; Burke, T. G. *J. Med. Chem.* **1999**, *42*, 3018.
- ²¹ Dallavalle, S.; Ferrari, A.; Biasotti, B.; Merlini, L.; Penco, S.; Gallo, G.; Marzi, M.; Tinti, M. O.; Martinelli, R.; Pisano, C.; Carminati, P.; Carenini, N.; Beretta, G.; Perego, P.; DeCesare, M.; Pratesi, G.; Zunino, F. *J. Med. Chem.* **2001**, *44*, 3264.
- ²² Lavergne, O.; Leseueur-Ginot, L.; Pla Rodas, F.; Bigg, D. C. H. *Bioorg. Med. Chem. Lett.* **1997**, *7*, 2235.
- ²³ Burke, T. G.; Bom, D.; *Ann. N.Y. Acad. Sci.* **2000**, *922*, 36.
- ²⁴ Du, W.; Curran, D. P.; Bevins, R. L.; Zimmer, S. G.; Zhang, J.; Burke, T. G. *Bioorg. Med. Chem.* **2002**, *10*, 103.
- ²⁵ Lavergne, O.; Leseueur-Ginot, L.; Pla Rodas, F.; Kasprzyk, P. G.; Pommier, J.; Demarquay, D.; Prévost, G.; Ulibarri, G.; Rolland, A.; Schiano-Liberatore, A.-M.; Harnett, J.; Pons, D.; Camara, J.; Bigg, D. C. H. *J. Med. Chem.* **1998**, *41*, 5410.
- ²⁶ Meth-Cohn, O.; Narine, B.; Tarnowski, B. *J. Chem. Soc. Perkin. Trans. I* **1981**, 1520.
- ²⁷ Lavergne, O.; Demarquay, D.; Bailly, C.; Lanco, C.; Rolland, A.; Huchet, M.; Coulomb, H.; Muller, N.; Baroggi, N.; Camara, J.; Le Breton, C.; Manginot, E.; Cazaux, J.-B.; Bigg, D. C. H. *J. Med. Chem.* **2000**, *43*, 2285.
- ²⁸ Gabarda, A. E.; Du, W.; Isarno, T.; Tangirala, R. S.; Curran, D. P. *Tetrahedron* **2002**, *58*, 6329.
- ²⁹ Han, X.; Stoltz, B. M.; Corey, E. J. *J. Am. Chem. Soc.* **1999**, *121*, 7600.
- ³⁰ a) Katsuki, T.; Sharpless, K. B. *J. Am. Chem. Soc.* **1980**, *101*, 5974. b) Hill, J. G.; Sharpless, K. B.; Exon, C. M.; Regeney, R. *Org. Synth.* **1985**, *63*, 66 (461).
- ³¹ Thomas, E. W. *J. Org. Chem.* **1986**, *51*, 2184.

-
- ³² Trécourt, F.; Mallet, M.; Marsais, F.; Quéguiner, G. *J. Org. Chem.* **1988**, *53*, 1367.
- ³³ Stork, G.; Takahashi, T. *J. Am. Chem. Soc.* **1977**, *99*, 1275.
- ³⁴ Piers, E.; Wong, T.; Ellis, K. A. *Can. J. Chem.* **1992**, 2058.
- ³⁵ a) Dess, D. B.; Martin, J. C. *J. Org. Chem.* **1983**, *48*, 4155. b) Ireland, R. E.; Liu, L. *J. Org. Chem.* **1993**, *58*, 2899.
- ³⁶ a) Johnson, R. A.; Sharpless, K. B. in *Catalytic Asymmetric Synthesis* (Ed.: I. Ojima), VCH, New York, 1993, Chapter 4.4. b) Becker, H.; Sharpless, K. B. *Angew. Chem. Int. Ed. Engl.* **1996**, *35*, 448. c) Seebach, D.; Gysel, U.; Kinkel, J. N. *Chimia* **1991**, *45*, 114. d) Akiyama, T.; Ishikawa, K.; Ozaki, S. *Synlett* **1994**, 275. e) Ley, S. V.; Cox, L. R. *J. Chem. Soc. Perkin Trans. I* **1997**, 3315. f) Soai, K.; Ishizaki, M.; Yokoyama, S. *Chem. Lett.* **1987**, 341. g) Ukaji, Y.; Yamamoto, K.; Fukui, M.; Fujisawa, T. *Tetrahedron Lett.* **1991**, *32*, 2919. h) Lee, E.; Choi, I.; Song, S. Y. *J. Chem. Soc. Chem. Commun.* **1995**, 321. i) Evans, D. A.; Ennis, M. D.; Le, T.; Mandel, N.; Mandel, G. *J. Am. Chem. Soc.* **1984**, *106*, 1154. j) Seebach, D.; Widler, L. *Helv. Chim. Acta.* **1982**, *65*, 1972.
- ³⁷ Evans, D. A.; Burgey, C. S.; Kozlowski, M. C.; Tregay, S. W. *J. Am. Chem. Soc.* **1999**, *121*, 686.
- ³⁸ Unpublished results, University of Pittsburgh.
- ³⁹ a) Belokon, Y. N.; Green, B.; Ikonnikov, N. S.; North, M.; Tararov, V. I. *Tetrahedron Lett.* **1999**, *40*, 8147. b) Tian, S. -K.; Deng, L. *J. Am. Chem. Soc.* **2001**, *123*, 6195. c) Tian, S. -K.; Hong, R.; Deng, L. *J. Am. Chem. Soc.* **2003**, *125*, 9900. d) Deng, H.; Isler, M. P.; Snapper, M. L.; Hoveyda, A. H. *Angew. Chem. Int. Ed.* **2002**, *41*, 1009.
- ⁴⁰ Hamashima, Y.; Kanai, M.; Shibasaki, M. *J. Am. Chem. Soc.* **2000**, *122*, 7412.

-
- ⁴¹ a) Boynard, L.; Rottländer, M.; Cahiez, G.; Konchel, P. *Angew. Chem. Int. Ed.* **1998**, *37*, 1701.
b) Berillon, L.; Lepretre, A.; Turch, A.; Ple, P.; Queguiner, G.; Cahiez, G.; Knochel, P. *Synlett* **1998**, 1359.
- ⁴² Comins, D. L.; Jacobine, A. F.; Marshall, J. L. ; Turnbull, M. M. *Synthesis* **1978**, 309.
- ⁴³ Takahasi, K.; Shibasaki, K.; Ogura, K.; Iida, H. *J. Org. Chem.* **1983**, *48*, 3566.
- ⁴⁴ Allen, C. F. H.; Vanallen, J. A. *Org. Synth. Collect. Vol. III*, Wiley, New York, 1965, 275.
- ⁴⁵ van Leusen, D.; van Leusen, A. M. *Org. React.* **2001**, *57*, 417.
- ⁴⁶ Oldenziel, O. H. ; van Leusen, D.; van Leusen, A. M. *J. Org. Chem.* **1977**, *42*, 3114.
- ⁴⁷ a) Kolb, H. C.; VanNieuwenhze, M. S.; Sharpless, K. B. *Chem. Rev.* **1994**, *94*, 2483. b) Becker, H.; Soler, M. A.; Sharpless, K. B. *Tetrahedron*, **1995**, *51*, 1345. c) Amberg, W.; Bennani, Y. L.; Chadha, R. K.; Crispino, G. A.; Davis, W. D.; Hartung J.; Jeong, K. -S.; Ogino, Y.; Shibata, T.; Sharpless, K. B. *J. Org. Chem.* **1993**, *58*, 844. d) Katsuki, T.; Sharpless, K. B. *J. Am. Chem. Soc.* **1980**, *101*, 5974. For reviews on stereoselective epoxidations of olefins, see e) Pfenninger, A. *Synthesis* **1986**, 89. f) Shwesinger, R.; Willaredt, J.; Bauer, T. in *Houbren-Weyl*; Hoffmann, R. W. Ed.; Thieme: Stuttgart, 1995; Vol. E21, p. 4599.
- ⁴⁸ Beckwith, a. L. J.; Cliff, M. D.; Schiesser, C. H. *Tetrahedron* **1992**, *48*, 4641.
- ⁴⁹ Ana E. Gabarda. In *Development of New Camptothecin analogs as Cancer Chemotherapeutic Agents: Library Synthesis of Homosilatecans and The First Asymmetric Synthesis of Homocamptothecin and Related Homosilatecans*. Ph.D. thesis, University of Pittsburgh, 2001.
- ⁵⁰ For reviews see a) Armstrong, S. K. *J. Chem. Soc. Perkin Trans. I* **1998**, 371. b) Grubbs, R. H.; Chang, S. *Tetrahedron* **1998**, *54*, 4413. c) Schuster, M.; Blechert, S. *Angew. Chem. Int. Ed.* **1997**, *36*, 2036.

-
- ⁵¹ Fürstner, A.; Thiel, O. R.; Ackermann, L.; Schanz, H. –J.; Nolan, S. P. *J. Org. Chem.* **2000**, *65*, 2204.
- ⁵² Wright, D. L.; Schulte II, J. P.; Page, M. A. *Org. Lett.* **2000**, *2*, 1847.
- ⁵³ Rayabarapu, D. K.; Cheng, C. –H. *J. Am. Chem. Soc.* **2002**, *124*, 5630.
- ⁵⁴ Molecular Operating Environment (MOE); 2004.03 ed.; Chemical Computing Group Inc.; 1010 Sherbrooke Street West, Suite 910, Montreal, Canada H3A 2R7.
- ⁵⁵ Eliel, E. L.; Wilen, S. H. *Stereochemistry of Organic Compounds*, John Wiley & sons, 1994, p. 503.
- ⁵⁶ Hautefaye, P.; Cimetière, B.; Pierré, A.; Léonce, S. ; Hickman, J. ; Laine, W. ; Bailly, C. ; Lavielle, G. *Bioorg. Med. Chem. Lett.* **2003**, *13*, 2731.
- ⁵⁷ David C. Bom. In *Implementation of a Radical Cascade Cyclization in Drug Discovery: Total Synthesis of Silatecans and Homosilatecans*. Ph.D. thesis, University of Pittsburgh, 2000.
- ⁵⁸ Hashimoto, N.; Aoyama, T.; Shiiri, T. *Chem. Pharm. Bull.* **1981**, *29*, 1475.
- ⁵⁹ a) Hertzberg, R. P.; Caranfa, M. J.; Hecht, S. M. *Biochemistry* **1989**, *28*, 4629. b) Horwitz, S. B.; Chang, C. K.; Grollman, A. P. *Mol. Pharmacol.* **1971**, *7*, 632.
- ⁶⁰ Martin, S. F.; Dwyer, M. P.; Hartmann, B.; Knight, K. S. *J. Org. Chem.* **2000**, *65*, 1305.
- ⁶¹ Crich, D.; Dudkin, V. *J. Am. Chem. Soc.* **2002**, *124*, 2263.
- ⁶² Govindachari, T. R.; Ravindranath, K. R.; Viswanathan, N. *J. Chem. Soc. Perkin Trans. 1* **1974**, 1215.
- ⁶³ Allaudeen, H. S.; Berges, D. A.; Hertzberg, R. P.; Johnson, R. K.; Kingsbury, W. D.; Petteway, S. R. Jr. *PCT Int. Appl.* (**1992**); WO 9207856.
- ⁶⁴ Kirihara, M.; Niimi, K.; Okumura, M.; Momose, T. *Chem. Pharm. Bull.* **2000**, *48*, 220.
- ⁶⁵ Takeuchi, Y.; Ogura, H.; Ishii, Y.; Koizumi, T. *Chem. Pharm. Bull.* **1990**, *38*, 2404.

-
- ⁶⁶ Wang, X.; Zhou, X.; Hecht, S. M. *Biochemistry* **1999**, *38*, 4374.
- ⁶⁷ Boehm, H. -J.; Banner, D.; Bendels, S.; Kansy, M.; Kuhn, B.; Mueller, K.; Obst-Sander, U.; Stahl, M. *ChemBioChem* **2004**, *5*, 637.
- ⁶⁸ Shibata, N.; Ishimaru, T.; Nakamura, M.; Toru, T. *Synlett* **2004**, 2509.
- ⁶⁹ Josien, H.; Ko, S. -B.; Bom, D.; Curran, D. P. *Chem. Eur. J.* **1998**, *4*, 67.
- ⁷⁰ Döbler, C.; Mehleretter, G. M.; Sundermeier, U.; Beller, M. *J. Am. Chem. Soc.* **2000**, *122*, 10289.
- ⁷¹ DAST fluorinations were performed on each intermediate of the synthetic sequence, i.e., the 20-hydroxy versions of **115**, **116**, **109** and **107** to determine the best step for fluorination. Pyridine lactone **115** proved to be ideal in terms of good yields and purity. Fluorination reaction of the other intermediates resulted either in multiple products or poorer yields as compared to that from **115**.
- ⁷² a) Lal, G. S. ; Pez, G. P. ; Pesaresi, R. J. ; Prozonic, F. M. *Chem. Commun.* **1999**, 215. b) , G. S. ; Pez, G. P. ; Pesaresi, R. J. ; Prozonic, F. M.; Cheng, H. *J. Org. Chem.* **1999**, *64*, 7048.
- ⁷³ Ma, Z. Z.; Hano, Y.; Nomura, T. ; Chen, Y. -J. *Heterocycles* **1997**, *46*, 541.
- ⁷⁴ Toyota, M.; Komori, C.; Ihara, M. *Heterocycles* **2002**, *56*, 101.
- ⁷⁵ Harayama, T.; Morikami, Y.; Shigeta, Y.; Abe, H.; Takeuchi, Y. *Synlett* **2003**, 847.
- ⁷⁶ a) Cagir, A.; Jones, S. H.; Eisenhauer, B. M. ; Gao, R. ; Hecht, S. M. *Bioorg. Med. Chem. Lett.* **2004**, *14*, 2051. b) Cagir, A.; Eisenhauer, B. M. ; Gao, R. ; Thomas, S. J.; Hecht, S. M. *Bioorg. Med. Chem.* **2004**, *12*, 6287.
- ⁷⁷ a) Dallavalle, S.; Merlini, L.; Beretta, G. L. ; Tinelli, S. ; Zunino, F. *Bioorg. Med. Chem. Lett.* **2004**, *14*, 5757. b) Yadav, J. S. ; Reddy, B. V. S. *Tetrahedron Lett.* **2002**, *43*, 1905. c) Wang, H.; Ganesan, A. *Tetrahedron Lett.* **1998**, *39*, 9097. d) Ross Kelly, T.; Chamberland, S.; Silva, R. A.

Tetrahedron Lett. **1999**, *40*, 2723. e) Molina, P.; Tárraga, A.; Gonzalez-Tejero, A. *Synthesis* **2000**, 1523.

⁷⁸ Pangborn, A. B.; Giardello, M. A.; Grubbs, R. H.; Rosen, R. K.; Timmers, F. J. *Organometallics*, **1996**, *15*, 1518.